NI 43-101 Technical Report – Mineral Resource Update on Bandeira Project, Araçuaí and Itinga, Minas Gerais State, Brazil

Prepared by **GE21 Consultoria Mineral Ltda**. on behalf of:

Lithium Ionic Corp.

Project GE21 nº: 240403
Effective date: March 5th, 2024

Qualified Persons:

Carlos José Evangelista Silva – MSc. (Geo), MAIG

Leonardo Rocha – BSc. (Geo), MAIG

Paulo Bergman – BSc. (Min Eng), FAusIMM

NI 43-101 Technical Report – Mineral Resource Update on Bandeira Project, Araçuaí and Itinga, Minas Gerais State, Brazil

GE21 Projeto nº: 240403

Effective date: March 5th, 2024

Issue date: May 27th, 2024

Version: Initial issue

Work directory: S:\Projetos\MGLIT-Empreendimento\240403-MRE-Bandeira\23_Relatorio

Copies: Lithium Ionic Corp. (1)
GE21 Consultoria Mineral Ltda. (1)

Version	Description	Author(s)	Date

DATE AND SIGNATURE PAGE

This Report, entitled “NI 43-101 Technical Report – Mineral Resource Update on Bandeira Project, Araçuaí and Itinga, Minas Gerais State, Brazil”, was prepared by Carlos José Evangelista Silva, Leonardo Silva Santos Rocha, and Paulo Roberto Bergman Moreira, on behalf of Lithium Ionic Corp.

Dated at Belo Horizonte, Brazil, on May 27th, 2024.

Original document signed and sealed

Carlos José Evangelista Silva, MSc (Geo), MAIG

Original document signed and sealed

Leonardo Silva Santos Rocha, BSc (Geog), MAIG

Original document signed and sealed

Paulo Bergman, BSc (Min Eng), FAusIMM

UNITS, SYMBOLS, AND ABBREVIATIONS

Units and Symbols	
“	Inches
°C	Celsius
%	Percentage
Au g/t	Grams of Gold per Tonne
Au	Gold
CDN$	Canadian Dollars
Cm	Centimetre(s)
E	East
Ga	Gigaannum
g/t	Grams per Tonne
Ha	Hectare(s)
hp	Horse Power
hr	Hour
k	Thousands
k$	Thousands of Dollars
kg	Kilogram
km	Kilometre(s)
kt	Thousands of Tonnes
kV	Kilovolt
l	Litre
m	Metres
m³/h	Cubic Metres per Hour
Mt	Megatonne
M	Millions
Mtpa	Million Tonnes per Annum
mg	Milligram

Units and Symbols	
Oz	Ounce
NE	Northeast
NW	Northwest
t/h	Tonnes per Hour
tpd	Tonnes per Day
USD	United States dollars ($)
V	Volts
w/v	Weight by volume

Abbreviations	
3D	Three Dimensional
AA	Atomic Absorption
AARL	Anglo American Research Laboratories
AHD	Average Hauling Distance
AI	Abrasion Index
AMPRD	Absolute Mean Paired Relative Difference
ANM	National Mining Agency of Brazil
ASL	Above Sea Level
BWI -	Bond Work Index
CA	Certificate of Authorization
CDN	Canadian
CFEM	Financial Compensation for Exploitation of Mineral Resources
Chl	Chlorite
CIM	Canadian Institute of Mining, Metallurgy and Petroleum
CoG	Cut-off Grade

Abbreviations	
CRM	Certified Reference Material
CSA	Canadian Securities Administrators
Cum	Cumulative
DDH	Diamond Drill Hole
DGPS	Differential Global Positioning System
DWT	Drop Weight Test
EBPP	Eastern Brazilian Pegmatite Province
EIA	Environmental Impact Assessment
Esp	Sphalerite
FA	Fire Assay
FS	Feasibility Study
GE21	GE21 Consultoria Mineral
GPS	Global Positioning System
GRG	Gravity Recoverable Gold Tests
Hem	Hematite
IBGE	Brazilian Institute of Geography and Statistics
ICU	Intensive Cyanidation Unity
JV	Joint Venture
LOM	Life of Mine
LCT	Lithium-Cesium-Tantalum
LP	Preliminary License
LPG	Liquefied Petroleum Gas
Mag	Magnetite
MAR	Metarenites
MGL	Metaconglomerate
MYL	Upper Schist and Schist
NI 43-101	National Instrument 43-101

Abbreviations	
NSR	Net Smelter Revenue
Py	Pyrite
P80	Passing 80%
QA/QC	Quality Assurance and Quality Control
QP	Qualified Person
Qtz	Quartz
ROM	Run of Mine
Sd	Siderite
Ser	Sericite
SO_2	Sulphur dioxide
SPI	SAG power index and
SR	Stripping Ratio
SRP	spodumene-rich pegmatites
TAH	Annual Rate per Hectare

TABLE OF CONTENTS

LIST OF TABLES

LIST OF FIGURES

1 EXECUTIVE SUMMARY

Lithium Ionic Corp. is a Canadian mining company exploring and developing its lithium properties in Brazil. Its flagship Itinga and Salinas projects cover 14,182 ha in the northeastern part of Minas Gerais state, a mining-friendly jurisdiction that is quickly emerging as a world-class hard-rock lithium district.

The Bandeira Project is situated in the same region as CBL's Cachoeira lithium mine, which has produced lithium for +30 years, as well as Sigma Lithium Corp.'s Grota do Cirilo project, which hosts the largest hard-rock lithium deposit in the Americas.

1.1 Introduction and Terms of Reference

GE21 Consultoria Mineral Ltda. ("GE21") was engaged by Lithium Ionic Corp. to prepare an Independent Technical Report ("ITR") containing a NI 43-101 Technical Report (The "Report") on Lithium Ionic's Bandeira deposit located in Minas Gerais State, Brazil (Project).

This Report titled "NI 43-101 Technical Report – Mineral Resource Update on Bandeira Project, Araçuaí and Itinga, Minas Gerais State, Brazil" outlines all relevant data about the Bandeira Project (The "Project"). They are technical information and data related to the drilling program and the status of the current Lithium Mineral Resources contained in the spodumene-bearing pegmatites.

1.1.1 Qualified Persons

The technical information for the MRE has been reviewed and approved by independent qualified persons as defined in NI 43-101.

GE21 is an independent mineral consulting firm based in Brazil formed by a team of professionals accredited by the Australian Institute of Geoscientists ("AIG") as Qualified Persons ("QP") for the declaration of Mineral Resources and Mineral Reserves in accordance with National Instrument 43-101 – Standards of Disclosure for Mineral Projects ("NI 43-101").

The independent QP responsible for this report's content on issues related to Mineral Resources is Carlos José Evangelista Silva (MAIG, M.Sc.), a Geologist with at least 17 years of experience in the mineral industry, including lithium mining companies.

The independent QP responsible for this report's content on issues related to data verification and QA/QC procedures is Leonardo Silva Santos Rocha (MAIG, M.Sc.), a Geologist who has at least 12 years of experience in the mineral industry, including lithium mining companies.

The independent QP responsible for this report's content on issues related to Mineral Processing and Metallurgical Tests, and Recovery Methods is Paulo Bergman (FAusIMM, B.Sc.), a Mining Engineer of GE21 Consultoria Mineral, who has at least 43 years of experience in mining projects.

Porfirio Cabaleiro Rodriguez (FAIG, B.Sc.) is the reviewer of this technical report. Mr. Rodriguez

has at least 45 years of experience in all aspects of mining project evaluation, from initial exploration to bankable feasibility studies. He is a senior mining engineer and managing director of GE21 Mineral Consulting.

1.2 Reliance on Other Experts

The authors have not independently verified ownership or mineral title beyond the information that Lithium Ionic has provided. The Property description presented in this Report is not intended to represent a legal or any other opinion as to title.

The Authors are not qualified to express any legal opinion concerning Property titles or current ownership.

1.3 Property Description and Location

The Bandeira Project (The "Project") covers 175 hectares within Lithium Ionic's large land package of 14,182 hectares and is located between the towns of Araçuaí and Itinga within Brazil's "Lithium Valley" - a hard rock lithium district that is quickly emerging as an important global lithium producer.

1.4 Accessibility, Climate, Local Resources, Infrastructure and Physiography

The Project is situated in the northeastern region of Minas Gerais State, Brazil, within the Jequitinhonha Valley, approximately 600 kilometres northeast of Belo Horizonte. Lithium Ionic fully owns the property. It is conveniently located about 75 kilometres south of the town of Salinas, with a population of approximately 42,000, and roughly 25 kilometres east of the town of Araçuaí, with a population of approximately 40,000. Access to the project is facilitated by well-maintained public and private roads, thanks to its proximity to National Roads 251 and 116.

The Project remains accessible year-round through a network of main and secondary service roads. National routes BR 116 and 262 provide access to the Port of Vitória in the State of Espírito Santo, located approximately 850 kilometres from the project site. This port offers potential export opportunities for any spodumene production from the project. Additionally, national roads BR 116 and BR 415 connect to the Ilhéus Port in the Bahia State, which is about 540 kilometres from the project and is an alternative shipping port option.

1.5 History

The Bandeira site and all other Mineral Tenures have not had any drilling activity before 2022.

1.6 Geological Setting and Mineralization

The Bandeira Project lies in the Middle Jequitinhonha River valley, northeastern Minas Gerais State, currently known as the Lithium Valley of Brazil. The region is part of the Eastern Brazilian

Pegmatite Province (EBPP), one of the largest pegmatitic provinces worldwide, with 150,000 km2 (cf. synthesis in Pedrosa-Soares et al., 2011). The EBPP is an outcome of magmatic and tectonic-metamorphic events that formed the Araçuaí Orogen from the Early Ediacaran (ca. 630 Ma) to the Late Cambrian (ca. 490 Ma). The significant EBPP pegmatite populations found within the Araçuaí Orogen have been grouped into twelve pegmatite districts (Pedrosa-Soares et al., 2011, 2023) that include residual pegmatites (representing late silicate melts released by fractional crystallization of parent granites) and/or anatectic pegmatites (formed directly from partial melting of country rocks).

The Itinga Pegmatite Field includes the spodumene mines and deposits of CBL (Companhia Brasileira de Lítio) and Sigma Lithium, as well as Lithium Ionic's properties of its Bandeira Project, such as the Bandeira spodumene deposit. The lithium ore bodies exploited in the CBL's underground mine, since the early 1990's, display a closely spaced swarm of relatively narrow (6 m thick on average) but long (up to 700 m along strike) non-zoned spodumene-rich pegmatites (SRP) with on average 25 vol% of disseminated spodumene (Romeiro and Pedrosa-Soares, 2005). In the Sigma Lithium properties, where several large spodumene-rich pegmatites are found (e.g., Barreiro, Murial, Xuxa; Delboni Jr. et al., 2023), an open pit mine is currently being developed on the Xuxa SRP deposit (15 m thick x 1800 m long x 500 m downdip open).

1.7 Deposit Types

According to the most accepted petrologic-metallogenetic classification of pegmatites, published by Cerný (1991) and updated by Cerný and Ercit (2005) and Cerný et al. (2012), all the spodumene-rich pegmatites found within the Bandeira deposit, as well as in the whole Cachoeira Pegmatite Group, belong to the rare element class, Li subclass, and albite-spodumene type.

Although generally included in the LCT (Lithium-Cesium-Tantalum) family, the non- to poorly zoned spodumene-rich pegmatites (SRP) found in the Bandeira deposit, as well as all the orebodies mined in CBL's Cachoeira Mine since the 1990's, the Xuxa and other spodumene-rich deposits of Sigma Lithium (Sá, 1977; Delboni et al., 2023), and the Outro Lado deposit of Lithium Ionic, are rather poor both in Ta and Cs when compared with the complex zoned LCT pegmatites.

1.8 Exploration

Trench sampling program, rock chip sampling programs, structural mapping and geophysical surveys were completed on the Property. A total of 26 trenches were completed until 2024 at the Bandeira target by Lithium Ionic totaling 1,401 m. Field work included rock samples in the field and a preliminary field mapping of visible outcrops.

Some basic field data such as outcrop attitude (strike and dip), foliation and cleavage which located several occurrences of spodumene never previously known or reported. Since this initial discovery, Lithium Ionic rapidly advanced the Project with drill testing of the target(s) and the pegmatite system.

1.9 Drilling

All drilling activities conducted within the Bandeira Property until March 2024 have been incorporated into the Mineral Resource estimation process. It is important to note that any drill holes completed in 2024 after this date, as well as pending sample assay results, have not been considered in the present resource statement Table 1-1.

Table 1-1 – Bandeira Drill Holes Summary

Source: GE21 2024

Drill Type	Year	Number Drill	Length (m)
DDH	2022	47	5,394
	2023	181	44,576
	2024	5	789
	Total	233	50,760

1.10 Sample Preparation, Analysis, and Security

Sample intervals in the mineralized zones are defined based on a 1.0m support. Mineralized samples must have a minimum length of 1.0m and a maximum length of 1.5m. In some specific situations, samples shorter than 1.0m can be generated.

Drill core samples are prepared and analyzed by an independent commercial laboratory (SGS Geosol). The SGS Geosol facility is certified in ISO 9001, ISO 14001, and ISO 17025. The sample shipment was delivered to the SGS Geosol facility in Vespasiano, Minas Gerais, Brazil, via a parcel transport company.

All samples received at SGS Geosol were inventoried and weighted before processing. Samples were dried at 105°C, crushed to 75% passing a 3 mm sieve, homogenized, split (jones riffle splitter), and pulverized (250 to 300 g of sample) in a steel mill to 95% passing 150 mesh.

Samples are prepared from NQ diameter drill cores (47.6mm core diameter). The sampling procedures described in this section reflect the current Standard Operational Procedures (SOP) in use by Lithium Ionic.

The sample batch composition includes 5 Quality Control Samples for every 30 regular samples. The Quality Control composition of the batches is described next:

- Coarse (Preparation) and Fine (Analytical) Blanks: 6% of the batch, or two blanks per batch, one of each type.
- Standards: 6% of the batch, or two standards per batch.
- Crushed Duplicates: 3% of the batch, or 1 sample per batch.
- Pulverized Duplicates: 3% of the batch, or 1 sample per batch.

Lithium Ionic has submitted Check Assay batches for analysis at the ALS Laboratory in Vancouver, British Columbia, Canada. This procedure is used to verify the reliability of the primary laboratory results by crosschecking it with a secondary reference laboratory.

In the QP opinion the sampling, sample preparation, security and analysis performed by Lithium Ionic and hired companies are suited for a Mineral Resource Estimation study. Quality Assurance procedures follow the industry's best practices, and Quality Control results are within industry standards, attesting to the quality of the Database information.

1.11 Data Verification

Mr. Carlos José E. Silva, an independent QP for Geology Exploration and Mineral Resource Estimate, carried out a site visit on the Bandeira Project between 13 and 14 September 2023, and the 12th of December 2023. Lithium Ionic allowed unlimited access to the Company's facilities during this time.

Mr. Leonardo Silva Santos Rocha, an independent QP for Geology Exploration and Mineral Resource Estimate, conducted an additional site visit on the Bandeira Project on the 11th of April 2024. The main purpose of this visit was to check on the additional infill drilling and geochemical data included in the current Mineral Resource Estimate. Lithium Ionic allowed unlimited access to the Company's facilities during this time.

All verified procedures related to sampling management, storage, logging, sample preparation and assay were checked, and it is considered inside acceptance limits and in compliance with mineral industry practices. Rock-type descriptions fit with the checked mineralization style.

1.12 Mineral Processing and Metallurgical Testing

The ROM from the Bandeira Project's underground mine consists of pegmatite mineralized with minerals such as spodumene, albite, quartz, muscovite, K-feldspar, cookeite, and minor amounts of petalite. The technological characterization of this material to define the process flowchart for size reduction, classification, and concentration by dense media was carried out using 2" (50.8 mm) diameter drill samples.

The technological characterization was carried out through chemical and mineralogical analyses, physical tests to determine hardness, particle size distribution in crushing tests, level of abrasiveness and metallurgical tests to understand the response of the material when subjected to the simulation of the industrial process of concentrating the mineral, spodumene.

1.13 Mineral Resources Estimates

A set of solid-grade shells for estimation domains was created using a 0.3% Li2O (%) threshold. These interpretations were then transformed into a series of implicit 3D models, aligned with the dominant strike directions of 235° and 140°. Additionally, weathering modelling was performed, considering the information provided in the logs. The model was built from implicit modelling using the Leapfrog 2023.2 software.

The MRE was constrained by a grade shell using a cut-off content of 0.5% Li2O to report the underground mining resource, this value is commonly adopted for SRP-type pegmatites in the

Lithium Valley province.

The updated MRE contains M&I resources of 23.68Mt grading 1.34% Li_2O, containing 783.0 thousand tonnes ("kt") of Lithium Carbonate Equivalent ("LCE"), the benchmark equivalent raw material used in the lithium industry, along with Inferred resources of 18.25Mt grading 1.37% Li_2O in the Inferred category, or 618.4kt of LCE (see MRE results in Table 1-2).

The MRE is based on 233 diamond drill holes comprising 50,760 metres of drilling completed between April 2022 and March 2024.

Table 1-2 – Bandeira Mineral Resource Estimates (base case cut-off grade of 0.5 % Li2O)

Source: GE21 2024

Deposit / Cut-Off Grade	Category	Resource (Mt)	Grade (% Li2O)	Contained LCE (kt)
Bandeira *(0.5% cut-off)*	Measured	3.32	1.38	113.1
	Indicated	20.36	1.33	669.6
	Measured + Indicated	23.68	1.34	783.0
	Inferred	18.25	1.37	618.4

Notes related to the Mineral Resource Estimate:
1. The spodumene pegmatite domains were modelled using composites with Li2O grades greater than
2. 0.3%
3. The mineral resource estimates were prepared following the CIM Standards and the CIM Guidelines, using geostatistical and/or classical methods, plus economic and mining parameters appropriate to the deposit.
4. Mineral Resources are not ore reserves or demonstrably economically recoverable.
5. Grades reported using dry density.
6. The effective date of the MRE is March 05, 2024.
7. The QP responsible for the MRE is the geologist Carlos Silva (MAIG #7868).
8. The MRE numbers provided have been rounded to the estimated relative precision. Values cannot be added due to rounding.
9. The MRE is delimited by Lithium Ionic Bandeira Target Claims (ANM).
10. The MRE was estimated using ordinary kriging in 12m x 12m x 4m blocks.
11. The MRE report table was produced in Leapfrog Geo software.
12. The reported MRE only contains fresh rock domains.
13. The MRE was restricted by RPEEE with grade shell using 0.5% Li2O cut-off.

1.14 Adjacent Properties

The Itinga Pegmatite Field includes the spodumene mines and deposits of CBL (Companhia Brasileira de Lítio) and Sigma Lithium.

The Lithium ore bodies exploited in the CBL's underground mine, since the early 1990's, display a closely spaced swarm of relatively narrow (6 m thick on average) but long (up to 700 m along strike) non-zoned spodumene-rich pegmatites (SRP) with on average 25 vol% of disseminated coarse-grained spodumene (Romeiro and Pedrosa-Soares, 2005).

In the Sigma Lithium properties, where several large spodumene-rich pegmatites are found (e.g., Barreiro, Murial, Xuxa; Delboni Jr. et al., 2023), an open pit mine is currently being developed on the Xuxa SRP deposit (15 m thick x 1800 m long x 500 m downdip open).

1.15 Interpretation and Conclusions

Mineral Resources were estimated and limited to the areas outlined using the Mining Rights

polygonal that comprise the Bandeira Property and the Reasonable Prospect for Eventual Economic Extraction - RPEEE.

The dataset provided by Lithium Ionic to MRE encompassed data from 233 surface diamond drill holes (totalling 50,760 meters) executed by Lithium Ionic data available from 2022 until March 5th, 2024. This Bandeira database contains 8,693 assay intervals covering 8,168 meters.

A set of solid-grade shells for estimation domains was created using a 0.3% Li2O (%) threshold. These interpretations were then transformed into a series of implicit 3D models, aligned with the dominant strike directions of 235° and 140°. Additionally, weathering modelling was performed, considering the information provided in the logs. The model was built from implicit modelling using the Leapfrog 2023.2 software.

The Ordinary Kriging (OK) estimation method was used on the Li2O% and Density variables based on the structural analysis results.

The mathematical/geostatistical criterion for classifying the resource was based on:

- The Measured Mineral Resource classification had as a reference the 50 meters of the Average Euclidean distance to sample (AvgD) used in ordinary kriging estimation with a minimum of five composites in at least three different drill holes.
- The Indicated Mineral Resource classification had as a reference the 100 meters of the Average Euclidean distance to sample (AvgD) used in ordinary kriging with a minimum of five composites in at least three different drill holes.
- The Inferred Mineral Resource classification is all remaining estimated blocks.

1.16 Recommendations

GE21 proposes the following recommendations for the continuous improvement of the Mineral Resource estimate:

- A 50x50m infill drilling program in the domain of the indicated resource classification that will focus on resource delineation improvement.
- A 100x100m infill drilling program in the domain of the inferred resource classification that will focus on resource delineation improvement.
- A density campaign to measure the density of drill hole cores by drying the samples in an oven, as well as waterproofing them. Compare the results with the methodology used in the current project procedure to check whether there is a bias in the results.
- Conduct an on-site density survey in the weathered zone.
- An updated mineral resource assessment is currently underway through the ongoing infill drilling program.

- Detail Geotechnical analysis, including a geotechnical-oriented diamond drilling campaign and logging, including sampling collecting for tensile, compressive and shear strength tests.
- Perform supplementary geotechnical investigations of planned infrastructure sites including at waste pile areas; supplementary geochemical tests (ARD); large-scale waste rock and tailings co-disposal stockpile field test.
- To implement the hydrological and hydrogeological studies for the project's next phases.

2 INTRODUCTION

GE21 Consultoria Mineral Ltda. (“GE21”) was engaged by Lithium Ionic Corp. to prepare an Independent Technical Report (“ITR”) containing a NI 43-101 Technical Report (The “Report”) on Lithium Ionic’s Bandeira deposit located in Minas Gerais State, Brazil (“Project”). This report titled “NI 43-101 Technical Report – Mineral Resource Update on Bandeira Project, Araçuaí and Itinga, Minas Gerais State, Brazil” outlines all relevant data about the Bandeira Project (“The Project”). They are technical information and data related to the drilling program and the status of the current Lithium Mineral Resources contained in the spodumene-bearing pegmatites.

The Project is located between Araçuaí and Itinga in Brazil’s “Lithium Valley” - a complex rock lithium district. The Update Mineral Resources (MRE) includes only the Bandeira lithium deposits.

Lithium Ionic Corp. is headquartered in Toronto, Ontario (36 Lombard Street, Floor 4, Toronto, ON, Canada, M5C 2X3) with management offices in Nova Lima (Alameda Oscar Niemeyer, 1033 – sls 133/134 Vila da Serra – Nova Lima – Minas Gerais- CEP 34006-065 – Brazil) and Araçuaí (Recife Street 96, Araçuaí, Minas Gerais – CEP 39600-000, Brazil). It is a publicly traded Canadian exploration and development company listed on the TSX Venture Exchange (“TSXV”). The Company is acquiring, exploring, and developing mineral properties, primarily focusing on exploring in Brazil. Exploration is conducted through the Company’s wholly owned Brazilian subsidiary, MGLIT Empreendimentos Ltda. (“MGLIT”) and Neolit Minerals Participações Ltda.

(“Neolit”).

2.1 Terms of Reference

This Report and the estimates herein comply with the requirements of the Canadian Securities Administrators’ National Instrument 43-101 – Standard of Disclosure for Mineral Projects (“NI 43101”) and Form 43-101F1 – Technical Report (“Form 43-101F1”).

2.2 Units and Currency

The International metric system was used to compile this report. The main currency used was the US dollar, and in some cases, the Reais (Brazil) or Canadian dollar, which is always indicated in these cases.

2.3 Effective Date

The effective date of this report is March 5th, 2024, and the information in this report, including the reported resource estimates, are all contained within a conceptual underground mineable MRE. The Report supports the disclosure by Lithium Ionic in the news release outlining the current MRE dated April 12, 2024.

2.4 Visits to the Project

The MGLIT Bandeira Project site visit was conducted by Mr. Carlos José Evangelista Silva between the 13th and 14th of September 2023 and the 12th of December 2023, and Mr. Leonardo Silva Santos Rocha on the 11th of April 2024.

During the site visit, the following activities were carried out:

- Data review, sampling, protocols, and procedures for QA QC of samples.
- Data collection procedures and review of the geological record procedure.
- Review of core sampling procedures and data management.
- Presentations and overview of how geological interpretation, modelling, and resource estimation are carried out by the company's in-house experts.

2.5 Qualified Experts

This technical report was prepared by GE21 and received contributions from Lithium Ionic (Table 2-1).

The QP responsible for the Mineral Resource Estimation, carried out at the Mineral Resources Update, is Geologist Carlos José Evangelista Silva, who has more than 15 years of relevant experience in Geology Exploration and Mineral Resource Estimation. Mr. Silva is a full-time employee of GE21 Consultoria Mineral. He has considerable experience dealing with commodities like iron ore, lithium, and gold. Mr. Silva is a member of the Australian Institute of Geoscientists (MAIG).

The QP responsible for the Mineral Resources Update site visit and QAQC procedures and results is Geologist Leonardo Silva Santos Rocha, who has more than 11 years of relevant experience in Geology Exploration, QA/QC procedures, and Mineral Resource Estimation. Mr. Rocha is a full-time employee of GE21 Consultoria Mineral. He has considerable experience dealing with iron ore, lithium, and gold commodities. Mr. Rocha is a member of the Australian Institute of Geoscientists (MAIG #7623).

The QP responsible for this report’s content on setion related to Mineral Processing and Metallurgical Tests, is Paulo Bergman (FAusIMM, B.Sc.), a Mining Engineer of GE21 Consultoria Mineral, who has more than 40 years of experience in mining projects. Mr. Bergman is a Fellow of the Australasian Institute of Mining and Metallurgy (FAusIMM).

Porfirio Cabaleiro Rodriguez (FAIG, B.Sc.) is the peer reviewer of this technical report. Mr. Rodriguez has at least 45 years of experience in all aspects of mining project evaluation, from initial exploration to bankable feasibility studies. He is a senior mining engineer and managing director of GE21 Mineral Consulting.

Each of the authors of this report has the required qualifications, experience, competence, and independence to be considered a "Qualified Person," as defined by NI 43-101.

Neither GE21 nor the authors of this report have or have had, any material interest vested in Lithium Ionic Corp. or any of its related entities. GE21's relationship with Lithium Ionic is strictly professional, consistent with that held between a client and an independent consultant. This report was prepared in exchange for payment based on fees stipulated in a commercial agreement. Payment of these fees is not dependent on the results of this Report.

Table 2-1 – Presents the QPs Matrix of Responsibility

Source: GE21 2024

Company	Professional	Site Visit	Responsibility
GE21	Carlos José Evangelista Silva	between the 13th and 14th of September 2023 and the 12th of December 2023	Items 2 to 10, 14 and partial responsibility on 1, 11,12, 25, 26 and 27.
GE21	Leonardo Silva Santos Rocha	11th of April 2024	Items 11 to 12 and partial responsibility on 1, 25, 26 and 27.
GE21	Paulo Bergman	-	Items 13, and partial responsibility 1, 25, 26 and 27.
GE21	Porfirio Cabaleiro Rodriguez	-	Report Peer Reviewer

Notes:
All QPs are responsible for the corresponding sections within Items related to the preceding Items of this Technical Report.

3 RELIANCE ON OTHER EXPERTS

3.1 Mining Law

The QPs did not assess the legal situation of the mining rights and the status of mining environmental licensing for this project. The Legal and Mining Law Discipline informed the professionals of the good standing of the asset to carry out all the necessary studies to prepare each of the chapters that make up the Project's Economic and Financial Feasibility Study.

This information is described in Chapter 4 and is mainly used to estimate resources and conduct a project financial analysis.

4 PROPERTY DESCRIPTION AND LOCATION

The Project is situated in the northeastern region of Minas Gerais State, Brazil, within the Jequitinhonha Valley area, approximately 600 km northeast of Belo Horizonte. It is positioned roughly 75 km south of the town of Salinas (population: approx. 42,000) and about 25 km east of Araçuaí (population: approx. 40,000), accessible via major paved roads (Figure 4-1).

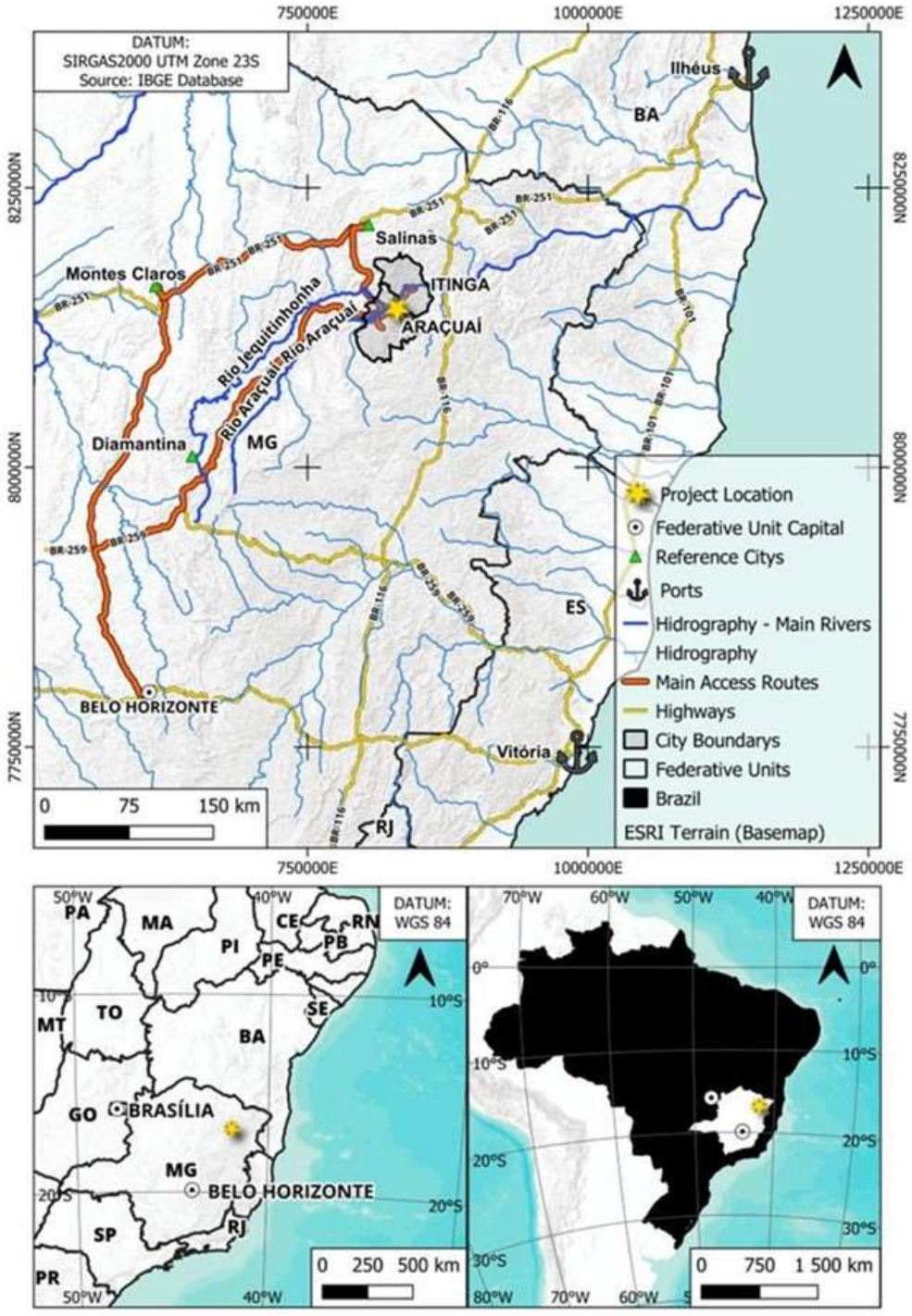

Figure 4-1 – Project Location

Source: GE21 2024

The area of mining right number 832439/2009 is located on the border of the municipalities of Araçuaí and Itinga, in the valley of the Piauí River. This mining right was requested from the National Mining Agency in 2016. The Piauí River, which cuts through the western portion of the Lithium Ionic (MGLIT) area, serves as the border between the municipalities of Araçuaí and Itinga. The area of the Bandeira project therefore covers parts of both municipalities (Figure 4-2).

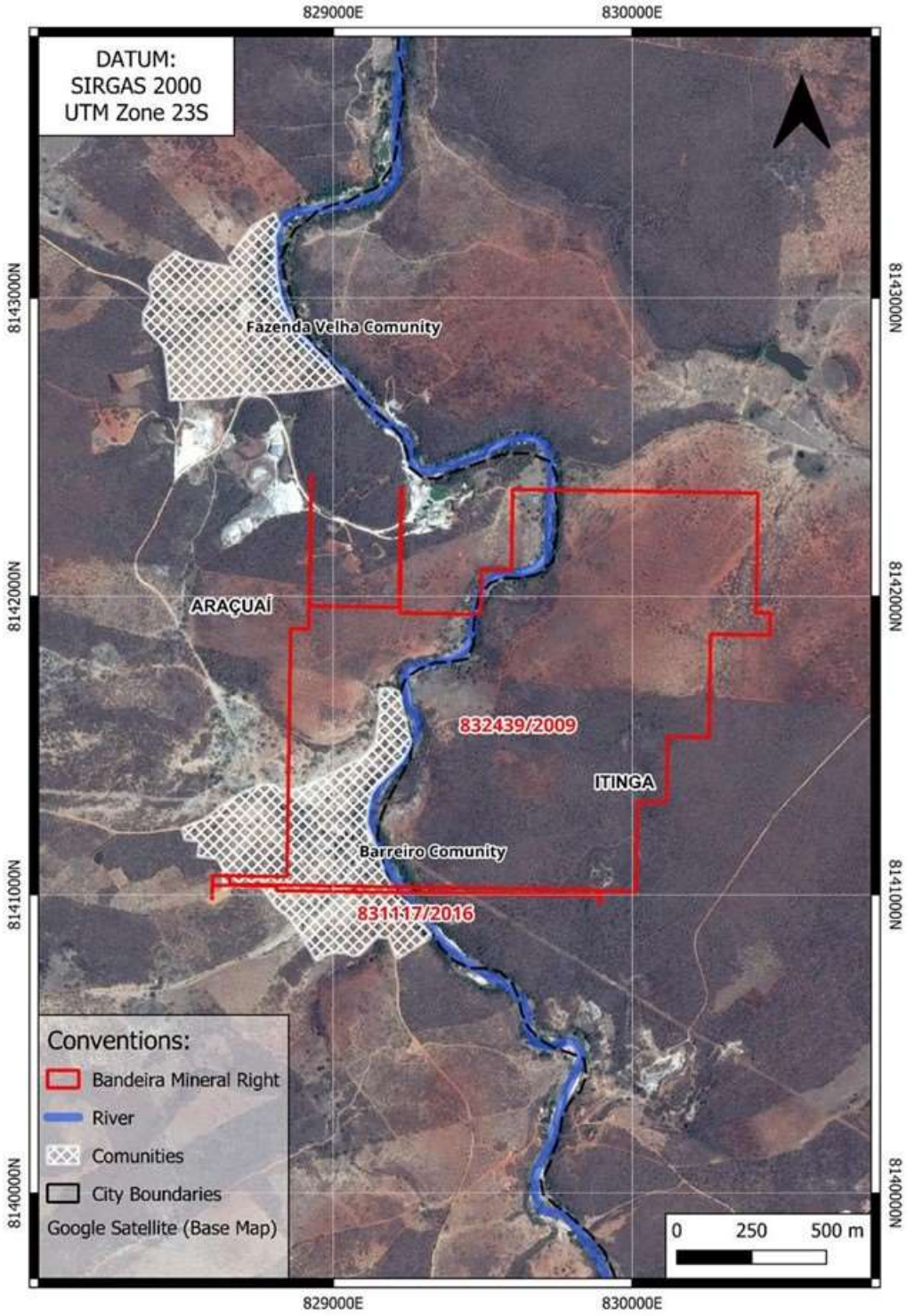

Figure 4-2 – Mining Rights of the Bandeira Project

Source: GE21 2024

4.1 History of the Process and Legal Status of ANM Case n° 832.439/2009

The exploration right to the area which is covered by the ANM process No. 832.439/2009 was requested on 10/22/2009 by FALCON METAIS LTDA for the exploration of Lithium minerals in an area covered by the municipalities of Itinga and Araçuaí, state of Minas Gerais.

On 05/06/2014, after the study was rectified, permit No. 3785/2014 was published, authorizing the applicant to research the substance for a period of 3 (three) years.

The start of the research was promptly communicated on 05/07/2014. The annual fees per hectare, referring to the first permit validity period, were duly paid.

On 03/03/2017, Falcon Metais submitted a Partial Research Report with a request for an extension of the license, and the publication of the approval took place on 04/28/2020, extending the term of validity of the license for 3 (three) years.

The holder again communicated the start of the research work and requested the installment payment of the TAH due in July/2020. This was granted by the ANM.

On 12/28/2020, a request for the Total Assignment of Mining Rights from Falcon Metais Ltda to MGLIT Empreendimentos Ltda. was filed. And, due to the assignment now being effected, a requirement was published for the assignee and current holder of the process, MGLIT EMPREENDIMENTOS LTDA and presented a Term of Assumption of Debt referring to the 2 (two) current installments of TAH. The requirement was fulfilled on 05/04/2021.

Subsequently, the TAHs of July 2021 and 2022 were paid, and the installments were considered paid on 02/02/2022.

The expiration date of the research permit was changed from 04/28/2023 to 09/30/2024 by ANM resolution no. 76/2021, which determined the suspension of material and procedural deadlines due to the state of public calamity resulting from the COVID-19 pandemic.

The original essential data of the area in question is below, according to the website, on May 6, 2024, of the ANM's own Mining Registry (Figure 4-3).

With an area of 156.77 hectares, the area of the DNPM 832.439/2009 process has its envelope defined according to the data below (Figure 4-4):

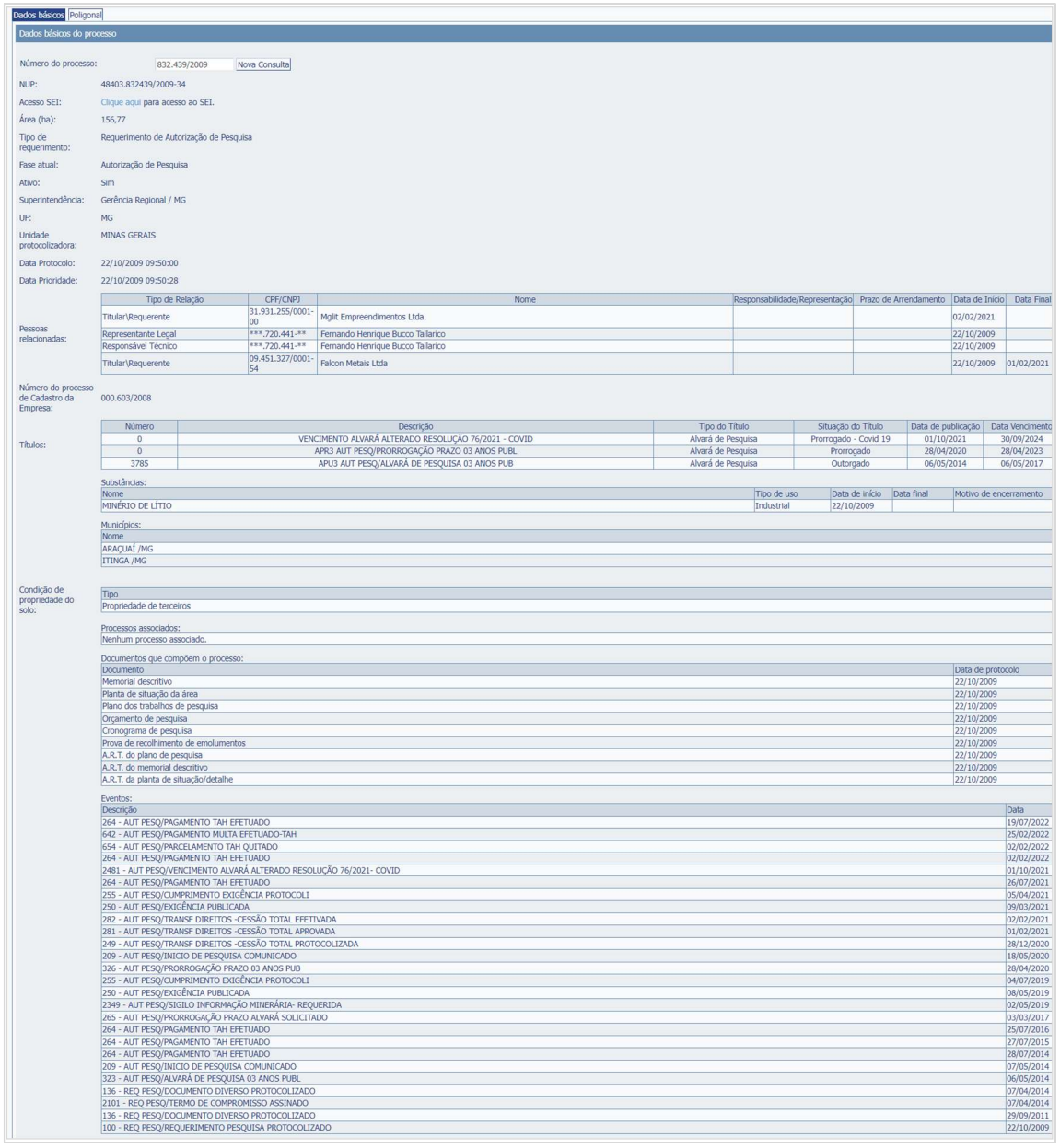

Dados básicos | Poligonal

Dados básicos do processo

Número do processo: 832.439/2009 [Nova Consulta]

NUP: 48403.832439/2009-34

Acesso SEI: Clique aqui para acesso ao SEI.

Área (ha): 156,77

Tipo de requerimento: Requerimento de Autorização de Pesquisa

Fase atual: Autorização de Pesquisa

Ativo: Sim

Superintendência: Gerência Regional / MG

UF: MG

Unidade protocolizadora: MINAS GERAIS

Data Protocolo: 22/10/2009 09:50:00

Data Prioridade: 22/10/2009 09:50:28

Pessoas relacionadas:

Tipo de Relação	CPF/CNPJ	Nome	Responsabilidade/Representação	Prazo de Arrendamento	Data de Início	Data Final
Titular\Requerente	31.931.255/0001-00	Mglit Empreendimentos Ltda.			02/02/2021	
Representante Legal	***.720.441-**	Fernando Henrique Bucco Tallarico			22/10/2009	
Responsável Técnico	***.720.441-**	Fernando Henrique Bucco Tallarico			22/10/2009	
Titular\Requerente	09.451.327/0001-54	Falcon Metais Ltda			22/10/2009	01/02/2021

Número do processo de Cadastro da Empresa: 000.603/2008

Títulos:

Número	Descrição	Tipo do Título	Situação do Título	Data de publicação	Data Vencimento
0	VENCIMENTO ALVARÁ ALTERADO RESOLUÇÃO 76/2021 - COVID	Alvará de Pesquisa	Prorrogado - Covid 19	01/10/2021	30/09/2024
0	APR3 AUT PESQ/PRORROGAÇÃO PRAZO 03 ANOS PUBL	Alvará de Pesquisa	Prorrogado	28/04/2020	28/04/2023
3785	APU3 AUT PESQ/ALVARÁ DE PESQUISA 03 ANOS PUB	Alvará de Pesquisa	Outorgado	06/05/2014	06/05/2017

Substâncias:

Nome	Tipo de uso	Data de início	Data final	Motivo de encerramento
MINÉRIO DE LÍTIO	Industrial	22/10/2009		

Municípios:

Nome
ARAÇUAÍ /MG
ITINGA /MG

Condição de propriedade do solo:

Tipo
Propriedade de terceiros

Processos associados:

Nenhum processo associado.

Documentos que compõem o processo:

Documento	Data de protocolo
Memorial descritivo	22/10/2009
Planta de situação da área	22/10/2009
Plano dos trabalhos de pesquisa	22/10/2009
Orçamento de pesquisa	22/10/2009
Cronograma de pesquisa	22/10/2009
Prova de recolhimento de emolumentos	22/10/2009
A.R.T. do plano de pesquisa	22/10/2009
A.R.T. do memorial descritivo	22/10/2009
A.R.T. da planta de situação/detalhe	22/10/2009

Eventos:

Descrição	Data
264 - AUT PESQ/PAGAMENTO TAH EFETUADO	19/07/2022
642 - AUT PESQ/PAGAMENTO MULTA EFETUADO-TAH	25/02/2022
654 - AUT PESQ/PARCELAMENTO TAH QUITADO	02/02/2022
264 - AUT PESQ/PAGAMENTO TAH EFETUADO	02/02/2022
2481 - AUT PESQ/VENCIMENTO ALVARÁ ALTERADO RESOLUÇÃO 76/2021- COVID	01/10/2021
264 - AUT PESQ/PAGAMENTO TAH EFETUADO	26/07/2021
255 - AUT PESQ/CUMPRIMENTO EXIGÊNCIA PROTOCOLI	05/04/2021
250 - AUT PESQ/EXIGÊNCIA PUBLICADA	09/03/2021
282 - AUT PESQ/TRANSF DIREITOS -CESSÃO TOTAL EFETIVADA	02/02/2021
281 - AUT PESQ/TRANSF DIREITOS -CESSÃO TOTAL APROVADA	01/02/2021
249 - AUT PESQ/TRANSF DIREITOS -CESSÃO TOTAL PROTOCOLIZADA	28/12/2020
209 - AUT PESQ/INICIO DE PESQUISA COMUNICADO	18/05/2020
326 - AUT PESQ/PRORROGAÇÃO PRAZO 03 ANOS PUB	28/04/2020
255 - AUT PESQ/CUMPRIMENTO EXIGÊNCIA PROTOCOLI	04/07/2019
250 - AUT PESQ/EXIGÊNCIA PUBLICADA	08/05/2019
2349 - AUT PESQ/SIGILO INFORMAÇÃO MINERÁRIA- REQUERIDA	02/05/2019
265 - AUT PESQ/PRORROGAÇÃO PRAZO ALVARÁ SOLICITADO	03/03/2017
264 - AUT PESQ/PAGAMENTO TAH EFETUADO	25/07/2016
264 - AUT PESQ/PAGAMENTO TAH EFETUADO	27/07/2015
264 - AUT PESQ/PAGAMENTO TAH EFETUADO	28/07/2014
209 - AUT PESQ/INICIO DE PESQUISA COMUNICADO	07/05/2014
323 - AUT PESQ/ALVARÁ DE PESQUISA 03 ANOS PUBL	06/05/2014
136 - REQ PESQ/DOCUMENTO DIVERSO PROTOCOLIZADO	07/04/2014
2101 - REQ PESQ/TERMO DE COMPROMISSO ASSINADO	07/04/2014
136 - REQ PESQ/DOCUMENTO DIVERSO PROTOCOLIZADO	29/09/2011
100 - REQ PESQ/REQUERIMENTO PESQUISA PROTOCOLIZADO	22/10/2009

Figure 4-3 – Consult Webpage, on May 6, 2024, the History and Situation on the Official Website of the Brazilian Government for Mineral Rights 832.439/2009

Source: https://sistemas.anm.gov.br/SCM/site/admin/dadosProcesso.aspx

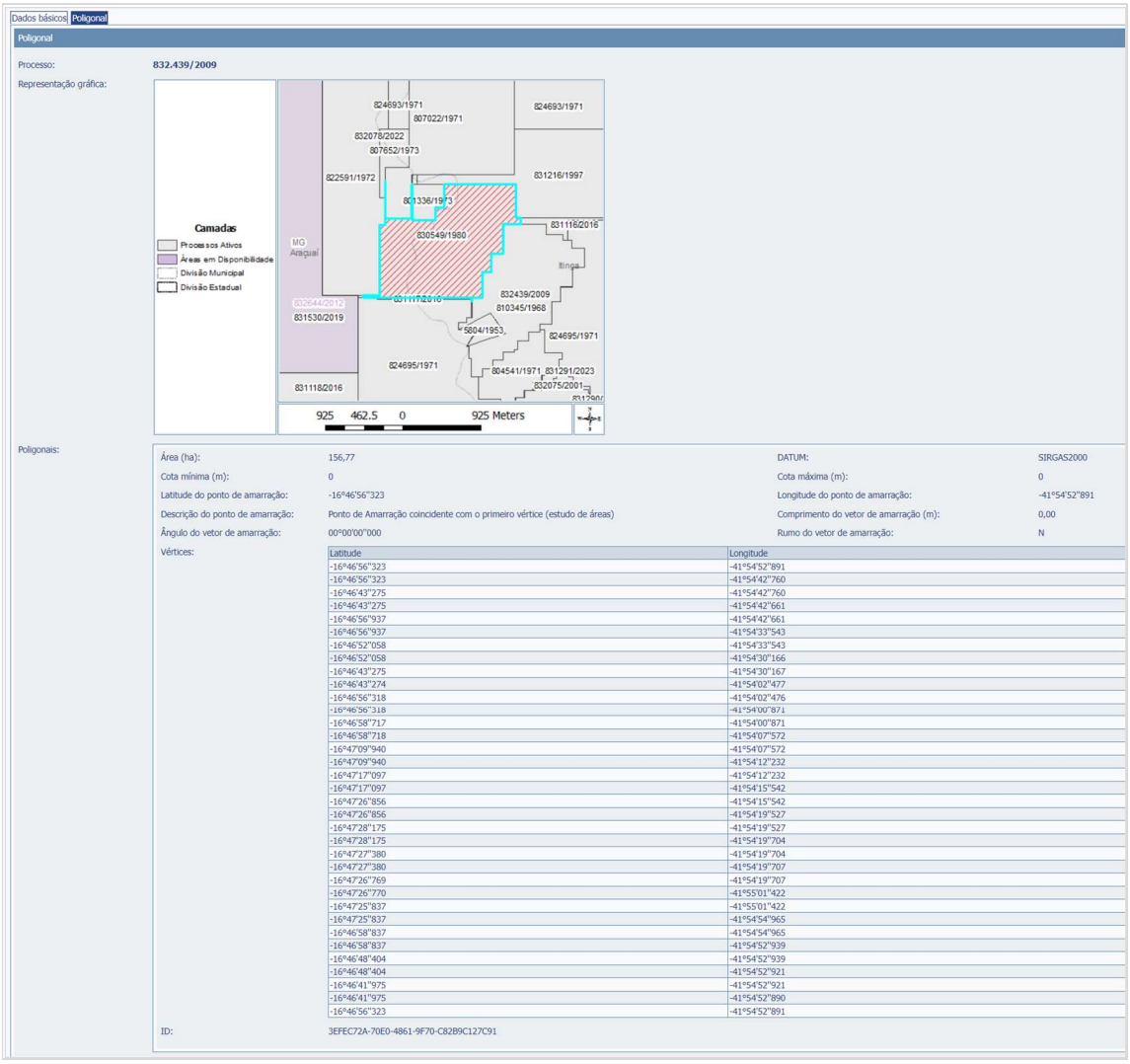

Latitude	Longitude
-16°46'56"323	-41°54'52"891
-16°46'56"323	-41°54'42"760
-16°46'43"275	-41°54'42"760
-16°46'43"275	-41°54'42"661
-16°46'56"937	-41°54'42"661
-16°46'56"937	-41°54'33"543
-16°46'52"058	-41°54'33"543
-16°46'52"058	-41°54'30"166
-16°46'43"275	-41°54'30"167
-16°46'43"274	-41°54'02"477
-16°46'56"318	-41°54'02"476
-16°46'56"318	-41°54'00"871
-16°46'58"717	-41°54'00"871
-16°46'58"718	-41°54'07"572
-16°47'09"940	-41°54'07"572
-16°47'09"940	-41°54'12"232
-16°47'17"097	-41°54'12"232
-16°47'17"097	-41°54'15"542
-16°47'26"856	-41°54'15"542
-16°47'26"856	-41°54'19"527
-16°47'28"175	-41°54'19"527
-16°47'28"175	-41°54'19"704
-16°47'27"380	-41°54'19"704
-16°47'27"380	-41°54'19"707
-16°47'26"769	-41°54'19"707
-16°47'26"770	-41°55'01"422
-16°47'25"837	-41°55'01"422
-16°47'25"837	-41°54'54"965
-16°46'58"837	-41°54'54"965
-16°46'58"837	-41°54'52"939
-16°46'48"404	-41°54'52"939
-16°46'48"404	-41°54'52"921
-16°46'41"975	-41°54'52"921
-16°46'41"975	-41°54'52"890
-16°46'56"323	-41°54'52"891

Figure 4-4 – Consult the Polygonal Webpage, on May 6, 2024, on the Brazilian Government's Official Website for Mineral Rights 832.439/2009

Source: https://sistemas.anm.gov.br/SCM/site/admin/dadosProcesso.aspx

5 ACCESSIBILITY, CLIMATE, LOCAL RESOURCES, INFRASTRUCTURE, AND PHYSIOGRAPHY

5.1 Accessibility

The Project is in northeastern Minas Gerais State, in the Municipalities of Itinga and Araçuaí, approximately 75 km south of Salinas and 600 km northeast of Belo Horizonte.

A public and private road network serves the Project well because of its proximity to National Highway BR-251 and BR-116. The Project is accessible year-round by a network of arterial and backcountry service roads.

National Highway BR-116 and BR-262 access the Port of Vitoria in Espirito Santo, approximately 850 km from the Project site. This port could represent a potential export exit for spodumene production from the Project. The National Highways BR-116 and BR-415 access

Ilhéus Port, which is 540 km from the project, they are an option as a shipping port (Figure 4-1).

5.2 Climate

The region is characterized by a hot, dry and semi-arid climate. The average temperature is 24.5ºC with an average annual rainfall of 750mm. The driest period of the year is June, and the wettest period is November. There is no harsh cold season. Exploration and mining activities can take place throughout the year.

The hot season lasts for 1.7 months, from September 10 to October 31, with an average daily high temperature above 91°F. The hottest month of the year in Araçuaí is February, with an average high of 91°F and low of 71°F.

The cool season lasts for 2.5 months, from May 26 to August 10, with an average daily high temperature below 86°F. The coldest month of the year in Araçuaí is July, with an average low of 62°F and high of 85°F. The weather conditions in Araçuaí/MG are detailed in the figures below (Figure 5-1 and Figure 5-2).

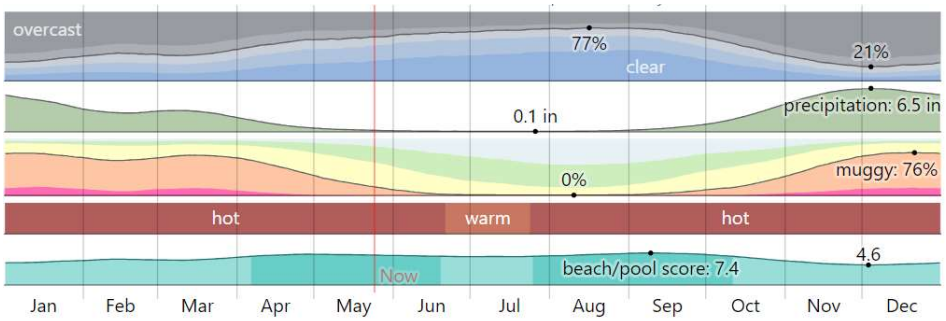

Figure 5-1 – Weather Conditions in Araçuaí/MG

Source: https://weatherspark.com/y/30709/Average-Weather-in-Ara%C3%A7ua%C3%AD-Minas-Gerais-Brazil-Year-Round

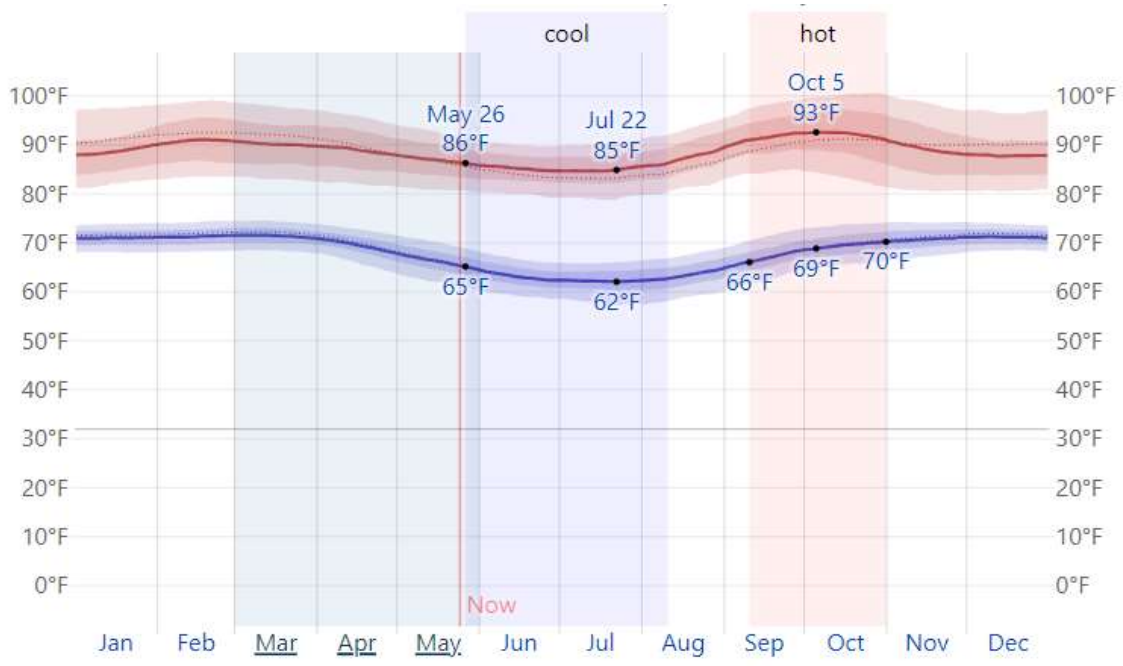

The daily average high (red line) and low (blue line) temperature, with 25th to 75th and 10th to 90th percentile bands. The thin dotted lines are the corresponding average perceived temperatures.

Average	Jan	Feb	Mar	Apr	May	Jun	Jul	Aug	Sep	Oct	Nov	Dec
High	89°F	91°F	90°F	89°F	87°F	85°F	85°F	87°F	91°F	92°F	89°F	88°F
Temp.	79°F	80°F	80°F	78°F	75°F	73°F	72°F	74°F	78°F	80°F	79°F	79°F
Low	71°F	71°F	71°F	70°F	66°F	63°F	62°F	63°F	67°F	69°F	71°F	71°F

Figure 5-2 – Maximum and Minimum Temperatures in Araçuaí/MG

Source: https://weatherspark.com/y/30709/Average-Weather-in-Ara%C3%A7ua%C3%AD-Minas-Gerais-Brazil-Year-Round

5.3 Local Resources and Infrastructure

Regarding the Bandeira Project, the largest and closest cities are Itinga and Araçuaí, with populations of 14,000 and 40,000 inhabitants, respectively. Araçuaí is served by a small airport and large commercial mobile phone networks.

In 2021, the average monthly wage in Araçuaí was 170% of the minimum wage. The proportion of unemployed persons in relation to the total population was 12.5%.

Araçuaí has 38.3% households with adequate sanitary sewage, 53.6% urban households on public roads with trees and 5.3% urban households with adequate urbanization (presence of culverts, sidewalks, paving and curbs).

The nearest medium-sized airport with regular commercial flights is located in Vitória da Conquista (BA), about 297 km north of Araçuaí, via BR-367 and BR-116. Another medium-sized airport is located in Montes Claros, 322 km from Araçuaí, accessed via federal highways BR-342 and BR-251. The nearest small airport, with regular commercial flights since December 2023, is

located in Salinas, around 110 km north of Araçuaí via BR-342.

5.4 Physiography

The topography of the area where the Project will be implemented has low hills, ravines and wide valleys, with elevation differences of less than 100 meters.

The Project area is characterized by thick thorn scrub and trees of medium height - except where it has been cleared for agriculture. The natural vegetation on the hilltops is typical of savannah grassland.

The Project occupies areas on both banks of the Piauí River, which will provide raw water to meet the demands of the mine, processing and concentration plants, and mining facilities, as shown in the aerial view in Figure 5-3.

Figure 5-3 – Physiography on Project

Source: Lithium Ionic 2024

6 HISTORY

6.1 History of Lithium

The history of lithium has an important relationship with Brazil. Between 1790 and 1800, José Bonifácio de Andrada e Silva, a native of the city of Santos, state of São Paulo, Brazilian naturalist, politician and scientist, was the one who first characterized and named spodumene and petalite, both anhydrous aluminum and lithium silicates, contained in samples from Sweden (ref. 1).

Most likely, prospectors already knew about lithium minerals in the Middle Jequitinhonha since the 18th century, although they did not know how to identify or value them. The occupation of the region was based on the discoveries of rock salt in the region of Salinas, and of gold in the Araçuaí River Valley from 1727 onwards, reaching the outskirts of Araçuaí in 1728. Since the early days of the mining of "chrysolite" (chrysoberyl) in the valley of the Piauí River, spodumene crystals have earned the nickname "rotten chrysolite" and "cambalacho", due to their similarity to chrysoberyl (cf. Sá, 1977 – ref. 2), as can still be heard today in conversations in the mines.

In 1823, Spix & Martius (1823) arrived at the headwaters of the Calhauzinho and Piauí Rivers in search of the sources of semi-precious stones, particularly chrysoberyl ("chrysolite"), which were already mined there, and described a "white granite with little mica, but with a lot of black tourmaline" (i.e., pegmatite).

In 1882, the first report of the occurrence of "trifana" (spodumene) in the Middle Jequitinhonha was due to Costa Sena (ref. 4). He identified "Andalusite, cimophana (chrysoberyl) and trifana, with sharp edges, in sands and gravel of the stream in the valley of the Piauí River, concluding that the primary deposits of these minerals would be located there".

Occurrences of spodumene were mentioned in the "Compendium of the Minerals of Brazil" (Ferraz, 1928 – ref. 5), among other pegmatite minerals. During the Second World War until the end of the Cold War, industrial beryl was widely exploited, starting in the region of Salinas and extending to the valleys of the Piauí and Jenipapo rivers (cf. Sá, 1977).

In Brazil, the production of lithium minerals began in the 1940s with the exploration of amblygonite (lithium phosphate) in the states of Ceará, Paraíba and Minas Gerais, to supply the chemical processing unit of Orquima (later Nuclemon), located in the neighbourhood of Santo Amaro, city of São Paulo. This lithium compound production unit operated until the late 1980s when it ceased its operation due to difficulties in the supply of raw materials and financial and environmental issues.

On pegmatites and the production of lithium minerals in the Jequitinhonha Valley, Haroldo de Sá, in his doctoral thesis, presented in 1977 at IG-USP, described the following:

- "In 1950, the farmer Avelar Pereira, who was exploiting beryl in the Jenipapo Mine, found in the place called Fumal, to the right of the Middle Piauí, a very dark and very heavy material, which was analyzed by Mr. Khalil Afgouni and found that it was cassiterite. At the same time, it was also known that amblygonite had existed in some pegmatites in the Piauí valley."
- "The cassiterite found near the Piauí stream attracted the attention of the companies Estanífera do Brasil and Produco (a subsidiary of Orquima) that settled in the region around 1952, and then began research and exploitation work on an industrial scale. At that time, the most important pegmatite bodies were the Fumal, Urubu and Generosa mines, the first two producing cassiterite and the last producing amblygonite."
- "Glycon de Paiva, in 1957, identified lepidolite in the Urubu and Generosa mines, and the first tons of this ore were exported to Japan in 1959."
- "At the Cachoeira mine (which is currently under CBL's mining right) spodumene production began in the late 1960s, to supply the demand of the domestic market."
- "Petalite, abundant in the region, was called "white slag" by the miners and was often confused with feldspar. Its correct identification took place at the end of the 1960s, and it soon went into production for export purposes."
- "Companhia Produco withdrew from the region in 1958, while Companhia Estanífera do Brasil maintained its activities until 1972, being succeeded by Companhia Arqueana de Minérios e Metais Ltda, which holds the mining and research rights in most of the area that comprises the valleys of the Piauí River, Jenipapo River and Tesouras River. This Company has today (i.e., in 1977) more than twenty pegmatite bodies producing petalite, spodumene, amblygonite, lepidolite, beryl, cassiterite and reduced quantities of tantalite-columbite, employing about a hundred workers. The mines are semi-mechanized and some of them have mechanized development." (cf. Sá, 1977.)

Khalil Afgouni & Haroldo de Sá published, in 1978, a article on lithium in the journal Energy (vol. 3, Pergamon Press, see ref. 6), entitled "Lithium Ore in Brazil", in which they state, at the end of the abstract of the work, that: “Another new use is in lithium batteries for electric cars and, if this application becomes a reality, Brazil will be a big consumer, ranking at the same level as the most developed countries in the world with the advantage of being one of the few countries capable of producing its own raw material.”

Correia-Neves, Pedrosa-Soares & Marciano published, in the Brazilian Journal of Geosciences (1986, ref. 7), a synthesis of studies on the Eastern Pegmatite Province of Brazil, applying, for the first time, petrological and metallogenetic concepts still current in the approach to litiniferous pegmatites, with emphasis, in particular, on the metallogenetic specialization of the Itinga Pegmatite Field for the production of spodumene and petalite, compared to other more lithium-poor pegmatite populations in the provinc

In 1985, Companhia Brasileira de Lithium (CBL) acquired from Companhia Arqueana de Minérios

e Metais Ltda, the mining rights and assets of the areas that include the Cachoeira Mine and its surroundings, having started producing spodumene concentrate in the early 1990s. In 1991, CBL acquired Nuclemon's chemical unit, which was paralyzed, and transferred it to Divisa Alegre, in the state of Minas Gerais, for processing spodumene concentrate. The first systematic study of the structural control of pegmatitic bodies and the variation of spodumene granulation at the Cachoeira Mine (CBL) was presented in the master's thesis of Júlio Romeiro (1998, IGC-UFMG).

In 2012, Sigma Lithium acquired several mining rights from Arqueana de Minérios e Metais Ltda, starting an exploration work to produce spodumene concentrate for export. In the second quarter of 2023, the concentration unit's commercial operation began to produce 270,000 tpa of spodumene, treating approximately 1.5 million tpa of ore from the Xuxa mine.

To encourage the development of the lithium production chain, the Brazilian government created the Lithium Decree, which was in force from 1992 until 2022.

Currently, in Brazil, there are three producers of spodumene concentrate: CBL, AMG, and Sigma Lithium, all of which are located in Minas Gerais. CBL is the only one that produces lithium compounds, such as carbonate and hydroxide.

6.2 Historical Exploration

All works in the Bandeira target started in 2022, and there is no historical exploration data.

6.3 Historical Mineral Resource Estimates

6.3.1 MRE August 10, 2023

SGS Geological Services (SGS), on behalf of Lithium Ionic Corp., prepared an MRE released on August 10, 2023; the effective date of this MRE was June 24, 2023 (Table 6-1).

This MRE includes an in-pit and an underground (below pit) Mineral Resources (estimated from the bottom of the pit). Highlights of the Mineral Resource Estimate are as follows:

The Bandeira in-pit Mineral Resource includes, at a base case cut-off grade of 0.5 % Li2O, 1.14 Mt grade 1.43 % Li2O, in the Measured category, 3.1 Mt grade 1.33 % Li2O, in the Indicated category and 5.9 Mt grade 1.40 % Li2O, in the Inferred category.

The Bandeira below-pit Mineral Resource includes, at a base case cut-off grade of 0.8 % Li2O, 3.0 Kt grade 1.1 % Li2O, in the Measured category, 0.35 Mt grade 1.26 % Li2O, in the Indicated category and 5.5 Mt grade 1.147 % Li2O, in the Inferred category.

Table 6-1 – Itinga Property; Bandeira In-Pit and Underground (below-pit) Mineral Resource Estimate, June 24, 2023

Source: SGS-Lithium Ionic 2023 - https://lithiumionic.com/investors/reports-filings/

Deposit/Cut-Off Grade	Category	Resource (Mt)	Grade (% Li2O)	Contained LCE (t)
Bandeira Open-Pit (0.5% Li_2O)	Measured	1.14	1.43	40,000
	Indicated	3.11	1.33	102,000
	Measured + Indicated	**4.24**	**1.36**	**142,000**
	Inferred	**5.92**	**1.40**	**205,000**
Bandeira Underground (0.8% Li_2O)	Measured	0.003	1.10	0
	Indicated	0.35	1.26	11,000
	Measured + Indicated	**0.36**	**1.26**	**11,000**
	Inferred	**5.53**	**1.47**	**201,000**
TOTAL	Measured	1,14	1.43	40,000
	Indicated	3,46	1.32	113,000
	Measured + Indicated	**4,60**	**1.35**	**153,000**
	Inferred	**11.45**	**1.43**	**406,000**

Notes related to the Mineral Resource Estimate:

1. The effective date of the MRE is June 24, 2023.
2. The classification of the current Mineral Resource Estimate into Measured, Indicated and Inferred is consistent with the current 2014 CIM Definition Standards - For Mineral Resources and Mineral Reserves.
3. All figures are rounded to reflect the relative accuracy of the estimate, and numbers may not be added due to rounding.
4. All Resources are constrained by continuous 3D wireframe models (constraining volumes) and are considered to have reasonable prospects for eventual economic extraction.
5. Mineral resources which are not mineral reserves do not have demonstrated economic viability. An Inferred Mineral Resource has a lower level of confidence than that applying to an Indicated Mineral Resource and must not be converted to a Mineral Reserve. It is reasonably expected that the majority of Inferred Mineral Resources could be upgraded to Indicated Mineral Resources with continued exploration.
6. The pit optimization results are used solely to test the “reasonable prospects for economic extraction” by an open pit and do not represent an attempt to estimate mineral reserves. There are no mineral reserves on the Project. The results are used as a guide to assist in the preparation of a Mineral Resource statement and to select an appropriate resource reporting cut-off grade.
7. It is envisioned that parts of the Bandeira deposit may be mined using open pit mining methods. In-pit mineral resources are reported at a cut-off grade of 0.5% Li2O within a conceptual pit shell,
8. The results from the pit optimization are used solely for the purpose of testing the “reasonable prospects for economic extraction” by an open pit and do not represent an attempt to estimate mineral reserves. There are no mineral reserves on the Property. The results are used as a guide to assist in the preparation of a Mineral Resource statement and to select an appropriate resource reporting cut-off grade.
9. It is envisioned that parts of the Bandeira deposit may be mined using underground mining methods. Underground (below-pit) Mineral Resources are estimated from the bottom of the pit (base of transition mineralization) and are reported at a base case cut-off grade of 0.8% Li2O. The underground Mineral Resource grade blocks were quantified above the base case cut-off grade, below the constraining pit shell and within the constraining mineralized wireframes.
10. Based on the size, shape, location and orientation of the Bandeira and Outro Lado deposit, it is envisioned that the deposit may be mined using low-cost underground bulk mining methods.
11. Bulk density values were determined based on physical test work from each deposit model and waste model.

6.3.2 PEA October 19, 2023

GE21 Consultoria (GE21), on behalf of Lithium Ionic Corp., prepared a Preliminary Economic Assessment Independent Technical Report (PEA) released on October 19, 2023, based on an updated MRE for the Bandeira Project summarized in Table 6-2. The Bandeira MRE contains

Measured and Indicated ("M&I") Resources of 13.72Mt grading 1.40% Li2O, containing 474,892 tonnes of Lithium Carbonate Equivalent ("LCE"), the benchmark equivalent raw material used in the lithium industry, in addition to Inferred Resources of 15.79Mt grading 1.34% Li2O, or 523,118 tonnes of LCE.

The updated MRE for Bandeira is based on 182 diamond drill holes conducted on the Bandeira property until August 30, 2023. This compares to drill data from 120 holes in the previous MRE for Bandeira announced on June 27, 2023. This additional drilling significantly expanded the MRE, with the tonnes in the Indicated category increasing by 196% compared to the previous Estimate.

Table 6-2 – Itinga Property; Bandeira Deposits Underground Mineral Resource Estimate, October 11, 2023

Source: GE21-Lithium Ionic 2023 - https://lithiumionic.com/investors/reports-filings/

Category	Resource (Mt)	Grade (% Li2O)	Contained LCE (t)
Measured	2.00	1.40	69,226
Indicated	11.72	1.40	405,666
Measured + Indicated	**13.72**	**1.40**	**474,892**
Inferred	**15.79**	**1.34**	**523,118**

Notes related to the Mineral Resource Estimate:

1. The spodumene pegmatite domains were modelled using composites with Li2O grades greater than 0.3%.
2. The Mineral Resource Estimates were prepared in accordance with the CIM Standards, and the CIM Guidelines, using geostatistical and/or classical methods, plus economic and mining parameters appropriate to the deposit.
3. Mineral Resources are not Ore Reserves and are not demonstrably economically recoverable.
4. Grades reported using Dry Density.
5. The effective date of the MRE is October 11, 2023.
6. The QP responsible for the Mineral Resources is geologist Carlos José Evangelista da Silva (MAIG #7868).
7. The MRE numbers provided have been rounded to the estimated relative precision. Values cannot be added due to rounding.
8. The MRE is delimited by Lithium Ionic Bandeira Target Claims (ANM).
9. The MRE was estimated using Ordinary Kriging in (12 x 12 x 4) m blocks.
10. The MRE Report Table was produced in Leapfrog Geo Software.
11. The reported MRE only contains Fresh Rock Domains.
12. The MRE was restricted by grade shell, simulating a UG method, using 0.5% Li2O cut-off.

6.3.3 MRE November 20, 2023

GE21 Consultoria (GE21), on behalf of Lithium Ionic Corp., prepared an update of the MRE released on November 20, 2023 (Table 6-3). This unpublished MRE is being used to develop the Feasibility Study by Atkins Réalis and is scheduled for publication by the end of the first half of 2024.

The Bandeira MRE contains Measured and Indicated ("M&I") Resources of 20.95Mt grading 1.39% Li2O, containing 696.52 tonnes of Lithium Carbonate Equivalent ("LCE"), the benchmark equivalent raw material used in the lithium industry, in addition to Inferred Resources of 16.91Mt grading 1.4% Li2O, or 583.53 tonnes of LCE.

The updated MRE for Bandeira is based on 7,351 assay intervals covering 6,895 meters, comprising 166 assays from trenches totalling 160 meters and 7,185 assay intervals from diamond drill holes totalling 6,735 meters.

Table 6-3 – Bandeira Deposits Underground Mineral Resource Estimate, November 20th, 2023

Source: GE21 2024

Category	Resource (Mt)	Grade (% Li2O)	Contained LCE (kt)
Measured	3.42	1.39	117.61
Indicated	17.52	1.34	578.92
Measured + Indicated	**20.95**	**1.35**	**696.52**
Inferred	**16.91**	**1.40**	**583.53**

Notes related to the Mineral Resource Estimate:

1. The spodumene pegmatite domains were modelled using composites with Li2O grades greater than 0.3%.
2. The mineral resource estimates were prepared by the CIM Standards and the CIM Guidelines, using geostatistical and classical methods, plus economic and mining parameters appropriate to the deposit.
3. Mineral Resources are not ore reserves or demonstrably economically recoverable.
4. Grades reported using dry density.
5. The effective date of the MRE was November 13, 2023.
6. Geologist Carlos José Evangelista da Silva (MAIG #7868) is the QP responsible for the Mineral Resources.
7. The MRE numbers provided have been rounded to estimate relative precision. Values cannot be added due to rounding.
8. The MRE is delimited by Lithium Ionic Bandeira Target Claims (ANM).
9. The MRE was estimated using ordinary kriging in 12m x 12m x 4m blocks.
10. The MRE report table was produced using Leapfrog Geo software.
11. The reported MRE only contains fresh rock domains.
12. The MRE was restricted by RPE3 with grade shell using 0.5% Li2O cut-off.
13. To convert percentage lithium (Li) to percentage lithium oxide (Li2O), multiply by 2.153; to convert Li to lithium carbonate (Li2CO3), multiply by 5.323. To convert a percentage of lithium oxide (Li2O) to lithium carbonate (Li2CO3), multiply by 2.472

7 GEOLOGICAL SETTING AND MINERALIZATION

7.1 Regional Lithium History and Geology

The Project lies in the Eastern Brazilian Pegmatite Province (EBPP), located in terranes of the Araçuaí Orogen (Figure 7-1 and Figure 7-3). The EBPP, one of the largest pegmatitic populations in the world with c. 150,000 km2, contains pegmatite districts located in eastern Minas Gerais (c. 90% of the whole province), southeastern Bahia, and Espírito Santo States of Brazil.

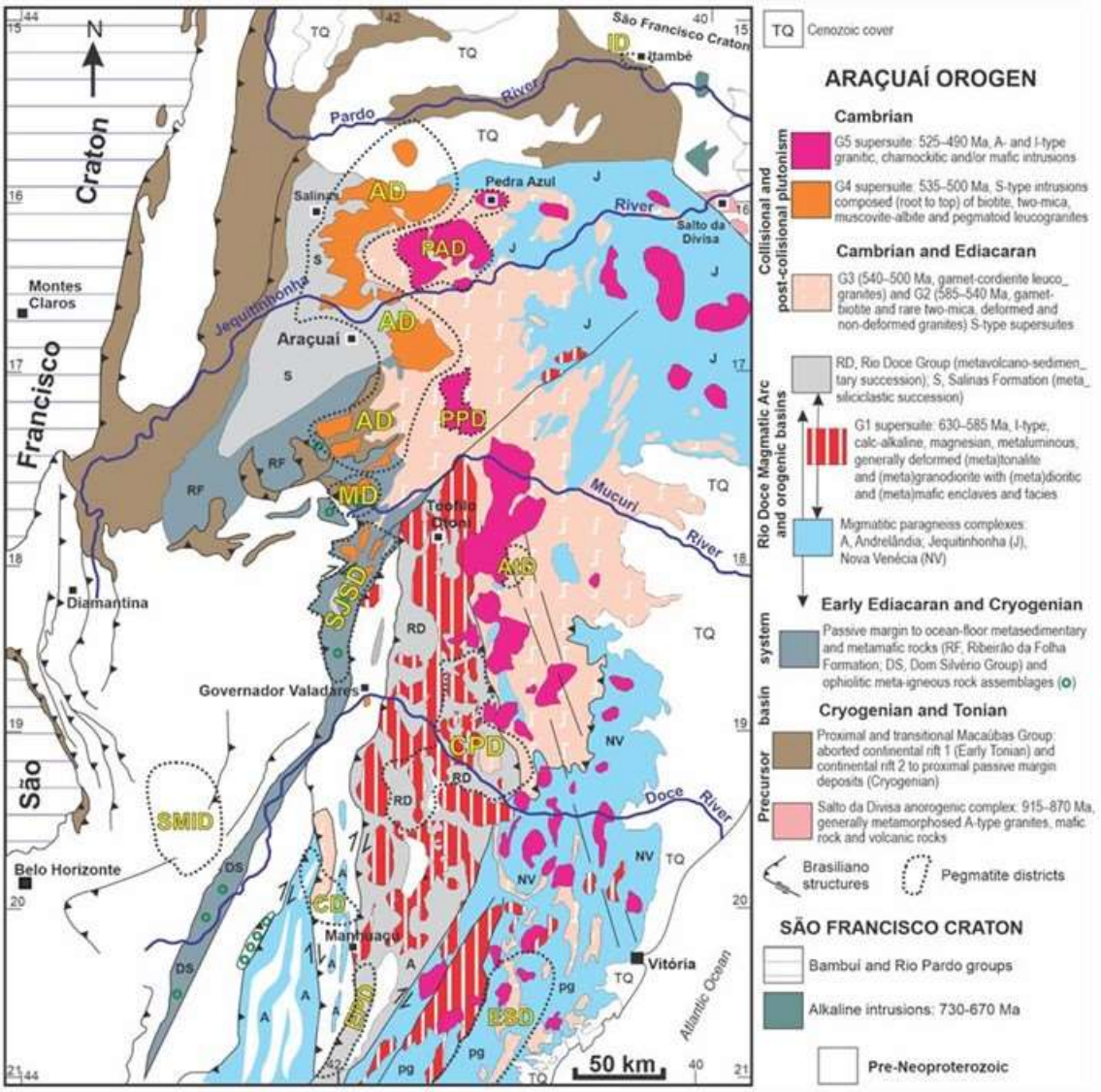

Figure 7-1 – Simplified Geologic Map of the Araçuaí Orogen

Legend: highlighting the granite supersuites and pegmatite districts of the Eastern Brazilian Pegmatite Province (cf. Pedrosa-Soares et al., 2011, 2023): AD, Araçuaí; AtD, Ataléia; CD, Caratinga; CPD, Conselheiro Pena; ESD, Espírito Santo; ID, Itambé; MD, Malacacheta; PAD, Pedra Azul; PPD, Padre Paraíso; SJSD, São José da Safira; SMID, Santa Maria de Itabira.

Source: modified from Pedrosa-Soares et al., 2020.

The Eastern Brazilian Pegmatite Province is the most important region in the history of pegmatite studies and development of lithium deposits in Brazil. Pegmatite gemstones are officially known

in Brazil since the last decades of the 17th century, when green tourmalines, initially mistaken for emeralds, were found by the explorer Fernão Dias Paes Leme in the region of São José da Safira, a pegmatite district very rich in gem-quality elbaite (Li-bearing tourmaline). Long after, in the first decades of the 19th century, pioneer naturalists and geologists, such as Eschwege, Spix, Martius, and Saint-Hilaire, described pegmatite gem deposits located in the Jequitinhonha and Doce river valleys. In 1818, Spix and Martius reached the headwaters of the Calhauzinho and Piauí rivers in the Araçuaí region (Figure 7-4), searching for the gemstones' primary sources, particularly chrysoberyl (then called "chrysolite" locally) that was already mined there. They found a "white granite with little mica, but rich in black tourmaline" (i.e., pegmatite). At that time, spodumene (discovered and named by the Brazilian mineralogist José Bonifácio de Andrada in a volume of the Journal der Chemie, 1800) was already called "rotten chrysolite" by pioneer prospectors and gemstone diggers ("garimpeiros" in Brazilian Portuguese) of the Jequitinhonha Valley. In 1866, Charles Hartt described the N45E-trending structure of the mica schists hosting very coarsegrained "granite" veins between Araçuaí and Itinga. In 1882, Costa Sena published the first paper directly referring to spodumene (also called "triphane" at that time) in the Middle Jequitinhonha region, after identifying "andalusite, cymophane (chrysoberyl) and triphane with sharp edges, in sands and gravels from streams of the Piauí river valley" and suggested that the primary deposits would also be located there. Several spodumene occurrences, among other pegmatite minerals, of the Middle Jequitinhonha Valley are described by Luiz Caetano Ferraz in his "Compendio dos Mineraes do Brasil", published in 1928.

The importance of pegmatites as economic mineral deposits greatly increased in Brazil from the Second World War, due to the large production of mica, beryl, and quartz to supply the military industry of allied countries, to the end of the Cold War in early 1990's. Just after the Second World War, in 1946, the largest pegmatitic populations of Brazil were grouped into provinces by Glaycon de Paiva. Among them the Eastern Brazilian Pegmatite Province was first defined. Since then, more than one thousand pegmatites have been mined there for gemstones, cassiterite, Li and Be ores, Nb-Ta oxides, industrial minerals (K-feldspar, muscovite, albite, quartz), collection and rare minerals, dimension stone, and minerals for esoteric purposes.

Historical milestones in the discoveries and mining of lithium deposits in the Araçuaí-Itinga region were reported by Haroldo de Sá in his PhD thesis (1977). According to him:

- "The discoveries and production of cassiterite, lepidolite, and amblygonite in pegmatites of the Piauí river valley (e.g., Fumal, Generosa, Jenipapo, and Urubu) by the Estanífera do Brasil and Produco companies dated back to the early 1950s. Although spodumene has been known for a long-time by gem diggers ("garimpeiros"), who called it "cambalacho" or "crisólita podre" (i.e., rotten chrysolite in reference to its similarity to chrysoberyl), its commercial production only started at the end of the 1960s at the Cachoeira mine (then owned by Companhia Estanífera do Brasil) to supply the increasing demand of the national market.

Petalite, formerly called "escória branca" (white scoria) and very often mistaken for feldspar, was correctly identified at the end of the 1960's and immediately mined for exportation by the

Companhia Estanífera do Brasil until 1972, followed by Companhia Arqueana de Minérios e Metais Ltda. Around 1977, this mining company has more than twenty distinct pegmatite bodies producing petalite, spodumene, amblygonite, lepidolite, beryl, cassiterite and columbite-tantalite."

For his PhD thesis (1977), Haroldo de Sá compiled map, sections and other data from the archives of the Companhia Arqueana de Minérios e Metais Ltda. and produced the first geochronological data for the local granites and pegmatites (whose similar ages, around 500 Ma, is evidence of a genetic link between them). He also produced the first geochemical data (K, Rb, Cs) for minerals of non-economic and pegmatites with mineralization of petalite, spodumene, lepidolite and/or pollucite. His spatial interpretation of the distribution and zoning of different Lirich pegmatites, even with present-day knowledge, remains realistic.

Khalil Afgouni, an outstanding pioneer of the lithium mining in Brazil and the owner of Companhia Arqueana de Minérios e Metais Ltda, together with Haroldo de Sá published a farseeing article entitled "Lithium Ore in Brazil" in the prestigious magazine Energy in 1978 (vol. 3, pp. 247-253). In the article, they predict that "another new use (for that metal) is in lithium batteries for electric cars and, if this application becomes reality, Brazil will be a big consumer, ranking at same level as the most developed countries in the world, with the advantage of being one of few countries producing its own raw material." Although this is not yet a full reality, the remarkable increase in lithium ore production in the Jequitinhonha Lithium Valley is a result of the invaluable heritage of Arqueana's discoveries of world-class lithium deposits.

The assets were later bought by CBL (Cachoeira mine) in the early 1990's and, more recently, by Sigma Lithium (Xuxa mine, and other spodumene and petalite deposits such as Barreiro, Maxixe, Murial, and others). That heritage continues to drive new companies to the region, whose exploration efforts have led to the discovery of subsurface spodumene deposits in areas lacking outcrops, such as the Bandeira deposit of Lithium Ionic.

Since the early 1980s, the region encompassing the Eastern Brazilian Pegmatite Province (EBPP) has been completely covered by systematic geological mapping (in 1:100,000 scale) and experienced an outstanding increasing in scientific studies supported by robust analytical data. That allowed genetic and metallogenetic links between pegmatite populations and the tectonomagmatic events of the regional geological evolution to be established. In fact, the EBPP is the result of the magmatic and tectono-metamorphic events that formed the Araçuaí Orogen from the Early Ediacaran (ca. 630 Ma) to the Late Cambrian (ca. 490 Ma).

These events comprise the regional deformation, metamorphism and partial melting of sedimentary and volcanic successions deposited in the Tonian-Cryogenian precursor (rift to passive margin) basin system and the Ediacaran orogenic (arc-related) basins (Figure 7-2), as well as of the continental basement. The melting events resulted in the production of huge volumes of orogenic granitic rocks and thousands of pegmatites grouped into five supersuites (G1 to G5; Figure 7-1, Table 7-1).

The sedimentary and volcano-sedimentary successions involved in the tectono-

metamorphicanatectic processes that generated granites and pegmatites show two contrasting distributions of U-Pb ages for detrital grains of zircon (Figure 7-2). One is a classic multimodal age spectrum of a basin system evolved from continental rift to passive margin, represented by the Macaúbas Group and Jequitinhonha Complex.

The other age distribution shows an unimodal spectrum typical of orogenic basins largely filled by material from a rather dominant zircon source (e.g., an active magmatic arc), representing the Salinas Formation and Rio Doce Group that host most Li-bearing pegmatites in the EBPP (Figure 7-1). The Salinas Formation, comprising quartz-mica schist (metapelite) with lenses of calcsilicate rock (metamarl), metawacke (metasandstone) and metaconglomerate, is the main host unit of Li-rich pegmatites in the whole EBPP, including the spodumene-rich pegmatites of the Bandeira deposit of Lithium Ionic.

Tectono-metamorphic events and the G1 to G5 granitic supersuites of the Araçuaí Orogen play distinct roles in relation to pegmatite abundance, distribution, genesis, and metallogenetic specialization, imposing important prospecting constraints with regards to metallic potential of distinct pegmatite populations along the EBPP (Table 7-2).

The G4 is the most important granitic supersuite related to Li-rich pegmatites, followed by the G2 supersuite, while the G5 and G1 supersuites are related to Be-rich pegmatites generally free of or poor in Li-minerals. Tourmaline-bearing pegmatites are widespread in the EBPP, except in some clusters of Be-rich and Li-rich pegmatites.

The G4 intrusions and batholiths show the classical distribution of granitic facies, from pluton root to top, found in other Li-rich pegmatite districts around the world, comprising biotite leucogranite, two-mica leucogranite, muscovite leucogranite, albite leucogranite and pegmatoid granite. Apatite, beryl, tourmaline, and garnet occur in the pegmatoid granites, and muscovite-albite leucogranites. The Salinas Formation is also the main host unit of G4 intrusions associated with Li-rich pegmatites (Figure 7-1).

7.1.1 Pegmatites

Granitic pegmatites represent silica-saturated magmas variably rich in H2O and bearing fluids, as well as in other hyperfusible (fluxing) components (e.g., Li, Na), crystallized in rather closed chemical systems (cf. Cerný, 1991; London, 2008). The EBPP comprises the two known genetic types of pegmatites, both formed during the evolution of the Araçuaí Orogen: i) the anatectic pegmatites generated directly from the partial melting of country rocks; and ii) the residual pegmatites, representing late silicate melts released by fractional crystallization of parental granites. Genetic affiliation and other criteria allow pegmatite districts to be distinguished in the EBPP (Figure 7-3; Table 7-2).

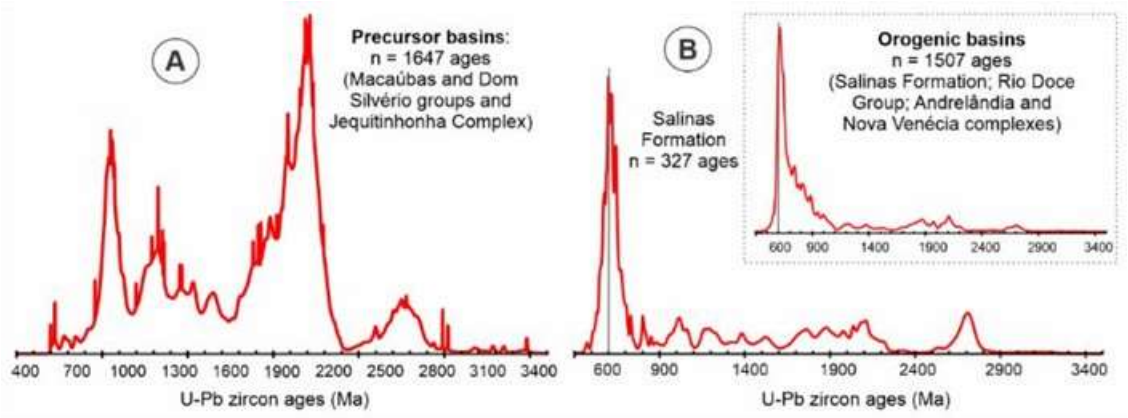

Figure 7-2 – Distributions of U-Pb Ages for Detrital Zircon Grains from Metamorphosed Sedimentary and Volcanic Rocks

Legend: (A) precursor basins (e.g., Macaúbas Group and Jequitinhonha Complex); and (B) orogenic basins (e.g., Salinas Formation, Rio Doce Group) of the Araçuaí Orogen within the Eastern Brazilian Pegmatite Province.
Source: Pedrosa-Soares et al., 2023.

Table 7-1 – Main Features of the Orogenic Igneous Supersuites of the Araçuaí Orogen

Supersuites	G_1	G_2	G_3	G_4	G_5
Ages (Ma)	**630 – 585**	**585 – 540**	**540 – 500**	**535 – 500**	**525 – 490**
Lithotypes	mostly tonalite and granodiorite, minor diorite to gabbronorite, with biotite, amphibole and/or pyroxenes; poor in pegmatites	mostly biotitegarnet syenogranite to alkali feldspar granite, garnet-rich monzogranite to tonalite, and garnet-two-mica granite, locally with sillimanite; associated with external rare element pegmatites	alkali feldspar granite to syenogranite with cordierite and/or garnet and/or sillimanite, free of or poor in biotite; poor in pegmatites	from pluton root to top: biotite granite, twomica leucogranite, muscovite and/or albite and/or schorlite granite, pegmatoid granite; associated with external rare element pegmatites	alkali feldspar granite to granodiorite, orthopyroxenebearing charnockitic rocks, basic (norite) to ultrabasic rocks, and beryl-topaz pegmatites

Supersuites	G_1	G_2	G_3	G_4	G_5
Ages (Ma)	**630 – 585**	**585 – 540**	**540 – 500**	**535 – 500**	**525 – 490**
Field Relations	batholiths and stocks, generally rich in dioritic to mafic enclaves and facies, showing solid-state deformation and migmatization, local well-preserved igneous fabrics, associated with the arc-related metavolcano-sedimentary Rio Doce Group	batholiths, stocks and stratoid bodies, showing solid-state deformation, metamorphism and migmatization, with common restites and xenoliths of metasedimentary rocks, and localized well-preserved igneous fabrics	mostly autochthonous, non-deformed patches, veins, and lodes of G_3 leucosome, and minor stocks, free of the regional foliation, hosted by migmatites with G_2 paleosome	balloon- to stratoid-shaped intrusions, postkinematic in relation to the regional ductile foliation, locally imposing late deformation on the regional structural trend (circumscribed intrusions)	balloon-shaped plutons and multiple intrusions, locally rich in mafic and/or microgranular enclaves with magma mixing features, and norite-rich bodies, postkinematic in relation to the regional ductile foliation
Geochemical Signatures	metaluminous to slightly peraluminous, magnesian, calcic to alkali-calcic, medium- to high-K, expanded calcalkaline series	strongly to weakly peraluminous, calc-alkalic to subalkalic (K > Na)	peraluminous, sub-alkalic (K > Na)	peraluminous, sub-alkalic (K > Na) to alkalic (Na > K)	metaluminous to slightly peraluminous, ferroan, high-K calc-alkalic, minor tholeiite
Petrogenetic Type	metaluminous Itype, locally peraluminous Itype	peraluminous Stype, locally peraluminous Itype	S-type	S-type	A-type and Itype
Tectonic Stage	pre-collisional to early collisional magmatic arc	late pre-collisional to late collisional	late collisional to post-collisional	post-collisional	post-collisional

Source: simplified from Pedrosa-Soares et al., 2023.

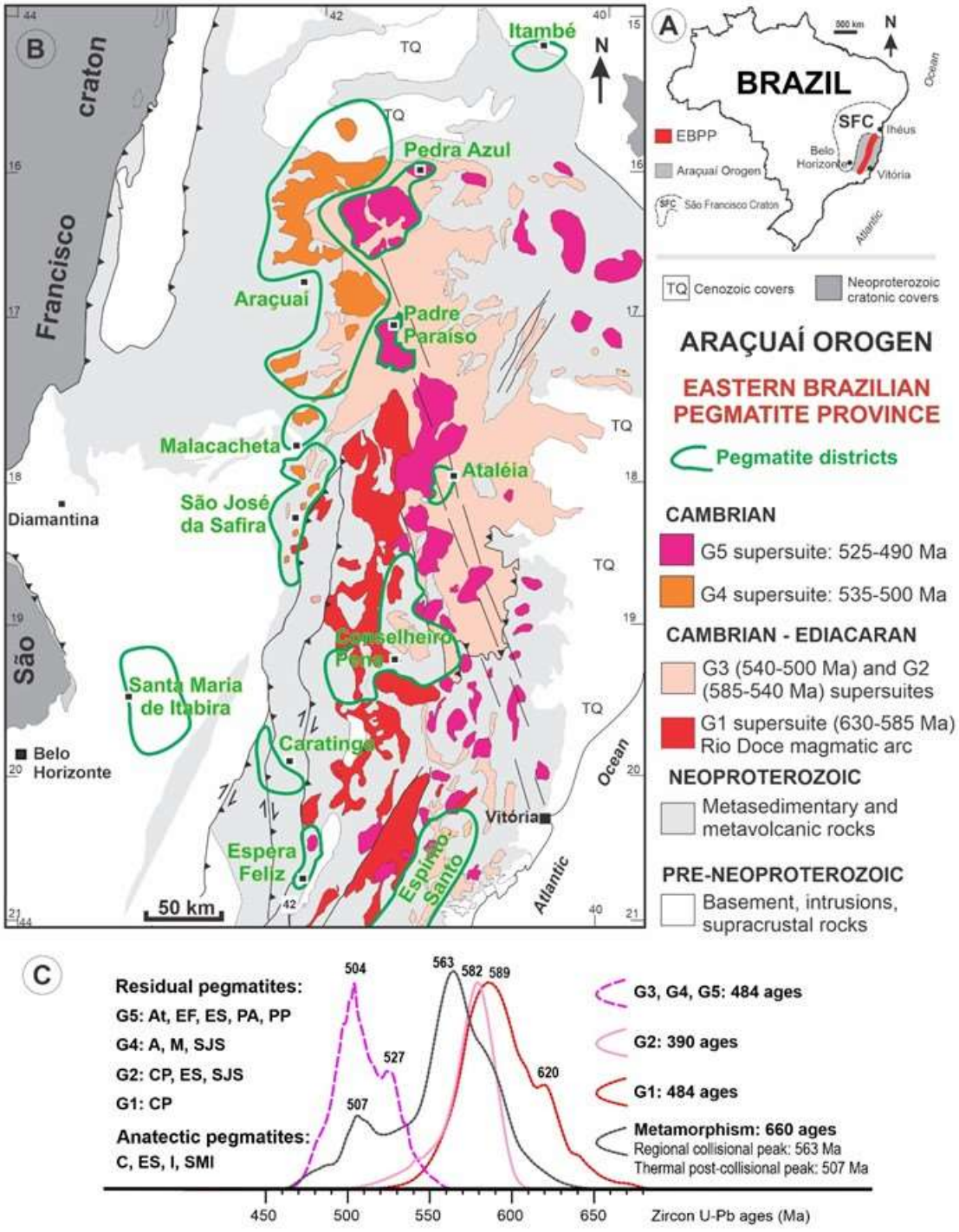

Figure 7-3 – Araçuaí Orogen – Eastern Brazilian Pegmatite Province

Legend: A) Location of Eastern Brazilian Pegmatite Province (EBPP). B) Simplified geological map highlighting the granite supersuites (G1 to G5) and EBPP pegmatite districts: A, Araçuaí; At, Ataléia; C, Caratinga; CP, Conselheiro Pena; EF, Espera Feliz; ES, Espírito Santo; I, Itambé; M, Malacacheta; PA, Pedra Azul; PP, Padre Paraíso; SMI, Santa Maria de Itabira; SJS, São José da Safira. C) Distribution of zircon U-Pb ages from orogenic granite supersuites (G1 to G5), regional metamorphism and post-collisional thermal events, correlated to pegmatite districts.
Source: Pedrosa-Soares et al., 2023.

The anatectic pegmatites are coarse-grained quartz-feldspathic bodies (i.e., granitic leucosomes) hosted by migmatitic gneisses and micaschists, mostly formed in the collisional tectonometamorphic event (585 – 540 Ma) and in the post-collisional thermal event (540 – 490 Ma). Therefore, their spatial distribution, and genetic and metallogenetic features are directly

related to the melted country rocks. Conversely, the residual pegmatites, especially those enriched in rare elements, have restricted spatial distributions and genetic links directly related to the distinct granite types from which they ultimately inherited their geochemical characteristics and metallogenetic specializations (Figure 7-3, Figure 7-2).

Therefore, residual pegmatites released from peraluminous, subalkalic to alkalic, hydrous, S-type, two-mica leucogranites formed from the partial melting of metasedimentary rocks might have a rather distinct metallogenetic specialization (e.g., richer in Li, Cs, Ta, Sn, and P) in relation to residual pegmatites (e.g., richer in Be, F, and Fe) from metaluminous, high-K calc-alkalic, ferroan, relatively anhydrous, A-type, amphibole-biotite granites formed from the partial melting of mainly igneous rocks. The first case (S-type granites) refers to Li-bearing pegmatites associated with the G4 and G2 supersuites, while the second (A-type granites) stands for the Be-bearing (but Li-free) pegmatites comprised by the G5 supersuite (Figure 7-3, Table 7-2).

Table 7-2 – Features of the Main Pegmatite Districts of the Eastern Brazilian Pegmatite Province

District names and ages (Ma)	Historical and present-day mineral production, and rare minerals	Genetic affiliation; class, subclass, type, subtype, and family (*)	Parent and host rocks
Itambé 508 Ma	K-feldspar, quartz crystals, mica, beryl, columbite, monazite	anatectic; muscovite-rare element, REE, allanitemonazite, NYF	biotite-hornblende gneisses, sillimanitefeldspar-mica schists
Pedra Azul 501 Ma	quartz, beryl (aquamarine), topaz	residual; REE, beryltopaz, NYF	A-type G_5 granites
Padre Paraíso 519 Ma	quartz, beryl (aquamarine), topaz, quartz crystals, goshenite, chrysoberyl	residual; REE, beryltopaz, NYF	A- and I-types G_5 granites and charnockites
Araçuaí 535-500 Ma	Greenish to pinkish spodumene, petalite, lepidolite, Li-phosphates, cookeite, cassiterite, columbitetantalite, industrial minerals (perthitic K-feldspar, albite, muscovite), tourmalines (elbaite, schorlite), beryl ore and gems (aquamarine, morganite), pollucite, quartz crystals, cleavelandite, herderite and other rare phosphates, topaz, bismuthinite	residual; mostly rare element and minor muscovite-rare element, Li, beryl, complex (spodumene, petalite, lepidolite, elbaite, amblygonite), albite-spodumene (SRP), albite, LCT	S-type G_4 leucogranites; low-P/high-T (andalusite, cordierite, sillimanite) to medium-PT (garnet, staurolite, kyanite, sillimanite) mica schists to paragneisses, metasandstones, calc-silicate rocks, metaultramafic rocks
Ataléia 502 Ma	quartz crystals, beryl (aquamarine), topaz, chrysoberyl	residual; REE, beryltopaz, NYF	A- and I-types G_5 granites and charnockites
São José da	tourmalines (elbaite, schorlite), industrial minerals (perthitic K-	residual; muscovite-rare element and rare element,	S-type G_4 and G_2 leucogranites; medium-PT

District names and ages (Ma)	Historical and present-day mineral production, and rare minerals	Genetic affiliation; class, subclass, type, subtype, and family (*)	Parent and host rocks
Safira 545-490 Ma	feldspar, albite, muscovite), beryl ore and gems (aquamarine, heliodor, morganite), lepidolite, Liphosphates, spodumene, garnet, cleavelandite, columbite-tantalite, cassiterite, bertrandite, microlite, zircon, rare phosphates	Li, beryl, complex (elbaite, lepidolite, Li-phosphates, spodumene), LCT	(garnet, staurolite, kyanite, sillimanite) mica schists to paragneisses, metasandstones, calc-silicate rocks, metaultramafic rocks
Conselheiro Pena 570-545 Ma	industrial minerals (perthitic Kfeldspar, albite, muscovite), tourmalines (elbaite, schorlite), beryl ore and gem, spodumene (kunzite), lepidolite, Liphosphates, quartz crystals, cleavelandite, columbite-tantalite, cassiterite, rare phosphates (arrojadite, barbosalite, brasilianite, childrenite, correianevesite, eosphorite, roscherite, vivianite, etc.)	residual; muscovite-rare element and rare element; Li, beryl, complex (elbaite, Li-phosphates, lepidolite, spodumene), LCT	S-type G_2 (and I-type G_1?) granites; medium-PT to intermediate low-P (garnet, staurolite, cordierite, kyanite, sillimanite), mica schists to paragneisses, metasandstones, calc-silicate rocks, metaultramafic rocks
Malacacheta 535-500 Ma	muscovite, beryl, chrysoberyl; alexandrite, sapphire	residual; muscovite-rare element, beryl, LCT; and anatectic to hydrothermal processes	S-type G_4 leucogranites; mica schists, meta-ultramafic rocks, migmatites
Santa Maria de Itabira, 545-500 Ma	emerald, alexandrite, aquamarine, amazonite	quartz-feldspathic hydrothermal deposits, and pegmatites	ultramafic schists, banded iron formations, migmatites
Caratinga, 570 Ma	kaolin, corundum (sapphire, ruby), beryl	anatectic; abyssal, ceramic	migmatitic paragneisses
Espera Feliz, 500	quartz crystals, beryl (aquamarine), topaz	residual; REE, beryltopaz; NYF	G_5 granites
Espírito Santo 570-500 Ma	kaolin, quartz, beryl (aquamarine), topaz, tourmalines (and spodumene?)	anatectic; ceramic; and residual; REE, beryltopaz, NYF (and LCT?)	migmatitic paragneisses, G_5 (and G_2?) granites

Source: Pedrosa-Soares et al., 2023, updated after Pedrosa-Soares et al., 2011; (*) Cerný et al., 1991, 2012; LCT, Lithium-Cesium-Tantalum; and NYF, Niobium-Fluorine pegmatites.

The EBPP was subdivided into twelve pegmatite districts based on the mineral production, genetic and metallogenetic affiliation and classification, parental granite type, host rocks and metamorphic regime, and crystallization ages of a relatively large and clustered pegmatite population (Figure 7-3; Table 7-2). Most of them are districts of residual pegmatites of the rare element class, distinguished by their affinities with the LCT (Lithium-Cesium-Tantalum) or NYF (Niobium-Yttrium-Fluorine) geochemical-metallogenetic families that, in turn, are related to distinct types of parental granites. Beryl-topaz (NYF) pegmatites cluster in districts almost

completely circumscribed or very close to A-type and I-type G5 intrusions, encompassing granitic and igneous charnockitic (orthopyroxene-bearing) rocks with features of magma mingling-mixing involving mafic melts.

Contrastingly, complex LCT pegmatites and albite-spodumene-rich pegmatites (SRP) are found in the external aureoles of S-type intrusions mostly composed of two-mica leucogranites with pegmatoid cupolas, generally hosted by metasedimentary rocks of the greenschist to amphibolite facies. Among the EBPP Li-bearing districts, the Araçuaí Pegmatite District stands out by having the largest historical and current production of lithium ore and the only world-class spodumene deposits of Brazil. Those deposits include the CBL, Sigma, and the newly discovered deposits by other companies, such as the Bandeira and other spodumene-rich deposits of Lithium Ionic Corporation.

The Araçuaí Pegmatite District includes several LCT pegmatite fields distinguished by their mineral production, pegmatite types and subtypes, and pressure-temperature (P-T) conditions of both the regional and contact metamorphisms (Figure 7-4). Besides complex LCT pegmatites, spodumene-rich pegmatites (SRP) are known in the Curralinho, Itinga, Neves-Tesouras and Salinas pegmatite fields. However, the Itinga Pegmatite Field remains the most important for spodumene production and prospecting, owing to the outstanding abundance of non-zoned to poorly zoned SRP ranging from a few to dozens of meters thick, hundreds to a few thousand meters in length along strike, and dozens to hundreds of meters in downdip width. Many spodumene orebodies mined by Arqueana, CBL and Sigma, as well as those discovered by Lithium Ionic at Bandeira and other targets, belong to the SRP (or albite-spodumene) type.

7.2 Structural Geology

In the Araçuaí Pegmatite District (Figure 7-4), the present-day structural framework was established after four deformation events (D1, D2, DG, and DNt). Two of them (D1, D2) are directly related to the regional tectono-metamorphic evolution of the Araçuaí Orogen in the Ediacaran-Cambrian. The third deformation event (DG) was caused by the widespread and voluminous intrusions of Cambrian G4 granites that caused thermal metamorphism and significant structural disturbance on the regional fabrics along areas relatively close to granitic stocks and batholiths (Pedrosa-Soares et al. 1987, 1993, 2011; Alkmim et al., 2006; Santos et al., 2009; Peixoto et al., 2017). Much later, the last deformation event (DNt) resulted from neotectonics reactivation in the Late Tertiary (Saadi and Pedrosa-Soares, 1989). The EdiacaranCambrian deformation events (D1, D2, and DG) formed the structural framework that passively hosts the rare element pegmatites in the Araçuaí District (Figure 7-4). The much younger neotectonic deformation (DNt) reworked prior structures in upper crustal levels in the Late Tertiary (Miocene), forming normal faults and graben basins (e.g., the Virgem da Lapa Graben, Figure 7-4) filled by the fluvial to lacustrine sandstone-mudstone piles of the São Domingos Formation that reach more than 100 m in thickness (Saadi and Pedrosa-Soares, 1989; Pedrosa-Soares, 1997). Locally, neotectonic faults may cut and displace blocks with pegmatite

deposits.

The D1 deformation results from regional tectono-metamorphic processes imposed by compressive stresses during the collisional stage (580-540 Ma) of the Araçuaí Orogen. Megascopic to macroscopic D1 structures are asymmetric tight folds with long limbs and short hinges, parasitic folds, and ductile shear zones related to thrust ramps and oblique to transcurrent strike-slip domains.

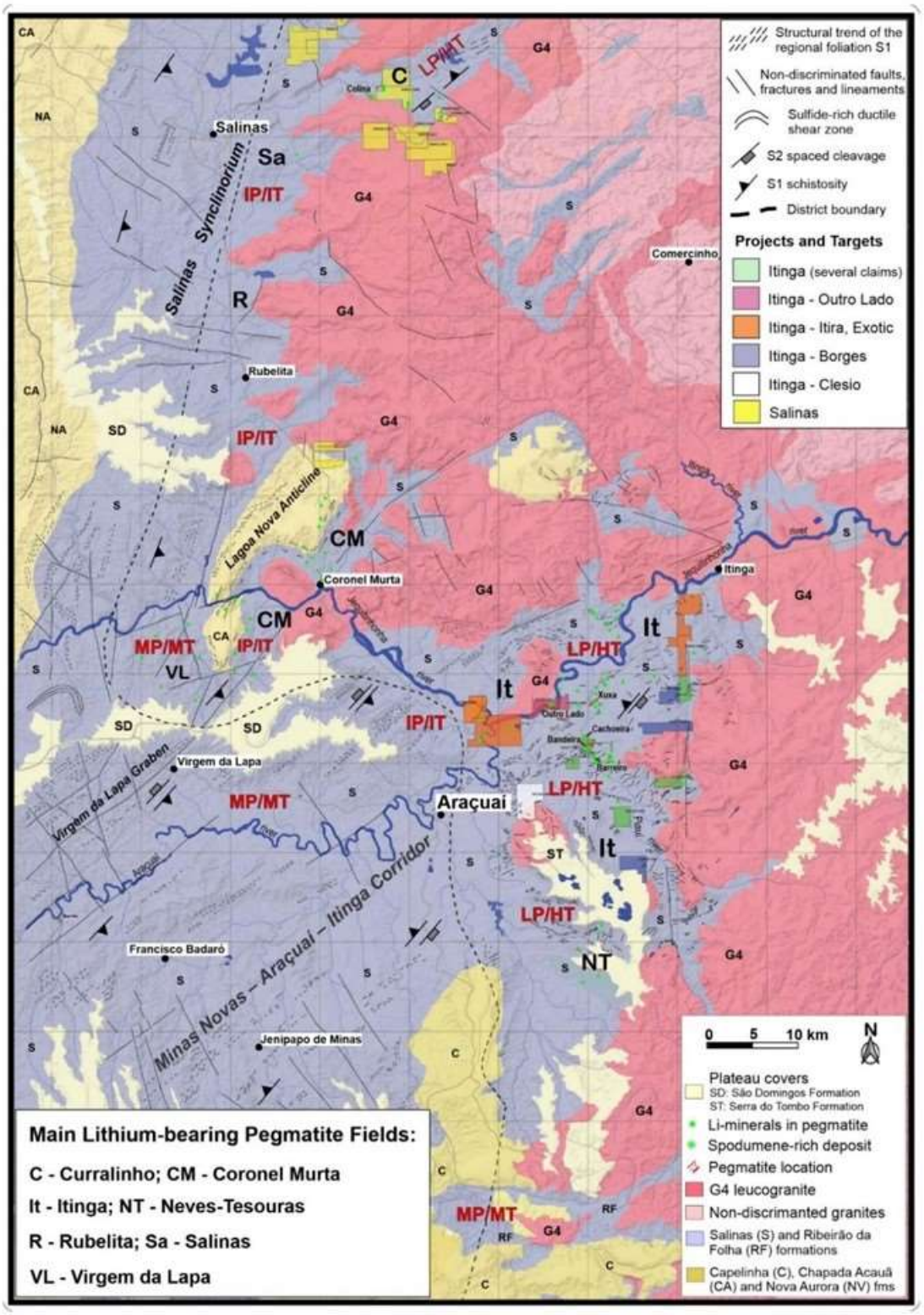

Figure 7-4 – Geological Map of the Araçuaí Pegmatite District

Legend: highlighting lithium-bearing pegmatite fields (see inbox), major tectonic domains (names in italics on map), metamorphic regimes according to relative pressure (P) and temperature (T) conditions (LP/HT, low-P/high-T; IP/IT, intermediate-low P and T; and MP/MT, medium P and T), spodumene active mines (Cachoeira, Xuxa) and main spodumene deposits: Bandeira and Outro Lado (Lithium Ionic), Barreiro (Sigma), and Colina (Latin Resources).

Source: modified and updated from Pedrosa-Soares et al., 2023, based on the district map by Paes et al., 2016.

The macroscopic to microscopic D1 structures include the main regional planar structure that

evolved from a cleavage to the schistosity S1 (Figure 7-5) that contains the L1 mineral/stretching lineation. S1 is generally (sub)parallel to the layering (S0) along D1 fold limbs, becoming an axialplane surface in fold hinges (Figure 7-5). Anastomosed and S-C foliations characterizes higher strain shear zones syn-kinematic to S1. Although it generally is a very penetrative structure, the S1 foliation also provides host surfaces for pegmatites.

Distinct metamorphic regimes related to the D1 deformation of schists and gneisses rich in micas have been recognized in the region encompassing the Araçuaí Pegmatite District (Pedrosa-Soares et al., 1984, 1993, 1996; Costa et al., 1984; Costa, 1989; Santos et al., 2009; Peixoto et al., 2017). In the western and southwestern sectors of the region (Figure 7-4), the S1 schistosity shows syn-kinematic (syn-S1) assemblages with Fe-rich garnet (almandine), staurolite, kyanite and/or sillimanite. Such index-minerals series is typical of a medium pressure and medium temperature (MP/MT) metamorphic regime (Figure 7-4). This, together with quantitative geothermobarometric data, characterize the M1 metamorphic event as a syn-collisional (syn-D1) Barrovian-type (MP/MT) metamorphism dating between 575 – 550 Ma. P and T increase from c. 3.5 kbar at 450 °C in the garnet zone at the southwest of Francisco Badaró, passing northeastwards through the staurolite, kyanite and sillimanite zones, and reaching up to 8.5 kbar at 650 °C at the southeast of Coronel Murta (Figure 7-4).

In the northeastern and northern sectors of the region, the S1 schistosity shows syn-kinematic (syn-S1) assemblages with biotite, Mn-rich garnet (spessartine), andalusite, cordierite and/or sillimanite. Such index-minerals series is typical of a low pressure and high temperature (LP/HT) metamorphic regime (Figure 7-4). From the most northeastern andalusite zone to the southwest of Itinga, quartz-feldspathic leucosomes with aplitic to pegmatitic textures formed from the breakdown of muscovite along the S1 foliation of cordierite-quartz-mica schists. Northeastwards, through the andalusite-cordierite, cordierite-sillimanite, sillimanite, and K-feldspar zones, increasing metamorphism and partial melting of quartz-mica schists formed migmatitic paragneisses in the eastern tip of the Itinga Pegmatite Field (Figure 7-4). Regionally, the metamorphic event (M2) records a low-P/high-T metamorphism with pressures from 2 kbar to 5.5 kbar under temperatures from 400 °C to 700 °C, at around 540-530 Ma. The M2 metamorphism reached partial melting conditions on quartz-mica schists of the Salinas Formation with increasing anatexis rates that formed leucosome-rich migmatites (diatexites) in the easternmost sector of the Araçuaí Pegmatite District. This implies that, in deeper crustal levels, the widespread anatexis on the Salinas Formation could have produced large volumes of S-type granitic magmas in the late collisional to post-collisional stages of the Araçuaí Orogen. Indeed, the time interval of the M2 metamorphism (540-530 Ma) fits well with the oldest ages of G4 granites (535-525 Ma). This, together with the fact that the M2 metamorphism culminated in partial melting of quartz-mica schists and paragneisses in the easternmost Araçuaí Pegmatite District, indicate that the S-type G4 magmas were formed from the anatexis of thick metasedimentary packages in deep levels of the Salinas Formation.

Along the boundary between the M1 and M2 metamorphic domains (Figure 7-4), the syn-S1

mineral assemblages include almandine and/or staurolite and andalusite and/or cordierite, characterizing an intermediate-low pressure (Buchan-type) metamorphic regime (IP/IT, Figure 7-4) transitional between the M1 Barrovian-type (MP/HT) and the M2 low-P/high-T (LP/HT) metamorphic regimes found in the Araçuaí Pegmatite Districts. Bearing in mind the relations between distinct pegmatite populations, their metallogenetic specializations and metamorphic regimes (Cerný, 1991; Cerný et al., 2012), such metamorphic characterization is of great importance for prospecting different rare element pegmatites, as Li-rich pegmatites are typically found in terranes with relatively low-P/high-T metamorphism.

Figure 7-5 – Photos from Outcrops and a Drill Core Showing Structures of the Deformation Events D1 and D2 on the Salinas Formation in the Araçuaí Pegmatite District

Legend: (A and B) Large tight fold (A) with a hinge (B) showing the sedimentary layering (S0) cut by the low-angle dip to flat axial-plane S1 cleavage. C) Tight folds with limbs transposed by S1 foliation. D) Hinges of tight folds with metamorphic quartz veins in quartz-mica schist. E) Spaced cleavage S2 cutting the schistosity S1, and sub-vertical joints (JA) cutting across both S1 and S2 in the Bandeira area. F) S2 spaced foliation marked by recrystallized mica, cutting the S1 schistosity in a drill core sample from the Bandeira deposit.

The D2 deformation developed from the late collisional to the post-collisional stages of the Araçuaí Orogen, when increasing decompression conditions, imposed by the orogen gravitational collapse, gradually replaced the tangential D1 compressive stresses. In the Araçuaí Pegmatite District, the D2 deformation comprises mostly brittle structures, such as the S2 spaced cleavage, joint families, and normal faults, as well as large open folds (flexures). The spacing between surfaces of the S2 cleavage ranges from less than one centimeter to decimeters (Figure 7-5). Locally, S2 may be very well developed in micaschists, becoming a tight crenulation cleavage to schistosity. The S2 spaced cleavage and other brittle structures, as being more open surfaces than the S1 schistosity, provided host surfaces for Li-rich pegmatites, generally the thicker ones, in the Itinga Pegmatite Field.

The latest Cambrian deformation event (DG) was caused by the intrusion of large volumes of Stype magmas that formed the G4 granites and cut across and disturbed the regional framework imprinted by the D1 and D2 deformations. The DG event deformed the regional structural trend of the host rocks around granitic plutons, forming radial fractures irradiating from the granitic plutons, and imprinting ring-shaped fracture systems that reworked regional structures around the intrusions. All these DG structures can host late orogenic rare element pegmatites.

During emplacement and cooling, the G4 plutons caused contact metamorphism on their country rocks and released residual silicate melts that formed pegmatites that either crystallized within the parental granite or migrated outwards and were hosted by D1, D2 and DG structures of the Salinas Formation and other metasedimentary units. While barren and beryl-bearing pegmatites are found both within parental G4 granites and country rocks, the Li-bearing pegmatites have been only found in places rather far from (> 1 km) granite massifs, emplaced in the Salinas Formation and other metasedimentary units. The G4 batholith emplaced along the whole eastern boundary of the Araçuaí Pegmatite District is formed by multiple coalescent plutons and places an eastern limit for the occurrence of Li-bearing pegmatites.

Regionally, the deformational events formed large structures with distinct implications for the occurrence and structural control of pegmatites in the Araçuaí District, such as the Salinas Synclinorium, the Lagoa Nova Anticline, and the Minas Novas - Araçuaí - Itinga Corridor (Figure 7-4).

The axial zone of the Salinas Synclinorium shows the best-preserved section of the Salinas Formation, comprising non-deformed to weakly deformed metawacke, metapelite and metaconglomerate, metamorphosed in the biotite and garnet zones of the low greenschist facies. This low-grade metasedimentary section reaches up to 2 km in thickness, with no evidence of pegmatite along the synclinorium keel. However, a Li-rich pegmatite cluster, including SRP bodies, was recently found to the east of the Salinas Synclinorium, along the andalusite-cordieritebearing, low-pressure/high-temperature metamorphic zone of the Curralinho Pegmatite Field (Figure 7-4).

In the case of the Lagoa Nova Anticline, although there are LCT pegmatites emplaced along its structural surfaces, no SRP was yet found there, much probably due to the rather unfavorable

pressure-temperature conditions of the regional and contact metamorphisms (between the medium PT (MP/MT) and intermediate PT (IP/IT) regimes).

The Minas Novas - Araçuaí - Itinga Corridor, in turn, plays a special role in the understanding of the structural control and the most favourable pressure-temperature conditions for the SRP occurrence in the Araçuaí Pegmatite District. That corridor has been characterized as a flowershaped transpressive (during D1) to transtensive (during D2) structure (Pedrosa-Soares et al., 1993, 1996; Alkmim et al., 2006) with the S1 foliation dipping to SE in the NW flank, and to NW in the SE flank (Figure 7-4).

In the Itinga Pegmatite Field, the S1 schistosity and S2 spaced cleavage show NE-trending strikes, with the S1 schistosity dipping to NW and the S2 cleavage dipping to SE (if they have not been disturbed by later deformations, i.e., DG and DNt). The S1 foliation, as well as the S2 spaced cleavage and other brittle surfaces (i.e., the flat-lying and subvertical joints) host many Li-rich pegmatites, with the thicker SRP bodies generally emplaced in more open surfaces of brittle structures.

The regional metamorphism associated with the S1 schistosity gradually increases from southwest to northeast along the corridor, reaching c. 3.5 kbar at c. 550 °C at the andalusite cordierite zone in the Piauí river valley, where the contact metamorphism was imposed by G4 granitic intrusions also under relatively low-pressure conditions. All those tectono-metamorphic and magmatic features favorable to SRP occurrence characterize the Itinga Pegmatite Field where several of the most important spodumene deposits already found in Brazil are located, such as those of the CBL and Sigma, and the SRP deposits of Lithium Ionic.

7.3 Local Geology

Field mapping in the Bandeira area revealed the existence of two geological units: (i) Salinas

Formation, characterized by banded quartz-mica schists with lenses of calcsilicate rocks; and (ii) G4 Supersuite, represented by an extensive pegmatite dike-swarm (pegmatite veins) composed of spodumene-rich orebodies and some non-mineralized pegmatites (Figure 7-6).

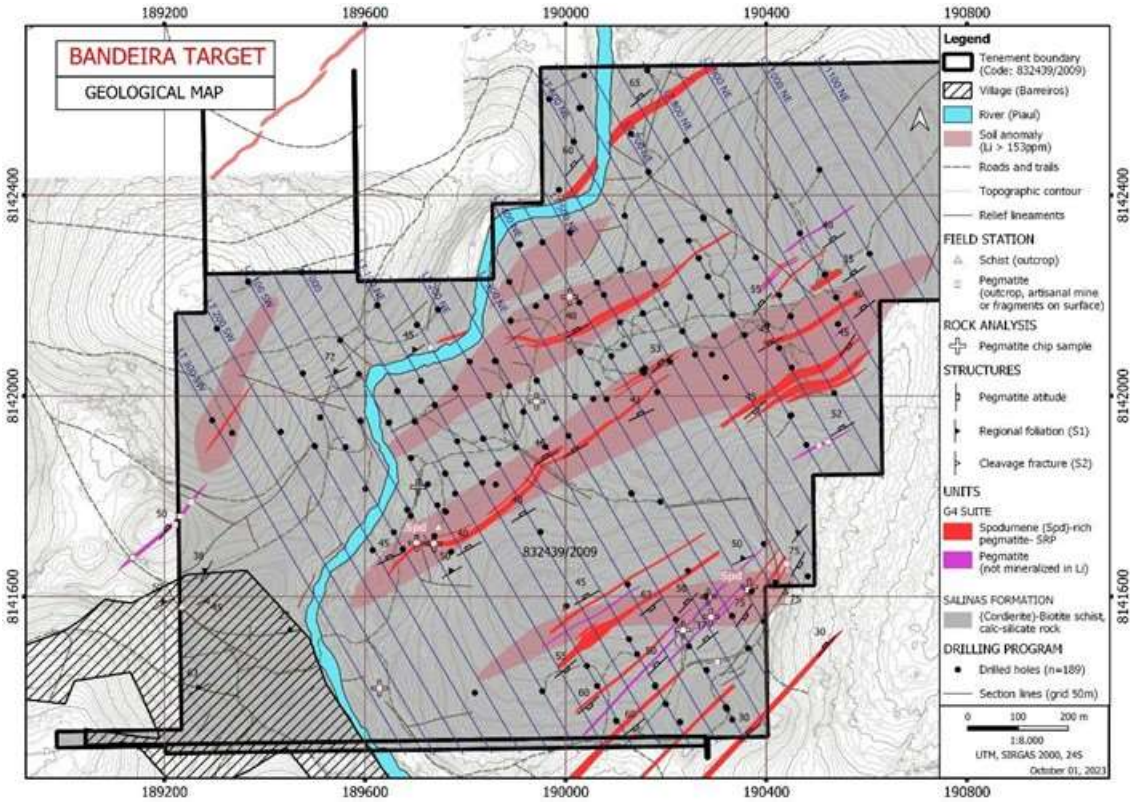

Figure 7-6 – Geological Map of the Bandeira Deposit

Figure Source: Lithium Ionic 2024

Owing to the significant weathering typical of tropical regions, the surface of the Bandeira area predominantly comprises recent residual soils resulting from the decomposition of the underlying rocks. The schist residual soil is a red to brown fine-grained (silt to clay) eluvium. In contrast, the pegmatite soil is typically a whitish, fine to coarse-grained, powdered eluvium, with a composition dominated by quartz, kaolinized feldspar and altered muscovite. In cases of lithium mineralization, this soil can also contain fine-grained, partially to almost wholly weathered spodumene fragments.

Based on the few exposed outcrops, the Salinas Formation in the Bandeira area is composed of biotite schist and cordierite-biotite schists of gray color and medium-grained size. When these rocks contain a higher concentration of mica, the schistosity is more penetrative and tends to be more fractured (Figure 7-7a). When the amount of quartz is greater, a preserved original bedding can be observed marked by the alternance of dark biotitic and light quartzfeldspathic layers (Figure 7-7b). Cordierite-biotite schist was also identified in the Bandeira target, and they are characterized by the enrichment of millimetric to centimetric cordierite porphyroblasts (Figure 7-7c), which can be stretched along the schistosity (syn-tectonic) or undeformed and latestage (post-tectonic). Based on observations in the drill cores it is also possible to verify the presence of calc-silicate rocks interlayered in the schists, which can be classified in three types (based on the mineralogy): (i) biotite-quartz schist; (ii) quartz-biotite schist; and (iii) cordieritequartz-biotite schist.

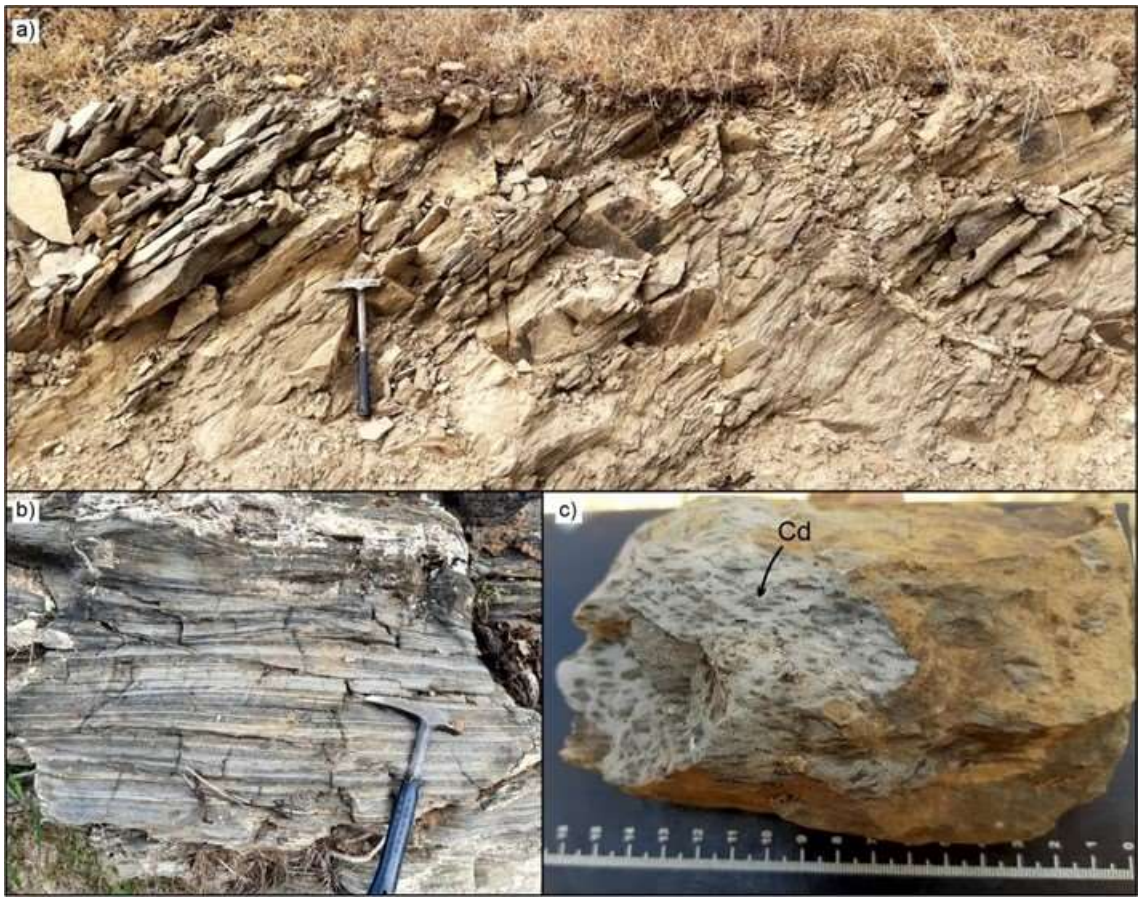

Figure 7-7 – Schists of the Salinas Formation Observed in the Bandeira Deposit

Legend: a) fractured biotite schist (UTM: 189,232 / 8,141,577); b) banded biotite-schist with preserved original bedding (UTM: 189,733 / 8,142,094); c) detail of the cordierite-biotite schist (UTM: 190,441 / 8,141,664). Coordinates in SIRGAS 2000, zone 24S. Abbreviation: Cd-cordierite.
Figure Source: Lithium Ionic 2024

The pegmatites in the Bandeira target constitute a swarm of several dikes with variable thicknesses (metric to decametric). They are normally concordant to the Salinas Formation schistosity (5055°NE/40-50°NW). The nature of the contact between the pegmatite and the host rock is abrupt and sharp (Figure 7-3a). Records of the pegmatites mineralized in lithium in the Bandeira area (i.e., Spodumene-Rich Pegmatites – SRP) can be observed in some exposed outcrops that show centimetric coreless to greenish spodumene crystals, with whitish colour when weathered. In such veins, it is common the occurrence of euhedral prismatic centimetric crystals with a preferred orientation indicative of mineral growth orthogonal to the borders of the dike (Figure 7-3b).

Based on the observations from these outcrops and the intercepts from the drill cores, it is possible to define the Bandeira mineralized bodies as non-zoned pegmatitic dikes with a simple and consistent mineralogy composed essentially of albite (33%), perthitic K-feldspar (25%), spodumene (19%), quartz (15%), and muscovite (5%). Accessory phases (3%) vary from petalite, columbite, tantalite, cassiterite, apatite, tourmaline, and sphalerite. The log analysis unveiled well preserved spodumene crystals of variable sizes, typically centimeter-scale and disseminated throughout the rock. Notably decimeter-sized crystals also occur (Figure 7-3b).

The concordant SRP pegmatites in the Bandeira area are dominantly concordant with the regional schistosity (S1) but discordant bodies, with similar strike and dipping to southeast, also occur. The best example are the pegmatites observed in the southeastern region (Figure 7-3), where a more flattened large discordant body fed smaller intrusions that dips towards southeast. These discordant bodies share identical mineralogical composition with the concordant bodies, leading to the interpretation as both products of the same coeval magmatism.

Figure 7-8 – Spodumene-Rich Pegmatites Observed in the Bandeira Deposit

Legend: a) pegmatite of ca. 2 m thick concordant to the regional foliation (S1) of the host schists; b) outcropping and weathered prismatic spodumene crystals that grew perpendicular to the contact; c) detail of the cordierite-biotite schist (UTM: 190,441 / 8,141,664). Coordinates in SIRGAS 2000, zone 24S. Abbreviation: Cd-cordierite.
Figure Source: Lithium Ionic 2024

7.4 Mineralization Model

The following text and illustrations were compiled from Pedrosa-Soares et al. (2023) and complemented with data from Lithium Ionic public and internal reports, if not otherwise specified.

The Bandeira spodumene deposit is located immediately to the southeast of the CBL's Cachoeira mine (Figure 7-9). This mine has played a major role in the understanding of the mineralogical, petrographic, geochemical, and structural features of spodumene-rich pegmatites (SRP) through the scientific and technical studies carried out on the Cachoeira Pegmatite Group, a specific

pegmatitic population of the Itinga Pegmatite Field (e.g., Sá, 1977; Afgouni and Sá, 1978; CorreiaNeves et al., 1986; Afgouni and Marques, 1997; Pedrosa-Soares et al., 2009, 2011, 2023; Romeiro, 1998; Quéméneur and Lagache, 1999; Romeiro and Pedrosa-Soares, 2005; Dias, 2015; Chaves et al., 2018; Luiz, 2023). The Cachoeira Pegmatite Group comprises a SRP swarm that has been mined at least since the 1970's by the Arqueana Company (Figure 7-10), followed by the production of spodumene ore in industrial scale by CBL since 1993 (Figure 7-11). It is yet the best characterized spodumene deposit in Brazil, providing solid information to support the mineralization model that was applied to the exploration work on the Bandeira deposit (Figure 7-4).

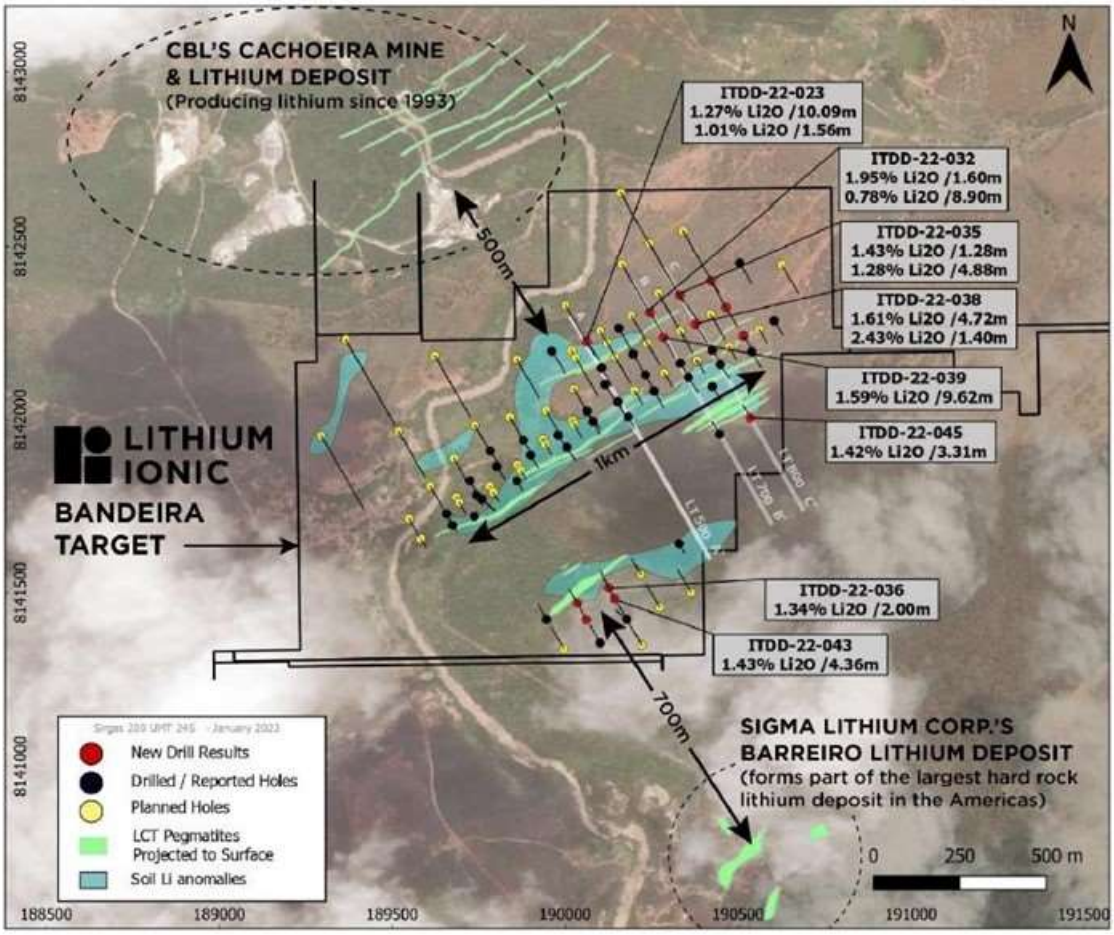

Figure 7-9 – Location of the Bandeira Deposit in Relation to the CBL's Cachoeira Mine and the Sigma's Barreiro Deposit

Source: Corporate Presentation, Lithium Ionic Corporation, March 2023, available at https://www.lithiumionic.com/projects/itinga-project/.

The typical SRP orebodies of the Cachoeira Pegmatite Group are non-zoned but rather inequigranular pegmatites composed of spodumene (on average 23 vol%), perthitic microcline, albite, quartz, and muscovite, generally totalizing more than 95% of the whole orebody volume. Montebrasite, beryl, cassiterite, columbite-tantalite, cookeite, zabuyelite and petalite are scarce accessory minerals.

The Cachoeira SRP cluster forms a pegmatite swarm characterized by a staggered (en-échelon)

spatial distribution of parallel to subparallel, locally branched orebodies showing lateral and vertical offsets among them (Figure 7-11 and Figure 7-12). They are roughly tabular bodies with lens-shaped terminations, ranging from decimeters up to 30 m in thickness orthogonal to dip, from a few meters to many hundreds of meters in length along strike, and up to many hundreds of meters downdip. The Cachoeira pegmatites were emplaced in the Salinas Formation that consists of banded cordierite-quartz-mica schist with intercalations of calcsilicate rock, recording P-T conditions suitable for SRP occurrence. In the Salinas Formation, the main host surfaces for pegmatites are the regional foliation (schistosity) S1 and the S2 spaced cleavage, although late joint surfaces can also host SRP bodies (Figure 7-10, Figure 7-11, and Figure 7-12).

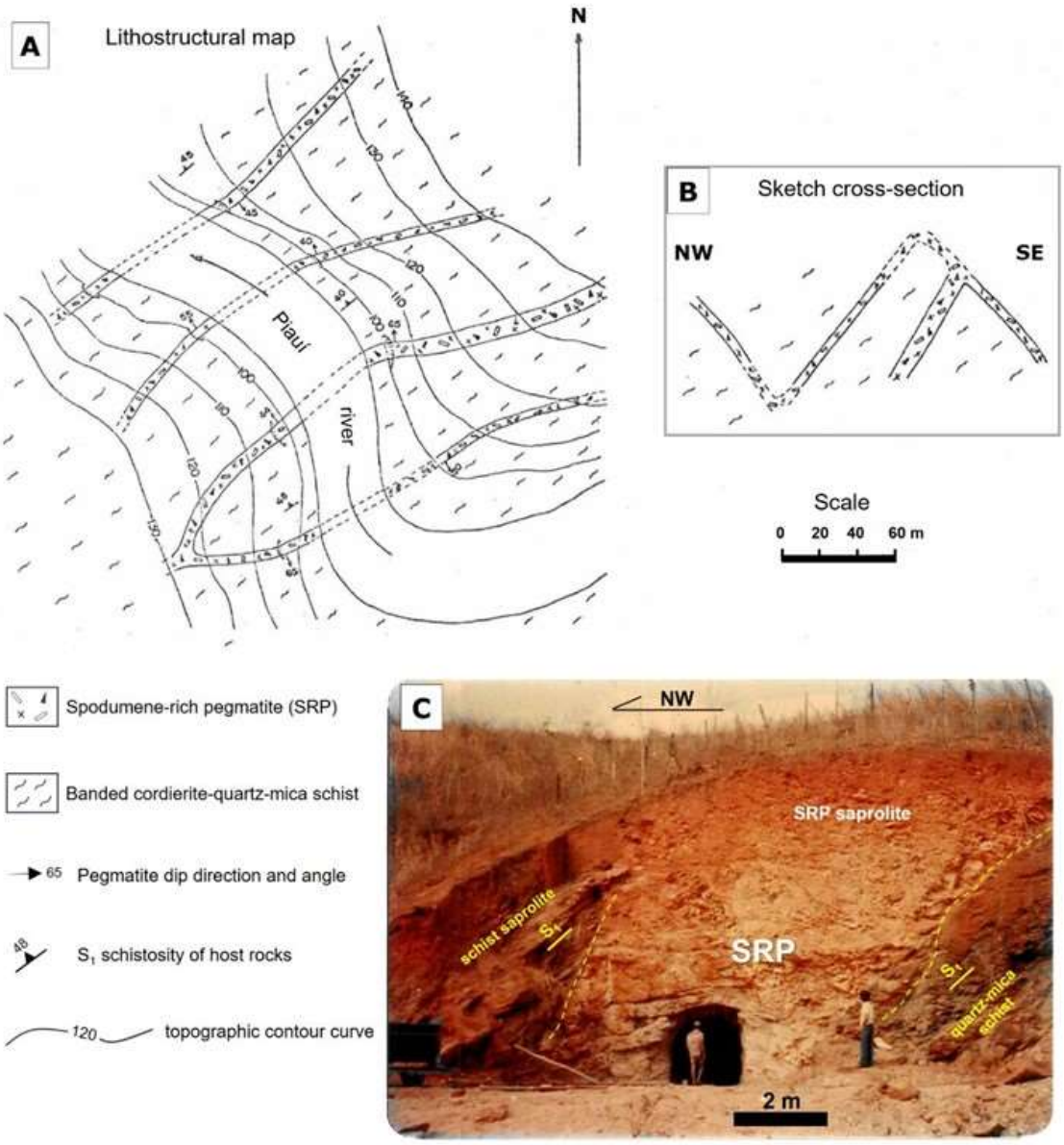

Figure 7-10 – The Cachoeira Mine in the Mid 1970's

Legend: A (map) and B (section) showing four NE-trending, parallel to sub-parallel, branched, tubular shaped, spodumene-rich pegmatites (SRP) both concordant with the NW-dipping S1 schistosity of host rocks and discordant with S1, (i.e., emplaced in the SE-dipping S2 spaced cleavage). C (photo) shows a concordant, c. 7 m thick SRP hosted by cordierite-quartz-mica schist, with both rocks increasingly weathered (saprolites to soils) towards the topographic surface.

Source: map, cross section, and photo adapted from Sá, 1977.

The tectonic structure of the Salinas Formation behaved passively during the intrusion of Li-rich magmas that crystallized as spodumene-rich pegmatites, which in turn do not record any evidence of ductile or brittle deformations (Figure 7-11 and Figure 7-12), except for small faults that locally cut pegmatite contacts and may be related to the latest D2 or DG deformations (Figure 7-12; see also section 7.2).

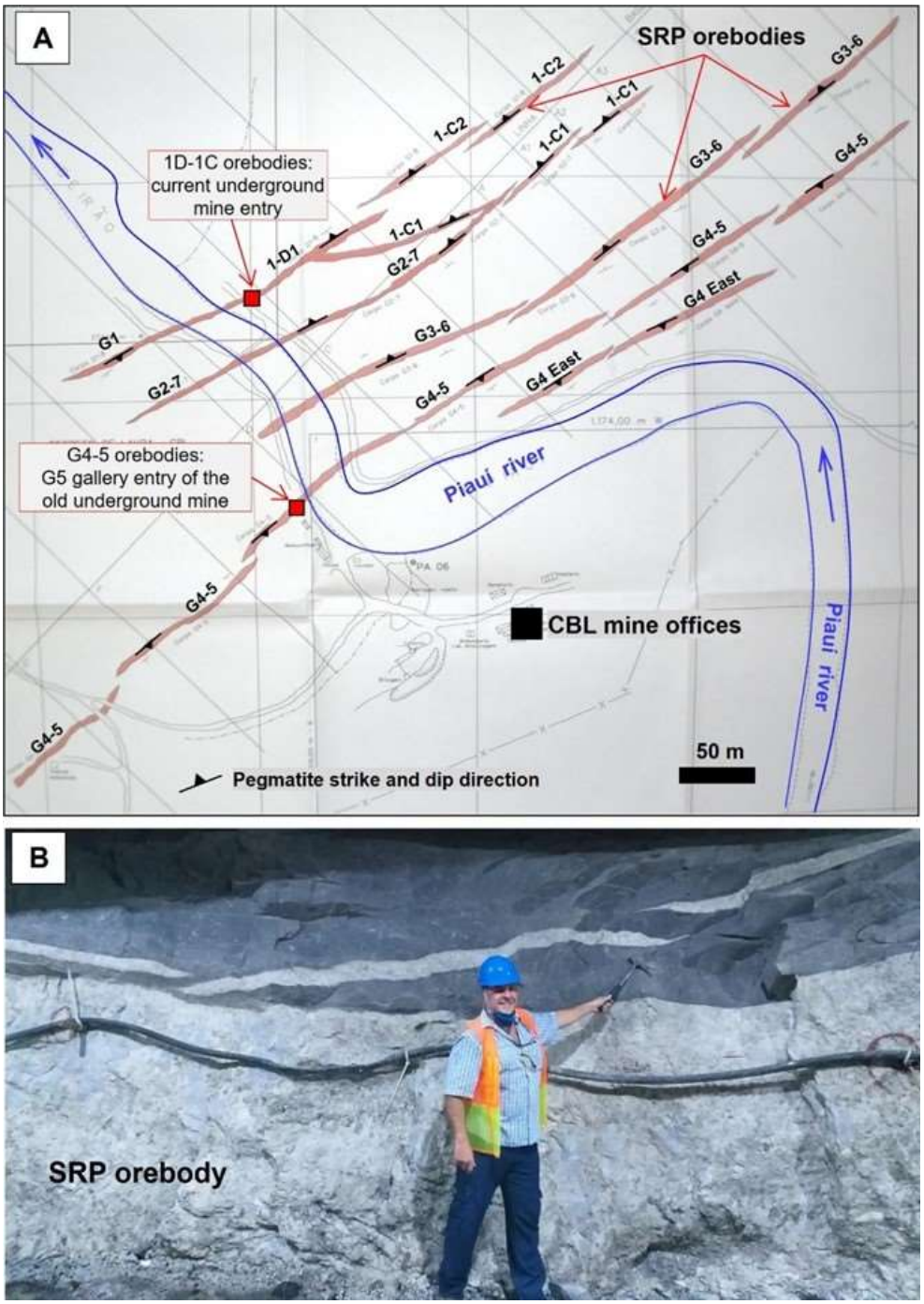

Figure 7-11 – Map of the Cachoeira Pegmatite Group in CBL's Mine Area

Legend: A) Showing the staggered (en-échelon) spatial pattern of parallel to subparallel, locally branched, NE-trending orebodies of spodumene-rich pegmatites (SRP, in light brown) with indications of mapped strike and dip directions of the pegmatite bodies. SRP concordant bodies, emplaced along the S1 schistosity, dip to NW. SRP discordant bodies, hosted by the S2 spaced cleavage, dip to SE. B) A fractal example of the en-échelon distribution pattern of SRP bodies shown by three smaller veins (above the main SRP orebody) in CBL's Cachoeira mine.
Source: adapted and updated from Romeiro, 1998; photo by A.C. Pedrosa-Soares, August 2022.

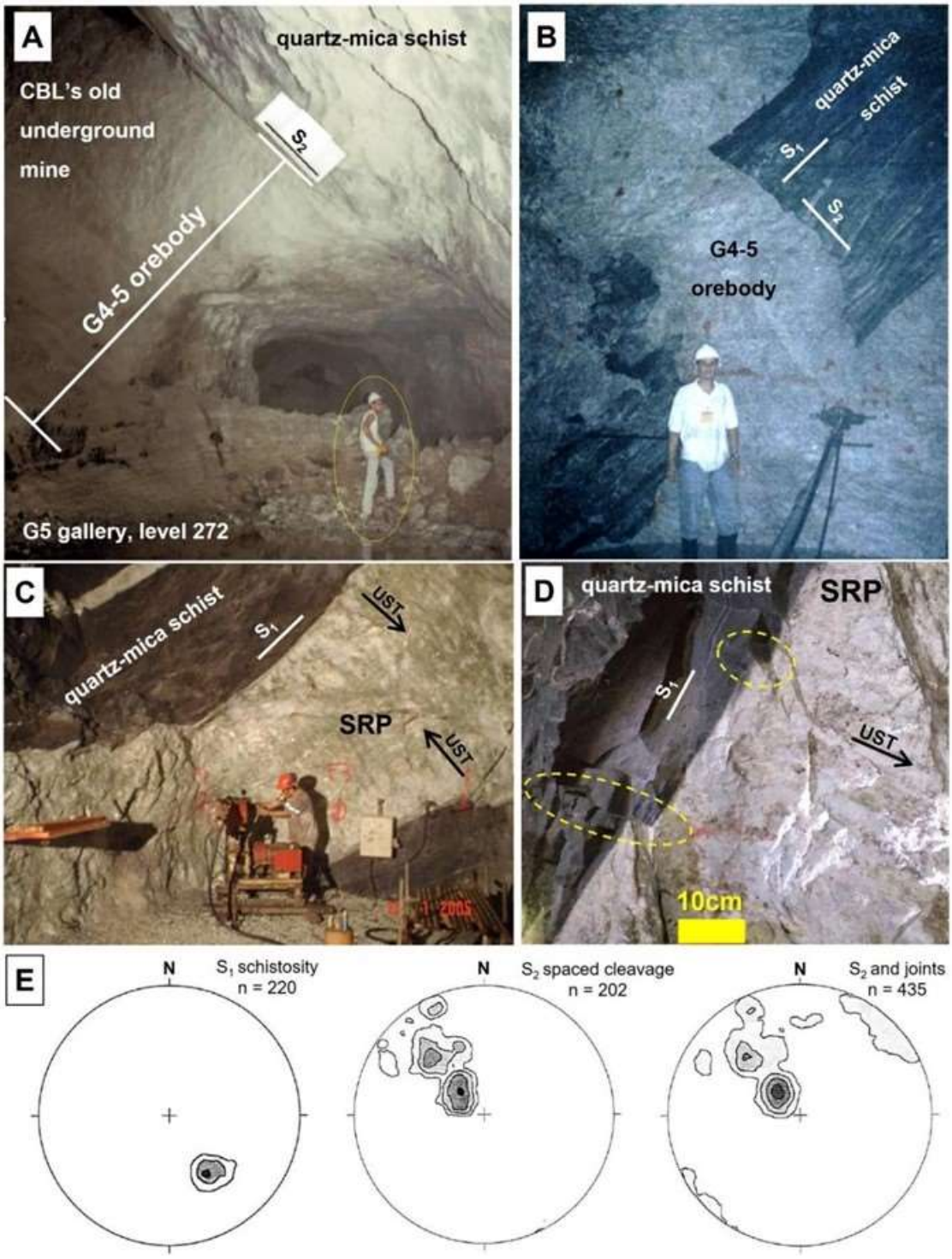

Figure 7-12 – Thirteen Photos from Spodumene-Rich Pegmatites (SRP) in the Cachoeira Underground Mine (CBL)

Legend: A) The G4-5 SRP in the G5 gallery, level 272, showing a discordant orebody (c. 7 m thick) hosted by the S2 spaced cleavage; B) A closing edge of the main G4-5 orebody, showing SRP branches cutting across the host quartz-mica schist; C) Mining front showing a concordant SRP orebody (1D/1C gallery) ranging from c. 3 m to more than 4 m thick, hosted by the S1 foliation dipping to NW, with unidirectional solidification texture (UST, black arrows) outlined by orientated greenish spodumene crystals orthogonal to the SRP contacts; D) Sharp lithological contact, concordant with S1, between a SRP and the host schist, showing small offsets along short brittle surfaces (yellow ellipses) and unidirectional solidification texture (UST, black arrow) outlined by oriented spodumene and feldspar; E) Stereograms (Schmidt projection, lower hemisphere) for the SRP host structures in the Cachoeira underground mine and surface outcrops showing that both S1 and S2 are Ne-trending but dip to opposite directions: S1 to NW and S2 to SE.

Source: A), B) photo from Romeiro, 1998; C), D) photo from Romeiro and Pedrosa-Soares, 2005; E) adapted from Romeiro, 1998.

Based on available information from the Cachoeira Pegmatite Group and CBL's underground mine (Figure 7-10 and Figure 7-12), a mineralization model for spodumene-rich pegmatites (SRP) was conceived to assist in the exploration work on the Bandeira target. After a soil geochemistry campaign, Li anomalies roughly parallel to the Cachoeira SRP swarm were revealed and, together with lithological and structural data from few outcrops, old diggings, and new exploration trenches (Figure 7-13) provided the basis for a very successful drilling campaign that discovered dozens of new SRP bodies rather close to each other from the near surface to more than 800 m in depth. The newly discovered Bandeira deposit comprises spodumene-rich orebodies, arranged along the same structural trend of Cachoeira's SRP swarm (Figure 7-14).

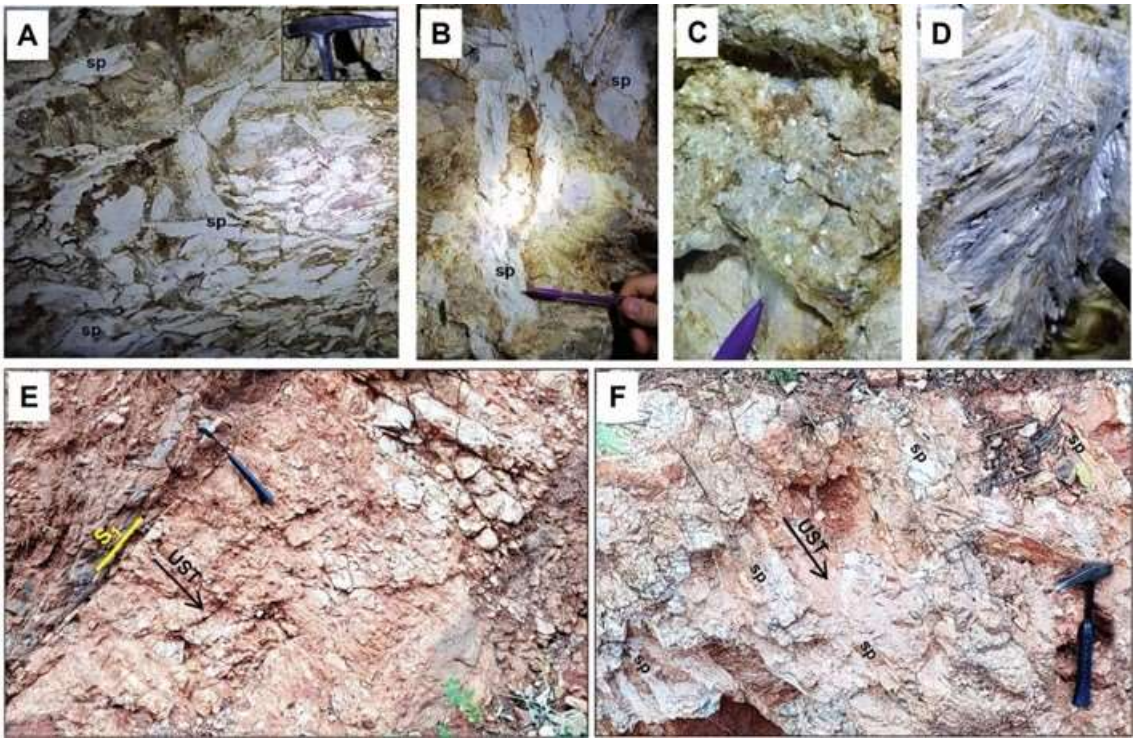

Figure 7-13 – Photos from Underground Galleries of an Old Digging for Gem Prospecting

Legend: showing a rather weathered pegmatite very rich in pseudomorphs of spodumene (sp) replaced by white clay (A and B), with local mica-rich rich metasomatic bodies, small miarolitic cavities and rare lepidolite books (D) at the pegmatite top. A new trench (E) revealed another rather weathered pegmatitic body concordant with the S1 foliation of the host quartz-mica schist, showing pseudomorphs of tabular-shaped spodumene (sp) replaced by white clay (F), depicting unidirectional solidification texture (UST) orthogonal to the pegmatite/schist contact.
Source: Garimpo in Brazilian Portuguese.

Following the regional NE-SW structural trend, the Bandeira deposit comprises SRP swarms of NE-striking orebodies mostly hosted by and concordant with the NW-dipping schistosity (S1), but also some discordant SRP emplaced along the SE-dipping fracture system (S2 spaced cleavage), as well as a few SRP bodies hosted by late flat-lying joints (Figure 7-14). The Bandeira pegmatites are tabular bodies with convex lens-shaped terminations, arranged in tight and staggered (enechellon) swarms, locally with branched connections linking ore bodies. Single SRP bodies normally reach hundreds of meters in length along the strike, ranging in thickness from a few decameters to decimeters, with the discordant SRP bodies tending to be thicker than the concordant ones. With known downdip-width up to 800 m, several Bandeira SRP bodies remain open in depth. The exploration drilling work revealed two main SRP swarms in the Bandeira

deposit: i) the northern swarm, with thicker, longer, and wider SRP bodies concordant to the S1 foliation of host rocks; and ii) the southern swarm, with somewhat smaller SRP bodies (Figure 7-14).

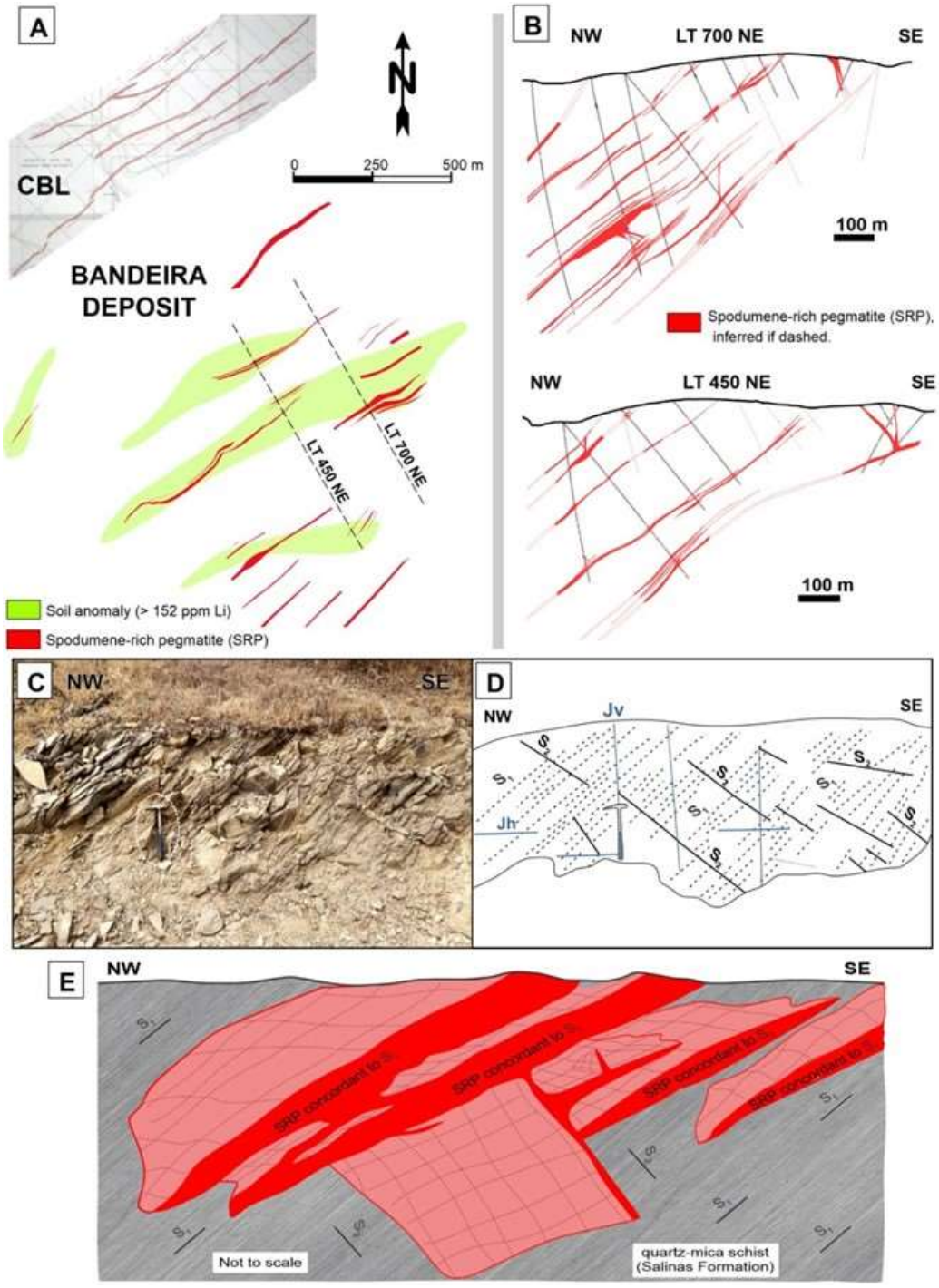

Figure 7-14 – Spodumene Pegmatites interpretations

Legenda: A) simplified map showing the distributions of Li anomalies in soil and drilled SRP bodies projected to surface in the Bandeira deposit, and CBL's SRP swarm (see Figure 7-11); B) simplified cross sections showing the SRP swarm discovered in depth by Lithium Ionic after exploration work; C) and D) outcrop and structural sketch illustrating the tectonic surfaces of the country rocks (Salinas Formation) that host pegmatites in the Bandeira deposit: S1, regional ductile foliation (schistosity); S2, post-S1 spaced cleavage; Jh, late horizontal joints; and Jv, late vertical joints; E) cartoon illustrating a model for the spatial distribution and lateral relations of SRP orebodies in the Bandeira deposit.

Source: map and sections for A and B from Lithium Ionic reports, and CBL map from Romeiro, 1998; C, D, and E by Geologist Anderson Victoria.

The host rocks of SRP orebodies in the Bandeira deposit are banded to laminated cordierite-quartz-mica schists, locally containing disseminated sulphide and/or graphite-rich bands, with intercalations of massive calcsilicate rocks (Figure 7-15 and Figure 7-16). Most cordierite forms ellipsoidal (egg-shaped) stretched poikiloblasts syn-kinematic to the regional S1 schistosity (Figure 7-15).

The banded to laminated quartz-mica schists represent metamorphosed sand-mud sediments, and the calcsilicate rocks are metamorphosed Ca-rich carbonate-mud sediments (marls). They show sharp contacts with the SRP orebodies that generally are concordant to the regional S1 foliation (often parallel to the compositional layering S0) but are also hosted by the S2 cleavage or foliation (Figure 7-16). The host schists may be enriched in decussate muscovite and/or biotite, black to green tourmaline, and recrystallized cordierite along narrow (cm to dm) fringes of contact metamorphism imposed by pegmatites (Figure 7-17). Although the host schists may be anomalous in lithium content close to pegmatites, they show no Li-ore mineral.

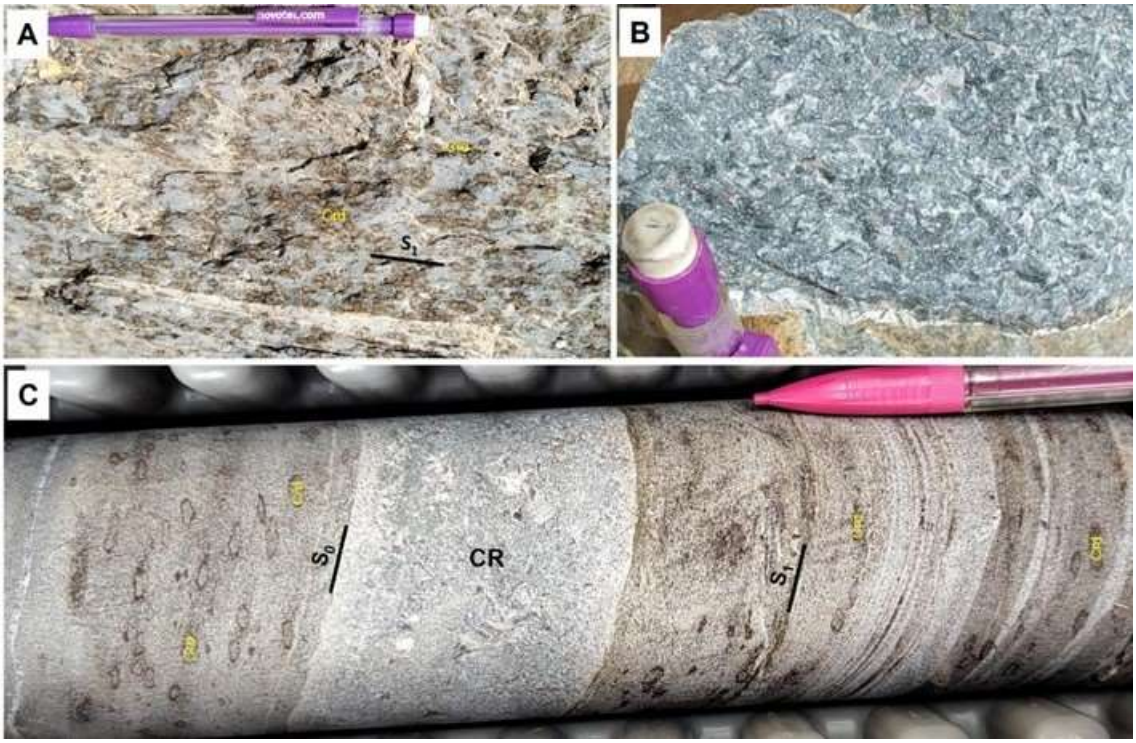

Figure 7-15 – Photos from host rocks of spodumene-rich orebodies in the Bandeira deposit

Legend: A) partially weathered cordierite-quartz-mica schist rich in poikiloblasts (dark spots) of eggshaped (ellipsoidal) cordierite (Crd) crowded of biotite and/or quartz inclusions and coronated by biotite; B) calcsilicate rock with porphyroblasts of amphibole (dark green) and grossular garnet (light pink) within a massive matrix (greenish gray) mostly composed of quartz and plagioclase; C) drill core segment showing the banded to laminated cordierite-quartz-mica schist with ellipsoidal cordierite (Crd; light spots coronated by biotite), light-colored quartz-rich laminae, and an intercalation of calcsilicate rock (CR).

The Bandeira spodumene orebodies show a rather simple mineralogical assemblage (Figure 7-16 and Figure 7-17), consisting of medium - to very coarse-grained spodumene phenocrysts, reaching up to 35 vol% on average, within a fine - to medium-grained matrix mostly composed of albite, perthitic K-feldspar (microcline), quartz, muscovite, and petalite, summing up to 95 vol% of the total matrix. The scarce accessory (mainly montebrasite, and Nb-Sn-Ta oxides) and

secondary minerals (cookeite, sericite, zabuyelita, Fe-Mn oxides, clay minerals) generally comprise less than 5 vol% in total. In drill cores, the spodumene crystals are mostly free of hydrothermal and weathering alterations and very poor in mineral inclusions (Figure 7-16 and Figure 7-17)). Conversely, surface outcrops, shallow diggings and exploration trenches cutting SRP bodies generally show weathered spodumene (Figure 7-13), forming pseudomorphs composed of white clay (kaolinite and montmorillonite). Rare spodumene-quartz intergrowth (SQUI) may be found associated with spodumene crystals (Figure 7-17). Petalite has been found in SRP's drill cores and thin sections, mostly occurring in the matrix as very fine- to fine-grained (sub-millimetric to 1 cm) crystals (Figure 7-17) and, more rarely, as coarser crystals locally found in rather restricted intervals.

The thicker SRP bodies may show a lithium-barren and thin marginal zone rich in albite, generally rather discontinuous, followed inwards by a thick internal zone rich in disseminated spodumene (although spodumene may also be more ROM in some domains than others along the internal zone). Owing to the upward migration of H2O-rich fluids, flat-lying SRP sections close to the hanging-wall contact, as well as the top termination (“head”) of high-angle dip bodies, may show metasomatic units with miarolitic cavities that partially replaced the primary mineral assemblage. Many SRP bodies lack the external lithium-barren zone, showing disseminated spodumene along virtually the whole orebody (Figure 7-16 and Figure 7-17)). Unidirectional solidification textures outlined by tabular to telescope-shaped spodumene crystals are common in the Bandeira’s SRP orebodies. Thin albite-rich pegmatites, barren to poor in lithium, are also found in the Bandeira pegmatite swarms.

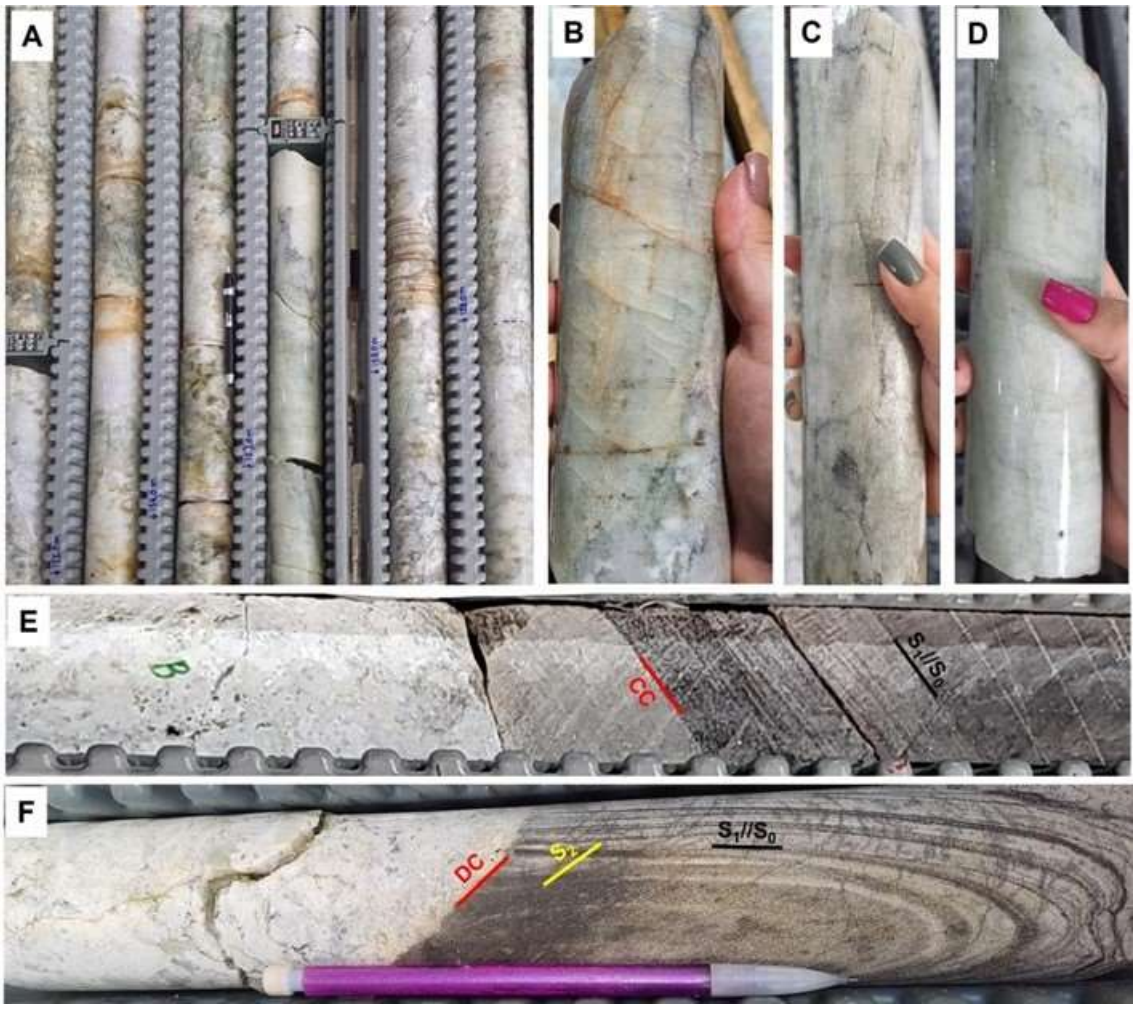

Figure 7-16 – Drill Core Samples from Spodumene-Rich Orebodies and Their Host Rocks in the Bandeira Deposit

Legend: A) Segment of a non-zoned SRP body with medium - to coarse-grained greenish spodumene disseminated in the quartz-albite-microcline-muscovite matrix; black minerals in spots and fracture fillings are Nb-Sn-Ta oxides and graphite. B to D) Features of roughly tabular, greenish to white spodumene crystals free of or poor in inclusions. E) Concordant contact (CC) between albite-rich pegmatite border and laminated quartz-mica schist; the host surface is the regional schistosity S1 parallel to the compositional (sedimentary) layering S0. F) Discordant contact (DC) between albite-rich pegmatite border and laminated cordierite-quartz-mica schist; the host surface is the S2 cleavage/foliation.

Source: photos by Geologist Fabiana Guimarães.

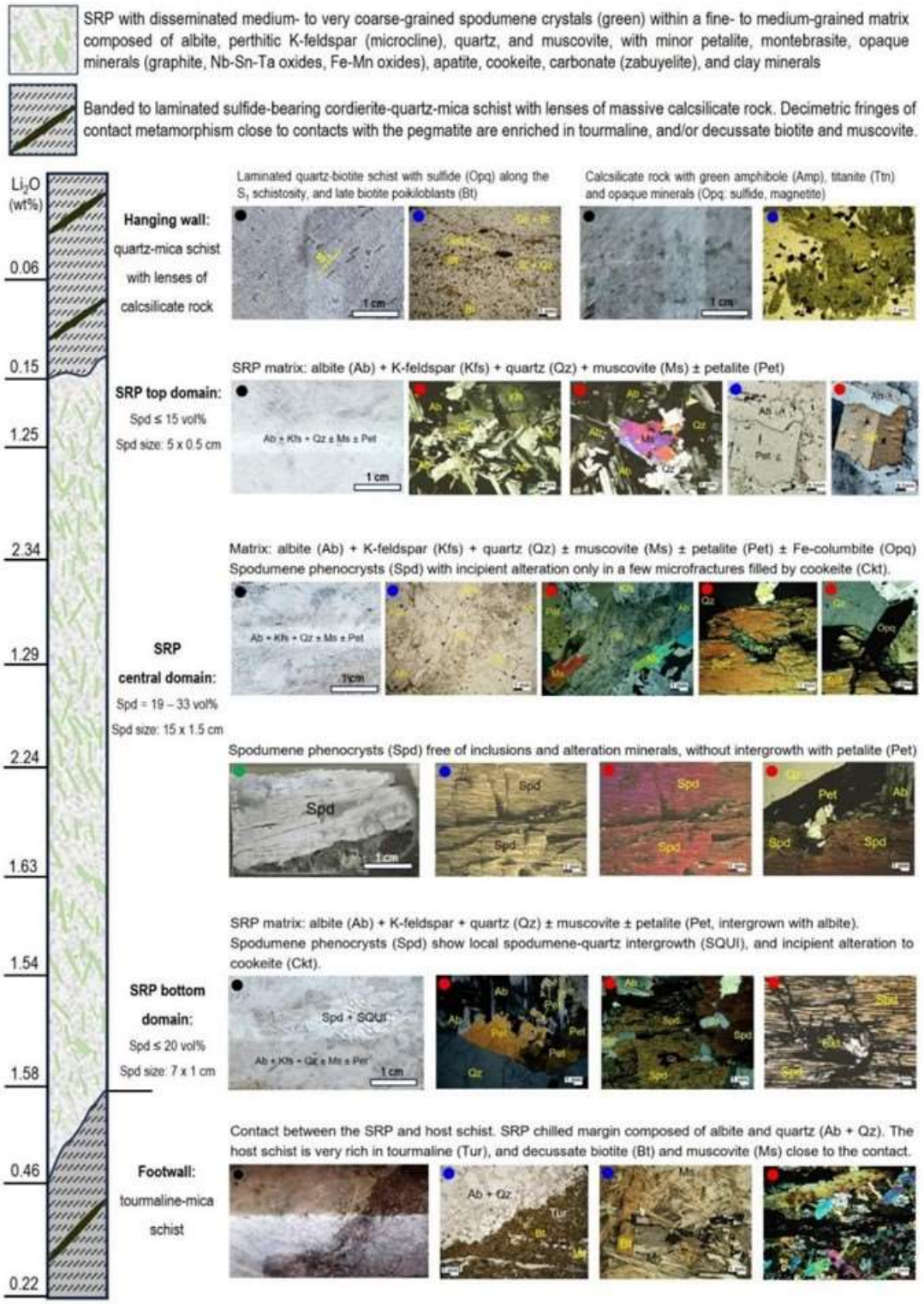

Figure 7-17 – Characterization Illustrated Summary for a Typical Spodumene-Rich Pegmatite (SRP) of the Bandeira Deposit, Based on Intercept with 6,75 m Thick and 1.99 wt% Li2O

Legend: pegmatitic textures based on average grain size (cm): fine < 2.5; medium = 2.5–10; coarse = 10– 30; and very coarse > 30. Spd size (e.g., 15 x 1.5 cm) based on average length and thickness of spodumene crystals. Photo types indicated by dots: black, photo from unpolished sample; blue, photomicrography under parallel polarizers light; green, photo from polished thin section; red: photomicrography under crossed polarizers light. Drill core and thin sections described by Geologists Fabiana Guimarães and Laura Wisniowscki, respectively.
Source: Pedrosa-Soares et al., 2023.

8 DEPOSIT TYPES

The following text and illustrations were compiled from Pedrosa-Soares et al. (2023) and complemented with data from Lithium Ionic public and internal reports, if not otherwise specified.

According to the most accepted petrologic-metallogenetic classification of pegmatites, published by Cerný (1991) and updated by Cerný and Ercit (2005) and Cerný et al. (2012), all the spodumene-rich pegmatites found within the Bandeira deposit, as well as in the whole Cachoeira Pegmatite Group, belong to the rare element class, Li subclass, and albite-spodumene type.

Although generally included in the LCT (Lithium-Cesium-Tantalum) family, the non- to poorly zoned spodumene-rich pegmatites (SRP) found in the Bandeira deposit, as well as all the orebodies mined in CBL's Cachoeira Mine since the 1990's (Romeiro and Pedrosa-Soares,

2005), the Xuxa and other spodumene-rich deposits of Sigma Lithium (Sá, 1977; Delboni et al., 2023), and the Outro Lado deposit of Lithium Ionic, are rather poor both in Ta and Cs when compared with the complex zoned LCT pegmatites (e.g., Generosa, Jenipapo, Murundu, Urubu and others) found in the Itinga Pegmatite Field (cf. Sá, 1977; Romeiro, 1998; Quéméneur and Lagache, 1999; Dias, 2015) and elsewhere (e.g., Cerný 1991; London, 2008; Cerný et al., 2012).

The SRP deposits consist of non-zoned to poorly zoned spodumene-rich pegmatites with spodumene reaching up to 35 vol% on average, and the total modal content of spodumene, albite, K-feldspar, quartz, and white mica (muscovite and/or Li-rich mica) summing up more than 90 vol% of the whole body. Therefore, SRP bodies are very poor in accessory minerals, which are generally represented by Li-micas, Li-phosphates, Nb-Sn-Ta oxides, cookeite, carbonate and graphite. They are also poor in secondary (metasomatic) units due to their rather fluid-poor (anhydrous) nature (Figure 7-12, Figure 7-16, and Figure 7-17).

As a corollary, the scarcity of rare elements, except for lithium, imposes constraints on the geochemical prospecting methods to be applied on searching for spodumene-rich deposits. Conversely, the high Li content (1.4 wt% Li2O on average) in SRP-type magmas promotes a significant decrease in the crystallization temperature and viscosity of the silicate melt, leading to the high mobility that allows such a Li-rich magmas to crystallize as very large but relatively narrow SRP bodies, with hundreds to thousands of meters in length and width, but only decimeters to a few decameters in thickness.

Therefore, for prospection and exploration work related to spodumene-rich deposits, it is very important to distinguish between the non- to poorly zoned spodumene-rich pegmatites (SRP, i.e., pegmatites of the albite-spodumene type) and the complex zoned LCT pegmatites.

9 EXPLORATION

Fieldwork was conducted in the Bandeira deposit with an approach encompassing chip rock sampling, soil sampling, a trench program, structural analysis and a drilling program. These activities aimed to achieve a more profound comprehension of the local geology and the identification of potential spodumene-rich pegmatites.

9.1 Chip Rock Sampling

Despite the extensive residual soil cover, the field mapping led to the recognition of pegmatites in artisanal mines (garimpos), in situ outcrops or fragments dispersed on the surface. Spodumene crystals were only identified in pegmatites found in artisanal mines and surrounding areas. The chip rock map (Figure 9-1) shows the location of each collected sample, with their respective lithium content (Li ppm), and the location of the outcropping pegmatites, mineralized in spodumene or not.

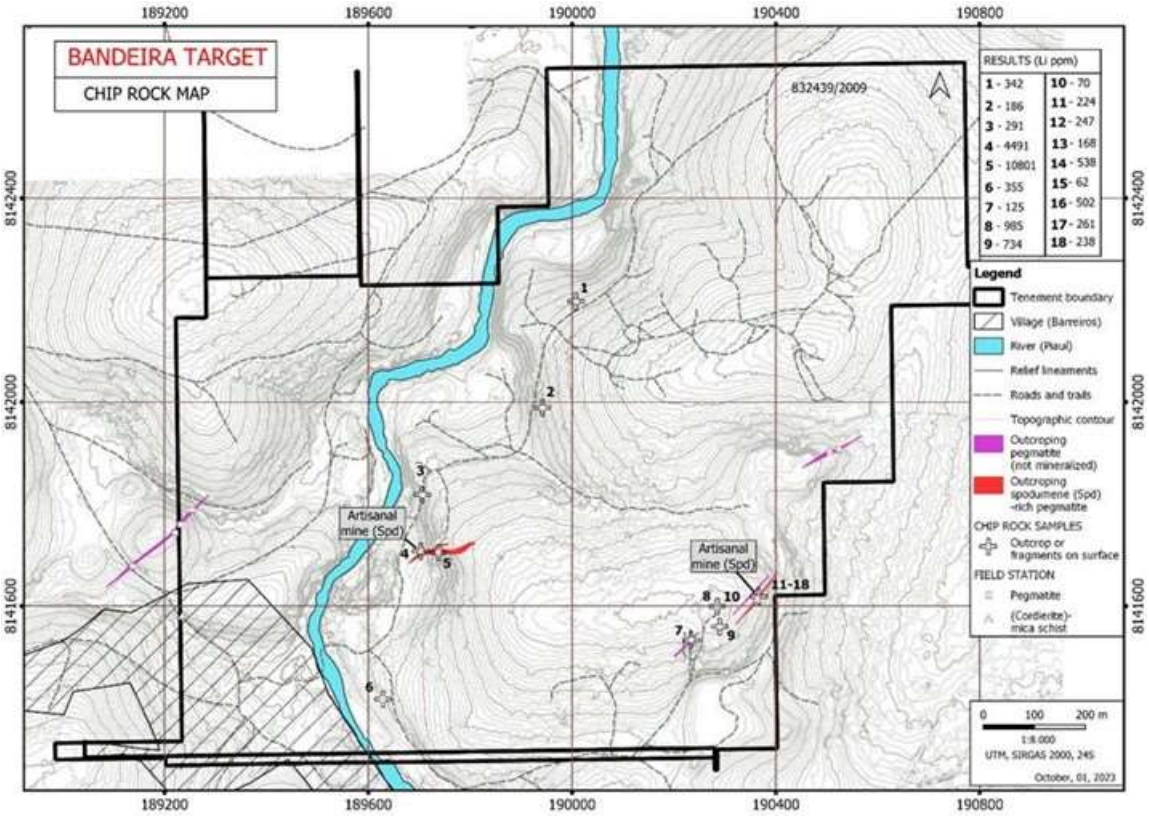

Figure 9-1 – Chip Rock Map in the Bandeira Deposit Emphasizing the Distribution of Each Collected Sample [Li (ppm)] and the Regions Where the Pegmatites are Exposed on the Surface

Source: Lithium Ionic 2024

9.2 Soil Sampling Program

The soil program in the Bandeira area was conducted in two distinct campaigns. In the first survey, the lines were oriented along the azimuth N120° and were spaced at regular intervals of 250

meters. Within each of these lines, samples were collected every 50 meters. In the second campaign, the lines were oriented at N150°, were spaced at regular intervals of 150 meters, and the samples were collected every 25 meters.

A total of 537 samples were collected in the Bandeira area, and the lithium content in the soil varied from 10 ppm to 573 ppm. Calculations based on the distribution of the results indicated a subdivision of the content as low grade (< 69 Li ppm), low to moderate grade (70-107 Li ppm), moderate to high grade (108-152 ppm), and high grade (> 153ppm). Based on the distribution of the results, it was possible to interpret at least five high-grade anomalous zones that represent more favourable spots to prospect spodumene-rich pegmatites (Figure 9-2). These anomalous regions are strongly oriented along the NE-SW direction, which is the same strike of the regional foliation and the mapped pegmatites in the Bandeira area and adjacent region.

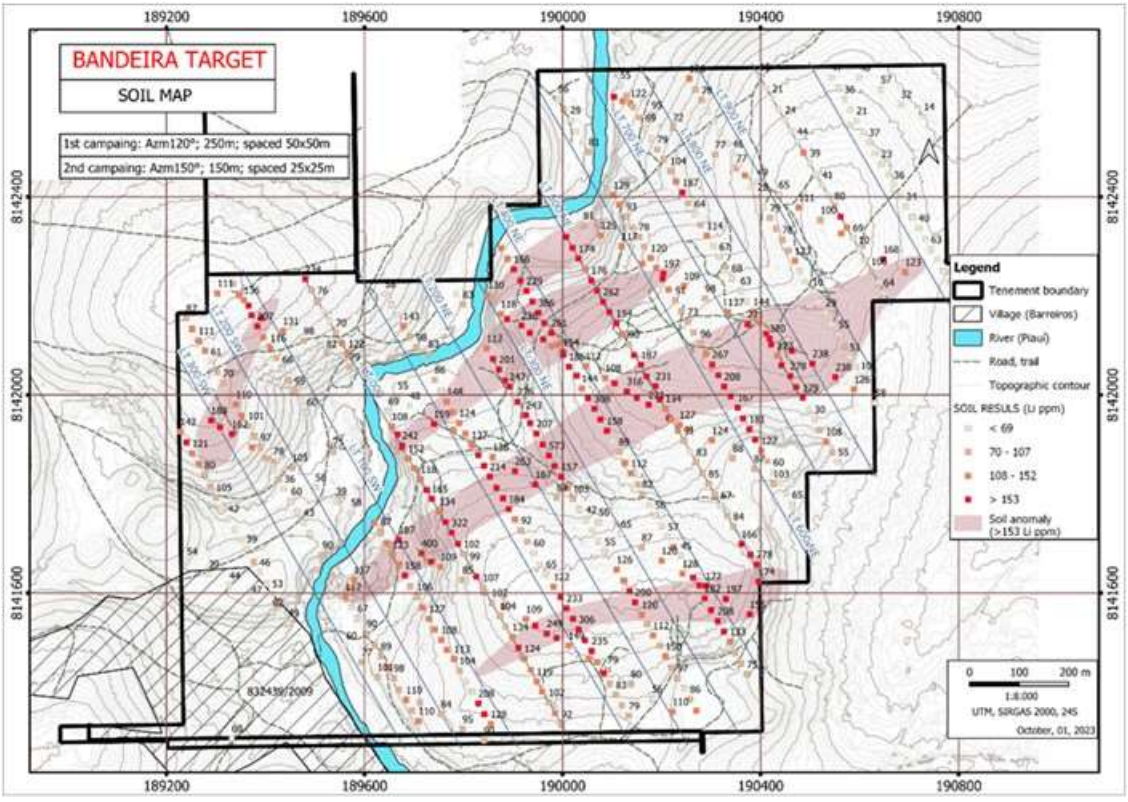

Figure 9-2 – Soil Geochemical Map of the Bandeira Deposit

Legend: the Remarkable NE-SW Anomalous Trend coincides with the Spodumene-Rich Pegmatites' Direction.
Source: Lithium Ionic 2024

9.3 Trench Program

After the soil geochemistry survey, a trench program was devised to investigate the anomalous areas. A total of 26 trenches were executed, totaling 1733 m of excavated lines (Table 9-1). The trenches were preferably positioned on top of the soil anomalies and the majority were positive, with pegmatite intercepts (Figure 9-3). Due to the high weathering, the exposed pegmatites are very decomposed in some trenches, exhibiting a characteristic whitish colour that shows a significant contrast with the horst schist (see an example of trench ITTRE-22-006 in Figure 9-4 a

and b). These pegmatites are friable, and it was possible to diagnose only quartz, kaolin and flake muscovite. In other trenches, however, it was possible to observe more preserved pegmatites, with visible spodumene centimetric crystals (see an example of trench ITTRE-22-001 in Figure 9-4 c and d). Independent of the conservation state, as part of the procedure, every pegmatite higher than 30cm mapped in the trench was sampled to verify the Li content (see channel sampling line on the pegmatite excavated in trench ITTRE-22-001 shown in the scheme of Figure 9-4 e).

In addition to confirming the presence of pegmatites and studying their mineral composition, the trenches played an important role in determining the strike and dip of the dikes. This valuable information contributed significantly to the mapping of the area and provided a higher level of confidence in planning the boreholes for the drilling campaign.

Table 9-1 – Summary of the Trenches Executed in the Bandeira Deposit

Source: Lithium 2024

TRENCH	X	Y	Z	AZIMUTH (°)	DIP (°)	LENGHT (m)
ITTRE-22-001	189772	8141689	296	308	0	43
ITTRE-22-002	190395	8141705	304	155	0	67
ITTRE-22-003	190156	8142046	336	150	0	41
ITTRE-22-003B	190158	8142055	336	146	0	11
ITTRE-22-004	189960	8141898	298	155	0	45
ITTRE-22-005	190401	8142141	343	151	0	47
ITTRE-22-006	190451	8142056	343	150	0	52
ITTRE-22-007	190292	8142082	340	149	0	50
ITTRE-22-008	190055	8141994	324	150	0	79
ITTRE-22-009	189941	8142179	325	150	0	74
ITTRE-22-010	189888	8142019	279	150	0	91
ITTRE-22-011	190001	8141581	324	150	0	140
ITTRE-22-012	190077	8142201	311	149	0	51
ITTRE-22-014	190280	8141600	325	150	0	53
ITTRE-22-015	190480	8141902	317	150	0	8
ITTRE-22-016	190124	8141624	353	150	0	66
ITTRE-22-017	190319	8142037	335	150	0	109
ITTRE-22-018	190189	8141789	339	150	0	102
ITTRE-22-020	190543	8142143	340	150	0	51
ITTRE-23-013	189710	8141979	278	150	0	78
ITTRE-23-014A	190244	8141651	324	150	0	53
ITTRE-23-019	190174	8141686	321	150	0	95
ITTRE-23-021	189819	8141408	350	150	0	98
ITTRE-23-023	189335	8141926	350	330	0	70
ITTRE-23-024	189978	8142317	275	150	0	67
ITTRE-23-025	190214	8142105	336	150	0	92
Total						**1733**

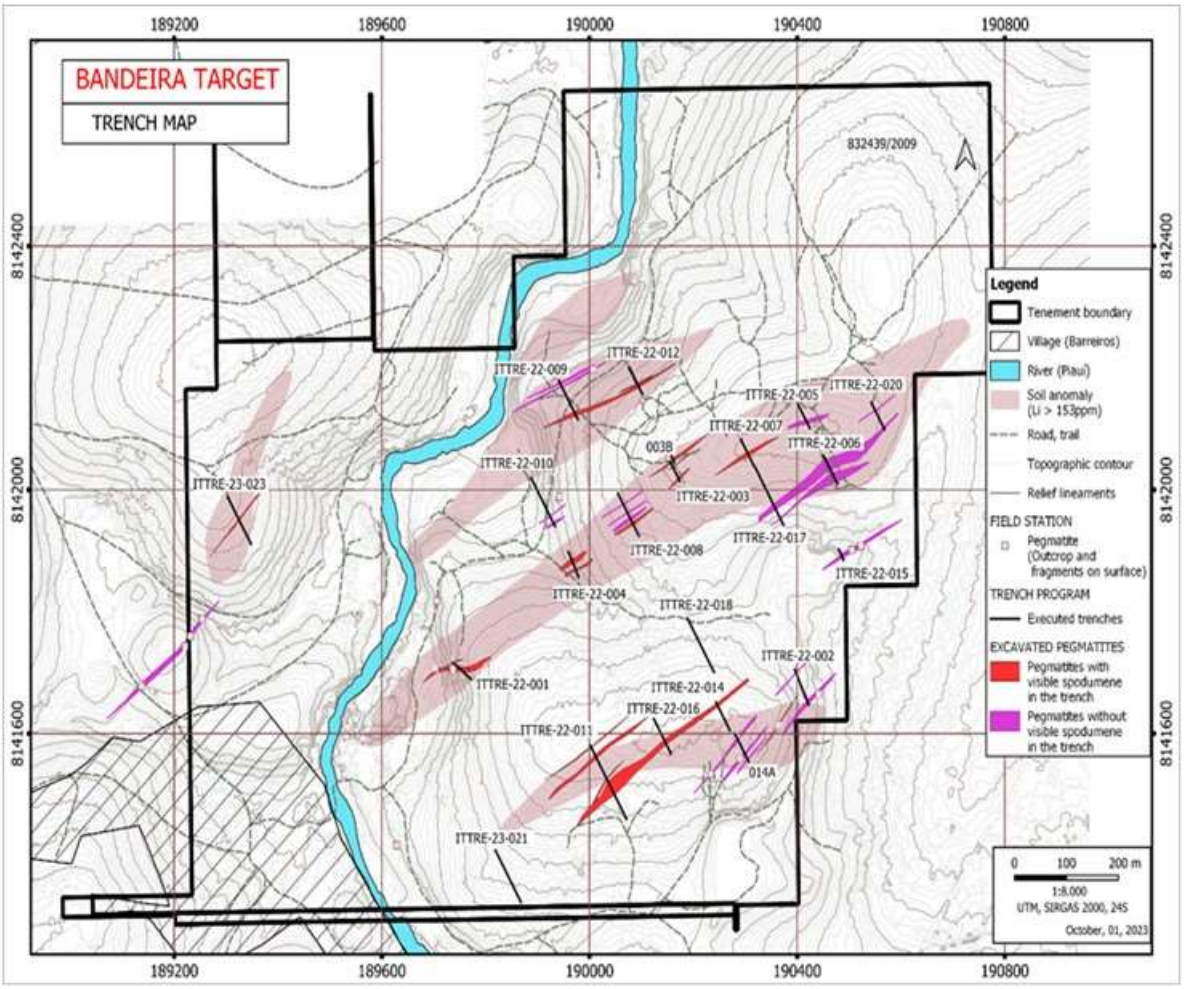

Figure 9-3 – Trench Map of the Bandeira Deposit

Legend: twenty-two trenches were executed, preferably in the soil anomalous region. Most of them intercepted pegmatites.

Source: Lithium Ionic 2024

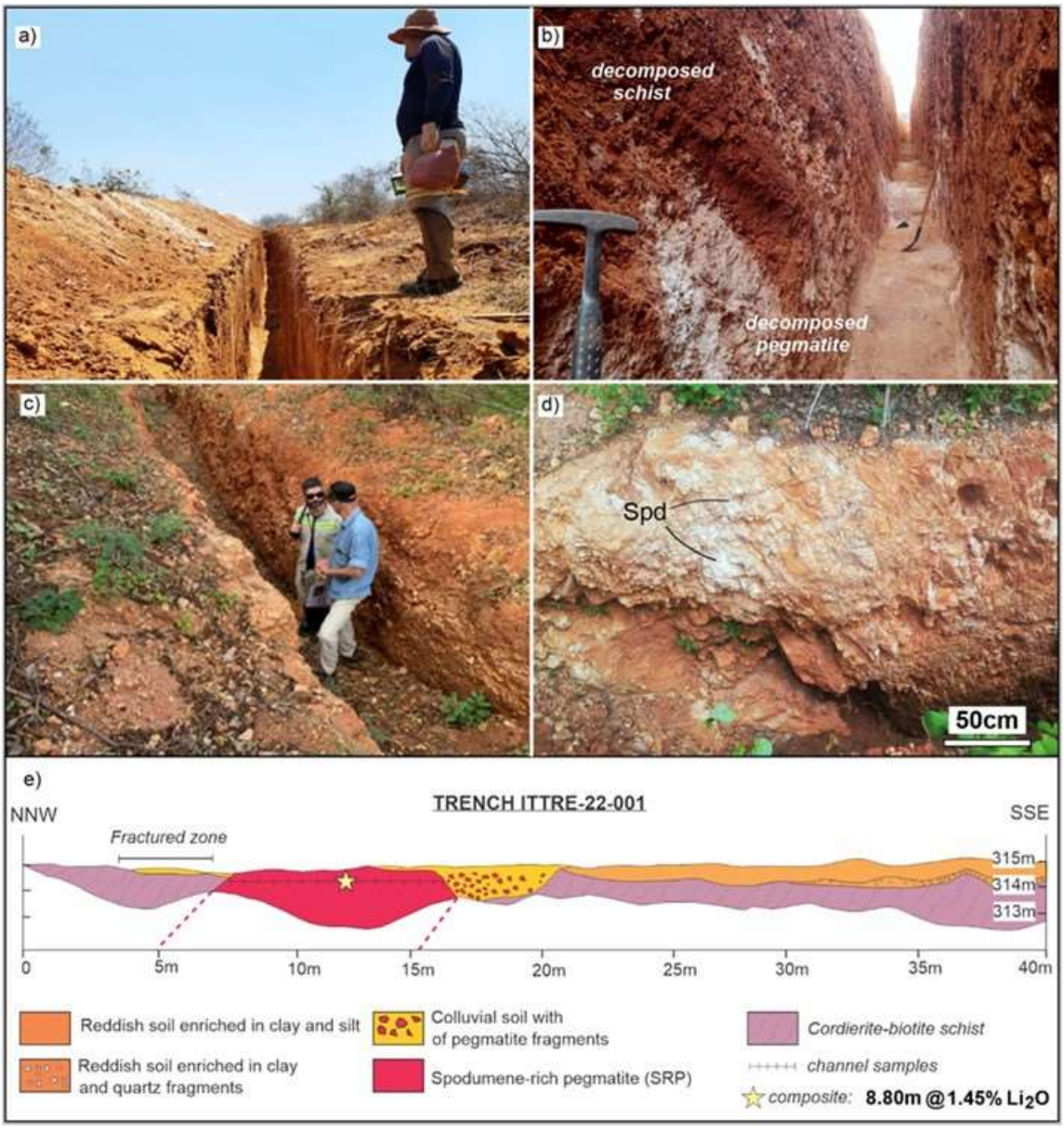

Figure 9-4 – Trenches

Legend: (a-b) photo of the trench ITTRE-22-006 and detail of the highly decomposed excavated whitish pegmatite contrasting to the host reddish decomposed schist; c-d) general aspect of the trench ITTRE-22-001 and detail of the spodumene crystals in the excavated pegmatite; e) scheme of the trench ITTRE-22-001 emphasizing the mapped units in the trench and the channel samples collected on the spodumene-rich pegmatite.
Source: a-b) UTM: 190451/ 8142056; SIRGAS 2000, 24S); c-d) UTM: 189772/ 8141689; SIRGAS 2000, 24S.

9.4 Structural Analysis

Although lacking outcrops, the few exposures of mica schists from the Salinas Formation are very relevant and helpful to understanding the structures in the Bandeira deposit. Ductile and brittle structures are recognized. The ductile structures were produced during the progressive metamorphism related to the syn-collisional phase of the Araçuaí orogen. In contrast, the brittle structures are younger and have been interpreted as related to the gravitational collapse of the orogen during the post-collisional phase. The structural map of the Bandeira target (Figure 9-5) shows the distribution of the structures and the projection of the non-exposed pegmatites. In that case, the attitude of each body was measured considering the interpreted geological model.

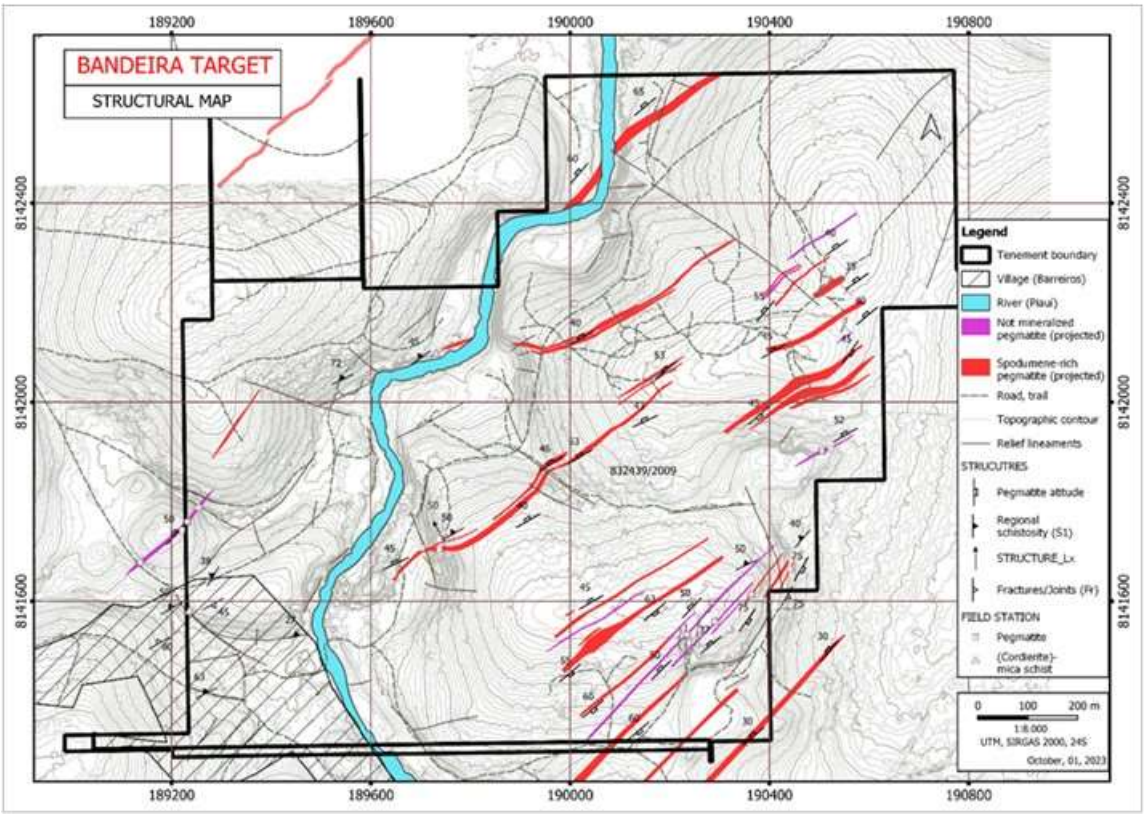

Figure 9-5 – Structural Map of the Bandeira Target Emphasizing the Distribution of the Mapped Structures

Source: Lithium Ionic 2024

The pegmatite veins are projections of the known intrusions based on the intercepts in drillholes. The attitude of each vein is based on the modelled veins.

The dominant ductile structural feature is the pervasive regional schistosity (S1), which exhibits a consistent orientation in both strike and dip across the entire area (modal: N50E/45NW). The stretched lineation (Lx) complements the ductile structural framework, often manifested as elongated micas or ellipsoidal cordierite porphyroblasts crystalized along S1. This lineation is downdip and indicates tectonic transport along the NW-SE direction.

The brittle structures are represented by a series of fractures, occasionally joints, that intersect the S1 schistosity and seem part of a conjugate system (Figure 9-6). Each structure was denoted as either F1 (fractures with a moderate dip to the southeast) or F2 (sub-vertical fractures), and their presence and prevalence may vary depending on the outcrop. The F1 structure seems more pervasive in the entire region, which also allows the interpretation of these structures as related to the development of a cleavage fracture system (secondary foliation S2). All these planar structures in the Bandeira area (S1, F1 and F2) consistently display a standard orientation along the NE-SW strike, with variations only in their dip angles.

Understanding the structural patterns in the host rocks is crucial for prospecting pegmatites since these structures serve as the surfaces that guide the migration of the silicate magmatic residues. Consequently, they profoundly influence the shape and continuity of the pegmatite bodies enriched in spodumene in the Bandeira area.

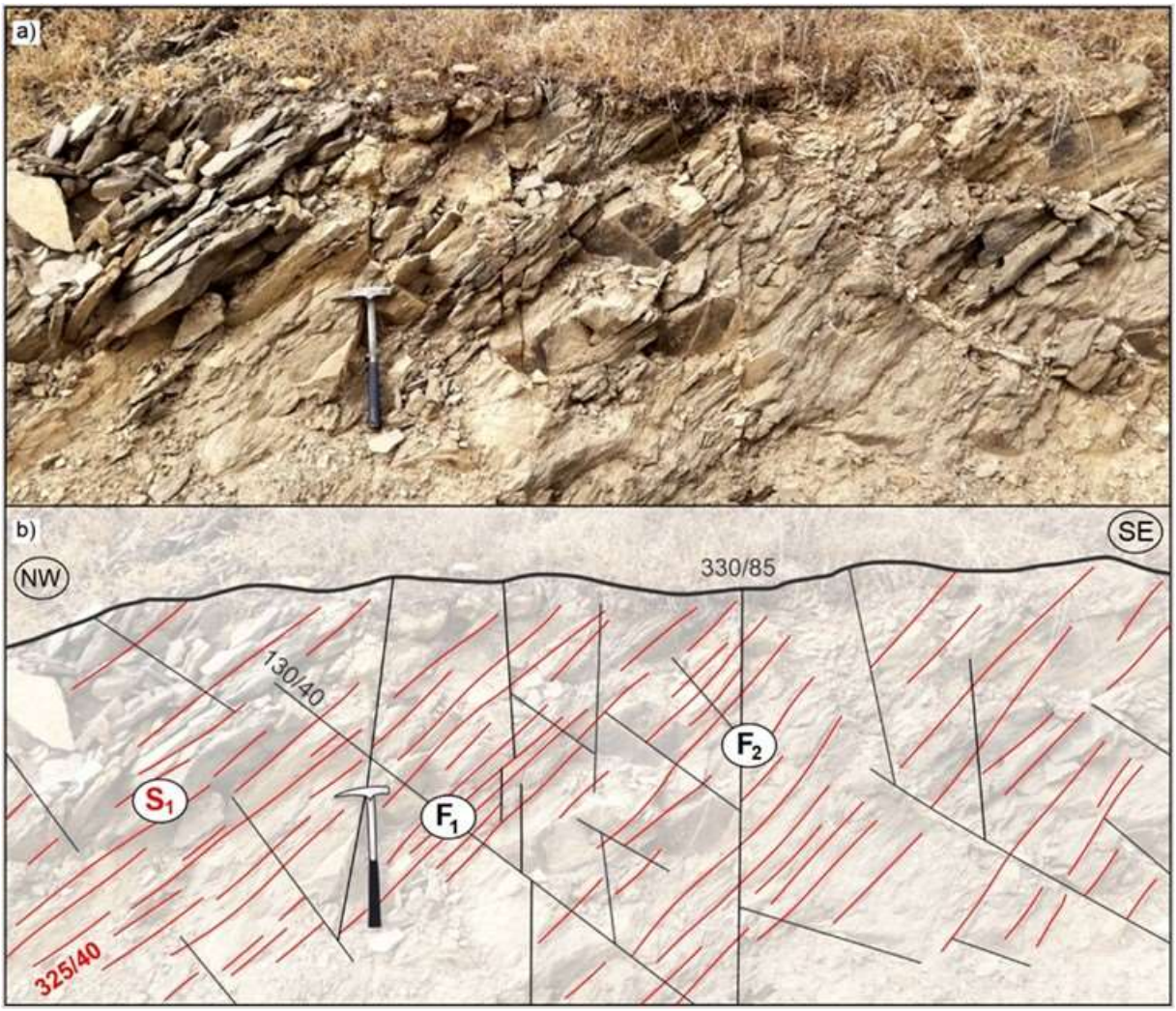

Figure 9-6 – Structural Planes in Bandeira Outcrop

Legend: a) fractured biotite-schist in the Bandeira area (UTM: 189,232 / 8,141,577); b) scheme emphasizing the interpreted structures in the same outcrop (a): regional ductile foliation (schistosity S1) and spaced brittle structures possibly related to conjugated system (F1, with moderate dip to southeast; and F2, subvertical).

9.5 Geophysical Surveys

A small-scale geophysical survey consisting of Induced Polarization was conducted on both Bandeira and Outro Lado prospects in 2022.

Induced polarization (IP) and resistivity (RES) are commonly used to delineate the resistive or conductive portions of the pegmatites subsurface. Although common in use by some operators, the inverted data is not always helpful or productive in the very early stages of exploration; however, in the case of Lithium Ionic, there were sufficient outcrops to measure some attitude data, so the general trend of the pegmatites could be extrapolated using the subsurface IP anomalies. Energy-induced data were acquired through the dipole-dipole arrangement in two distinct areas: Area 1 involved six lines and totaled 5,150 m linear. Area 2 had five lines totaling 2,850 m linear profiling executed in March and April 2022.

The principle for this prospecting method is based on the injection of current through several electrodes into the ground. Data acquired depended on the resistivity values at each point, terrain

geometry and the electrodes' geometric arrangement (arrays). For an uninterrupted flow of current, the induced polarization depends on the terrain's impedance and the current's frequency. The induced polarization can be measured in the time and frequency domains. Despite being complex, IP resembles the discharge of a capacitor (time domain), or the impedance variation of an alternating current (frequency domain) can be measured. Once processed, the raw data can be viewed in 2D or, if available, in a 3D environment. Resistivity and induced polarization data were acquired in Areas 1 and 2 with the dipole-dipole arrangement (AB=MN=25 m). The map in Figure 9-7 shows the location of the lines and measuring stations of the Chargeability and Resistivity data. Some pseudo-sections of apparent chargeability and apparent resistivity 2D models of the processed data are shown below.

Source: Stevanato, 2022

Figure 9-7 – Location of the Lines and Measuring Stations of the Chargeability and Resistivity Data of Area 1 and Area 2 of the Lithium Project

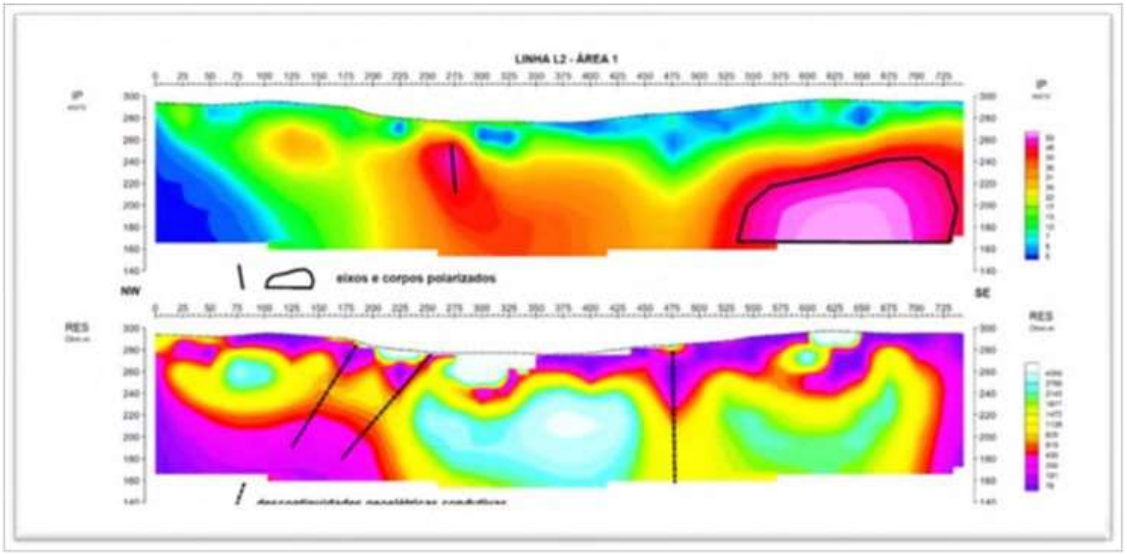

Figure 9-8 – Depth Model of the Chargeability (Top Panel) and the Actual Resistivity (Bottom Panel) of Line 2 of Area 1

Source: Stevanato, 2022.

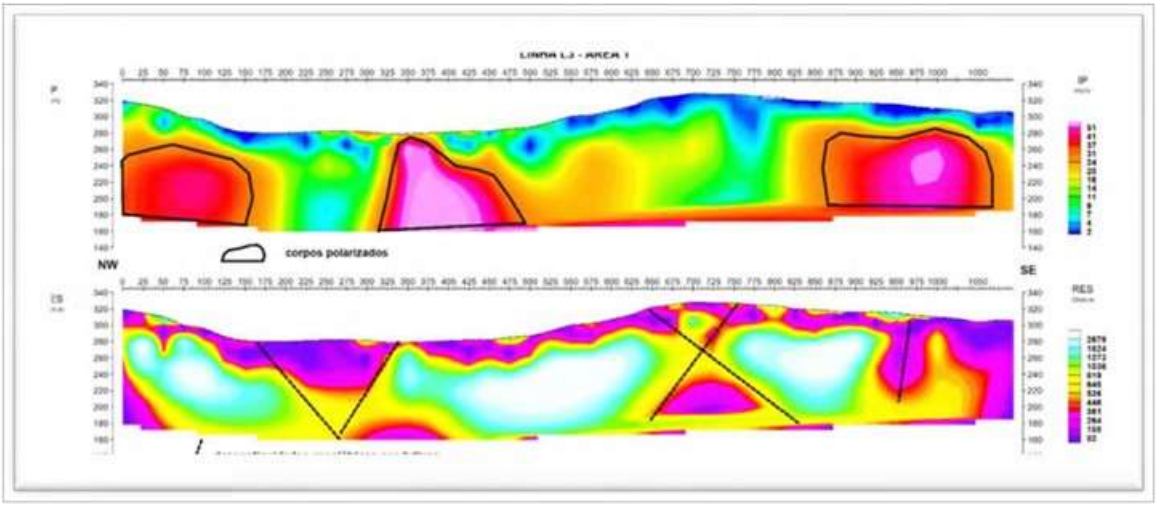

Figure 9-9 – Depth Model of the Actual Chargeability (Top Panel) and the Actual Resistivity (Bottom Panel) of Line 3 of Area 1

Source: Stevanato, 2022.

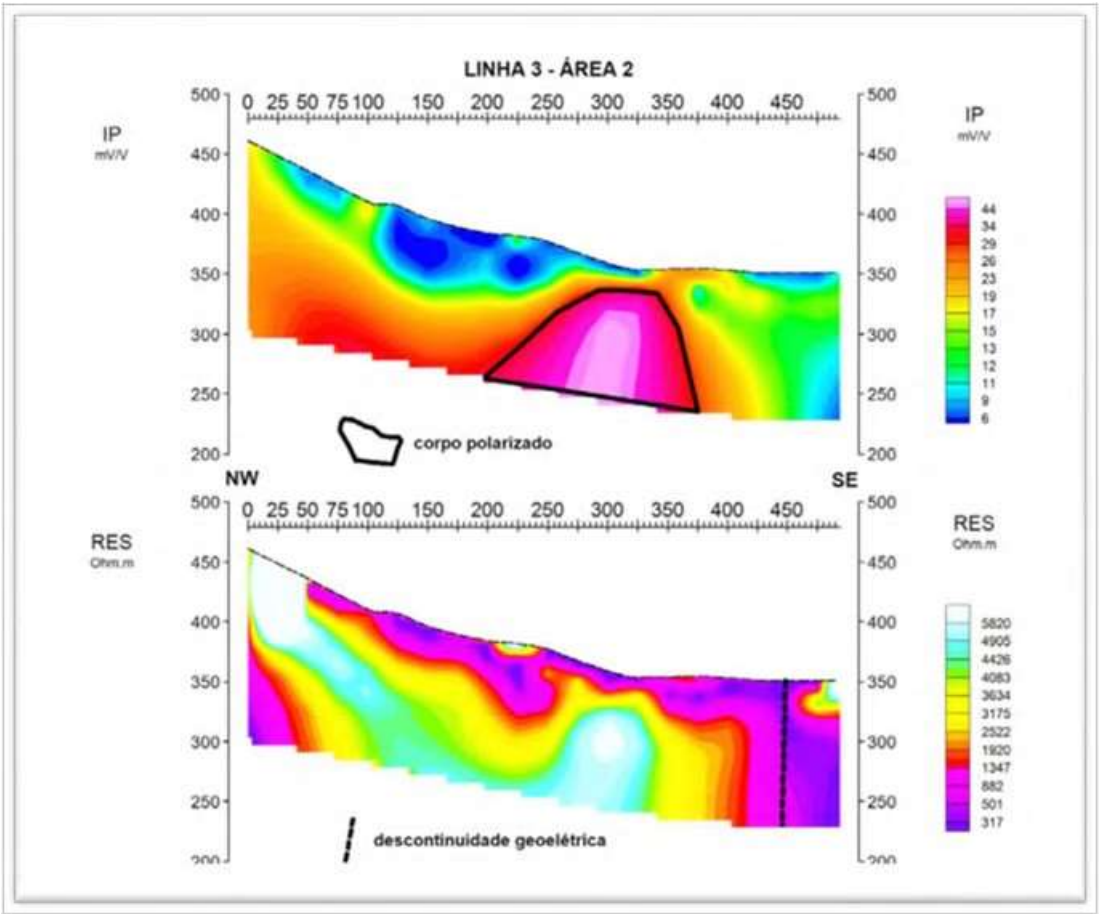

Figure 9-10 – Depth Model Chargeability (Top Panel) and Resistivity (Bottom Panel) of Line 3 Area 2

Source: Stevanato, 2022.

The Geophysical-Geological model was designed from the accurate resistivity data of Line 3 of Area 1. This model was parameterized from the log data of the ITDD-22-001 rotary drilling and is composed of a unit of shales throughout the length measured by geophysics. Superimposed on this homogeneous unit is another consisting of soil and conductive shale that in the probing

carried out intercepted the pegmatite lenses to a depth of 13.7 meters. Other interpretations suggest the presence of conductive geoelectric discontinuities that probably correspond to fault and/or fracture systems.

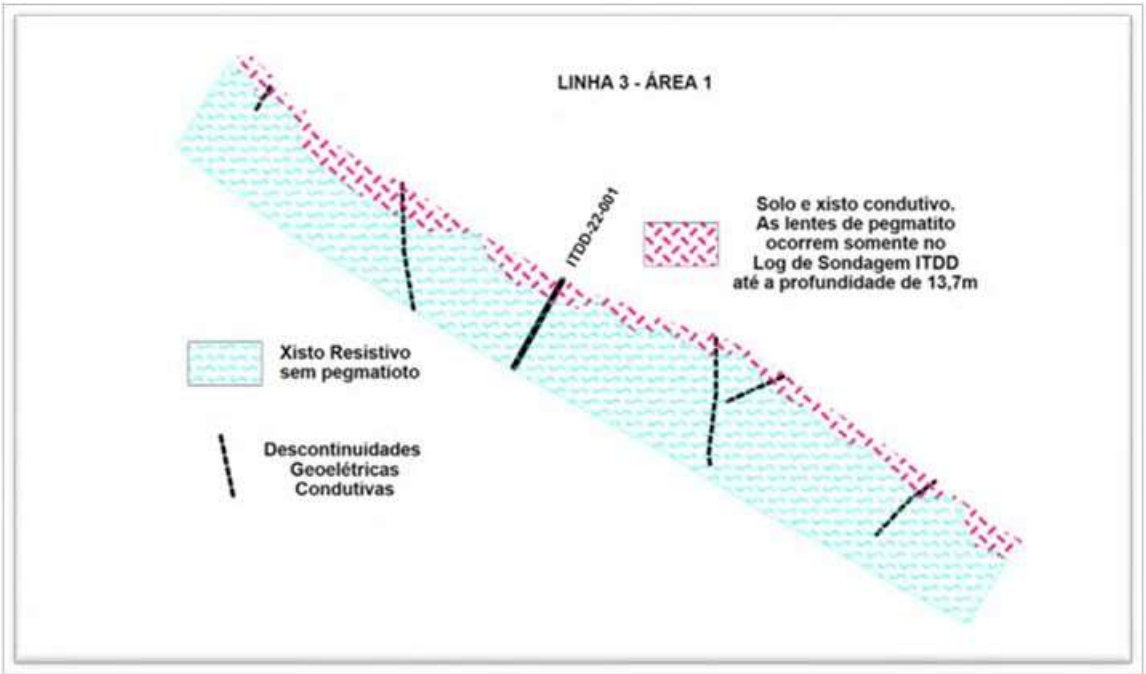

Figure 9-11 – Conceptual Geological Model from Geophysics Data

Source: Stevanato, 2022.

The inverted data was reviewed by Lithium Ionic geoscientists to determine some baseline information to choose a general attitude of the pegmatitic dykes and, if possible, to assist in designing some drill hole targets.

10 DRILLING

10.1 Lithium Ionic Drilling Campaigns

As of November 13, 2023, Lithium Ionic has successfully executed 242 diamond drill holes within the Bandeira Property, as detailed in Table 10-1 and Figure 10-1 to Figure 10-3.

All diamond drilling activities conducted within the Bandeira Property until March 2024 have been incorporated into the Mineral Resource estimation process. It is important to note that any drill holes completed in 2024 after this date and pending sample assay results have not been considered in the present resource statement.

Table 10-1 – Bandeira Drill Holes Summary

Source: GE21 2024

Drill Type	Year	Number Drill	Length (m)
DDH	2022	47	5,394
	2023	181	44,576
	2024	5	789
	Total	233	50,760

10.2 Drill Type

All drilling operations were conducted using core techniques with HQ and NQ core size specifications, featuring a 63.5mm and 47.6 mm core diameter, respectively. This approach was chosen to ensure the retrieval of pristine and representative core samples, which are essential for accurate geological logging, adequate sample support, and to secure a material supply for future metallurgical testing purposes.

10.3 Drilling Companies in Bandeira Project

Three Brazilian-based companies undertook the 2022-2024 Drill Program in Bandeira:

- Servdrill Perfuração e Sondagens Ltda (http://servdrill.com.br/);
- Servitec Foraco Sondagem AS (https://www.foraco.com.br/);
- GEOSOL Ltda (https://www.geosol.com.br).

10.4 Drill Collar Monuments

All Drill Core Monuments were surveyed by a Differential GPS and the monuments were placed by the driller once the hole had been completed.

10.5 Drillhole Surveying

The drill holes were drilled with a plunge between 50º to 90º. Core holes are generally oriented at azimuth 340° and 152°, perpendicular to both general orientations of the pegmatite intrusions.

MGLIT used the REFLEX GYRO IQ downhole survey tool to obtain all downhole survey data.

According to The REFLEX GYRO-IQ™ website, the tool can maintain high accuracy of surveys. The device is connected to a cloud-based data hub, with a secure chain of custody and QA/QC application with real-time access to drilling survey data. Data transfer from field to office ensures minimum clerical errors related to processing and interpretation.

MGLIT rented the downhole Reflex tool and completed all hole surveys at various locations and attitudes, where all necessary surveys were done in real-time. MGLIT staff had quick access to results through the cloud-based data hub. The design of the high-speed survey allowed Lithium Ionic field staff (including geologists and drillers) to obtain the following:

- Survey speeds of more than 150 meters surveyed per minute,
- There were no significant issues with the accuracy of results, which was confirmed once holes were plotted on a 3D modelling software.
- Continuous survey data comes from the tool's north-seeking sensors assisted with GPS.

The report's authors have no way to verify the accuracy of the survey method; hence, the authors will rely on the statements and information provided by MGLIT.

10.6 Core Orientation

MGLIT began implementing REFLEX ACT III to establish core orientation for drill holes within the Bandeira project after July 2023. As of the effective date, core orientation has been determined for four drill holes. Lithium Ionic has consistently integrated core orientation into its drilling program and will now prioritize its application in strategically significant sections of the geological model moving forward."

The Reflex core orientation system is based on recovering the core barrel orientation after a run. The Reflex orientation tool begins the orientation process by inserting the device in the core barrel using a specially made shoe. The tool records core barrel orientation each minute during a core run. The Reflex sleeve that attaches to the upper drill rod measures the direction of the top-of-hole using built-in accelerometers. Upon completion of a run, the drill string is left undisturbed while the communication tool, which is on the surface, counts down the time to the next reading; after this, the barrel can be withdrawn. On the surface, the tool is inserted into the end of the barrel, and the barrel is rotated until it indicates that the barrel is in the same up-down position as it was in the hole. The core, barrel, and shoe are then marked using a level to confirm verticality upward position. After the line is split, the top of the core marks is transferred along the length of the recovered core.

The Report's authors have no way to verify the accuracy of the orientation method; the authors will rely on the statements and information provided by MGLIT.

10.7 Drill Core Chain Custody

The drill cores are primarily stored in plastic or wooden boxes.

It is always transported by the drilling companies from the drilling site directly to the MGLIT core sheds in Araçuaí. MGLIT's staff receives all core boxes delivered.

10.8 Core Logging Procedures

Lithium Ionic adheres to a core logging methodology, carried out by geologists and technicians.

In summary, the following procedures are conducted:

- Preparation of drilling site.
- Collar Drilling location.
- Verify and validate meterage and quality of drill cores in the field.
- Core survey drilling.
- Photographs of the core box.
- Detailed petrographic and geological structural core logging.
- Geotechnical logging (RQD, weathering types).
- Sample geochemistry logging programming and QA/QC procedures.
- Drill core density determinations for each programmed sample.
- Core sample preparation for geochemistry analysis.
- Logistics protocols for sending samples to the laboratory.

Each procedure has its respective sheet and is stored in digital form within Lithium Ionic customized database system.

10.9 Ore Drilling Intercepts

Drill spacing typically ranges from 50m to 150m, with narrower spacing observed in the central portion of the drill pattern and wider spacing towards the pattern's edges. The ore intercepts vary in thickness, ranging from approximately 85% of the true width to nearly the true width of the mineralization.

The average pegmatite intersection spans from 0.3m to 40m, with an average true thickness of about 5m. In total, 760 mineralized intercepts from diamond drill holes (DDH) were utilized for modelling the 34 mineralized solids within the Bandeira Project. Each solid was assigned a numerical code in the tag column.

Figure 10-4 to Figure 10-7 list the mineralized intervals from Bandeira drill holes that were incorporated into the 3D modelling of the mineralized solids (Figure 10-8 and Figure 10-9).

10.10 QP's Comments

No significant drilling, sampling or recovery factors would impact the outcome of the drilling results and the estimated MRE (covered in section 14).

In the Author's opinion, based on a review of all possible information, the drilling procedures put in place by MGLIT meet acceptable industry standards, and the data can be and has been used for Geological and Resource Modelling

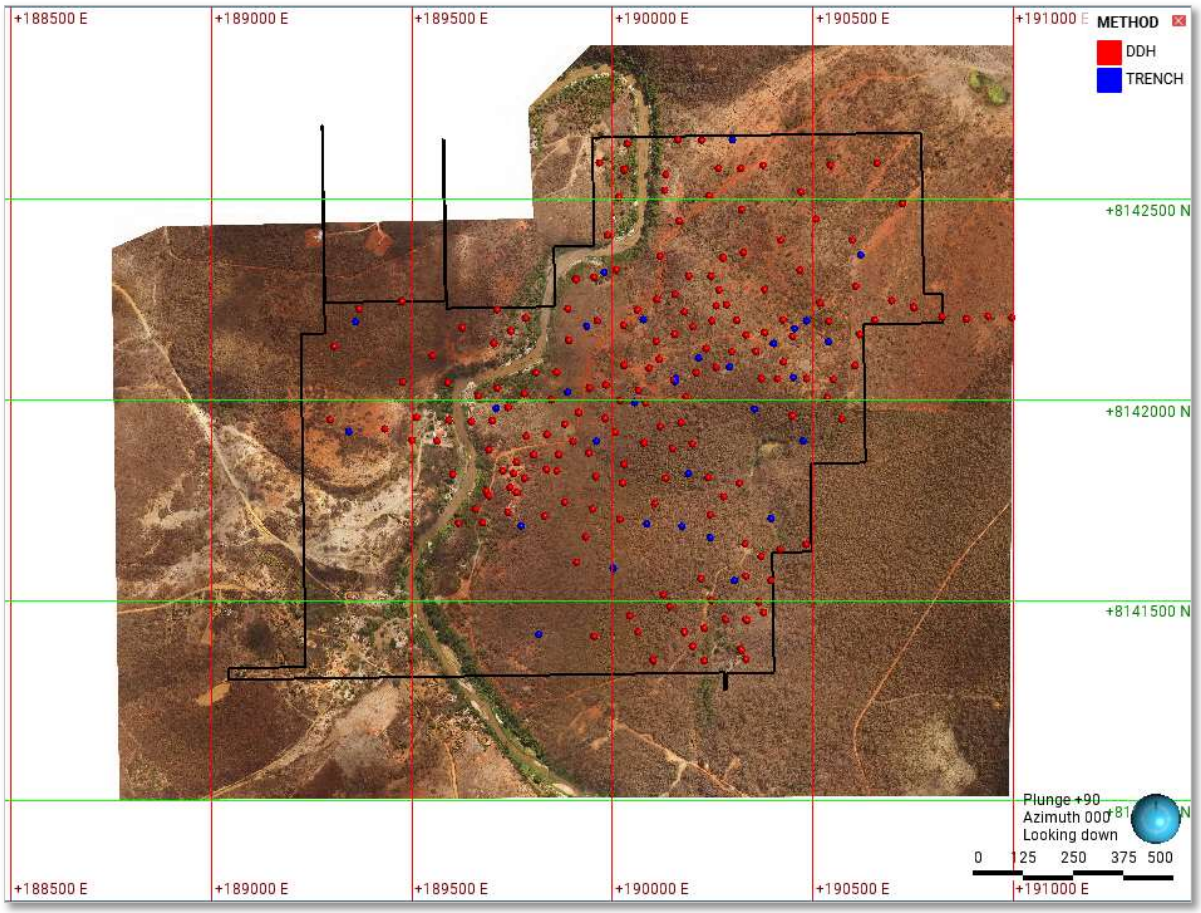

Figure 10-1 – MGLIT Drill Holes and Trenches

Source: GE21 2024

HOLE-ID	LOCATION-X	LOCATION-Y	LOCATION-Z	maxdepth	METHOD	CampaignType	Year
ITDD-22-001	189738	8141720	296	100.55	DDH	MRR	2022
ITDD-22-002	189760	8141770	302	96.25	DDH	MRR	2022
ITDD-22-002T	189761	8141769	302	45.05	DDH	MET	2023
ITDD-22-003	190330	8141641	323	60.30	DDH	MRR	2022
ITDD-22-004	190153	8142051	336	75.60	DDH	MRR	2022
ITDD-22-004B	190153	8142051	336	40.40	DDH	MRR	2022
ITDD-22-005	190183	8142008	336	68.45	DDH	MRR	2022
ITDD-22-006	190116	8142101	331	124.90	DDH	MRR	2022
ITDD-22-007	189861	8141823	302	70.50	DDH	MRR	2022
ITDD-22-008	189744	8141782	299	75.08	DDH	MRR	2022
ITDD-22-009	190426	8142095	345	109.70	DDH	MRR	2022
ITDD-22-010	190379	8142168	341	4.40	DDH	MRR	2022
ITDD-22-011	189803	8141864	292	100.25	DDH	MRR	2022
ITDD-22-012	189901	8141897	288	99.80	DDH	MRR	2022
ITDD-22-013	189881	8141940	284	99.95	DDH	MRR	2022
ITDD-22-014	189784	8141910	285	102.60	DDH	MRR	2022
ITDD-22-015	189675	8141694	275	50.90	DDH	MRR	2022
ITDD-22-016	189980	8141955	308	102.55	DDH	MRR	2022
ITDD-22-017	189725	8141824	293	100.30	DDH	MRR	2022
ITDD-22-018	190064	8142024	326	153.65	DDH	MRR	2022
ITDD-22-019	189658	8141728	276	101.80	DDH	MRR	2022
ITDD-22-020	190082	8141993	327	91.30	DDH	MRR	2022
ITDD-22-021	190258	8142082	339	130.90	DDH	MRR	2022
ITDD-22-022	190006	8141920	311	100.35	DDH	MRR	2022
ITDD-22-023	190063	8142225	304	148.70	DDH	MRR	2022
ITDD-22-023T	190061	8142224	304	49.10	DDH	MET	2023
ITDD-22-024	190156	8142264	313	180.35	DDH	MRR	2022
ITDD-22-025	190233	8142129	335	130.00	DDH	MRR	2022
ITDD-22-026	190357	8142121	342	121.40	DDH	MRR	2022
ITDD-22-027	190449	8142159	342	109.15	DDH	MRR	2022
ITDD-22-028	190333	8142162	339	111.90	DDH	MRR	2022
ITDD-22-029	189962	8142198	299	170.90	DDH	MRR	2022
ITDD-22-030	190426	8142200	337	110.30	DDH	MRR	2022
ITDD-22-030T	190425	8142199	337	61.30	DDH	MET	2023
ITDD-22-031	190540	8142196	339	130.00	DDH	MRR	2022
ITDD-22-032	190245	8142309	320	163.10	DDH	MRR	2022
ITDD-22-033	190516	8142242	339	100.10	DDH	MRR	2022
ITDD-22-033A	190517	8142242	339	21.70	DDH	MRR	2022
ITDD-22-034	190043	8141461	311	120.50	DDH	MRR	2022
ITDD-22-035	190326	8142368	320	204.90	DDH	MRR	2022
ITDD-22-036	190127	8141515	317	121.10	DDH	MRR	2022
ITDD-22-037	189954	8141411	305	121.50	DDH	MRR	2022
ITDD-22-038	190379	8142276	327	150.35	DDH	MRR	2022
ITDD-22-039	190284	8142238	331	150.45	DDH	MRR	2022
ITDD-22-040	190063	8141421	306	151.35	DDH	MRR	2022
ITDD-22-041	190467	8142324	338	150.75	DDH	MRR	2022
ITDD-22-042	190606	8142283	341	110.20	DDH	MRR	2022
ITDD-22-043	190143	8141485	314	150.90	DDH	MRR	2022
ITDD-22-044	190420	8142398	334	201.90	DDH	MRR	2022
ITDD-22-045	190536	8142005	333	100.60	DDH	MRR	2022
ITDD-22-046	190179	8141423	305	120.45	DDH	MRR	2022
ITDD-22-047	190507	8142451	340	157.35	DDH	MRR	2022
ITDD-22-048	190448	8141960	326	100.00	DDH	MRR	2022
ITDD-22-048T	190450	8141961	326	84.40	DDH	MET	2023
ITDD-22-049	190179	8141421	305	109.00	DDH	MRR	2022
ITDD-22-050	190200	8142183	327	150.75	DDH	MRR	2022
ITDD-23-051	190101	8141351	298	90.70	DDH	MRR	2023
ITDD-23-052	190166	8142446	294	480.75	DDH	MRR	2023
ITDD-23-053	190109	8142146	325	140.90	DDH	MRR	2023
ITDD-23-054	189739	8141981	275	144.85	DDH	MRR	2023
ITDD-23-055	190101	8141352	298	130.15	DDH	MRR	2023
ITDD-23-056	190228	8141350	299	75.60	DDH	MRR	2023
ITDD-23-058	189739	8141982	275	155.75	DDH	MRR	2023
ITDD-23-059	190229	8141349	299	57.05	DDH	MRR	2023
ITDD-23-060	190165	8142447	292	490.15	DDH	MRR	2023
ITDD-23-061	190281	8141453	297	105.25	DDH	MRR	2023
ITDD-23-062	190163	8142649	278	433.05	DDH	MRR	2023
ITDD-23-063	190281	8141452	297	121.15	DDH	MRR	2023
ITDD-23-065	190130	8142523	283	504.90	DDH	MRR	2023
ITDD-23-066	190332	8141354	297	150.95	DDH	MRR	2023
ITDD-23-067	190364	8141497	301	129.70	DDH	MRR	2023
ITDD-23-068	189692	8141876	287	136.30	DDH	MRR	2023
ITDD-23-069	190364	8141496	302	220.25	DDH	MRR	2023
ITDD-23-070	190163	8142649	280	422.60	DDH	MRR	2023
ITDD-23-071	190332	8141561	320	153.45	DDH	MRR	2023
ITDD-23-072	189691	8141876	287	140.30	DDH	MRR	2023
ITDD-23-073	190016	8142507	275	480.20	DDH	MRR	2023
ITDD-23-074	189848	8142000	276	120.75	DDH	MRR	2023
ITDD-23-075	190395	8141550	303	169.05	DDH	MRR	2023
ITDD-23-076	190009	8142325	276	260.10	DDH	MRR	2023
ITDD-23-077	190220	8141554	322	100.10	DDH	MRR	2023
ITDD-23-078	189625	8142181	306	361.70	DDH	MRR	2023
ITDD-23-079	190483	8141640	320	170.65	DDH	MRR	2023
ITDD-23-080	190241	8142509	305	310.35	DDH	MRR	2023
ITDD-23-081	190418	8141628	304	172.30	DDH	MRR	2023
ITDD-23-082	190009	8142326	275	298.00	DDH	MRR	2023
ITDD-23-083	190017	8142506	275	420.25	DDH	MRR	2023
ITDD-23-083T	190015	8142504	276	74.25	DDH	MET	2023
ITDD-23-084	189625	8142181	306	305.15	DDH	MRR	2023
ITDD-23-085	190246	8141501	315	115.10	DDH	MRR	2023
ITDD-23-086	190241	8142509	305	340.55	DDH	MRR	2023
ITDD-23-087	190322	8141375	296	89.85	DDH	MRR	2023
ITDD-23-087T	190320	8141379	296	75.00	DDH	MET	2023
ITDD-23-088	190118	8142359	300	303.80	DDH	MRR	2023
ITDD-23-089	190371	8141611	317	184.20	DDH	MRR	2023
ITDD-23-090	190037	8142639	276	589.15	DDH	MRR	2023
ITDD-23-091	189367	8142228	335	544.20	DDH	MRR	2023
ITDD-23-092	189847	8142001	277	129.95	DDH	MRR	2023
ITDD-23-093	190200	8141385	302	75.30	DDH	MRR	2023
ITDD-23-093T	190199	8141386	302	60.05	DDH	MET	2023
ITDD-23-094	189943	8142030	300	109.35	DDH	MRR	2023
ITDD-23-095	189746	8142172	277	249.85	DDH	MRR	2023
ITDD-23-096	189942	8142031	300	118.40	DDH	MRR	2023
ITDD-23-097	189780	8141805	299	48.75	DDH	MRR	2023
ITDD-23-098	189760	8141845	294	350.20	DDH	MRR	2023
ITDD-23-099	189836	8141914	284	79.10	DDH	MRR	2023
ITDD-23-100	189691	8141761	278	49.90	DDH	MRR	2023
ITDD-23-101	189835	8141915	284	100.40	DDH	MRR	2023
ITDD-23-102	189745	8142173	277	262.35	DDH	MRR	2023
ITDD-23-103	189511	8141957	273	221.30	DDH	MRR	2023
ITDD-23-104	189684	8141773	278	67.05	DDH	MRR	2023
ITDD-23-105	189907	8142302	277	421.35	DDH	MRR	2023
ITDD-23-106	189700	8141948	279	141.80	DDH	MRR	2023
ITDD-23-107	189588	8142044	273	240.80	DDH	MRR	2023
ITDD-23-108	189760	8141846	294	95.05	DDH	MRR	2023
ITDD-23-109	189780	8142016	275	315.65	DDH	MRR	2023
ITDD-23-110	189915	8141968	288	72.10	DDH	MRR	2023
ITDD-23-111	189834	8141827	299	41.45	DDH	MRR	2023
ITDD-23-112	189699	8141949	279	320.05	DDH	MRR	2023
ITDD-23-113	189601	8141814	273	108.60	DDH	MRR	2023

Figure 10-2 – Bandeira Drill Holes

Source: GE21 2024

HOLE-ID	LOCATION-X	LOCATION-Y	LOCATION-Z	maxdepth	METHOD	CampaignType	Year
ITDD-23-114	189916	8141968	288	91.60	DDH	MRR	2023
ITDD-23-115	189866	8141864	294	47.50	DDH	MRR	2023
ITDD-23-116	189859	8142069	276	139.45	DDH	MRR	2023
ITDD-23-117	189891	8142149	297	220.05	DDH	MRR	2023
ITDD-23-118	189592	8141949	273	183.95	DDH	MRR	2023
ITDD-23-119	189779	8142016	275	138.50	DDH	MRR	2023
ITDD-23-120	189859	8142070	277	279.85	DDH	MRR	2023
ITDD-23-121	189891	8142150	297	361.55	DDH	MRR	2023
ITDD-23-122	189591	8141950	273	340.20	DDH	MRR	2023
ITDD-23-123	189712	8142030	275	350.90	DDH	MRR	2023
ITDD-23-124	190154	8142164	327	130.00	DDH	MRR	2023
ITDD-23-125	189648	8141947	273	330.10	DDH	MRR	2023
ITDD-23-126	190154	8142165	327	170.10	DDH	MRR	2023
ITDD-23-127	190029	8142087	320	150.95	DDH	MRR	2023
ITDD-23-128	189591	8141950	273	205.55	DDH	MRR	2023
ITDD-23-129	189665	8142009	274	199.00	DDH	MRR	2023
ITDD-23-130	190154	8142164	327	300.25	DDH	MRR	2023
ITDD-23-131	190029	8142088	320	301.00	DDH	MRR	2023
ITDD-23-132	189664	8142010	274	210.35	DDH	MRR	2023
ITDD-23-133	189561	8141898	277	184.25	DDH	MRR	2023
ITDD-23-134	189648	8141947	273	164.75	DDH	MRR	2023
ITDD-23-134T	189647	8141946	273	38.55	DDH	MET	2023
ITDD-23-135	190179	8142220	321	250.40	DDH	MRR	2023
ITDD-23-136	190248	8142197	331	334.35	DDH	MRR	2023
ITDD-23-137	189664	8142010	274	400.60	DDH	MRR	2023
ITDD-23-138	189476	8142045	298	330.10	DDH	MRR	2023
ITDD-23-139	189550	8142111	304	366.90	DDH	MRR	2023
ITDD-23-140	190208	8142068	338	80.05	DDH	MRR	2023
ITDD-23-141	190297	8142120	339	61.35	DDH	MRR	2023
ITDD-23-142	190111	8142251	306	200.15	DDH	MRR	2023
ITDD-23-143	190190	8142309	316	439.45	DDH	MRR	2023
ITDD-23-144	190247	8142198	331	119.85	DDH	MRR	2023
ITDD-23-145	189625	8142180	306	330.25	DDH	MRR	2023
ITDD-23-146	189809	8142068	274	295.30	DDH	MRR	2023
ITDD-23-147	190110	8142251	306	510.05	DDH	MRR	2023
ITDD-23-148	190310	8142199	335	349.95	DDH	MRR	2023
ITDD-23-149	189367	8142227	335	469.20	DDH	MRR	2023
ITDD-23-150	189861	8142069	276	349.40	DDH	MRR	2023
ITDD-23-151	189474	8142246	327	442.00	DDH	MRR	2023
ITDD-23-152	190190	8142309	316	315.35	DDH	MRR	2023

HOLE-ID	LOCATION-X	LOCATION-Y	LOCATION-Z	maxdepth	METHOD	CampaignType	Year
ITDD-23-153	189295	8141951	322	450.00	DDH	MRR	2023
ITDD-23-154	190266	8142274	325	550.25	DDH	MRR	2023
ITDD-23-155	190110	8142252	305	241.45	DDH	MRR	2023
ITDD-23-156	190189	8142309	316	340.55	DDH	MRR	2023
ITDD-23-157	189888	8142227	285	379.65	DDH	MRR	2023
ITDD-23-158	189474	8142246	327	481.30	DDH	MRR	2023
ITDD-23-159	190027	8142186	309	489.15	DDH	MRR	2023
ITDD-23-160	190091	8142079	329	259.20	DDH	MRR	2023
ITDD-23-161	190276	8142353	312	420.45	DDH	MRR	2023
ITDD-23-162	189367	8142228	335	486.70	DDH	MRR	2023
ITDD-23-163	190031	8142574	277	534.45	DDH	MRR	2023
ITDD-23-164	189954	8142306	275	480.30	DDH	MRR	2023
ITDD-23-165	189910	8142302	276	367.40	DDH	MRR	2023
ITDD-23-166	190132	8141805	310	121.00	DDH	MRR	2023
ITDD-23-167	189703	8142142	284	412.20	DDH	MRR	2023
ITDD-23-168	190131	8141806	310	145.60	DDH	MRR	2023
ITDD-23-169	190322	8142475	321	445.05	DDH	MRR	2023
ITDD-23-170	189950	8141728	314	141.00	DDH	MRR	2023
ITDD-23-171	190019	8141998	317	249.15	DDH	MRR	2023
ITDD-23-172	190274	8142355	312	392.05	DDH	MRR	2023
ITDD-23-173	189950	8141729	314	150.10	DDH	MRR	2023
ITDD-23-174	189704	8142141	284	370.00	DDH	MRR	2023
ITDD-23-175	190028	8142573	275	550.15	DDH	MRR	2023
ITDD-23-176	190018	8141999	318	255.25	DDH	MRR	2023
ITDD-23-177	189954	8142306	276	390.70	DDH	MRR	2023
ITDD-23-178	189500	8141899	273	211.00	DDH	MRR	2023
ITDD-23-179	189432	8141928	294	249.90	DDH	MRR	2023
ITDD-23-180	189987	8142411	276	508.65	DDH	MRR	2023
ITDD-23-181	189588	8142043	273	250.30	DDH	MRR	2023
ITDD-23-182	190322	8142475	322	380.65	DDH	MRR	2023
ITDD-23-183	189500	8141899	273	200.60	DDH	MRR	2023
ITDD-23-184	190274	8142356	313	420.50	DDH	MRR	2023
ITDD-23-185	190027	8142574	276	591.60	DDH	MRR	2023
ITDD-23-186	189305	8142134	331	421.25	DDH	MRR	2023
ITDD-23-187	189500	8141900	273	220.05	DDH	MRR	2023
ITDD-23-188	189967	8142591	276	664.10	DDH	MRR	2023
ITDD-23-189	189615	8141692	277	120.20	DDH	MRR	2023
ITDD-23-191	189753	8141816	296	80.35	DDH	GEOTEC	2023
ITDD-23-192	189783	8142204	276	380.55	DDH	MRR	2023
ITDD-23-193	190571	8141953	323	150.20	DDH	MRR	2023

HOLE-ID	LOCATION-X	LOCATION-Y	LOCATION-Z	maxdepth	METHOD	CampaignType	Year
ITDD-23-194	190025	8141793	302	150.35	DDH	MRR	2023
ITDD-23-195	189983	8142037	312	106.20	DDH	GEOTEC	2023
ITDD-23-196	190024	8141794	302	150.90	DDH	MRR	2023
ITDD-23-197	190258	8142235	330	110.30	DDH	GEOTEC	2023
ITDD-23-198	190447	8141960	326	118.35	DDH	MRR	2023
ITDD-23-199	189711	8142225	293	450.55	DDH	MRR	2023
ITDD-23-200	189910	8141596	322	100.30	DDH	MRR	2023
ITDD-23-201	190550	8142051	337	50.00	DDH	GEOTEC	2023
ITDD-23-202	190028	8142086	320	280.50	DDH	MRR	2023
ITDD-23-203	190199	8141891	324	150.15	DDH	MRR	2023
ITDD-23-204	190029	8141840	303	40.10	DDH	GEOTEC	2023
ITDD-23-205	190484	8142053	342	50.00	DDH	GEOTEC	2023
ITDD-23-206	190412	8142053	341	50.00	DDH	GEOTEC	2023
ITDD-23-207	190119	8141934	326	50.00	DDH	GEOTEC	2023
ITDD-23-208	190371	8142053	340	13.50	DDH	GEOTEC	2023
ITDD-23-209	190228	8141432	301	75.00	DDH	GEOTEC	2023
ITDD-23-210	190170	8141944	330	607.85	DDH	MRR	2023
ITDD-23-211	190082	8141993	327	233.05	DDH	MRR	2023
ITDD-23-212	190149	8141879	322	150.20	DDH	MRR	2023
ITDD-23-213	190336	8141450	300	130.85	DDH	GEOTEC	2023
ITDD-23-214	190079	8141894	317	45.10	DDH	GEOTEC	2023
ITDD-23-215	189981	8141954	307	233.35	DDH	MRR	2023
ITDD-23-216	189881	8141940	284	228.15	DDH	MRR	2023
ITDD-23-217	190238	8141807	315	90.60	DDH	MRR	2023
ITDD-23-218	190332	8141452	299	93.35	DDH	MRR	2023
ITDD-23-219	189914	8141970	288	220.15	DDH	MRR	2023
ITDD-23-220	190106	8141742	314	99.45	DDH	MRR	2023
ITDD-23-221	190336	8141451	300	220.80	DDH	MRR	2023
ITDD-23-222	189803	8141863	292	223.60	DDH	MRR	2023
ITDD-23-223	190018	8141703	315	118.05	DDH	MRR	2023
ITDD-23-224	189835	8141827	299	193.15	DDH	MRR	2023
ITDD-23-225	189933	8141659	320	106.90	DDH	MRR	2023
ITDD-23-226	189865	8141865	294	199.15	DDH	MRR	2023
ITDD-23-227	189940	8141867	291	214.35	DDH	MRR	2023
ITDD-23-228	190377	8141470	301	153.20	DDH	MRR	2023
ITDD-23-229	189830	8141711	312	147.35	DDH	MRR	2023
ITDD-23-230	190077	8141892	317	187.20	DDH	MRR	2023
ITDD-23-231	189880	8141745	312	156.60	DDH	MRR	2023
ITDD-23-232	190028	8141840	303	165.50	DDH	MRR	2023
ITDD-23-233	189958	8141810	303	170.55	DDH	MRR	2023

HOLE-ID	LOCATION-X	LOCATION-Y	LOCATION-Z	maxdepth	METHOD	CampaignType	Year
ITDD-23-234	190243	8141714	319	199.45	DDH	MRR	2023
ITDD-23-235	190277	8141759	314	232.80	DDH	MRR	2023
ITDD-23-236	190316	8141793	309	230.75	DDH	MRR	2023
ITDD-23-237	190376	8142585	324	100.35	DDH	COND	2023
ITDD-23-238	190470	8142519	334	100.45	DDH	COND	2023
ITDD-23-239	190544	8142585	332	100.05	DDH	COND	2023
ITDD-23-240	190659	8142591	328	100.20	DDH	COND	2023
ITDD-23-241	190723	8142490	328	100.40	DDH	COND	2023
ITDD-23-242	190598	8142398	342	100.45	DDH	COND	2023
ITDD-23-243	190696	8142247	333	100.50	DDH	COND	2023
ITDD-23-244	190320	8142578	316	100.00	DDH	COND	2023
ITDD-23-245	190264	8142578	304	100.30	DDH	MRR	2023
ITDD-23-246	190616	8142164	335	70.00	DDH	MRR	2023
ITDD-23-247	190617	8142163	335	110.60	DDH	MRR	2023
ITDD-23-248	190751	8142232	333	87.95	DDH	MRR	2023
ITDD-23-249	190752	8142230	333	150.30	DDH	MRR	2023
ITDD-24-250	190654	8142199	334	69.65	DDH	MRR	2024
ITDD-24-251	190822	8142208	341	217.15	DDH	MRR	2024
ITDD-24-252	190605	8142086	334	121.45	DDH	MRR	2024
ITDD-24-253	190605	8142086	334	199.75	DDH	MRR	2024
ITDD-24-254	190133	8142562	283	200.20	DDH	HYDRO	
ITDD-24-255	190222	8142648	288	181.65	DDH	MRR	2024

Figure 10-3 – Bandeira Drill Collars

Source: GE21 2024

holeid	from	to	Legth	Li2O %	Domain
ITDD-22-001	8.50	13.70	5.20	1.53	1
ITDD-22-001	19.00	19.45	0.45	1.37	01B-SW
ITDD-22-002	33.08	38.74	5.66	2.02	1
ITDD-22-004B	37.45	38.13	0.68	0.44	1
ITDD-22-006	54.90	57.60	2.70	2.23	1
ITDD-22-007	18.20	18.75	0.55	0.50	01A-SW
ITDD-22-007	21.62	27.58	5.96	1.33	1
ITDD-22-008	45.45	46.80	1.35	0.13	1
ITDD-22-011	53.14	59.89	6.75	1.99	1
ITDD-22-012	33.70	34.45	0.75	0.74	01A-SW
ITDD-22-012	36.23	36.71	0.48	2.16	1
ITDD-22-012	37.03	42.03	5.00	1.70	1
ITDD-22-013	53.18	57.08	3.90	1.56	01A-SW
ITDD-22-013	62.90	65.66	2.76	1.66	1
ITDD-22-014	77.10	82.80	5.70	1.14	1
ITDD-22-015	6.16	8.74	2.58	1.04	1
ITDD-22-015	10.97	11.70	0.73	0.66	01B-SW
ITDD-22-016	39.50	45.35	5.85	1.27	1
ITDD-22-017	62.21	67.15	4.94	1.06	1
ITDD-22-018	44.96	45.96	1.00	0.52	1
ITDD-22-019	29.83	33.57	3.74	1.97	1
ITDD-22-021	23.50	24.19	0.69	0.74	1
ITDD-22-021	31.90	34.73	2.83	1.29	04-NE
ITDD-22-021	36.53	37.33	0.80	0.31	04-NE
ITDD-22-022	14.31	18.31	4.00	0.55	1
ITDD-22-023	33.50	34.26	0.76	0.96	02-NE
ITDD-22-023	38.53	43.59	5.06	2.13	02A-NE
ITDD-22-023	114.34	115.90	1.56	1.01	1
ITDD-22-024	28.14	31.00	2.86	2.04	02-NE
ITDD-22-024	32.22	33.86	1.64	2.34	02-NE
ITDD-22-024	36.35	37.35	1.00	1.07	02A-NE
ITDD-22-024	117.39	118.76	1.37	0.07	1
ITDD-22-024	159.72	161.72	2.00	2.46	04-NE
ITDD-22-025	57.47	58.08	0.61	0.33	1
ITDD-22-025	67.62	71.31	3.69	2.22	04-NE
ITDD-22-027	22.78	29.09	6.31	0.43	04-NE
ITDD-22-028	34.30	35.35	1.05	2.17	04B-NE

holeid	from	to	Legth	Li2O %	Domain
ITDD-22-028	38.64	40.25	1.61	1.95	1
ITDD-22-028	51.39	53.39	2.00	0.67	04-NE
ITDD-22-029	17.35	17.75	0.40	0.28	02C-NE
ITDD-22-029	41.46	42.25	0.79	1.56	02-NE
ITDD-22-029	44.28	46.93	2.65	1.29	02A-NE
ITDD-22-029	145.91	149.08	3.17	1.21	1
ITDD-22-030	46.60	53.30	6.70	1.49	04-NE
ITDD-22-032	13.18	14.33	1.15	0.29	02-NE
ITDD-22-032	18.35	19.95	1.60	1.95	02A-NE
ITDD-22-032	130.30	133.92	3.62	0.71	1
ITDD-22-032	134.34	135.34	1.00	0.39	1
ITDD-22-032	137.40	139.20	1.80	1.58	04-NE
ITDD-22-033	6.25	10.23	3.99	0.00	04B-NE
ITDD-22-033A	6.05	10.05	4.00	0.41	04B-NE
ITDD-22-034	17.42	18.42	1.00	0.30	SE-A
ITDD-22-035	103.27	105.17	1.90	1.04	04A-NE
ITDD-22-035	111.93	113.21	1.28	1.43	04B-NE
ITDD-22-035	128.48	129.24	0.76	0.56	1
ITDD-22-035	171.62	176.50	4.88	1.28	04-NE
ITDD-22-035	179.30	181.02	1.72	0.56	04C-NE
ITDD-22-036	39.10	45.10	6.00	0.90	SE-A
ITDD-22-038	43.26	44.66	1.40	2.43	04A-NE
ITDD-22-038	55.73	56.81	1.08	0.39	04B-NE
ITDD-22-038	67.32	71.32	4.00	1.04	1
ITDD-22-038	98.13	104.85	6.72	1.24	04-NE
ITDD-22-039	86.24	91.95	5.71	2.13	1
ITDD-22-039	94.19	95.86	1.67	1.71	04-NE
ITDD-22-040	55.90	56.90	1.00	0.37	SE-A
ITDD-22-041	37.16	37.97	0.81	0.60	04A-NE
ITDD-22-043	38.05	42.41	4.36	1.43	SE-A
ITDD-22-044	157.06	158.03	0.97	0.32	1
ITDD-22-045	21.65	24.65	3.00	0.22	10-NE
ITDD-22-045	34.94	38.78	3.84	0.40	09-NE
ITDD-22-045	41.57	44.88	3.31	1.42	09-NE
ITDD-22-046	63.00	68.00	5.00	1.17	SE-A
ITDD-22-048	57.50	60.11	2.61	0.70	10-NE
ITDD-22-048	69.39	74.20	4.81	1.08	09-NE

holeid	from	to	Legth	Li2O %	Domain
ITTRE-22-004	12.80	14.80	2.00	0.56	01A-SW
ITTRE-22-004	14.80	15.80	1.00	0.22	01A-SW
ITTRE-22-012	33.20	37.20	4.00	0.28	02-NE
ITTRE-22-012	42.06	44.06	2.00	0.38	02A-NE
ITTRE-22-012	44.06	46.06	2.00	0.16	02A-NE
ITDD-22-050	80.70	81.00	0.30	0.63	1
ITDD-22-050	96.60	99.31	2.71	0.81	04-NE
ITDD-22-049	64.87	67.87	3.00	0.86	SE-A
ITDD-23-051	56.98	59.68	2.70	0.64	SE-A
ITDD-23-052	99.96	100.73	0.77	0.87	02-NE
ITDD-23-052	108.25	109.28	1.03	1.32	02A-NE
ITDD-23-052	110.98	111.94	0.96	0.60	02A-NE
ITDD-23-052	205.44	209.44	4.00	1.79	1
ITDD-23-052	223.63	225.63	2.00	2.33	04-NE
ITDD-23-052	255.36	256.10	0.74	1.62	04C-NE
ITDD-23-052	256.39	257.46	1.07	0.56	04C-NE
ITDD-23-052	279.04	280.00	0.96	0.74	05A-NE
ITDD-23-052	308.20	310.33	2.13	1.32	05-NE
ITDD-23-052	311.08	312.46	1.38	0.80	05-NE
ITDD-23-052	327.28	328.28	1.00	0.51	05B-NE
ITDD-23-052	381.30	386.00	4.70	1.11	06-NE
ITDD-23-052	392.20	398.52	6.32	1.37	06A-NE
ITDD-23-052	415.48	416.48	1.00	1.20	06B-NE
ITDD-23-052	433.13	435.39	2.26	2.16	07-NE
ITDD-23-052	436.36	438.74	2.38	2.14	07-NE
ITDD-23-052	439.79	440.30	0.51	0.65	07-NE
ITDD-23-053	74.65	77.19	2.54	1.95	1
ITDD-23-054	118.00	123.00	5.00	1.66	1
ITDD-23-055	36.97	38.95	1.98	0.24	SE-A
ITDD-23-056	37.75	49.02	11.27	0.88	SE-A
ITDD-23-058	122.55	128.55	6.00	1.96	1
ITDD-23-059	28.72	32.96	4.24	1.32	SE-A
ITDD-23-060	111.44	112.13	0.69	2.00	02-NE
ITDD-23-060	170.03	171.08	1.05	1.34	02B-NE
ITDD-23-060	171.85	172.38	0.53	0.47	02B-NE
ITDD-23-060	173.29	174.36	1.07	1.10	02B-NE
ITDD-23-060	225.23	229.50	4.27	2.03	1

holeid	from	to	Legth	Li2O %	Domain
ITDD-23-060	252.75	254.57	1.82	0.04	04-NE
ITDD-23-060	283.30	284.48	1.18	2.16	04C-NE
ITDD-23-060	315.98	316.93	0.95	2.25	05A-NE
ITDD-23-060	319.40	321.20	1.80	0.99	05A-NE
ITDD-23-060	332.62	334.00	1.38	1.49	05-NE
ITDD-23-060	399.67	402.45	2.78	1.79	06-NE
ITDD-23-060	405.94	408.44	2.50	0.81	06A-NE
ITDD-23-060	444.29	449.43	5.14	1.44	07-NE
ITDD-23-061	61.50	78.58	17.08	1.43	SE-A
ITDD-23-061	78.58	79.27	0.69	0.07	SE-A
ITDD-23-061	79.52	80.19	0.67	0.34	SE-A
ITDD-23-062	104.43	124.43	20.00	1.62	03-NE
ITDD-23-062	167.88	168.86	0.98	0.30	02D-NE
ITDD-23-062	349.55	353.47	3.92	1.05	04-NE
ITDD-23-062	384.50	385.60	1.10	0.67	04C-NE
ITDD-23-062	386.68	388.67	1.99	1.67	04C-NE
ITDD-23-063	41.67	55.24	13.57	1.73	SE-A
ITDD-23-065	159.62	164.60	4.98	1.12	02-NE
ITDD-23-065	203.93	208.16	4.23	1.53	02B-NE
ITDD-23-065	216.53	217.63	1.10	1.30	02E-NE
ITDD-23-065	271.20	277.29	6.09	2.53	1
ITDD-23-065	321.20	324.22	3.02	1.24	04-NE
ITDD-23-065	336.67	339.41	2.74	1.32	04C-NE
ITDD-23-065	354.23	378.23	24.00	1.32	05A-NE
ITDD-23-065	390.10	397.82	7.72	1.88	05-NE
ITDD-23-065	400.74	403.08	2.34	1.30	05B-NE
ITDD-23-065	431.25	434.45	3.20	0.67	06-NE
ITDD-23-065	441.88	445.37	3.49	2.04	06A-NE
ITDD-23-065	456.28	457.62	1.34	0.42	07-NE
ITDD-23-065	458.05	459.74	1.69	1.01	07-NE
ITDD-23-065	460.29	461.88	1.59	1.17	07-NE
ITDD-23-065	463.95	465.95	2.00	0.38	07-NE
ITDD-23-065	484.11	485.10	0.99	1.12	08-NE
ITDD-23-066	28.16	37.16	9.00	0.73	SE-A
ITDD-23-067	86.96	103.96	17.00	1.21	SE-A
ITDD-23-068	92.23	93.97	1.74	1.03	1
ITDD-23-068	112.79	114.45	1.66	0.38	01B-SW

holeid	from	to	Legth	Li2O %	Domain
ITDD-23-069	58.55	60.55	2.00	0.18	SE-A
ITDD-23-069	60.55	75.48	14.93	1.44	SE-A
ITDD-23-070	78.30	84.30	6.00	1.06	03-NE
ITDD-23-070	84.30	89.30	5.00	0.04	03-NE
ITDD-23-070	89.30	97.30	8.00	1.32	03-NE
ITDD-23-070	152.73	156.40	3.67	1.83	02D-NE
ITDD-23-070	332.74	336.36	3.62	2.15	04-NE
ITDD-23-070	339.94	341.09	1.15	0.72	04C-NE
ITDD-23-070	341.39	343.42	2.03	1.41	04C-NE
ITDD-23-071	86.49	90.49	4.00	0.90	SE-A
ITDD-23-072	99.14	100.94	1.80	1.37	1
ITDD-23-072	113.69	117.69	4.00	1.38	01B-SW
ITDD-23-073	77.82	83.66	5.84	1.99	03-NE
ITDD-23-073	206.62	213.30	6.68	1.99	02-NE
ITDD-23-073	243.54	245.10	1.56	1.43	02B-NE
ITDD-23-073	246.82	247.63	0.81	0.79	02B-NE
ITDD-23-073	298.08	299.08	1.00	0.81	1
ITDD-23-073	352.92	360.92	8.00	1.66	04-NE
ITDD-23-073	408.21	411.86	3.65	1.83	05A-NE
ITDD-23-073	412.04	412.34	0.30	0.76	05A-NE
ITDD-23-073	413.90	423.97	10.07	1.30	05A-NE
ITDD-23-073	425.10	426.35	1.25	1.25	05A-NE
ITDD-23-073	443.07	447.07	4.00	2.10	05-NE
ITDD-23-074	85.77	89.55	3.78	1.58	01A-SW
ITDD-23-074	89.55	89.96	0.41	0.25	01A-SW
ITDD-23-074	90.06	90.40	0.34	0.63	01A-SW
ITDD-23-074	95.31	95.91	0.60	1.98	1
ITDD-23-074	96.52	96.75	0.23	0.00	1
ITDD-23-074	96.84	100.25	3.41	1.98	1
ITDD-23-075	109.00	112.38	3.38	1.44	SE-A
ITDD-23-075	112.38	113.03	0.65	0.07	SE-A
ITDD-23-075	113.57	115.18	1.61	0.09	SE-A
ITDD-23-075	115.18	119.43	4.25	0.98	SE-A
ITDD-23-075	130.10	141.90	11.80	1.00	08-NE
ITDD-23-076	82.64	84.05	1.41	2.03	02-NE
ITDD-23-076	85.55	86.84	1.29	2.24	02A-NE
ITDD-23-076	165.53	166.49	0.96	2.05	1

Figure 10-4 – Mineralized Intercepts by Bandeira Drill Holes

Source: GE21 2024

holeid	from	to	Legth	Li2O %	Domain
ITDD-23-076	167.12	168.98	1.86	1.43	1
ITDD-23-078	313.14	314.34	1.20	0.62	01A-SW
ITDD-23-078	315.48	315.94	0.46	0.04	01A-SW
ITDD-23-078	316.38	317.90	1.52	1.54	01A-SW
ITDD-23-078	321.95	323.43	1.48	0.86	1
ITDD-23-078	324.44	337.78	13.34	1.56	1
ITDD-23-080	65.52	65.63	0.11	0.22	02D-NE
ITDD-23-080	255.45	256.94	1.49	2.87	04-NE
ITDD-23-080	258.05	258.77	0.72	3.00	04-NE
ITDD-23-080	260.45	261.66	1.21	1.99	04-NE
ITDD-23-080	274.70	275.70	1.00	0.53	04C-NE
ITDD-23-081	120.07	129.07	9.00	1.49	08-NE
ITDD-23-081	144.40	149.12	4.72	1.50	08A-NE
ITDD-23-082	50.63	56.40	5.77	2.17	02C-NE
ITDD-23-082	99.92	102.23	2.31	1.04	02-NE
ITDD-23-082	196.20	201.00	4.80	1.48	1
ITDD-23-083	59.09	66.12	7.03	1.37	03-NE
ITDD-23-083	171.31	177.15	5.84	1.90	02-NE
ITDD-23-083	225.68	226.38	0.70	0.71	02B-NE
ITDD-23-083	230.83	231.48	0.65	1.09	02E-NE
ITDD-23-083	310.73	314.78	4.05	1.11	04-NE
ITDD-23-083	371.44	372.42	0.98	0.43	05-NE
ITDD-23-083	372.67	379.76	7.09	2.29	05-NE
ITDD-23-084	273.30	274.06	0.76	0.92	01A-SW
ITDD-23-084	275.42	278.93	3.51	1.60	1
ITDD-23-084	279.20	284.87	5.67	1.16	1
ITDD-23-085	73.40	74.47	1.07	0.21	SE-A
ITDD-23-086	69.92	72.11	2.19	1.48	02D-NE
ITDD-23-086	272.46	274.84	2.38	1.52	04-NE
ITDD-23-086	276.00	282.45	6.45	1.07	04-NE
ITDD-23-086	282.97	283.27	0.30	0.60	04-NE
ITDD-23-086	293.70	299.86	6.16	1.33	04C-NE
ITDD-23-087	53.24	56.07	2.83	0.70	SE-A
ITDD-23-087	56.92	58.73	1.81	1.90	SE-A
ITDD-23-087	60.20	64.85	4.65	1.38	SE-A
ITDD-23-087	65.45	66.15	0.70	0.85	SE-A
ITDD-23-087	67.79	69.96	2.17	1.88	SE-A

holeid	from	to	Legth	Li2O %	Domain
ITDD-23-088	83.32	86.32	3.00	0.96	02-NE
ITDD-23-088	199.94	202.63	2.69	1.59	04-NE
ITDD-23-088	206.00	210.19	4.19	1.87	04-NE
ITDD-23-088	272.46	274.62	2.16	2.21	05-NE
ITDD-23-088	287.18	287.96	0.78	0.74	05C-NE
ITDD-23-088	294.83	295.63	0.80	0.48	05B-NE
ITDD-23-089	63.26	72.02	8.76	1.37	SE-A
ITDD-23-089	155.53	161.53	6.00	1.22	08-NE
ITDD-23-090	161.74	169.95	8.21	1.03	03-NE
ITDD-23-090	253.07	255.80	2.73	0.66	02-NE
ITDD-23-090	259.50	263.50	4.00	1.80	02-NE
ITDD-23-090	386.98	389.98	3.00	1.62	1
ITDD-23-090	442.90	445.66	2.76	1.79	04-NE
ITDD-23-090	465.61	466.26	0.65	1.05	04C-NE
ITDD-23-090	466.85	471.85	5.00	1.72	04C-NE
ITDD-23-090	564.45	567.45	3.00	1.56	06-NE
ITDD-23-090	580.60	581.60	1.00	0.47	07-NE
ITDD-23-091	62.26	63.07	0.81	0.43	01E-SW
ITDD-23-091	426.04	427.97	1.93	0.89	01D-SW
ITDD-23-091	479.83	482.00	2.17	2.04	1
ITDD-23-091	486.04	489.24	3.20	0.82	1
ITDD-23-092	92.81	95.83	3.02	1.57	01A-SW
ITDD-23-092	103.81	109.42	5.61	1.23	1
ITDD-23-093	43.65	51.65	8.00	1.47	SE-A
ITDD-23-094	80.58	81.72	1.14	1.25	1
ITDD-23-094	82.97	83.37	0.40	1.73	1
ITDD-23-094	83.88	88.26	4.38	2.17	1
ITDD-23-095	46.35	48.48	2.13	0.70	02C-NE
ITDD-23-095	202.91	203.63	0.72	0.54	01A-SW
ITDD-23-095	205.40	206.91	1.51	1.13	01A-SW
ITDD-23-095	216.19	217.88	1.69	1.98	1
ITDD-23-095	218.84	223.07	4.23	1.38	1
ITDD-23-096	88.95	90.40	1.45	1.03	1
ITDD-23-096	91.20	97.18	5.98	1.91	1
ITDD-23-097	38.70	44.12	5.42	1.48	1
ITDD-23-098	62.59	67.59	5.00	1.64	1
ITDD-23-098	194.04	196.69	2.65	1.02	05-NE

holeid	from	to	Legth	Li2O %	Domain
ITDD-23-099	63.04	65.04	2.00	1.91	01A-SW
ITDD-23-099	67.96	72.49	4.53	1.10	1
ITDD-23-100	27.85	28.85	1.00	0.26	1
ITDD-23-100	32.49	33.49	1.00	0.40	01B-SW
ITDD-23-101	76.74	81.74	5.00	1.55	1
ITDD-23-102	52.60	56.09	3.49	1.16	02C-NE
ITDD-23-102	202.45	204.35	1.90	0.99	01A-SW
ITDD-23-102	226.35	226.90	0.55	2.01	1
ITDD-23-102	228.55	233.36	4.81	1.63	1
ITDD-23-103	197.00	200.00	3.00	1.33	1
ITDD-23-104	55.89	57.89	2.00	0.84	1
ITDD-23-104	58.89	59.89	1.00	0.84	01B-SW
ITDD-23-105	97.01	99.52	2.51	1.47	02C-NE
ITDD-23-105	110.73	116.40	5.67	1.49	02-NE
ITDD-23-105	214.09	215.79	1.70	0.96	01A-SW
ITDD-23-105	220.44	229.59	9.15	1.32	1
ITDD-23-105	370.38	372.70	2.32	1.46	05-NE
ITDD-23-105	373.42	375.38	1.96	1.19	05-NE
ITDD-23-106	133.08	135.23	2.15	0.95	01B-SW
ITDD-23-107	194.96	195.83	0.87	0.46	01A-SW
ITDD-23-107	197.74	199.94	2.20	1.37	1
ITDD-23-107	209.54	213.54	4.00	1.81	01B-SW
ITDD-23-108	75.26	81.26	6.00	1.59	1
ITDD-23-108	81.26	81.89	0.63	0.10	1
ITDD-23-108	86.52	88.52	2.00	1.73	01B-SW
ITDD-23-109	120.09	126.07	5.98	1.34	1
ITDD-23-109	126.60	127.08	0.48	1.34	1
ITDD-23-109	127.30	127.60	0.30	0.32	1
ITDD-23-109	247.87	255.66	7.79	1.69	05-NE
ITDD-23-110	55.33	56.10	0.77	1.35	01A-SW
ITDD-23-110	58.58	62.84	4.26	2.15	1
ITDD-23-111	27.80	34.40	6.60	1.51	1
ITDD-23-113	97.33	99.89	2.56	1.75	1
ITDD-23-114	66.26	67.26	1.00	0.38	01A-SW
ITDD-23-114	71.78	78.15	6.37	0.96	1
ITDD-23-115	34.08	41.00	6.92	1.26	1
ITDD-23-116	112.82	117.36	4.54	2.18	01A-SW

holeid	from	to	Legth	Li2O %	Domain
ITDD-23-116	132.52	132.78	0.26	0.49	1
ITDD-23-116	133.12	134.17	1.05	1.32	1
ITDD-23-117	35.00	36.69	1.69	0.21	02A-NE
ITDD-23-117	143.90	145.00	1.10	2.81	01A-SW
ITDD-23-117	166.63	169.18	2.55	0.74	1
ITDD-23-118	155.35	156.56	1.21	1.76	01A-SW
ITDD-23-118	160.13	160.82	0.69	0.40	1
ITDD-23-118	161.16	164.07	2.91	1.12	1
ITDD-23-120	109.66	114.98	5.32	1.33	01A-SW
ITDD-23-120	115.28	115.92	0.64	0.84	01A-SW
ITDD-23-120	126.06	127.18	1.12	0.52	1
ITDD-23-120	253.93	259.63	5.70	1.86	05-NE
ITDD-23-112	124.79	131.18	6.39	1.74	1
ITDD-23-112	142.43	144.36	1.93	1.20	01B-SW
ITDD-23-119	118.90	119.42	0.52	0.31	01A-SW
ITDD-23-119	124.13	130.85	6.72	1.57	1
ITDD-23-121	36.85	37.50	0.65	0.31	02-NE
ITDD-23-121	38.85	40.85	2.00	0.80	02-NE
ITDD-23-121	44.74	45.12	0.38	0.73	02A-NE
ITDD-23-121	163.40	164.25	0.85	2.07	01A-SW
ITDD-23-121	165.12	169.82	4.70	2.15	01A-SW
ITDD-23-121	182.04	183.59	1.55	2.59	1
ITDD-23-121	331.55	337.47	5.92	1.83	05-NE
ITDD-23-122	157.52	158.16	0.64	0.73	01A-SW
ITDD-23-122	164.11	168.11	4.00	1.49	1
ITDD-23-123	150.16	150.51	0.35	0.38	01A-SW
ITDD-23-123	151.75	159.40	7.65	2.39	1
ITDD-23-123	285.88	286.88	1.00	0.73	05-NE
ITDD-23-124	80.04	81.04	1.00	0.70	1
ITDD-23-125	133.72	134.77	1.05	0.29	1
ITDD-23-125	144.94	147.92	2.98	1.44	01B-SW
ITDD-23-126	105.80	108.37	2.57	1.02	1
ITDD-23-127	81.91	82.66	0.75	1.11	1
ITDD-23-128	178.46	178.94	0.48	1.38	1
ITDD-23-128	179.31	183.31	4.00	2.43	1
ITDD-23-129	153.61	155.00	1.39	0.83	01A-SW
ITDD-23-129	157.10	160.35	3.25	1.40	1

holeid	from	to	Legth	Li2O %	Domain
ITDD-23-130	88.49	91.08	2.59	1.15	1
ITDD-23-130	201.33	203.33	2.00	0.60	05-NE
ITDD-23-130	240.32	242.41	2.09	1.46	05B-NE
ITDD-23-131	99.48	101.48	2.00	1.98	1
ITDD-23-131	272.94	278.00	5.06	0.96	05-NE
ITDD-23-132	69.56	72.73	3.17	1.66	01C-SW
ITDD-23-132	166.14	167.86	1.72	1.75	01A-SW
ITDD-23-132	168.98	169.88	0.90	1.31	01A-SW
ITDD-23-132	172.68	178.59	5.91	1.59	1
ITDD-23-133	150.20	154.79	4.59	1.20	1
ITDD-23-134	32.45	34.95	2.50	2.43	01C-SW
ITDD-23-134	135.63	137.16	1.53	0.50	01A-SW
ITDD-23-134	138.85	141.96	3.11	2.24	1
ITDD-23-135	111.38	112.27	0.89	0.13	1
ITDD-23-135	136.02	137.59	1.57	2.96	04-NE
ITDD-23-135	205.63	206.63	1.00	0.35	05-NE
ITDD-23-135	247.22	248.46	1.24	0.31	05B-NE
ITDD-23-136	75.02	75.76	0.74	0.43	1
ITDD-23-136	85.97	89.97	4.00	1.73	04-NE
ITDD-23-136	283.33	286.25	2.92	0.19	06-NE
ITDD-23-136	318.38	319.63	1.25	0.28	07-NE
ITDD-23-136	328.82	329.29	0.47	1.26	07A-NE
ITDD-23-137	81.68	85.18	3.50	1.48	01C-SW
ITDD-23-137	182.18	183.70	1.52	0.92	01A-SW
ITDD-23-137	185.16	185.66	0.50	1.81	01A-SW
ITDD-23-137	186.06	187.39	1.33	1.38	01A-SW
ITDD-23-137	189.80	196.65	6.85	1.44	1
ITDD-23-137	207.90	208.90	1.00	0.50	01B-SW
ITDD-23-138	289.52	291.29	1.77	1.56	1
ITDD-23-138	292.62	296.62	4.00	0.97	1
ITDD-23-140	27.30	28.08	0.78	0.57	1
ITDD-23-140	28.83	30.62	1.79	1.22	1
ITDD-23-141	39.98	44.45	4.47	1.32	1
ITDD-23-141	47.25	49.25	2.00	0.52	04-NE
ITDD-23-141	49.58	51.61	2.03	0.69	04-NE
ITDD-23-142	36.36	40.36	4.00	1.39	02-NE
ITDD-23-142	40.36	41.36	1.00	1.39	02A-NE

Figure 10-5 – Mineralized Intercepts by Bandeira Drill Holes

Source: GE21 2024

holeid	from	to	Legth	Li2O %	Domain
ITDD-23-142	126.70	128.70	2.00	2.05	1
ITDD-23-144	82.50	82.98	0.48	2.34	1
ITDD-23-144	94.46	99.42	4.96	1.85	04-NE
ITDD-23-139	304.00	315.16	11.16	1.63	1
ITDD-23-143	48.05	49.46	1.41	1.18	02-NE
ITDD-23-143	49.87	52.40	2.53	2.21	02A-NE
ITDD-23-143	156.45	158.76	2.31	0.71	1
ITDD-23-143	164.12	167.19	3.07	1.34	04-NE
ITDD-23-143	168.75	169.75	1.00	1.43	04-NE
ITDD-23-143	187.65	188.03	0.38	2.99	04C-NE
ITDD-23-143	189.75	190.05	0.30	0.32	04C-NE
ITDD-23-143	190.45	191.02	0.57	0.65	04C-NE
ITDD-23-143	231.53	233.40	1.87	0.64	05-NE
ITDD-23-143	251.16	251.77	0.61	0.94	05C-NE
ITDD-23-143	341.86	344.37	2.51	1.52	06-NE
ITDD-23-143	347.82	349.48	1.66	0.73	06A-NE
ITDD-23-143	359.64	361.75	2.11	0.42	06B-NE
ITDD-23-143	383.35	384.95	1.60	1.79	07-NE
ITDD-23-143	385.37	388.72	3.35	1.89	07-NE
ITDD-23-143	398.90	400.75	1.85	2.40	07A-NE
ITDD-23-145	283.58	284.05	0.47	1.70	01A-SW
ITDD-23-145	290.15	290.59	0.44	2.33	1
ITDD-23-145	290.95	302.05	11.10	1.38	1
ITDD-23-146	132.78	134.82	2.04	0.34	01A-SW
ITDD-23-146	142.88	147.88	5.00	1.29	1
ITDD-23-146	267.31	276.18	8.87	1.57	05-NE
ITDD-23-147	41.30	44.43	3.13	1.96	02-NE
ITDD-23-147	45.04	47.62	2.58	1.35	02A-NE
ITDD-23-147	138.02	140.27	2.25	1.11	1
ITDD-23-147	268.30	271.03	2.73	1.63	05-NE
ITDD-23-147	285.15	287.81	2.66	1.57	05C-NE
ITDD-23-147	307.66	310.36	2.70	2.16	05B-NE
ITDD-23-147	391.75	392.34	0.59	1.87	07-NE
ITDD-23-147	393.84	395.03	1.19	0.75	07-NE
ITDD-23-147	395.79	396.24	0.45	0.47	07-NE
ITDD-23-147	396.66	398.68	2.02	1.30	07-NE
ITDD-23-147	399.92	401.23	1.31	0.63	07-NE

holeid	from	to	Legth	Li2O %	Domain
ITDD-23-147	404.20	405.27	1.07	1.00	07A-NE
ITDD-23-147	406.79	409.13	2.34	1.12	07A-NE
ITDD-23-147	430.72	436.67	5.95	2.01	08-NE
ITDD-23-147	479.02	480.29	1.27	1.25	08A-NE
ITDD-23-147	481.53	481.90	0.37	0.95	08A-NE
ITDD-23-147	483.52	486.52	3.00	2.13	08A-NE
ITDD-23-147	488.57	489.06	0.49	2.05	08B-NE
ITDD-23-148	60.55	61.40	0.85	1.07	04B-NE
ITDD-23-148	62.30	64.65	2.35	0.50	1
ITDD-23-148	73.61	77.87	4.26	1.17	04-NE
ITDD-23-148	257.50	260.54	3.04	3.18	06-NE
ITDD-23-148	262.83	266.60	3.77	1.39	06A-NE
ITDD-23-148	317.40	320.17	2.77	2.11	07-NE
ITDD-23-148	326.16	328.99	2.83	1.44	07A-NE
ITDD-23-149	46.51	48.45	1.94	1.52	01E-SW
ITDD-23-149	434.80	438.60	3.80	1.94	1
ITDD-23-149	439.41	440.56	1.15	1.61	1
ITDD-23-150	123.60	129.60	6.00	1.74	01A-SW
ITDD-23-150	142.44	146.34	3.90	2.15	1
ITDD-23-150	293.11	301.75	8.64	1.45	05-NE
ITDD-23-151	8.66	10.35	1.69	0.68	01E-SW
ITDD-23-151	348.98	351.05	2.07	1.17	01D-SW
ITDD-23-151	411.87	421.66	9.79	1.84	1
ITDD-23-152	53.19	55.35	2.16	0.44	02-NE
ITDD-23-152	56.15	58.31	2.16	1.29	02A-NE
ITDD-23-152	165.09	166.09	1.00	0.42	1
ITDD-23-152	183.78	185.86	2.08	0.30	04-NE
ITDD-23-152	250.73	252.51	1.78	0.92	05A-NE
ITDD-23-152	272.95	274.60	1.65	1.52	05-NE
ITDD-23-152	291.98	295.53	3.55	2.02	05B-NE
ITDD-23-154	108.52	113.42	4.90	1.57	1
ITDD-23-154	116.50	118.26	1.76	0.56	04-NE
ITDD-23-154	119.76	121.15	1.39	1.46	04-NE
ITDD-23-154	296.12	298.14	2.02	1.58	06-NE
ITDD-23-154	302.70	303.78	1.08	2.80	06A-NE
ITDD-23-154	305.07	306.29	1.22	2.38	06A-NE
ITDD-23-154	308.01	308.78	0.77	1.09	06A-NE

holeid	from	to	Legth	Li2O %	Domain
ITDD-23-154	310.17	310.99	0.82	0.77	06A-NE
ITDD-23-154	332.07	335.08	3.01	1.80	06B-NE
ITDD-23-154	336.32	337.38	1.06	0.68	06B-NE
ITDD-23-154	337.82	338.28	0.46	0.90	06B-NE
ITDD-23-154	359.89	361.12	1.23	2.19	07-NE
ITDD-23-154	361.50	363.56	2.06	1.89	07-NE
ITDD-23-154	369.23	370.37	1.14	1.24	07A-NE
ITDD-23-155	44.50	49.50	5.00	1.71	02-NE
ITDD-23-155	49.50	50.49	0.99	1.71	02A-NE
ITDD-23-155	149.36	151.36	2.00	1.67	1
ITDD-23-156	63.03	67.36	4.33	1.30	02A-NE
ITDD-23-156	209.37	211.94	2.57	0.90	04-NE
ITDD-23-156	213.86	218.63	4.77	2.02	04-NE
ITDD-23-156	290.10	292.08	1.98	0.94	05A-NE
ITDD-23-156	299.55	301.20	1.65	1.11	05-NE
ITDD-23-156	301.70	302.52	0.82	1.30	05-NE
ITDD-23-156	305.01	306.31	1.30	1.41	05-NE
ITDD-23-156	313.78	317.61	3.83	1.78	05B-NE
ITDD-23-157	78.37	79.17	0.80	0.77	02-NE
ITDD-23-157	87.20	89.20	2.00	0.93	02A-NE
ITDD-23-157	190.25	194.07	3.82	0.61	01A-SW
ITDD-23-157	203.54	205.60	2.06	1.78	1
ITDD-23-157	354.35	359.35	5.00	1.53	05-NE
ITDD-23-158	13.30	14.55	1.25	1.44	01E-SW
ITDD-23-158	393.02	396.02	3.00	1.09	01D-SW
ITDD-23-158	444.60	445.03	0.43	1.22	01A-SW
ITDD-23-158	445.93	446.80	0.87	0.86	01A-SW
ITDD-23-158	453.28	453.59	0.31	0.39	1
ITDD-23-158	453.97	455.14	1.17	2.92	1
ITDD-23-158	456.50	468.92	12.42	2.02	1
ITDD-23-160	66.94	67.50	0.56	0.50	1
ITDD-23-160	230.18	230.77	0.59	1.50	05-NE
ITDD-23-160	234.27	237.37	3.10	1.18	05-NE
ITDD-23-161	13.66	14.34	0.68	1.77	02-NE
ITDD-23-161	25.12	25.77	0.65	1.41	02A-NE
ITDD-23-161	129.12	133.12	4.00	1.27	1
ITDD-23-161	174.56	177.56	3.00	2.57	04C-NE

holeid	from	to	Legth	Li2O %	Domain
ITDD-23-161	313.74	315.43	1.69	2.10	06-NE
ITDD-23-161	322.93	324.22	1.29	0.95	06A-NE
ITDD-23-161	326.51	327.94	1.43	1.10	06A-NE
ITDD-23-161	351.41	354.37	2.96	1.16	06B-NE
ITDD-23-161	377.01	378.76	1.75	0.15	07-NE
ITDD-23-162	53.69	56.49	2.80	1.10	01E-SW
ITDD-23-162	395.57	398.57	3.00	1.56	01D-SW
ITDD-23-162	458.62	462.24	3.62	1.22	1
ITDD-23-163	204.32	206.32	2.00	0.87	02-NE
ITDD-23-163	245.30	245.81	0.51	0.20	02B-NE
ITDD-23-163	256.24	257.48	1.24	1.78	02E-NE
ITDD-23-163	298.22	299.76	1.54	0.66	1
ITDD-23-163	301.28	302.28	1.00	0.21	1
ITDD-23-163	348.35	349.35	1.00	0.14	04-NE
ITDD-23-163	354.35	359.42	5.07	0.72	04C-NE
ITDD-23-163	382.72	385.73	3.01	1.03	05A-NE
ITDD-23-163	387.92	389.09	1.17	1.51	05A-NE
ITDD-23-163	392.27	394.69	2.42	1.26	05A-NE
ITDD-23-163	395.05	397.65	2.60	0.96	05A-NE
ITDD-23-163	404.30	410.30	6.00	0.75	05-NE
ITDD-23-163	425.03	434.90	9.87	2.11	05B-NE
ITDD-23-163	469.10	473.67	4.57	1.75	06-NE
ITDD-23-163	474.65	477.57	2.92	1.79	06A-NE
ITDD-23-163	511.31	517.88	6.57	1.62	07-NE
ITDD-23-164	64.12	65.36	1.24	1.46	02C-NE
ITDD-23-164	80.29	83.39	3.10	1.22	02-NE
ITDD-23-164	87.48	100.06	12.58	1.50	02A-NE
ITDD-23-164	170.49	173.30	2.81	1.73	1
ITDD-23-164	325.78	326.42	0.64	1.82	05-NE
ITDD-23-164	328.68	333.75	5.07	0.74	05-NE
ITDD-23-164	415.18	417.35	2.17	0.86	07-NE
ITDD-23-164	418.75	419.65	0.90	0.54	07-NE
ITDD-23-164	424.78	427.02	2.24	0.84	07A-NE
ITDD-23-164	434.58	437.39	2.81	0.78	08-NE
ITDD-23-164	438.59	443.52	4.93	2.06	08-NE
ITDD-23-165	79.48	80.70	1.22	0.20	02C-NE
ITDD-23-165	100.21	101.21	1.00	0.35	02-NE

holeid	from	to	Legth	Li2O %	Domain
ITDD-23-165	195.00	202.00	7.00	2.08	1
ITDD-23-165	202.64	202.99	0.35	0.72	1
ITDD-23-165	338.94	342.77	3.83	1.42	05-NE
ITDD-23-166	89.68	90.72	1.04	1.58	05D-NE
ITDD-23-166	97.55	99.71	2.16	2.03	05-NE
ITDD-23-167	65.42	67.10	1.68	0.12	02C-NE
ITDD-23-167	228.46	229.56	1.10	0.81	01A-SW
ITDD-23-167	230.45	238.50	8.05	1.93	1
ITDD-23-167	345.55	351.27	5.72	1.86	05-NE
ITDD-23-168	88.20	88.79	0.59	1.07	05D-NE
ITDD-23-168	116.69	120.59	3.90	0.88	05-NE
ITDD-23-169	32.29	33.27	0.98	1.71	02D-NE
ITDD-23-169	199.77	200.44	0.67	0.43	04B-NE
ITDD-23-169	214.79	215.79	1.00	0.53	1
ITDD-23-169	241.60	243.89	2.29	1.27	04-NE
ITDD-23-169	359.01	360.46	1.45	2.26	06-NE
ITDD-23-170	101.62	106.04	4.42	1.46	05-NE
ITDD-23-171	51.37	52.05	0.68	1.22	1
ITDD-23-171	52.69	54.96	2.27	0.64	1
ITDD-23-171	208.35	208.77	0.42	1.74	05D-NE
ITDD-23-171	222.89	228.56	5.67	1.95	05-NE
ITDD-23-172	15.84	16.93	1.09	1.89	02-NE
ITDD-23-172	26.83	27.74	0.91	1.11	02A-NE
ITDD-23-172	136.38	140.13	3.75	1.78	1
ITDD-23-172	180.94	185.33	4.39	1.58	04C-NE
ITDD-23-172	317.72	320.13	2.41	2.05	06-NE
ITDD-23-172	331.69	332.79	1.10	2.92	06A-NE
ITDD-23-172	350.08	352.13	2.05	0.52	06B-NE
ITDD-23-172	353.90	354.98	1.08	2.17	06B-NE
ITDD-23-172	368.65	368.95	0.30	1.89	07-NE
ITDD-23-172	369.88	371.88	2.00	1.84	07-NE
ITDD-23-173	122.48	129.13	6.65	1.50	05-NE
ITDD-23-174	55.70	57.78	2.08	0.74	02C-NE
ITDD-23-174	211.36	212.40	1.04	0.72	01A-SW
ITDD-23-174	213.11	214.99	1.88	2.09	1
ITDD-23-174	216.09	221.72	5.63	1.58	1
ITDD-23-174	342.54	346.82	4.28	1.65	05-NE

Figure 10-6 – Mineralized Intercepts by Bandeira Drill Holes

Source: GE21 2024

holeid	from	to	Legth	Li2O %	Domain
ITDD-23-175	214.57	216.09	1.52	0.64	02-NE
ITDD-23-175	275.37	276.40	1.03	0.38	02E-NE
ITDD-23-175	323.64	325.56	1.92	1.85	1
ITDD-23-175	383.34	385.19	1.85	1.02	04C-NE
ITDD-23-175	398.59	402.11	3.52	1.63	05A-NE
ITDD-23-175	404.49	407.49	3.00	1.50	05A-NE
ITDD-23-175	479.11	480.55	1.44	0.60	06-NE
ITDD-23-175	484.82	488.20	3.38	1.86	06A-NE
ITDD-23-175	488.20	488.80	0.60	0.27	06A-NE
ITDD-23-175	489.59	492.19	2.60	2.58	06A-NE
ITDD-23-175	502.82	503.65	0.83	1.52	07-NE
ITDD-23-175	524.36	525.90	1.54	1.43	08-NE
ITDD-23-175	526.83	528.21	1.38	1.78	08-NE
ITDD-23-175	529.05	529.94	0.89	1.38	08-NE
ITDD-23-176	56.11	57.66	1.55	1.54	1
ITDD-23-176	60.09	61.88	1.79	1.24	1
ITDD-23-176	221.74	223.08	1.34	0.91	05D-NE
ITDD-23-176	230.14	235.14	5.00	1.57	05-NE
ITDD-23-177	78.86	79.52	0.66	0.10	02C-NE
ITDD-23-177	110.89	113.89	3.00	1.12	02-NE
ITDD-23-177	199.14	200.30	1.16	1.03	01A-SW
ITDD-23-177	204.16	209.98	5.82	2.18	1
ITDD-23-177	354.96	355.75	0.79	1.86	05-NE
ITDD-23-177	356.86	359.59	2.73	1.35	05-NE
ITDD-23-177	362.09	363.55	1.46	1.54	05-NE
ITDD-23-178	171.00	173.18	2.18	0.67	1
ITDD-23-180	171.59	177.38	5.79	1.78	02-NE
ITDD-23-180	264.35	269.85	5.50	1.15	1
ITDD-23-180	390.61	393.13	2.52	1.41	05-NE
ITDD-23-180	393.51	401.35	7.84	2.06	05-NE
ITDD-23-181	203.14	205.32	2.18	1.26	01A-SW
ITDD-23-181	223.00	229.00	6.00	1.02	1
ITDD-23-182	30.47	31.47	1.00	0.40	02D-NE
ITDD-23-182	151.73	152.75	1.02	0.32	04A-NE
ITDD-23-182	181.36	182.40	1.04	0.77	04B-NE
ITDD-23-182	201.09	202.74	1.65	1.21	1
ITDD-23-182	226.06	228.07	2.01	1.33	04-NE

holeid	from	to	Legth	Li2O %	Domain
ITDD-23-182	228.72	231.25	2.53	1.49	04-NE
ITDD-23-182	358.81	359.69	0.88	0.35	06-NE
ITDD-23-183	177.37	178.64	1.27	3.40	1
ITDD-23-184	21.01	22.05	1.04	0.56	02-NE
ITDD-23-184	156.12	159.73	3.61	1.03	1
ITDD-23-184	188.74	189.51	0.77	0.28	04-NE
ITDD-23-184	201.67	203.01	1.34	0.99	04C-NE
ITDD-23-184	203.67	205.70	2.03	2.91	04C-NE
ITDD-23-184	207.71	210.57	2.86	1.21	04C-NE
ITDD-23-184	337.76	338.67	0.91	0.38	06-NE
ITDD-23-184	339.45	341.69	2.24	1.87	06-NE
ITDD-23-184	348.01	349.42	1.41	1.94	06A-NE
ITDD-23-184	384.79	385.63	0.84	0.44	07-NE
ITDD-23-184	386.31	387.52	1.21	0.93	07-NE
ITDD-23-185	240.77	244.06	3.29	1.84	02-NE
ITDD-23-185	360.36	365.03	4.67	1.54	1
ITDD-23-185	417.41	420.23	2.82	0.98	04-NE
ITDD-23-185	434.34	437.34	3.00	1.22	04C-NE
ITDD-23-185	443.78	447.25	3.47	1.10	05A-NE
ITDD-23-185	520.91	521.41	0.50	0.04	06-NE
ITDD-23-185	529.52	531.92	2.40	3.57	06A-NE
ITDD-23-185	539.78	540.32	0.54	0.59	07-NE
ITDD-23-185	567.15	569.57	2.42	2.00	08-NE
ITDD-23-186	16.90	17.95	1.05	0.22	01E-SW
ITDD-23-187	196.58	198.86	2.28	1.85	1
ITDD-23-189	70.07	72.93	2.86	0.97	1
ITDD-23-188	130.48	139.59	9.11	2.45	03-NE
ITDD-23-188	272.46	275.86	3.40	2.07	02-NE
ITDD-23-188	347.55	356.50	8.95	1.30	02B-NE
ITDD-23-188	391.25	392.79	1.54	0.26	1
ITDD-23-188	393.13	394.86	1.73	0.55	1
ITDD-23-188	461.28	461.99	0.71	0.67	04-NE
ITDD-23-188	463.82	465.66	1.84	1.05	04-NE
ITDD-23-188	466.64	471.60	4.96	1.71	04-NE
ITDD-23-188	483.13	485.78	2.65	0.39	04C-NE
ITDD-23-188	581.89	582.23	0.34	0.03	06-NE
ITDD-23-188	631.34	633.20	1.86	1.86	08-NE

holeid	from	to	Legth	Li2O %	Domain
ITDD-23-188	634.37	643.24	8.87	1.59	08-NE
ITDD-23-192	196.40	197.60	1.20	1.40	01A-SW
ITDD-23-192	198.71	202.91	4.20	1.66	01A-SW
ITDD-23-192	210.10	210.75	0.65	1.46	1
ITDD-23-192	346.48	348.84	2.36	1.11	05-NE
ITDD-23-192	349.42	355.84	6.42	1.73	05-NE
ITDD-23-193	48.07	49.34	1.27	0.24	10-NE
ITDD-23-193	65.08	68.85	3.77	1.39	09-NE
ITDD-23-194	96.22	96.94	0.72	1.02	05D-NE
ITDD-23-194	114.65	115.58	0.93	1.34	05-NE
ITDD-23-194	117.31	119.50	2.19	1.83	05-NE
ITDD-23-195	80.91	81.95	1.04	1.36	1
ITDD-23-195	83.20	84.24	1.04	0.00	1
ITDD-23-195	84.75	86.51	1.76	0.61	1
ITDD-23-196	110.73	111.46	0.73	1.41	05D-NE
ITDD-23-196	113.06	113.82	0.76	2.01	05D-NE
ITDD-23-196	137.13	138.60	1.47	1.88	05-NE
ITDD-23-196	140.15	146.05	5.90	1.61	05-NE
ITDD-23-197	94.36	95.84	1.48	0.57	1
ITDD-23-197	97.91	102.40	4.49	1.76	04-NE
ITDD-23-198	67.98	71.67	3.69	0.91	10-NE
ITDD-23-198	93.91	99.94	6.03	1.26	09-NE
ITDD-23-200	69.11	72.49	3.38	1.06	05-NE
ITDD-23-202	85.10	86.07	0.97	3.68	1
ITDD-23-202	87.04	87.62	0.58	1.04	1
ITDD-23-202	252.08	253.19	1.11	1.20	05D-NE
ITDD-23-202	258.82	262.81	3.99	1.83	05-NE
ITDD-23-203	83.29	83.69	0.40	0.81	05-NE
ITDD-23-209	41.61	51.61	10.00	1.13	SE-A
ITDD-23-199	127.38	129.42	2.04	2.03	02C-NE
ITDD-23-199	270.33	272.10	1.77	0.93	01A-SW
ITDD-23-199	288.91	294.47	5.56	1.59	1
ITDD-23-199	408.52	413.16	4.64	0.74	05-NE
ITDD-23-211	197.53	198.63	1.10	1.54	05D-NE
ITDD-23-211	211.54	212.82	1.28	0.40	05-NE
ITDD-23-212	110.38	112.78	2.40	1.21	05D-NE
ITDD-23-212	124.48	124.98	0.50	0.71	05-NE

holeid	from	to	Legth	Li2O %	Domain
ITDD-23-213	54.87	59.87	5.00	1.37	SE-A
ITDD-23-213	59.87	60.32	0.45	0.08	SE-A
ITDD-23-213	61.02	61.68	0.66	0.84	SE-A
ITDD-23-213	62.69	64.69	2.00	1.24	SE-A
ITDD-23-213	64.69	66.03	1.34	0.13	SE-A
ITDD-23-213	66.67	98.66	31.99	1.36	SE-A
ITDD-23-213	100.85	102.87	2.02	1.12	SE-A
ITDD-23-218	56.17	72.40	16.23	1.65	SE-A
ITDD-23-215	37.48	43.52	6.04	1.36	1
ITDD-23-215	187.71	188.49	0.78	0.38	05D-NE
ITDD-23-215	188.95	189.90	0.95	0.49	05D-NE
ITDD-23-215	203.86	208.94	5.08	2.44	05-NE
ITDD-23-215	209.38	212.54	3.16	0.92	05-NE
ITDD-23-216	55.24	60.12	4.88	1.54	01A-SW
ITDD-23-216	65.36	70.42	5.06	1.13	1
ITDD-23-216	197.59	206.18	8.59	1.59	05-NE
ITDD-23-219	56.49	57.17	0.68	1.16	01A-SW
ITDD-23-219	58.54	62.54	4.00	0.76	01A-SW
ITDD-23-219	67.05	69.31	2.26	0.53	1
ITDD-23-219	197.86	200.53	2.67	1.62	05-NE
ITDD-23-220	66.48	66.89	0.41	2.38	05D-NE
ITDD-23-220	68.46	69.48	1.02	0.77	05D-NE
ITDD-23-220	76.92	78.00	1.08	1.60	05-NE
ITDD-23-222	57.30	63.57	6.27	1.22	1
ITDD-23-222	197.78	202.62	4.84	1.45	05-NE
ITDD-23-223	64.00	64.70	0.70	1.20	05D-NE
ITDD-23-223	94.04	98.19	4.15	1.49	05-NE
ITDD-23-221	113.37	124.56	11.19	1.61	SE-A
ITDD-23-221	127.64	167.10	39.46	1.87	SE-A
ITDD-23-224	28.43	34.32	5.89	1.96	1
ITDD-23-224	166.46	170.87	4.41	1.67	05-NE
ITDD-23-224	171.28	172.45	1.17	2.45	05-NE
ITDD-23-225	78.99	81.13	2.14	1.85	05-NE
ITDD-23-225	83.80	85.97	2.17	0.72	05-NE
ITDD-23-226	35.27	42.50	7.23	2.12	1
ITDD-23-226	171.61	179.57	7.96	1.53	05-NE
ITDD-23-227	9.76	11.66	1.90	1.73	1

holeid	from	to	Legth	Li2O %	Domain
ITDD-23-227	12.58	14.82	2.24	1.18	1
ITDD-23-227	149.37	154.62	5.25	2.19	05D-NE
ITDD-23-227	179.03	181.93	2.90	1.67	05-NE
ITDD-23-228	98.34	106.93	8.59	1.46	SE-A
ITDD-23-228	110.13	122.94	12.81	1.43	SE-A
ITDD-23-229	122.55	124.72	2.17	1.30	05-NE
ITDD-23-230	136.25	137.06	0.81	1.63	05D-NE
ITDD-23-230	161.98	162.79	0.81	1.09	05-NE
ITDD-23-230	163.40	167.49	4.09	1.85	05-NE
ITDD-23-210	139.91	142.91	3.00	1.79	05-NE
ITDD-23-210	219.57	223.51	3.94	1.98	07-NE
ITDD-23-210	256.99	259.01	2.02	1.75	08-NE
ITDD-23-210	285.60	287.94	2.34	1.22	08A-NE
ITDD-23-210	298.00	300.05	2.05	0.83	08B-NE
ITDD-23-210	301.85	302.98	1.13	1.92	08B-NE
ITDD-23-231	129.79	130.53	0.74	1.31	05-NE
ITDD-23-231	131.14	132.27	1.13	0.99	05-NE
ITDD-23-231	133.26	136.35	3.09	1.57	05-NE
ITDD-23-232	116.40	116.98	0.58	0.86	05D-NE
ITDD-23-232	138.70	145.95	7.25	1.35	05-NE
ITDD-23-233	125.59	126.30	0.71	0.67	05D-NE
ITDD-23-233	127.47	129.17	1.70	0.47	05D-NE
ITDD-23-233	146.75	148.90	2.15	1.27	05-NE
ITDD-23-234	95.12	97.53	2.41	1.44	07-NE
ITDD-23-234	147.34	148.34	1.00	0.27	08-NE
ITDD-23-235	104.46	105.70	1.24	1.87	07-NE
ITDD-23-235	107.81	111.29	3.48	1.62	07-NE
ITDD-23-235	167.04	171.04	4.00	1.29	08-NE
ITDD-23-235	188.10	189.10	1.00	0.40	08A-NE
ITDD-23-235	206.29	207.29	1.00	0.14	08B-NE
ITDD-23-236	101.89	104.89	3.00	1.39	07-NE
ITDD-23-236	173.04	174.04	1.00	0.35	08-NE
ITDD-23-159	16.50	18.75	2.25	0.43	02-NE
ITDD-23-159	23.36	25.16	1.80	0.77	02A-NE
ITDD-23-159	115.78	117.32	1.54	0.34	1
ITDD-23-159	278.40	279.00	0.60	1.24	05D-NE
ITDD-23-159	287.50	289.55	2.05	1.28	05-NE

holeid	from	to	Legth	Li2O %	Domain
ITDD-23-159	291.65	292.65	1.00	1.25	05-NE
ITDD-23-159	350.16	351.23	1.07	0.91	07-NE
ITDD-23-159	351.66	353.08	1.42	1.09	07-NE
ITDD-23-159	372.21	379.28	7.07	1.78	08-NE
ITDD-23-159	425.97	426.72	0.75	2.01	08A-NE
ITDD-23-159	428.03	429.06	1.03	2.91	08A-NE
ITDD-23-159	430.60	431.54	0.94	2.81	08A-NE
ITDD-23-159	431.98	433.53	1.55	1.72	08A-NE
ITDD-23-159	435.46	437.60	2.14	2.42	08A-NE
ITDD-23-159	445.38	446.60	1.22	3.23	08B-NE
ITDD-23-159	448.60	450.94	2.34	1.80	08B-NE
ITDD-23-243	45.06	54.06	9.00	1.52	11-NE
ITDD-23-246	45.70	50.70	5.00	1.17	11-NE
ITDD-23-247	86.62	96.77	10.15	0.95	11-NE
ITDD-23-248	71.41	76.41	5.00	1.02	11-NE
ITDD-23-249	122.10	124.10	2.00	0.56	11-NE
ITDD-24-250	43.42	49.42	6.00	1.09	11-NE
ITDD-24-251	193.16	197.00	3.84	1.28	11-NE
ITDD-24-252	94.07	101.07	7.00	1.14	11-NE
ITDD-24-253	181.75	188.30	6.55	1.01	11-NE

Figure 10-7 – Mineralized Intercepts by Bandeira Drill Holes

Source: GE21 2024

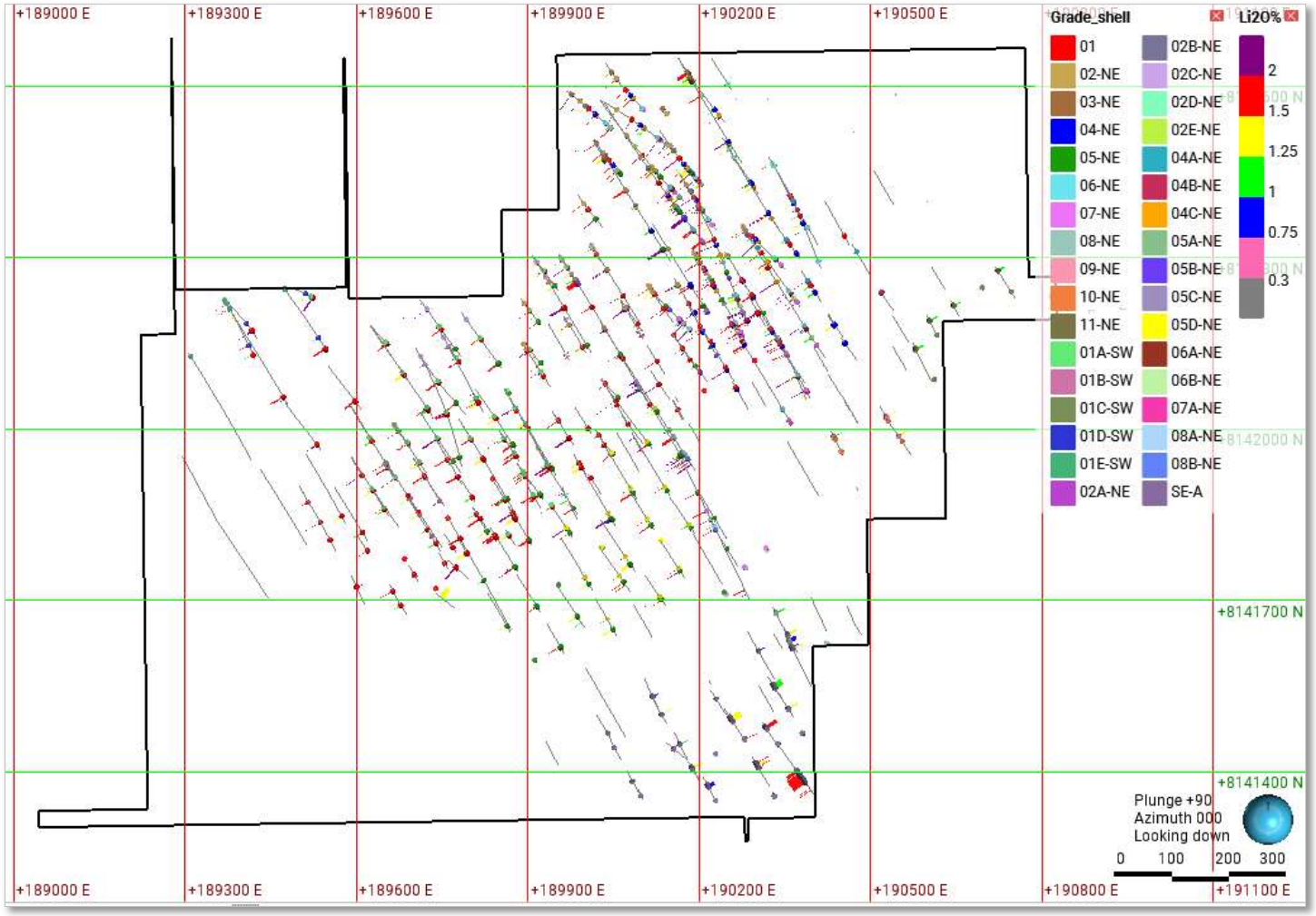

Figure 10-8 – Horizontal Projection of Bandeira Drilling Holes with Mineralized Intercepts

Source: GE21 2024

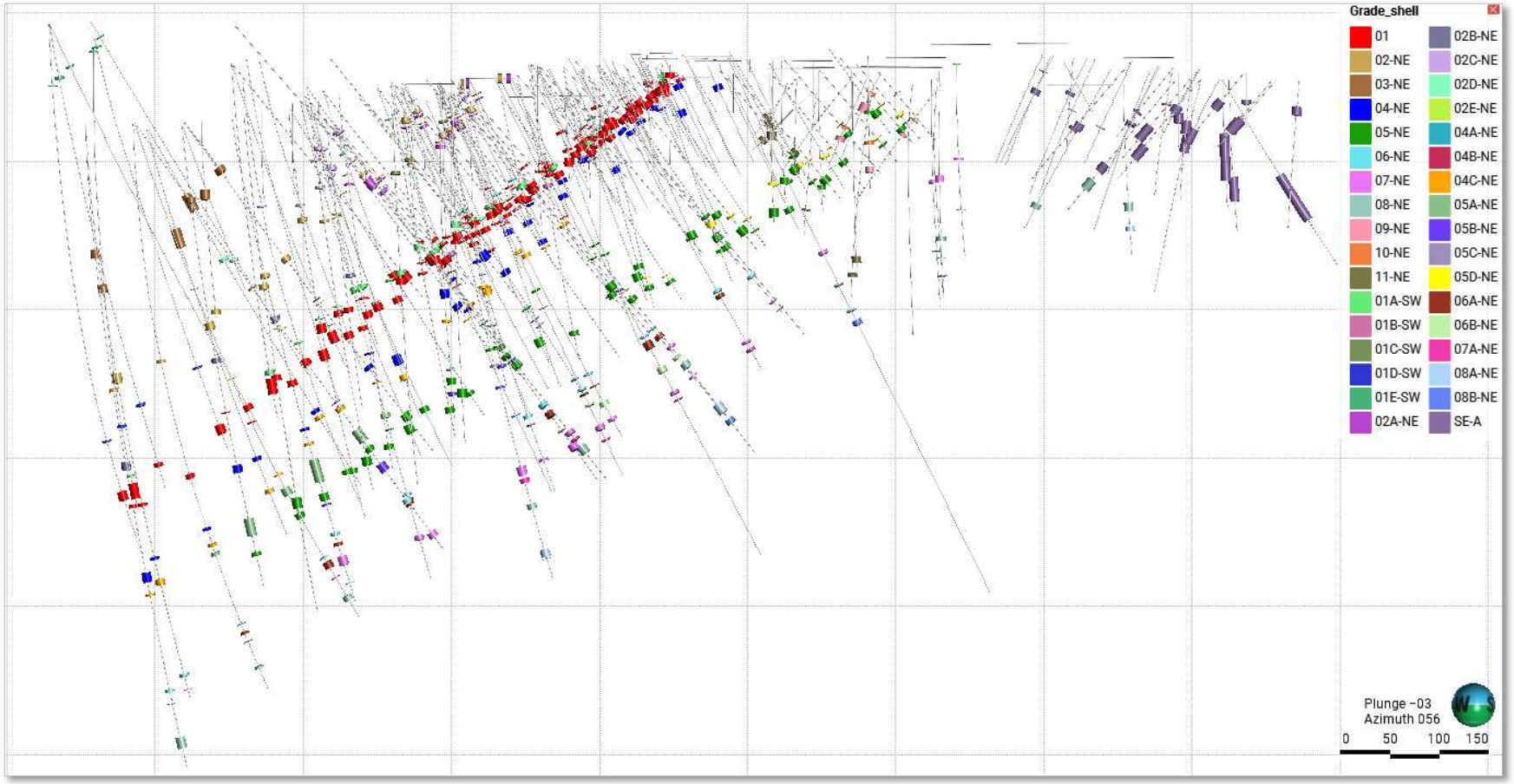

Figure 10-9 – Oblique View of Drill Holes with Mineralized Intercept

Source: GE21 2024

11 SAMPLE PREPARATION, ANALYSES AND SECURITY

11.1 Sampling

Samples are prepared from NQ diameter drill cores (47.6mm core diameter). The sampling procedures described in this section reflect the current Standard Operational Procedures (SOP) in use by Lithium Ionic.

Sample intervals in the mineralized zones are defined based on a one-meter support. Mineralized samples must have a minimum length of 1.00m and a maximum length of 1.50m. In some specific situations, samples shorter than 1.00m can be generated. These situations are described in detail in the SOP.

Outside the mineralized domains, the sampling support is 1.50m, and samples can range from 1.00m to 3.00m.

The visual indicators for sample interval definition include lithological contacts, structures, and mineralization.

The sample collection and sample definition procedures adopted by Lithium Ionic are described below:

- Drill core is brought in by the drilling contractor team, one or more times per shift, from the drill rig to a drill logging and sampling area.
- The disposition and orientation of boxes are checked, and the depth lengths are marked.
- Core boxes are photographed (three boxes per picture) and logged.
- Sample intervals are marked with a pencil in the core box.
- Before sampling, the drill core is marked by a line drawn along the core at high angles to the foliation to orient the saw cut. The left side of the core is selected as a sample. The remaining half of the core is retained for future reference.
- Sample tags are attached to the core box at the end of each sample.
- Sample bags are numbered before sampling.
- Sample tags are inserted in the bags only after samples are bagged.
- After the samples are tagged and bagged, they are weighted.
- The core is cut lengthwise along the core axis. A Geologist defines the position of the cut, and a Geology Technician performs the cutting.
- For weathered material, a spatula or a machete is used to split the sample into two subsamples along the drilling direction.
- Fresh rock cores are cut in half using a diamond saw and flushed with water between cuts.

- After bagging, the samples are weighted, and the weight is registered.
- Batches are assembled and sent to the laboratory.

The standard batch size is 35 samples, consisting of 29 core samples and six quality control samples.

11.2 Sample Preparation, Security and Custody Chain of Custody

Samples are defined and marked on-site after logging and entering the data into the database. Cores are split in half using a diamond saw. Half of the core is retained in the core box, while the other half is stored in plastic bags, accompanied by a printed sample tag, and sent to the lab.

Drill core samples are prepared and analyzed by an independent commercial laboratory (SGS Geosol). The SGS Geosol facility is certified in ISO 9001, ISO 14001, and ISO 17025. The sample shipment is delivered to the SGS Geosol facility in Vespasiano, Minas Gerais, Brazil, via a parcel transport company. At all times, samples are in the custody and control of the Company's representatives until delivery to the laboratory, where samples are held in a secure enclosure until processing. SGS Geosol sends a confirmation e-mail with details of samples received upon delivery. The chain of custody of the batches was carefully maintained from collection at the drill rig to delivery at the laboratory to prevent accidental contamination or mixing of samples and render active tampering as tricky as possible.

All samples received at SGS Geosol are inventoried and weighed before processing. Samples are dried at 105°C, crushed to 75% passing <3 mm sieve, homogenized, split (jones riffle splitter), and pulverized (250 to 300 g of sample) in a steel mill to 95% passing 150 mesh.

11.3 Sample Analysis

After the preparation, the core samples are analyzed by SGS Geosol. The chemical assays are performed using SGS's analytical method ICP90A, a multi-element analysis using fusion by sodium peroxide (Na2O2) and an ICP-OES analysis. If lithium results are above 15000 ppm, SGS Geosol re-analyzes for lithium through the ICP90Q_Li method, similar to the ICP90A but with higher Detection Limits.

All chemical analysis conducted by SGS Geosol are reported to Lithium Ionic on PDF certificates, accompanied by an MS Excel digital file.

11.4 Density Measurements

The density SOP currently in use by Lithium Ionic states that density measurements should be taken for every geochemical sample generated. When the drill core quality does not allow for the density assay, this should be registered in the density sampling plan with a specified tag. The high frequency of the density sampling aims to acquire a statistically robust database.

Three samples should be taken for the geochemical samples with more heterogeneity: one on

the top of the sample, the other in the middle and one further in the base. Homogenous geochemical samples should generate only one density sample. Density samples must have a minimum length of 10 cm and a maximum of 25 cm. The density assay procedures do not include drying or sample sealing. Density is commonly measured in the unsampled half-cores, reflecting a faster and more dynamic drillhole data collection process. All density data is stored in a database. A summary of the procedures described in the density SOP is presented next:

- Sample selection and registration in the density plan.
- Weighing of the sample.
- Weighing of the sample while submerged.
- Density values are acquired from the following formula:
  - D = PA / (PA – PB).
  - D = Density.
  - PA = Sample weight (in the air).
  - PB = Sample weight (submerged in water).

The density assay procedures do not include drying or sample sealing with paraffin. Not implementing the mentioned procedures might be acceptable considering the deposit's climate and lithological characteristics.

For a more conclusive evaluation of the effect of those procedures on the density results, GE21 recommends duplicate density assays, using the SOP procedure in one sample and a procedure that includes drying and sealing in the other sample. For the sealed samples, the density formula to be used is:

Ds = Ps / [(Pp – Pj) – (Pp – Ps) * dp] Ds = Dry Density.

Ps =Dry sample weight (in the air).

Pp = Sealed sample weight (in the air).

Pj = Sealed sample weight (submerged in water). Dp = Paraffin density.

11.5 Quality Assurance and Quality Control (QA/QC)

The Quality Assurance and Quality Control program implemented was proposed by the independent company GE21. The sample batch composition includes 5 Quality Control Samples for every 30 regular samples. The Quality Control composition of the batches is described next:

- Coarse (Preparation) and Fine (Analytical) Blanks: 6% of the batch, or two blanks per batch, one of each type.
- Standards: 6% of the batch, or two standards per batch.
- Crushed Duplicates: 3% of the batch, or 1 sample per batch.
- Pulverized Duplicates: 3% of the batch, or 1 sample per batch.

Additionally, one sample is selected for the Check Assay procedure for every sample batch, representing 3% of the batch. Check samples are chosen from the pulverized material of a regular sample reserved by the primary laboratory. These samples are sent to a secondary laboratory, ALS Vancouver, monthly. ALS Vancouver is ISO 17025 accredited.

The same control sample proportion criteria should be respected on Check Assay batches: 2 standards, two blanks, and two duplicates. Particle Size Analysis (PSA) is also performed on the Check Assay samples. Figure 11-1 presents the batch composition scheme for batches with mineralized samples or zones and unmineralized batches. Table 11-1 shows the proportion of Quality Control samples in the Lithium Ionic geochemical database.

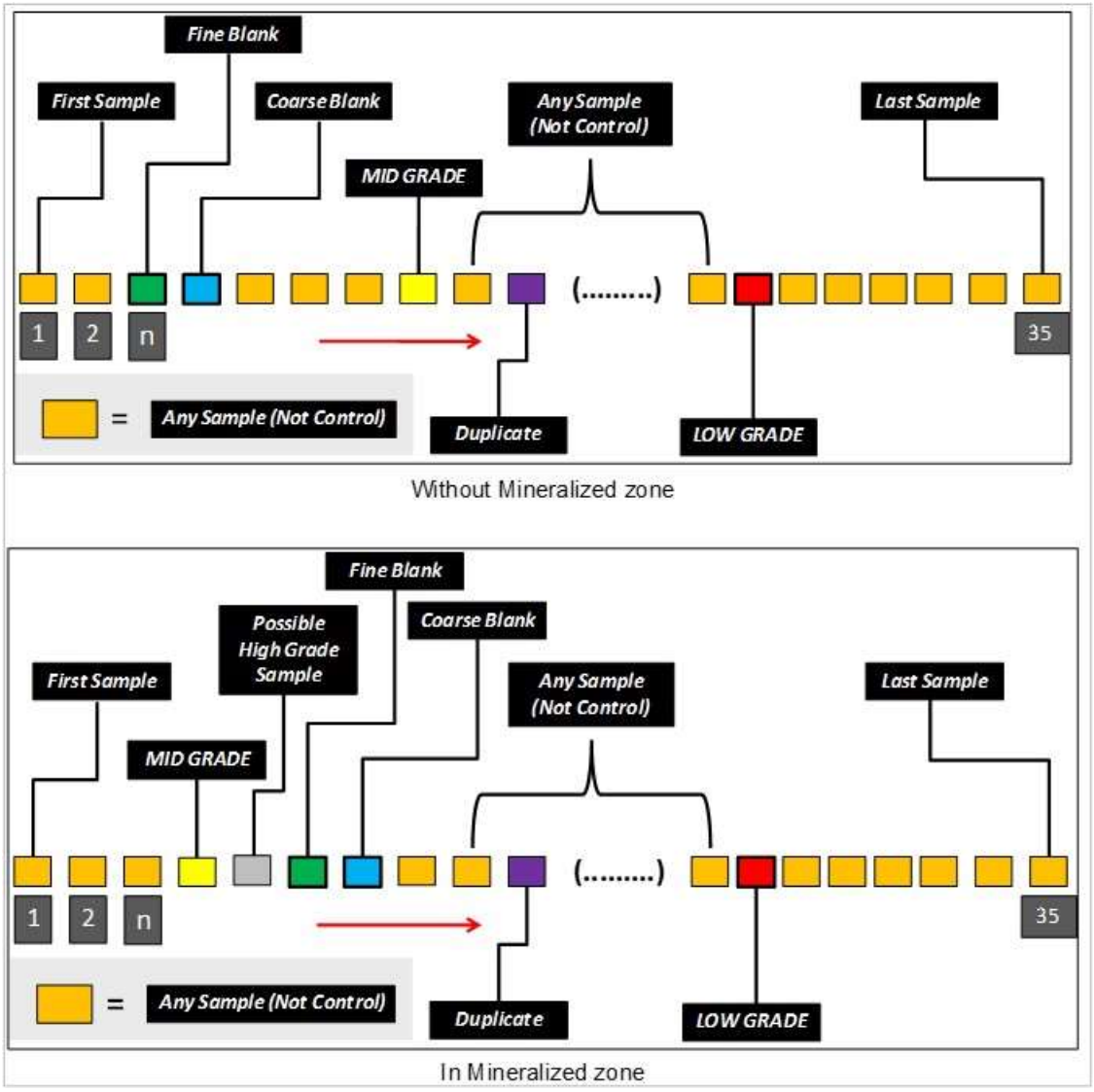

Figure 11-1 – QA/QC Program

Source: GE21 2024

Table 11-1 – QA/QC Program Summary

Source: GE21 2024

CRM/SRM	Crushed Duplicates	Pulverized Duplicates	Preparation Blanks	Analytical Blanks	Check-Assay	Total QA/QC Samples	Total Database
556	273	273	279	279	72	1732	10437
5.3%	2.6%	2.6%	2.7%	2.7%	0.7%	16.6%	100.0%

11.5.1 Preparation Blank – Coarse Blank

Preparation blank samples are inserted in the sample batch before the physical preparation of the samples. This measure helps to track any contamination problems that might occur in the granulometric reduction or sample-splitting processes. Blank samples are inserted at the beginning of the possibly mineralized intervals, following the sequence:

- Mineralized sample.
- Analytical/Fine Blank.
- Preparation/Coarse Blank.
- If an unmineralized batch is assembled, blank samples must be inserted at the beginning of the batch.
- Lithium Ionic uses a commercial blank, ITAK-QG-01, as its Coarse Blank material. More than 95% of the Coarse Blank samples are below the 5x Detection Limit threshold, indicating no major contamination. Figure 11-2 presents the Preparation Blank control chart for Lithium.

Type of Control	Blank
Reference	BLK_QG_01
Variable	Li_ppm
Number of analysis	279

Code	BLK_QG_01
Detection Limit	10
Standard desviation	12
Upper limit (5*DL)	50

Minimum	10
Maximum	129
Average	15
Median	10

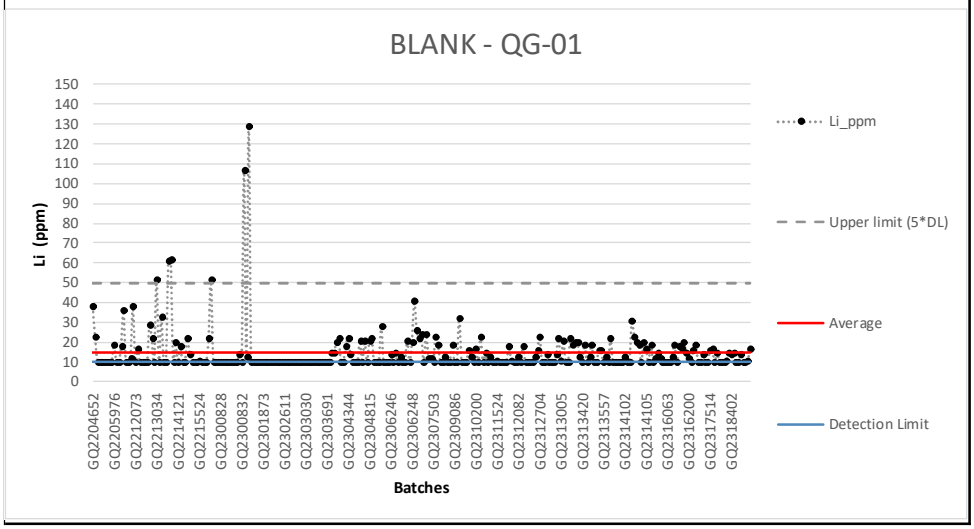

Figure 11-2 – Blank Control Chart – ITAK QG-01

Source: GE21 2024

11.5.2 Analytical Blank – Fine Blank

Analytical or Fine Blank samples are inserted in the analytical batches after the samples' physical preparation. This type of blank sample is used to assess contamination problems that might occur in the sample digestion or sample fusion processes and to evaluate analytical equipment (in this case, ICP-OES) miscalibrations. Blank Samples are inserted at the beginning of the possibly mineralized intervals, following the sequence:

- Mineralized sample.
- Analytical/Fine blank.
- Preparation/Coarse blank.

If an unmineralized batch is assembled, blank samples must be inserted at the beginning of the batch.

For its QA/QC Program, Lithium Ionic used three types of commercial Fine Blank controls: ITAK-QF-15, ITAK-QF-16 and ITAK-QF-18. Only two in 279 control samples inserted have returned grades higher than the 5x Detection Limit threshold, indicating no systematic contamination or calibration problems in the final stages of the geochemical analysis. Figure 11-3 to Figure 11-5 present the Analytical Blanks control charts for Lithium:

Type of Control	Blank
Reference	BLK_QF_15
Variable	Li_ppm
Number of analysis	38

Code	BLK_QF_15
Certificate Value	18.7
Standard desviation	13
Upper limit (5*DL)	50

Minimum	10
Maximum	62
Average	18
Median	12

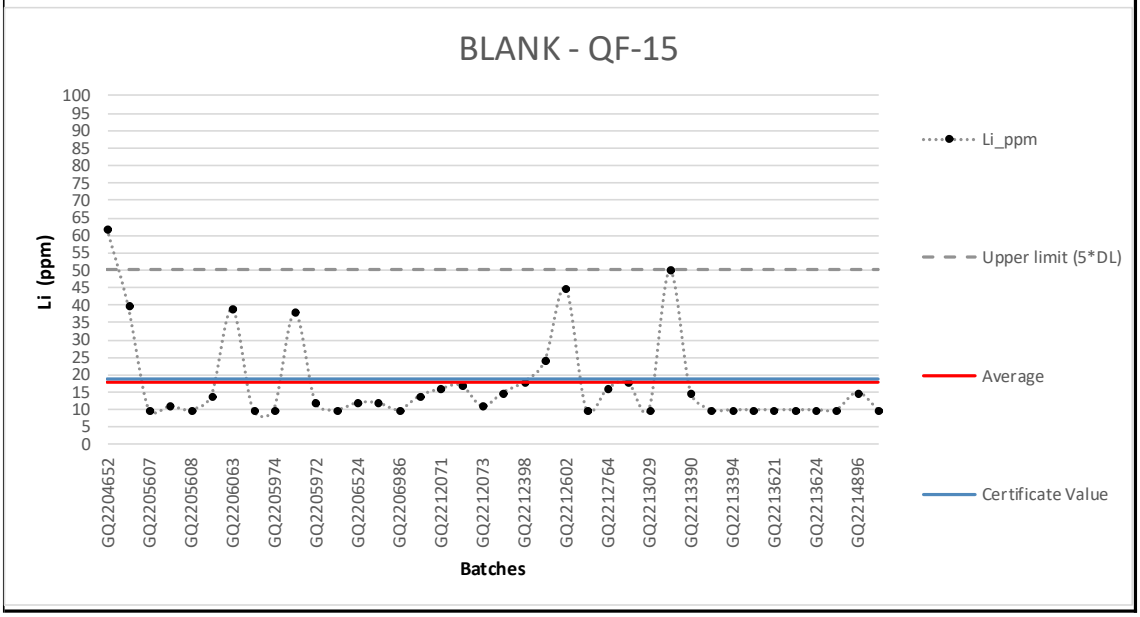

Figure 11-3 – Blank Control Chart – ITAK QF-15

Source: GE21 2024

Type of Control	Blank
Reference	BLK_QF_16
Variable	Li_ppm
Number of analysis	228

Code	BLK_QF_16
Certificate Value	36.6
Standard desviation	6
Upper limit (5*DL)	50

Minimum	10
Maximum	74
Average	14
Median	12

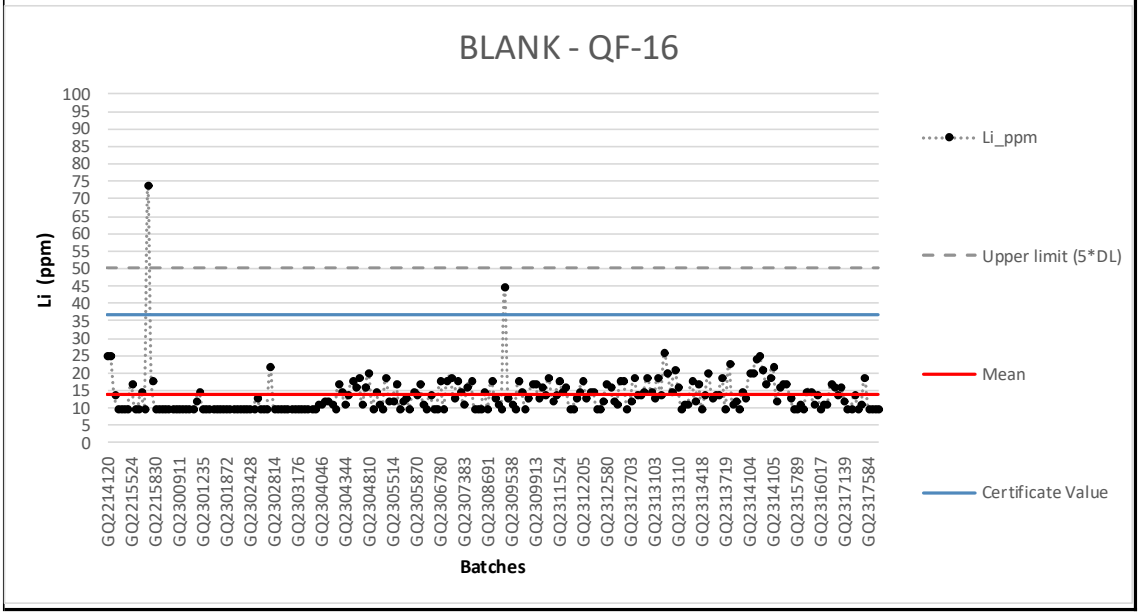

Figure 11-4 – Blank Control Chart – ITAK QF-16

Source: GE21 2024

Type of Control	Blank
Reference	BLK_QF_18
Variable	Li_ppm
Number of analysis	13

Code	BLK_QF_18
Certificate Value	18.3
Standard desviation	4
Upper limit (5*DL)	50

Minimum	10
Maximum	22
Average	13
Median	10

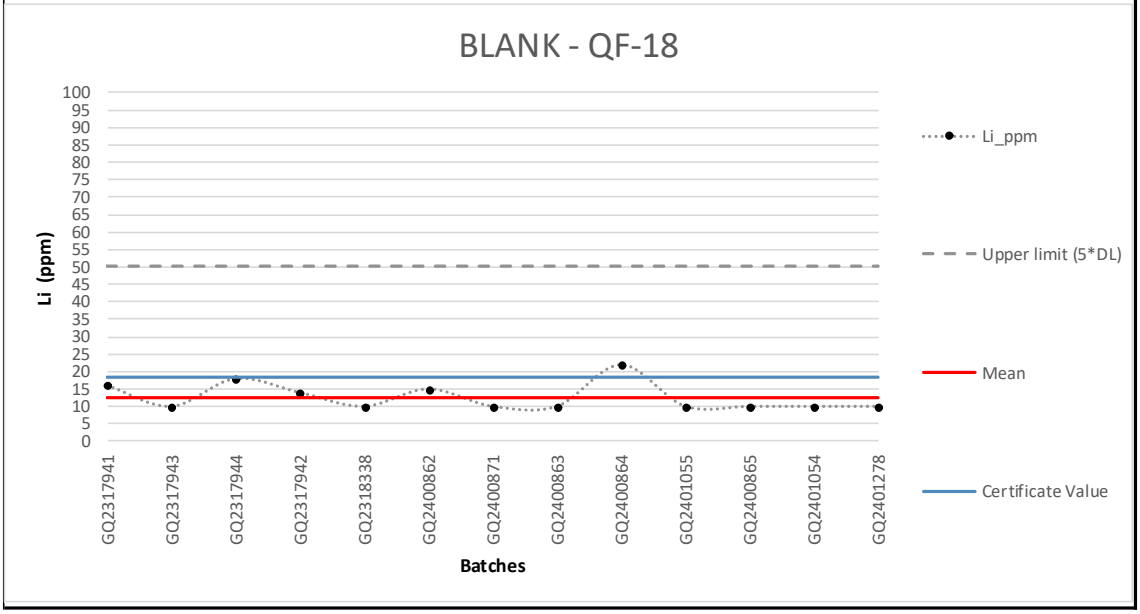

Figure 11-5 – Blank Control Chart – ITAK QF-18

Source: GE21 2024

11.5.3 Certified/Standard Reference Material – CRM/SRM

Certified or Standard Reference Materials are reference materials for which one or more parameters have been certified by a technically valid and recognized procedure. A certifying body has issued a Certificate or other accurate documentation. These materials are used as quality control samples to evaluate the accuracy of the analytical methods and procedures.

Lithium Ionic uses 4 CRMs/SRMs: ITAK – 1100, ITAK – 1101, OREAS 750 and OREAS 752. These Reference Materials evaluate high, medium, and low-grade assay results.

Medium-grade or high-grade Reference Materials are inserted at the beginning of the possible mineralized zones. The insertion can occur immediately or a few samples before the mineralized zone. The low-grade Materials are inserted at the end of the zone where the Geologist interprets mineralization. The insertion can be immediately after or a few samples after the mineralized zone. The order of the Reference Materials can be changed based on geological features or mineralization characteristics.

Figure 11-6 to Figure 11-9 present Lithium's CRM/SRM control charts. More than 80% of the samples are constrained within the 2x Standard Deviation limits.

Type of Control	STANDARD
Reference	ITAK-1100
Variable	Li_ppm
Number of analysis	182

Code	ITAK-1100
Certificate Value	2430
Upper limit (95%CL)	2526
Lower limit (95%CL)	2334

Minimum	2256
Maximum	2680
Mean	2478
Standard deviation	76
Bias	1.97%

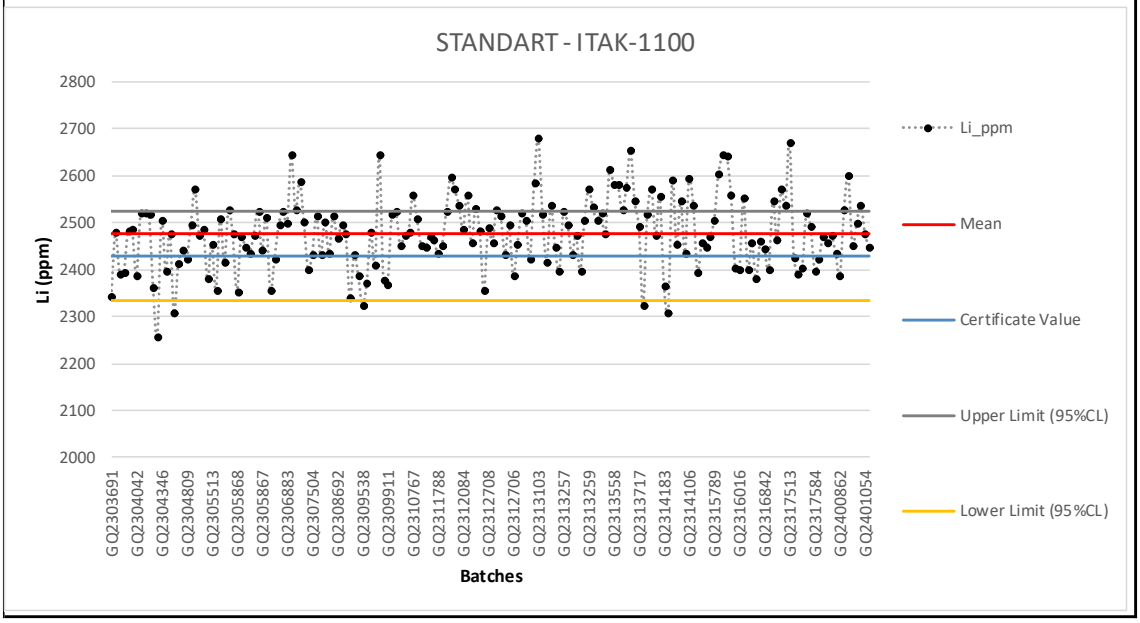

Figure 11-6 – Standard Reference Material Chart – ITAK 1100

Source: GE21 2024

Type of Control	STANDARD
Reference	ITAK-1101
Variable	Li_ppm
Number of analysis	176

Code	ITAK-1101
Certificate Value	6710
Upper limit (95%CL)	6950
Lower limit (95%CL)	6470

Minimum	6436
Maximum	7201
Mean	6840
Standard deviation	152
Bias	1.94%

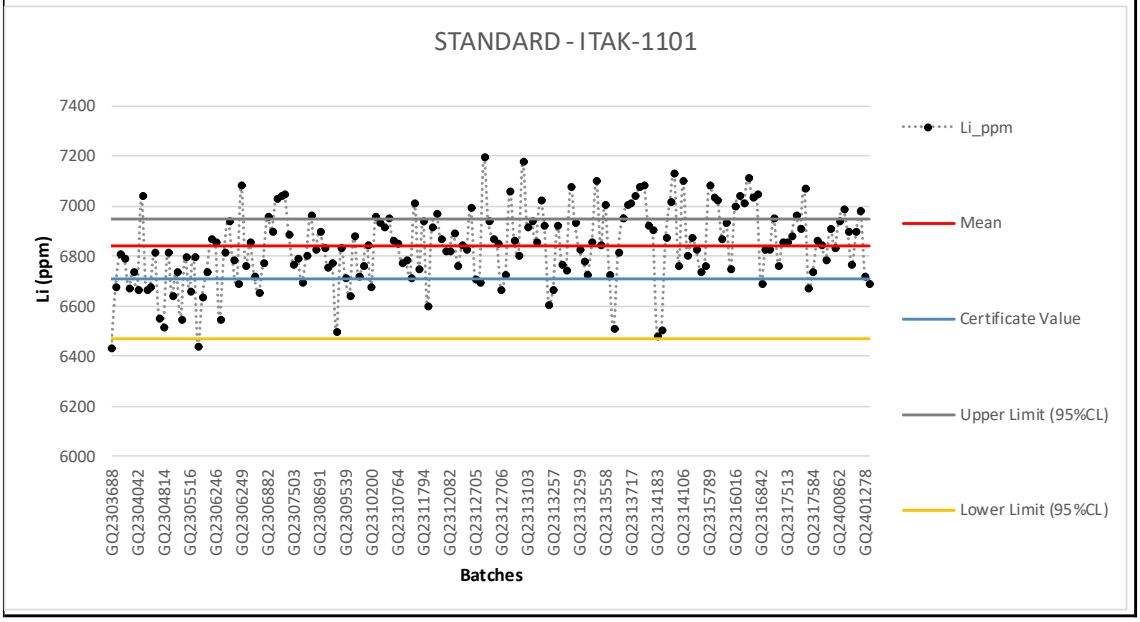

Figure 11-7 – Standard Reference Material Chart – ITAK 1101

Source: GE21 2024

Type of Control	STANDARD
Reference	OREAS_750
Variable	Li_ppm
Number of analysis	97

Code	OREAS_750
Certificate Value	2300
Upper limit (95%CL)	2350
Lower limit (95%CL)	2250

Minimum	2093
Maximum	2515
Mean	2284
Standard deviation	92
Bias	-0.67%

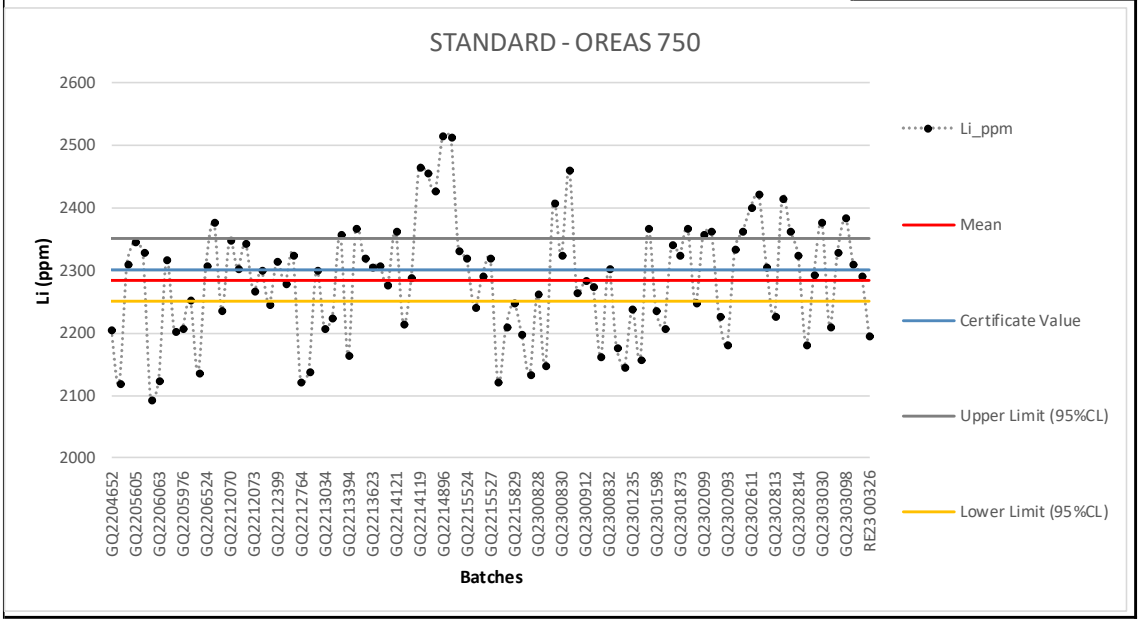

Figure 11-8 – Standard Reference Material Chart – OREAS 750

Source: GE21 2024

Type of Control	STANDARD
Reference	OREAS_750
Variable	Li_ppm
Number of analysis	97

Code	OREAS_750
Certificate Value	2300
Upper limit (95%CL)	2350
Lower limit (95%CL)	2250

Minimum	2093
Maximum	2515
Mean	2284
Standard deviation	92
Bias	-0.67%

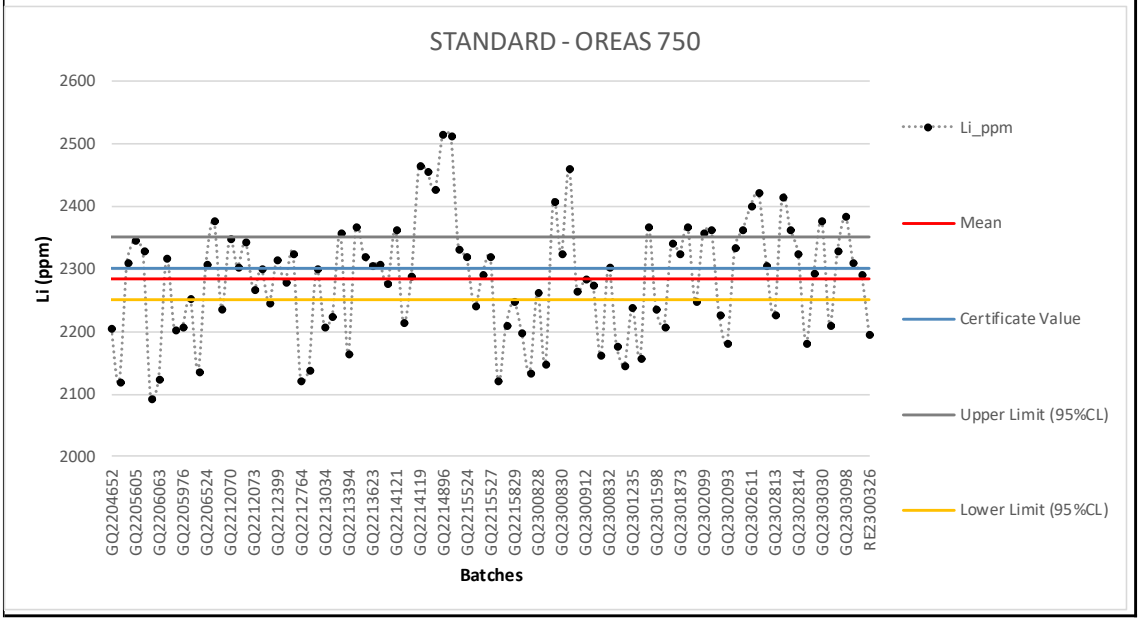

Figure 11-9 – Standard Reference Material Chart – OREAS 752

Source: GE21 2024

11.5.4 Crushed Duplicates

Duplicates are used in the Quality Control program to evaluate the precision of geochemical analysis. Insertion of blind duplicates of crushed (75% passing in 3mm sieve) material is used to test the laboratory's reproducibility and determine if the sample preparation process generates bias or imprecision in the results.

A total of 273 crushed duplicates were evaluated. Control charts for this control type show high correlations and good reproducibility, with over 90% of the samples falling below the 20% HARD limit. Figure 11-10 presents the control chart.

Type of control	Duplicate
Reference	3mm
Variable	Li_ppm
Accuracy limit	10%
Number of pairs	273

	SMP	DUP
Minimum	17	10
Maximum	17130	18020
Average	5414	5400
Median	5270	5102
Inside HARD Limits	95.24%	

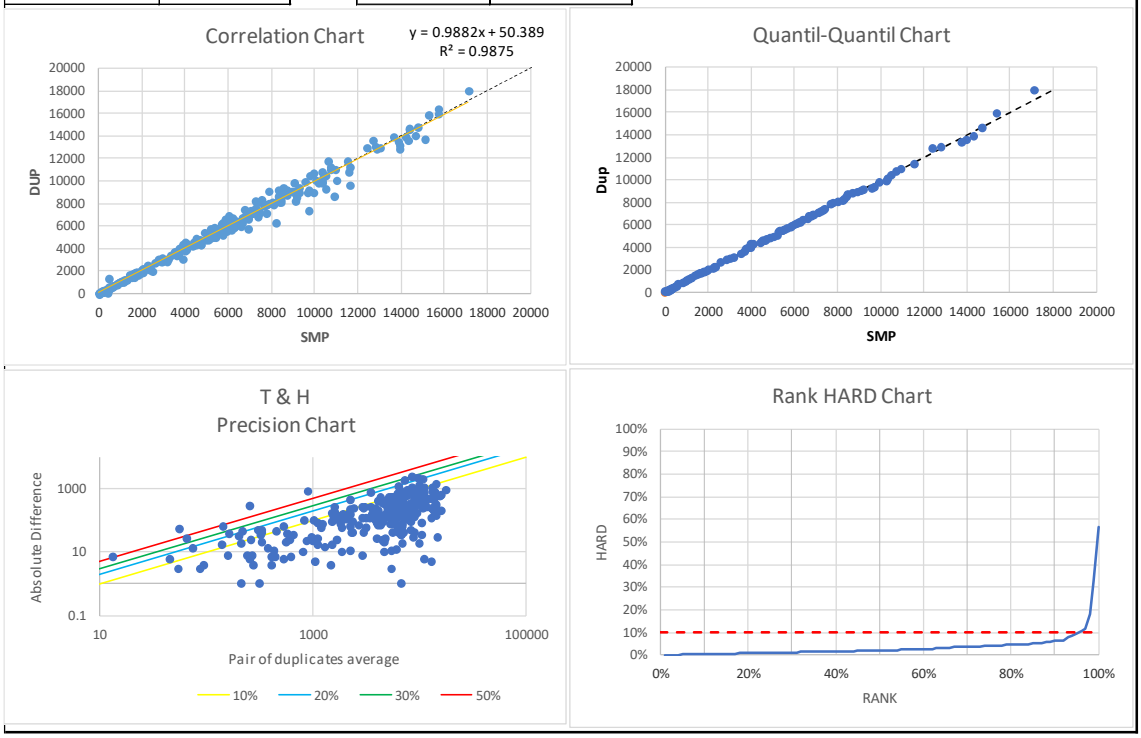

Figure 11-10 – Crushed Duplicates Control Chart

Source: GE21 2024

11.5.5 Pulverized Duplicates

Duplicates are used in the quality control program to evaluate the precision of the geochemical analysis. The insertion of blind duplicates of pulverized material (95% passing 150# sieve) is used to test the laboratory's reproducibility and determine if the milling process is not generating bias or imprecision in the results.

A total of 273 pulverized duplicates were evaluated. Control charts for this control type show high correlations and good reproducibility, with approximately 91% of the samples falling below the 5% HARD limit. Figure 11-11 presents the control chart.

Type of control	Duplicate
Reference	150#
Variable	Li_ppm
Accuracy limit	5%
Number of pairs	273

	SMP	DUP
Minimum	32	19
Maximum	23330	22900
Average	7357	7338
Median	7231	7132
Inside HARD Limits	90.84%	

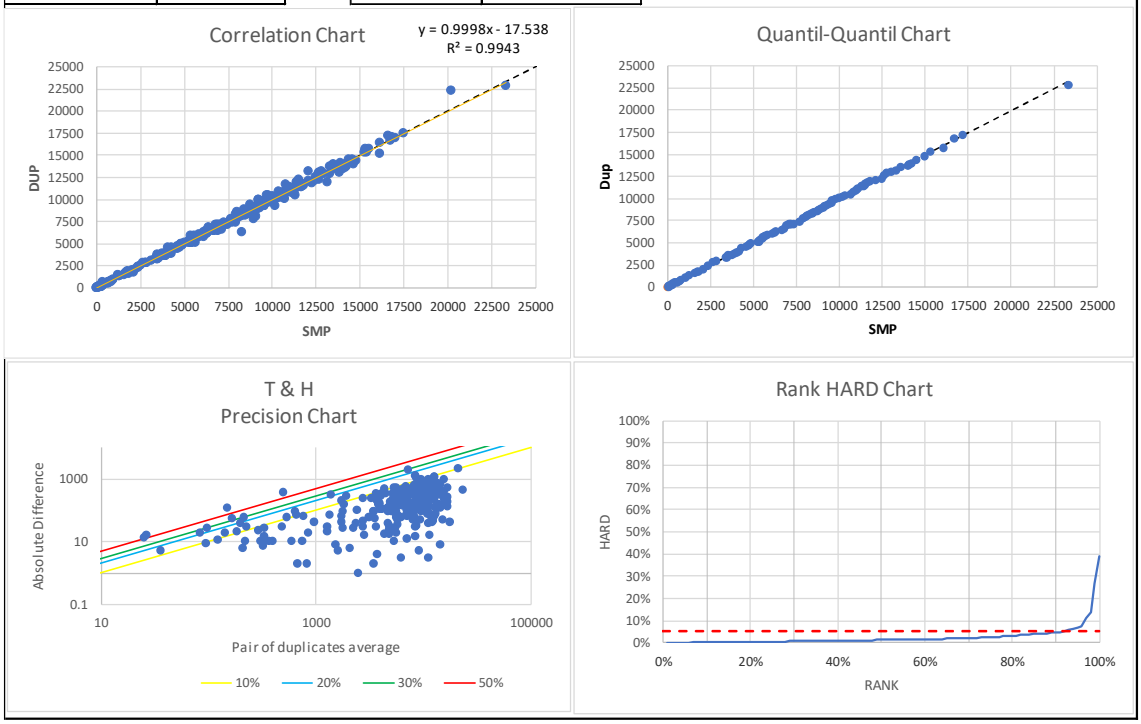

Figure 11-11 – Pulverized Duplicates Control Chart

Source: GE21 2024

11.5.6 Check Assay

Lithium Ionic has submitted Check Assay batches for analysis at the ALS Laboratory in Vancouver, British Columbia, Canada. This procedure is used to verify the reliability of the primary laboratory results by crosschecking it with a secondary reference laboratory. Check Assay results are presented in the following control chart (Figure 11-12). Only 1 sample of 72 has returned a pair above the 30% HARD limit, representing 1.4% of the total Check Assays, presenting the control chart of the Check Assay results.

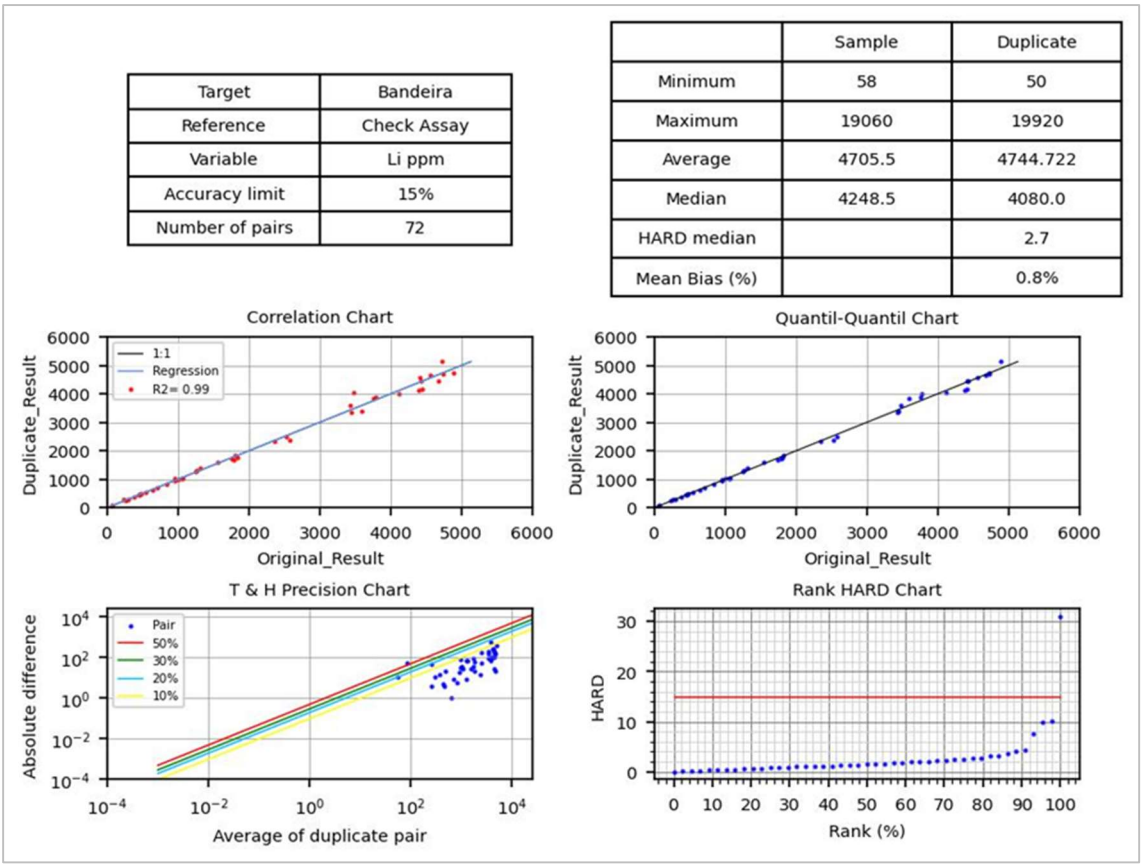

Figure 11-12 – Check the Assay Control Chart

Source: GE21 2024

11.6 QP Opinion

The QP's opinion is that sampling, sample preparation, security and analysis performed by Lithium Ionic and hired companies are suited for a Mineral Resource Estimation study. Quality Assurance procedures follow the industry's best practices, and Quality Control results are within industry standards, attesting to the quality of the Database information.

12 DATA VERIFICATION

12.1 QP Verification

GE21 team members have conducted several field visits since 2022 at the Bandeira Project in Araçuaí to verify the company's infrastructure, the procedures in the course, and the results obtained from the activities carried out by Lithium Ionic staff.

Mr. Carlos José Evangelista Silva, an independent QP for Geology Exploration and Mineral Resource Estimate, conducted a site visit on the Bandeira Project between the 13th and 14th of September 2023 and the 12th of December 2023. Lithium Ionic allowed unlimited access to the Company's facilities during this time.

The QP inspected mainly the following points:

- Drilling Sites and Trenches (Figure 12-1 to Figure 12-4):
  - Collar landmarks.
  - Trenches.
  - Drilling Rigs.
  - Drill Core Shed House (Figure 12.5 to Figure 12-13):
  - Installations and Overall core shed procedures flowchart.
  - Core box archive and Drillhole landmark checking.
  - Drill core saw and Drill core sample bags.
  - Batches of sample bags.
  - Pulverized and crushed samples were returned from labs.
  - Density test procedures by water displacement methodology.
  - Physical file storage for drill hole loggings and bulletins.
  - Check the mineralization style and sampling procedures.
- The assay data was cross-checked within the drill sample database. Digital assay records were randomly selected and scrutinized against the available laboratory assay certificate reports.
- Additionally, a comprehensive review of the assay database was conducted to identify errors, including overlaps, interval gaps, and typographical errors in assay values. The database generally exhibited high accuracy, requiring no adjustments to the assay values contained within.

Mr. Leonardo Silva Santos Rocha, an independent QP for Geology Exploration and Mineral Resource Estimate, conducted an additional site visit on the Bandeira Project on the 11th of April 2024. The main purpose of this visit was to check on the additional infill drilling and geochemical data included in the current Mineral Resource Estimate. Lithium Ionic allowed unlimited access

to the Company's facilities during this time.

The QP inspected mainly the following points:

- Drilling sites (Figure 12-14 and Figure 12-15):
  - Collar landmarks of selected infill drilling.
  - Drill Core Shed House (Figure 12-16 and Figure 12-17):
  - Installations and Overall core shed procedures flowchart.
  - Core box archive and Drillhole landmark checking.
  - Batches of sample bags.
  - Density test procedures by water displacement methodology.
  - Physical file storage for drill hole loggings and bulletins.
  - Check the mineralization style and sampling procedures.
- The assay data was cross-checked within the drill sample database. Digital assay records were randomly selected and scrutinized against the laboratory assay certificate reports and core samples in the core shed.

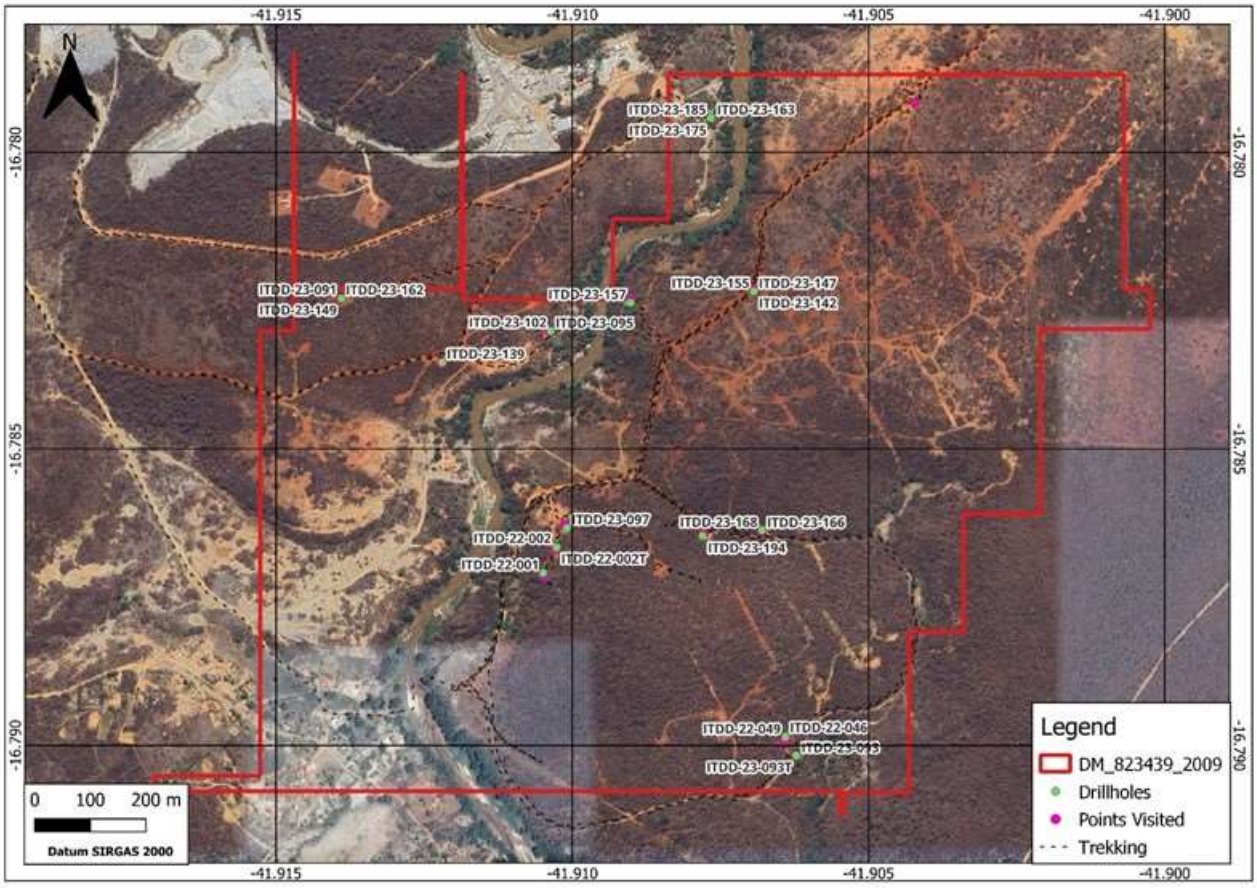

Figure 12-1 – Visited Points on Lithium Ionic Bandeira Property by QP Carlos J. E. Silva

Source: GE21 2024

Pegmatite Vein with Spodumene Outcrop

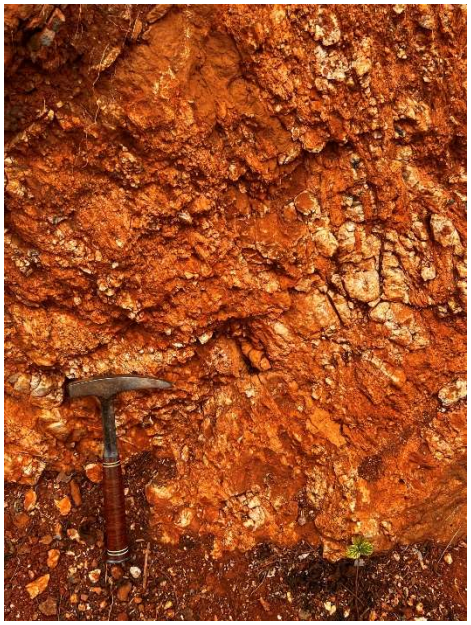

Pegmatite Vein with Spodumene Outcrop

Trench ITTRE-22-001 – Pegmatite Vein with Spodumene Outcrop

Trech ITTRE-22-001 – Spodumene Pegmatite Vein Outcrop

Figure 12-2 – Spodumene Pegmatites Outcrops and Trench on Lithium Ionic Bandeira Property

Source: GE21 2023 taken by QP Carlos J. E. Silva

	
Collar landmarks - Drilling Site ITDD-23-196	**Drilling Site ITDD-23-196**
	
Collar landmarks - Drilling Site ITDD-23-162	**Drilling Site ITDD-23-162**
	
Collar landmarks - Drilling Site ITDD-23-093	**Drilling Site ITDD-23-093**

Figure 12-3 – Collar Moments Lithium Ionic Bandeira Property

Source: GE21 2023 taken by QP Carlos J. E. Silva

Drill Rig on site of the Bandeira, drilling in 13/09/2023 the DDH ITDD-23-192 - azimuth 140 – dip ~70

Drill Rig on site of the Bandeira, drilling in 13/09/2023 – DDH ITDD-23-192 - Technicians recovering the cores and using the REFLEX ACT III for core orientation

Drill Rig on site of the Bandeira, drilling in 13/09/2023 - DDH ITDD-23-192 – Spodumene in pegmatite veins cores recovered from drilling – depth 355m

Drill Rig on site of the Bandeira, drilling in 13/09/2023 the DDH ITDD-23-192 - REFLEX GYRO IQ used by Lithium Ionic Staff to do the survey measurement

Figure 12-4 – Drilling Rig and Survey Equipment on Lithium Ionic Bandeira Property

Source: GE21 2023 taken by QP Carlos J. E. Silva

Office and Core Shed House 1 of the Lithium Ionic in Araçuaí-MG-Brazil – external view

Office and Core Shed House 1 of the Lithium Ionic in Araçuaí-MG-Brazil – internal view

Core Shed House 2 of the Lithium Ionic in Araçuaí-MG-Brazil – external view

Core Shed House 2 of the Lithium Ionic in Araçuaí-MG-Brazil – internal view

Core Shed House 3 of the Lithium Ionic in Araçuaí-MG-Brazil – external view

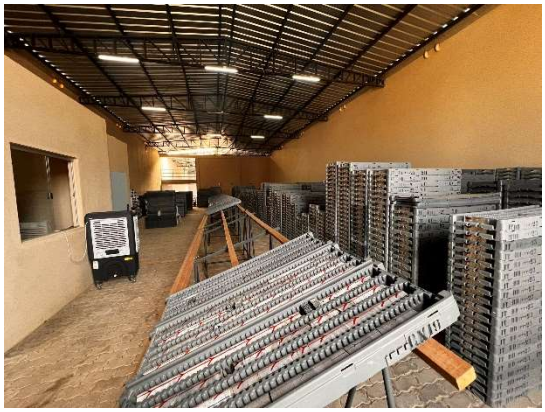

Core Shed House 3 of the Lithium Ionic in Araçuaí-MG-Brazil - internal view

Figure 12-5 – Lithium Ionic Core Shed Storage Houses in Araçuaí

Source: GE21 2023 taken by QP Carlos J. E. Silva

Core boxes storage – House 2

Core boxes storage – House 3

Storage of the pulverized samples and crushed samples after return from Labs

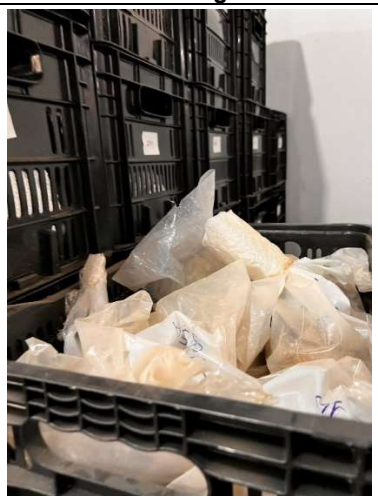

Storage of the pulverized samples and crushed samples after return from Labs

Core boxes storage

Core boxes storage

Figure 12-6 – Cores Boxes Storage in Lithium Ionic Core Shed Houses

Source: GE21 2023 taken by QP Carlos J. E. Silva

The technician is working with the cores.

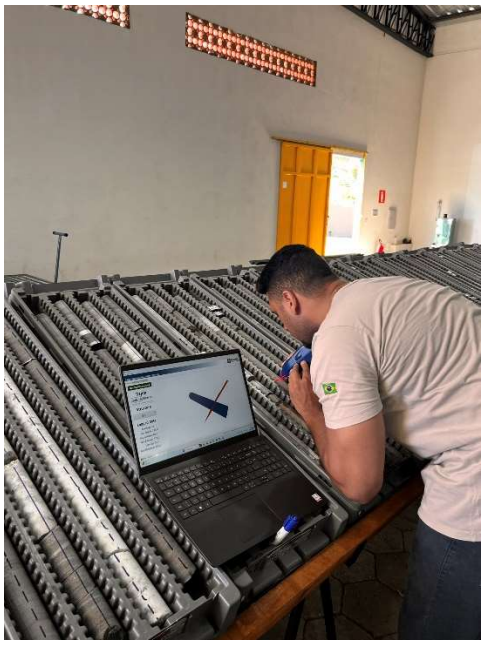

Geologists are doing the structural and geological logs.

Cores after sampling with assays identified

Cores sampled and identified to send to labs.

Figure 12-7 – Lithium Ionic Staff Working in Logs and Sampling Procedures

Source: GE21 2023 taken by QP Carlos J. E. Silva

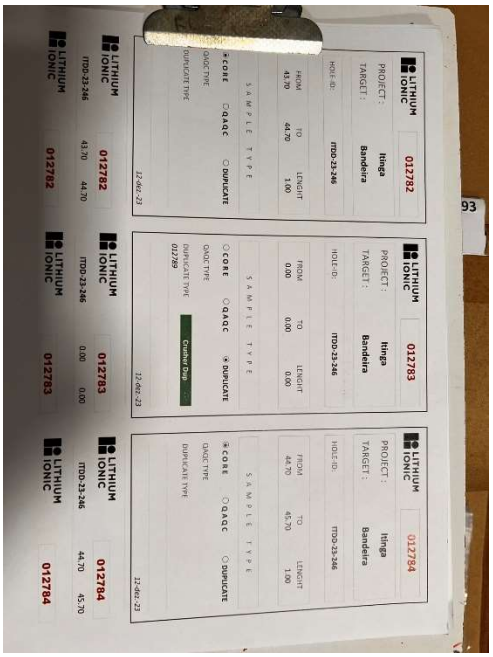

DHH standardized sample identification

DDH batch of samples ready to be sent to the laboratory

Stock of the Standards used in QA/QC procedures

Stock of the Blank used in QA/QC procedures

Figure 12-8 – Lithium QA/QC Standards Stock and Sampling Standards

Source: GE21 2023 taken by QP Carlos J. E. Silva

Density measurement – dry core weight

Density measurement – core weight underwater

Drill core cutting saw.

Drill core cutting saw sediment settling tank.

Figure 12-9 – Lithium Ionic Density Procedures and Drill Core Cutting Saw

Source: GE21 2023 taken by QP Carlos J. E. Silva

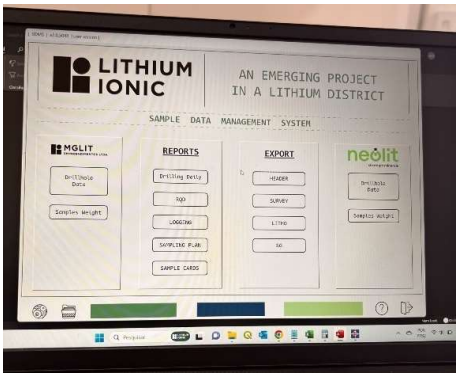

Customized database management system for mineral research from Lithium Ionic

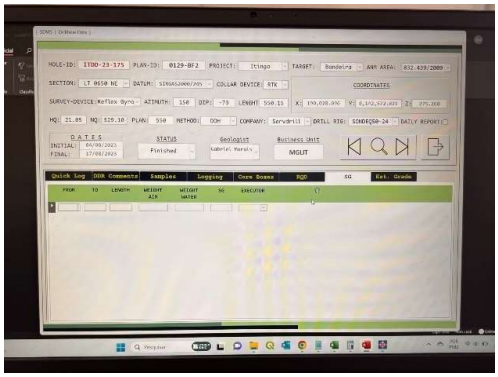

Customized database management system for mineral research from Lithium Ionic – Registration of Collar Drilling

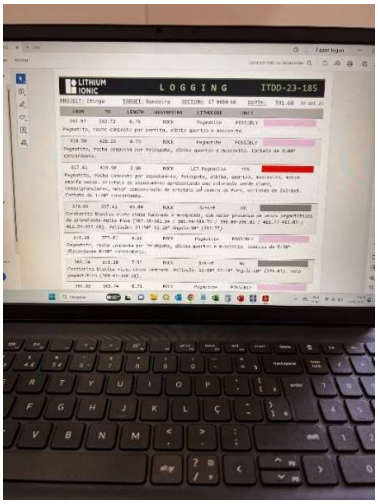

Customized database management system for mineral research from Lithium Ionic -Registration of the Geological log

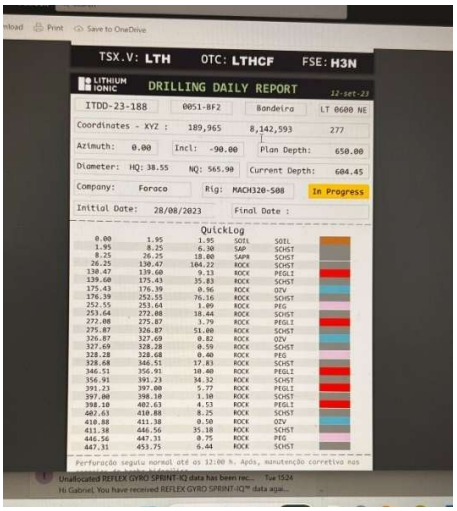

Customized database management system for mineral research from Lithium Ionic -Registration of the Drilling daily report

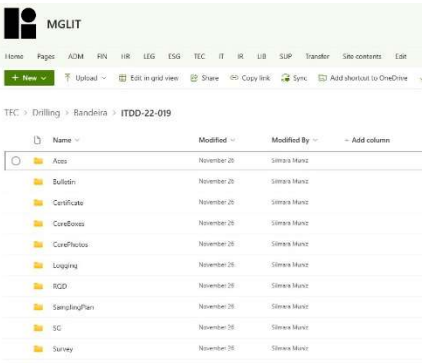

Lithium Ionic Cloud data center

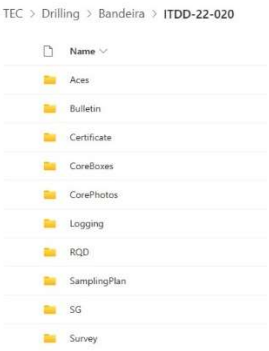

Lithium Ionic Cloud data center – DDH folders

Figure 12-10 – Lithium Ionic Data Base System Interface and Cloud Data Center

Source: GE21 2023 taken by QP Carlos J. E. Silva

Physical Drillhole Files Storage

Folders with drill-hole documents

Folder of the DDH ITDD-23-196 - with drill hole documents -

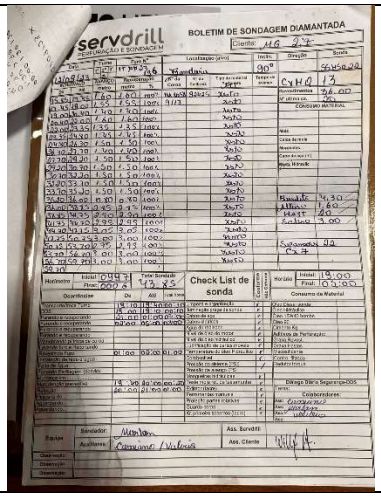

Folder of the DDH ITDD-23-196 - Daily Drilling Bulletin

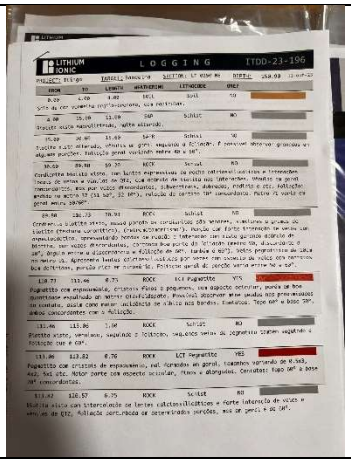

Folder of the DDH ITDD-23-196 – geological log

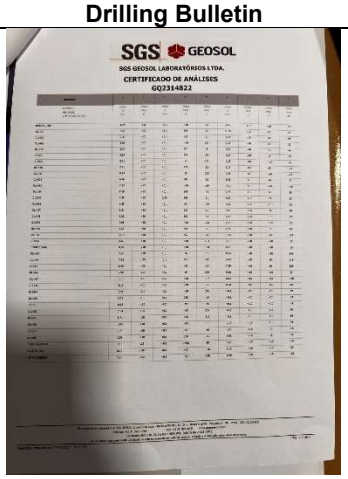

Folder of the DDH ITDD-23-196 – assay results, certificates

Figure 12-11 – Lithium Ionic Physical Drillhole Files Storage

Source: GE21 2023 taken by QP Carlos J. E. Silva

Core boxes of the modelled mineralized spodumene zone – ITDD-23-147 – – 207,80m depth, detail of the Spodumene crystal

Core boxes of the modelled mineralized spodumene zone – ITDD-23-139 – 305m depth, detail of the Spodumene crystal

Core boxes of the modelled mineralized spodumene zone – ITDD-23-162 – 460,5m depth - detail of the Spodumene crystal

Core boxes of the modelled mineralized spodumene zone – ITDD-23-163 – 146m depth, detail of the Spodumene crystal

Figure 12-12 – Lithium Ionic Bandeira Property Spodumene Pegmatites Intercepts

Source: GE21 2023 taken by QP Carlos J. E. Silva

Core boxes of the modelled mineralized spodumene zone – ITDD-23-120 – 109m to 115m

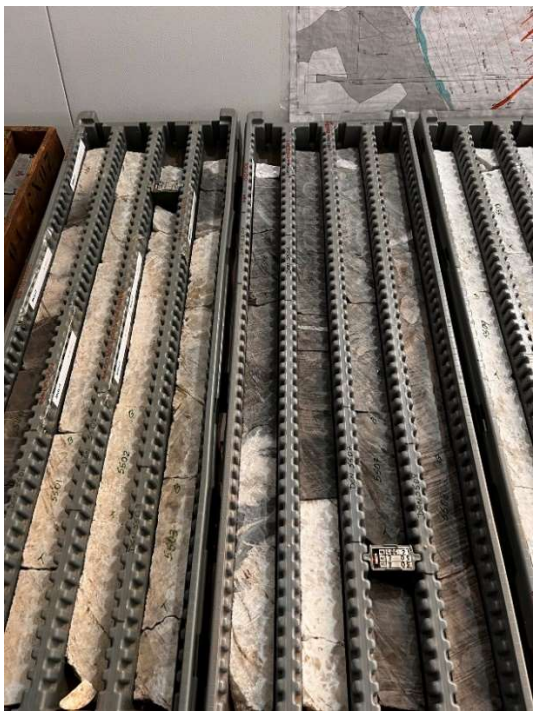

Core boxes of the modelled mineralized spodumene zone – ITDD-23-091 – 479m to 489m

Core boxes of the modelled mineralized spodumene zone – ITDD-23-091 – 479m to 489m - samples identification

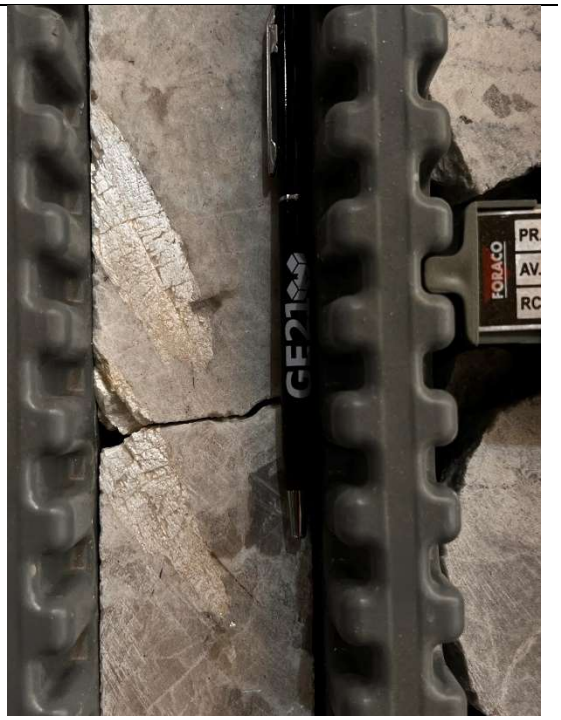

Core boxes of the modelled mineralized spodumene zone – ITDD-23-120 – 111m depth, detail of the Spodumene crystal

Figure 12-13 – Lithium Ionic Bandeira Property Spodumene Pegmatites Intercepts

Source: GE21 2023 taken by QP Carlos J. E. Silva

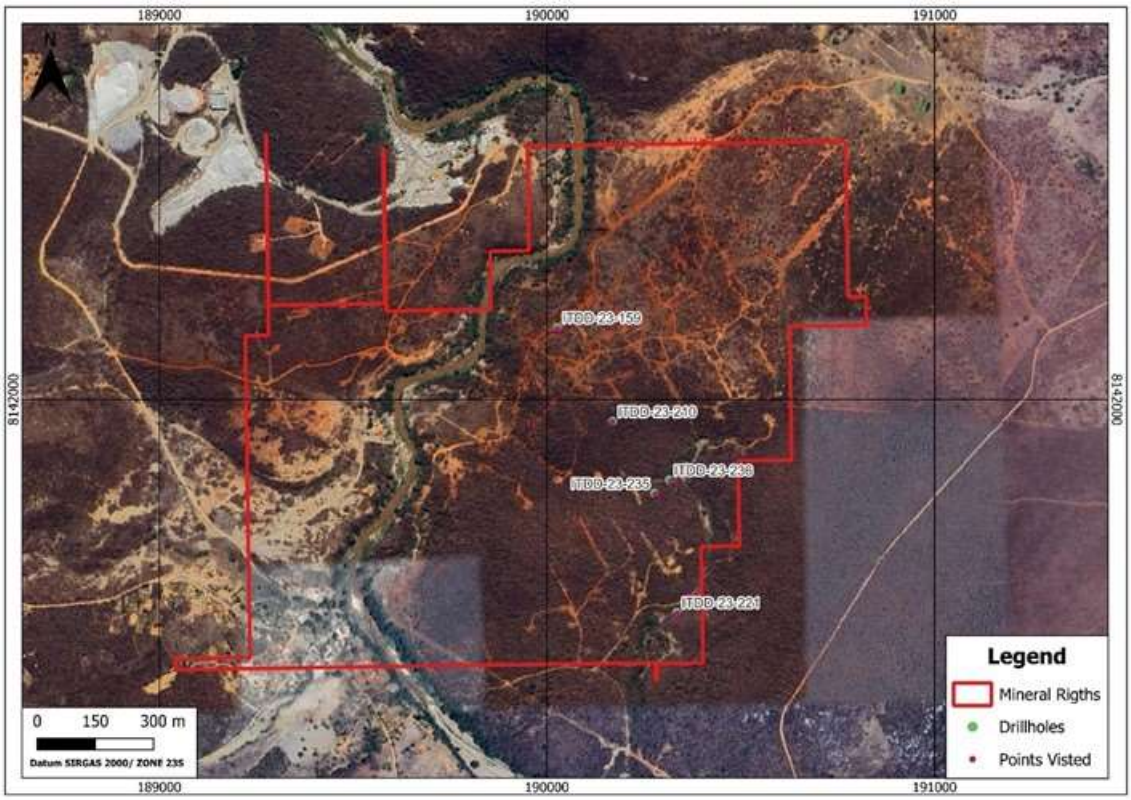

Figure 12-14 – Visited Points on Lithium Ionic Bandeira Property by QP Leonardo Rocha

Source: GE21 2024

	
Collar landmarks - Drilling Site ITDD-23-120	**Drilling Site ITDD-23-210**
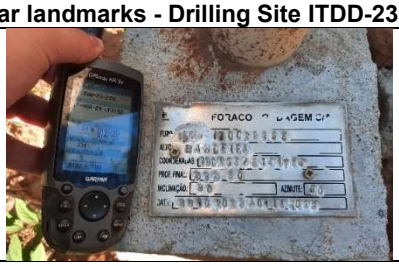	
Collar landmarks - Drilling Site ITDD-23-235	**Drilling Site ITDD-23-235**
	
Collar landmarks - Drilling Site ITDD-23-236	**Drilling Site ITDD-23-236**
	
Collar landmarks - Drilling Site ITDD-23-221	**Drilling Site ITDD-23-221**
	
Collar landmarks - Drilling Site ITDD-23-159	**Drilling Site ITDD-23-159**
	
Pegmatite Vein with Spodumene (detail) Outcrop	**Pegmatite Vein contact with Schist Spodumene Outcrop**

Figure 12-15 – Collar landmarks and Outcrops in Lithium Ionic Bandeira Property

Source: GE21 2024 taken by QP Leonardo S. S. Rocha

Folder of the DDH ITDD-23-236 - with drill hole documents -

Folder of the DDH ITDD-23-236 - Daily Drilling Bulletin

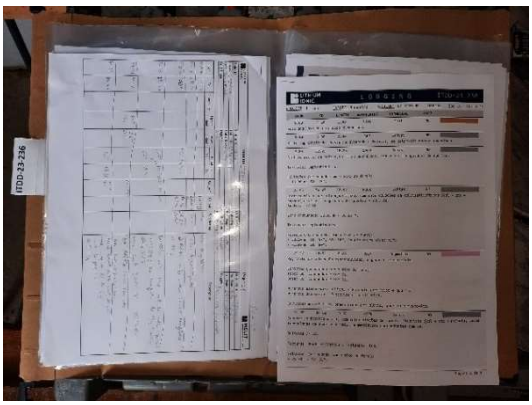

Folder of the DDH ITDD-23-236 – geological log

Folder of the DDH ITDD-23-236 – assay results, certificates

Core boxes storage shed

DDH batch of samples ready to be sent to the laboratory

Stock of the Standards and Blanks used in QA/QC procedures

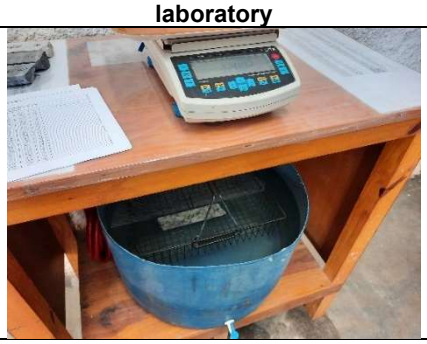

Bulk Density Measurement

Figure 12-16 – Lithium Ionic Physical Drillhole Files Storage

Source: GE21 2024 taken by QP Leonardo S. S. Rocha

Core boxes of the modelled mineralized spodumene zone – ITDD-23-236 – – 174m depth, detail of the Spodumene crystal

Core boxes of the modelled mineralized spodumene zone – ITDD-23-235 – 108m depth, detail of the Spodumene crystal

Core boxes of the modelled mineralized spodumene zone – ITDD-23-159 – 446m depth - detail of the Spodumene crystal

Core boxes of the modelled mineralized spodumene zone – ITDD-23-210 – 220m depth, detail of the Spodumene crystal

Figure 12-17 – Lithium Ionic Bandeira Property Spodumene Pegmatites Intercepts

Source: GE21 2024 taken by QP Leonardo S. S. Rocha

12.2 QP Opinion

No major issues were identified with the database. The QP's opinion is that the practices and procedures used to generate the Lithium Ionic database are sufficient to support Mineral Resource estimation. Some observations that were recorded during visits as they relate to the generation, collection, control, and storage of exploration data on-site at Araçuaí-MG are:

- The site visits included reviewing the QA/QC, field checks of the core shed, drilling in progress, review of density procedures, and discussions of the current geological interpretations with geologists of Lithium Ionic.
- Drill hole collars have a physical identification marker. The markers comprise a concrete pad with a metal plate designating the drilling contractor, drill hole number, drilling area, orientation, coordinate location, start and end date drilled, and total depth. A PVC pipe protruding from the marker provides a physical record of the drill hole orientation.
- All core boxes were labelled and adequately stored in a core shed house. Sample tags were present in the boxes, and it was possible to validate sample numbers and confirm the presence of mineralization in witness half-core samples from the mineralized zone.
- The QP considered the Drill Hole Logging as standard industry practice logging procedures, which Lithium Ionic has standardized. They reviewed logging procedures for randomly selected drill cores and verified the completeness of the logs.
- Lithium Ionic has its database software. Data storage procedures at Lithium Ionic are considered within standard industry practice. As part of the validation process, 12 holes were verified. Database validation was conducted with the Lithium Ionic staff according to standard validation procedures, including a review of collar locations, drill hole deviations and database check-assay review. QP found no inconsistencies in the database.
- An extensive database of wet density information was collected during the exploration phase. Assessing density samples' moisture and porosity impact on bulk density measurements is strongly recommended.
- The QP checked the Lithium Ionic procedures for sampling management, storage, logging, sample preparation, and assay. They are considered inside acceptance limits and in compliance with mineral industry practices.
- Rock-type descriptions fit with the checked mineralization style. Lithium Ionic has demonstrated that it understands geology.

13 MINERAL PROCESSING AND METALLURGICAL TESTING

The underground mine ore body at Bandeira Project are spodumene-rich pegmatites, SRP type (cf. Pedrosa-Soares et al., 2023), characterized by being non-zoned to poorly zoned pegmatites, rich in spodumene crystals (average in size 5 to 30 cm) disseminated in a matrix composed of albite, quartz, perthitic microcline (i.e., potassium feldspar with exsolved albite lamellae), muscovite, and petalite, totaling over 90% volume, with subordinate amounts (up to 10% volume) of accessory and alteration minerals, such as lithium minerals (cookeite, montebrasite, triphylite, and zabuyelite), apatite, Nb-Sn-Ta and Fe-Mn oxides, graphite, and clay minerals (kaolinite and montmorillonite).

The technological characterization includes chemical and mineralogical analyses, physical tests for hardness determination, particle size distribution in crushing assays, abrasiveness level, and metallurgical tests to identify the ore's response when subjected to simulation of the industrial process of ore mineral concentration (in this case, spodumene).

13.1 Ore Mineralogical Characterization

The lithium minerals present in the pegmatites of the Bandeira Deposit have been routinely characterized through systematic logging of drilling cores. From core intervals selected samples are taken through the description of thin polished sections under an optical microscope. Those descriptions, macroscopic (log) and microscopic (thin sections), are accompanied by modal evaluation (in vol%) of spodumene versus matrix contents, and within the matrix, the quantities of minerals identified, particularly those that may significantly interfere with ore processing. As a result of these descriptions, the lithium minerals identified in the pegmatites of the Bandeira Deposit are listed in Table 13-1. In addition to the lithium minerals listed in Table 13-1, the spodumene ore from the Bandeira Deposit contains the following main gangue minerals (average modal values in vol%): albite, quartz, perthitic potassium feldspar and muscovite.

Other accessory minerals, besides those listed in Table 13-1, typically present in amounts less than 1% volume, include: apatite, beryl, cassiterite, columbite-tantalite (including Fe-columbite determined by SEM-EDS), and graphite.

Table 13-1 – Lithium Minerals Identified at Bandeira Pegmatite Deposit

Source: Lithium Ionic 2024

Mineral	Formula	Specific Density g/cm³	Dureza Mohs	Li_2O %weight	Li_2O* %weight
Montebrasite	$LiAl(PO_4)(OH)$	3,0 – 3,1	5,5 – 6,0	10,21	9,0
Cookeite	$(Al,Li)_3Al_2(Si,Al)_4O_{10}(OH)_8$	2,6 – 2,7	2,5 – 3,5	2,86	2,5
Elbaíte	$Na(Li,Al)_3Al_6(BO_3)_3Si_6O_{18}(OH)_4$	2,9 – 3,1	7,5	4,07	4,0
Spodumene	$LiAlSi_2O_6$	3,1 – 3,2	6,5 – 7,0	8,03	7,4

Mineral	Formula	Specific Density g/cm³	Dureza Mohs	Li_2O %weight	Li_2O* %weight
Spodumene parcially alterated	-	< 3,1	< 6,5	-	< 7,4
Lepidolite (polilitionite – trilitionite)	$KLi_2Al(Si_4O_{10})(F,OH)_2$ – $K(Li_{1.5}Al_{1.5})(AlSi_3O_{10})(F,OH)_2$	2,8 - 2,9	2,5 - 3,5	6,46 – 7,70	7,1
Litiofilite – Trifilite	$LiMn(PO_4)$ – $LiFe(PO_4)$	3.4 – 3.6	4	9,53 – 9,47	9,0
Petalite (cristal)	$LiAlSi_4O_{10}$	2,4	6,5	4,90	4,7
Petalite alterated (*mass*)	-	< 2,4	< 6,5	< 4,90	3,0
Zabuyelite	Li_2CO_3	2,09	3	40,44	40,0

Source: www.mindat.org; and Pöllmann & König, 2021, available at https://doi.org/10.3390/min11101058.

The mineralogical characterization of the Bandeira ore was conducted using X-ray diffraction (XRD) analysis with a Bruker-AXS D8 Advance ECO instrument, utilizing CuKa radiation (40kV/25mA) with a Ni filter, a step size of 0.02º 2Θ, and an accumulated counting time of 192 seconds per step with a position-sensitive linear detector of the silicon drift type, LynxEye XE, collected from 5 to 105º 2Θ in θ-2θ geometry on the goniometer. Quantitative analysis was calculated using the total multiphase spectrum refinement method (Rietveld method), by fundamental parameters, with Bruker-AXS Diffrac. Topas software, version 6.

The average mineralogical analysis for the 07 (seven) ore variability is presented in Table 13-2. The ore variability results are presented in the item 13.4 of this chapter.

Table 13-2 – Mineralogical Composition Average of 7 Metallurgical Drill Holes – X-Ray Difraction, Rietveld Method

Source: Lithium Ionic 2024

Mineral	% Weight
Albite	31,70
Quartz	26,50
Microcline	15,00
Spodumene	14,30
Moscovite	6,10
Montebrasite	3,30
Petalite	1,10
Others (Polilitionite, Elbaíte, Cookeite and Pyrite)	2,00

Thin section microscopy and visual modal analyses also revealed some accessory minerals with total contents of less than 1% in volume: sphalerite, blue tourmaline, beryl, cassiterite, columbite/tantalite, iron columbite, lithiophilite/triphylite, apatite, zabuyelite and graphite.

13.2 Ore Chemical Analysis

The average chemical analyses for the Bandeira Deposit, considering samples from the 07

metallurgical drill holes of the ore variability study and the mean values from the geological database (7,516 chemical analysis, cutoff grade of Li2O>0.5%), are presented in Table 13-3.

Table 13-3 – Average Chemical Composition of the 07 Drill Holes of Bandeira Deposit

Source: Lithium Ionic 2024

Metal Oxides	Metallurgical drill holes, % weight	Geological Data Base, % weight
Li_2O, %	1,40	1,37
Fe_2O3, %	0,69	0,70
Al_2O_3, %	15,40	14,40
K_2O, %	2,30	2,58
P_2O_5, %	0,87	0,85
CaO, %	0,41	0,45
SnO_2, ppm	437,00	280,00
Ta_2O_5, ppm	82,00	80,00
Nb_2O_5, ppm	160,00	130,00

Source: reference in the database, maps, and sections: PEGL.

13.3 Metallurgical Testing

Preliminary metallurgical tests using Heavy Liquid Separation (HLS) were conducted by SGS Geosol. Ore sorting tests were carried out by TOMRA in Germany and at Steinert in Brazil. Ore variability test work campaign was develop in different research center and laboratories like SGS Geosol, SGS Chile, CETEM and Metso Outotec.

13.3.1 Preliminary HLS Test at SGS Geosol

Samples from drill holes ITDD-22-001, 002, and 007 were combined to generate a composite and sent to SGS Geosol. This sample was prepared according to the procedure shown in Figure 13-1, to proceed with HLS test. The objective of this test is to evaluate the performance of dense media separation in obtaining lithium concentrate for the Bandeira Project, according to market specifications, by varying the particle size distribution and density of the dense media.

20 kg sample was dried and crushed in a jaw crusher with openings of 31.5, 25.4, and 12.7 mm to obtain material 100% passing 12.7 mm. After this, particle size analysis was conducted using a sequence of sieves of 12.7, 6.3, 1.7, and 0.5 mm. For each size fraction, a representative sample was collected for chemical analysis. HLS tests were conducted at densities of 3.0, 2.9, 2.8, and 2.7 g/cm³, for the size fractions -12.7+6.3 mm, -6.3+1.7 mm, and -1.7+0.5 mm.

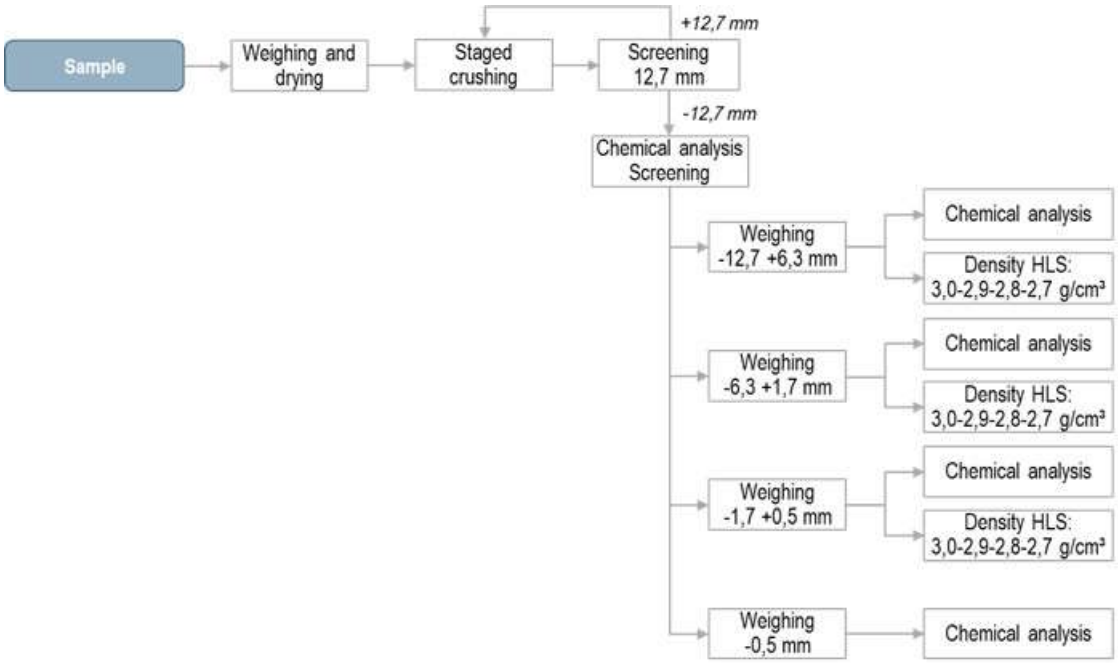

Figure 13-1 – Bandeira Composite Sample Preparation Procedure

Source: Lithium Ionic 2024

The particle size distribution of the material passing 100% through 12.7 mm is presented in Figure 13-2. It is worth noting that approximately 12% of the mass does not have suitable particle size for the dense media separation stage, meaning it is smaller than 0.5 mm. The Bandeira Project considers a future study of concentration of the fine fraction (-0,5 mm) using gravity equipment or flotation.

Chemical analysis identified the predominant presence of aluminum oxide (17.10%), potassium oxide (2.39%), and lithium oxide (1.63%), as shown in Figure 13-3. The presence of aluminum can be mainly attributed to albite, K-feldspar, and spodumene. Potassium is predominantly present in K-feldspar, while lithium is in spodumene. Regarding iron oxide, the main contaminant for market specifications, the concentration in the ore is 0.23%. The mineral origin of iron is mainly schists (biotite). Besides the presence of iron, another point of concern regarding the schists is its density, which can vary between 2.40 and 3.05 g/cm³, similar to the cut-off density used for dense media separation commonly employed for spodumene concentration, considering the density of the mineral of interest varies between 3.15 and 3.20 g/cm³ (PEIXOTO, et al., 2016).

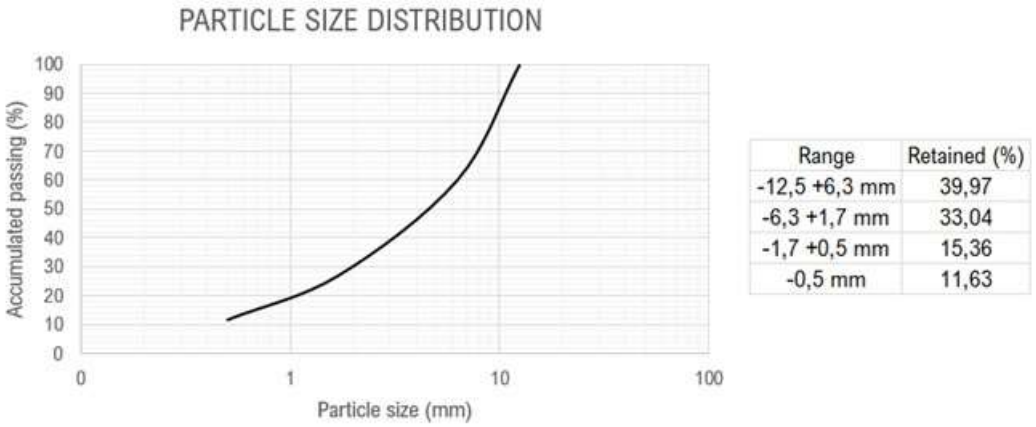

Range	Retained (%)
-12,5 +6,3 mm	39,97
-6,3 +1,7 mm	33,04
-1,7 +0,5 mm	15,36
-0,5 mm	11,63

Figure 13-2 – Product Size Distribution after Crushing at 12,7 mm

Source: Lithium Ionic 2024

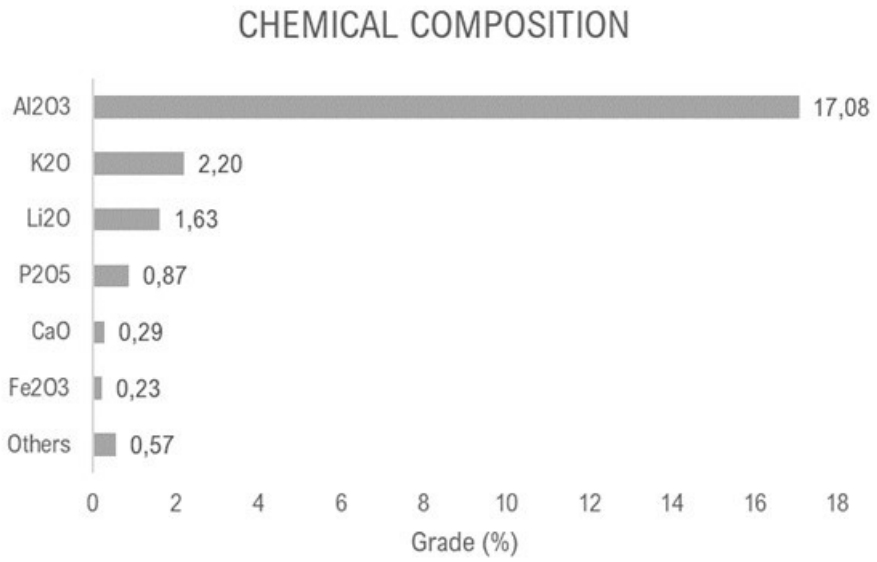

Figure 13-3 – Bandeira Composite Sample Chemical Analysis

Source: Lithium Ionic 2024

The Heavy Liquid Separation tests were conducted for each particle size fraction; (i) -12.7 +6.3 mm, (ii) -6.3 +1.7 mm and (iii) -1.7 +0.5 mm, using organic liquid to evaluate the optimal density to achieve the market specification of lithium concentrate, i.e., a minimum of 5.5% Li2O and a maximum of 1% Fe2O3. The densities evaluated were (i) 2.7 g/cm³, (ii) 2.8 g/cm³, (iii) 2.9 g/cm³, and (iv) 3.0 g/cm³, for which solution with different proportions of methylene iodide (density: 3.29 g/cm³) and acetone (density: 0.79 g/cm³) were prepared.

Tests for the particle size fractions of -12.7 +6.3 mm and -6.3 +1.7 mm were conducted in beakers, while the test for the finer particle size fraction (-1.7 +0.5 mm) was carried out using a separating funnel. The test involves mixing the ore and the dense media solution in the reactor (beaker or separating funnel) and waiting for separation. Afterward, the sunken material, the dense media, and the floated material are collected separately. Densities were evaluated sequentially according to Figure 13-4, and for each stage, chemical composition and mass partition were assessed.

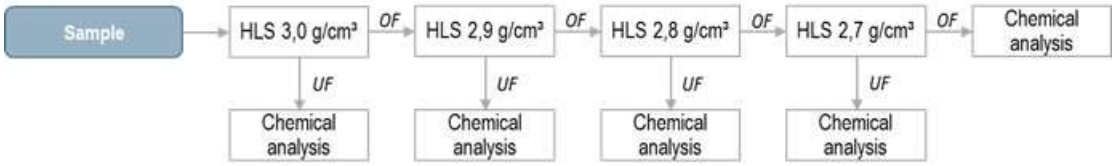

Figure 13-4 – HLS Test Flowsheet

Source: Lithium Ionic 2024

From the results presented in Figure 13-5, the cumulative content of Li2O and Fe2O3 per each density for the three particle size fractions evaluated can be observed. This value was calculated based on the individual content of each sample and the mass partition.

It can be noted that the cut-off density increases with particle size. For finer particles, it is possible to obtain a concentrate meeting the specification using a cut-off density of 2.7 g/cm3. However, for the intermediate particle size range, the cut-off should be performed at 2.8g/cm3, and for the coarser material, at 2.9 g/cm3.

It is observed that the Li2O content in the floated material for the coarser particles is approximately three times higher than the content in the floated material for the finer particles. This indicates lower liberation of spodumene in the coarser particle size range.

Regarding iron oxide, it is found that the maximum content limit was met for all tested densities.

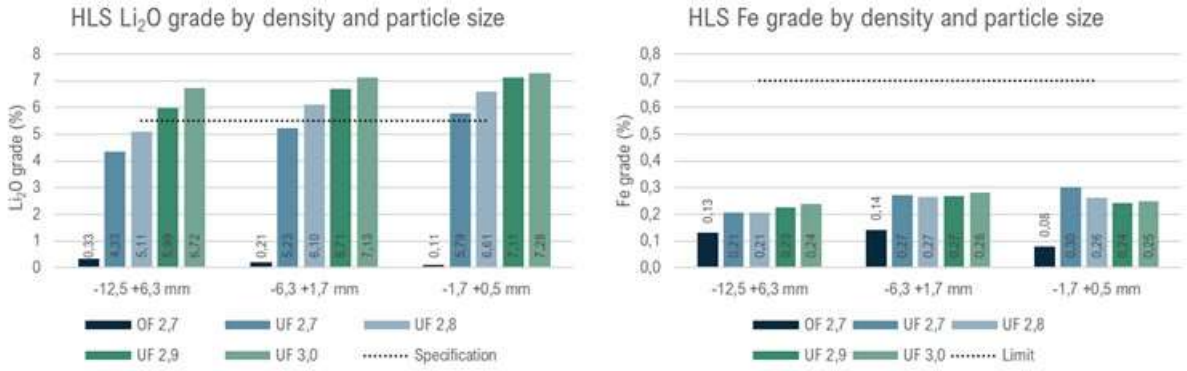

Figure 13-5 – Li2O and Fe2O3 Chemical Analysis Results for Each HLS Step

Source: Lithium Ionic 2024

The recovery results by particle size range and the overall recovery of the HLS are presented in Figure 13-6, along with the Li2O content in the concentrate. For the particle size range -12.7 +6.3 mm, the cut density was 2.84 g/cm³, representing a recovery of 70.5%. These values were obtained by interpolation. For the -6.3 +0.5 mm range, the density was 2.71 g/cm³ and the recovery was 90.1%. However, considering the loss of fines, i.e., fractions smaller than 0.5 mm, which represent 12% of the mass and 11% of the lithium, the HLS recovery was 74.8%.

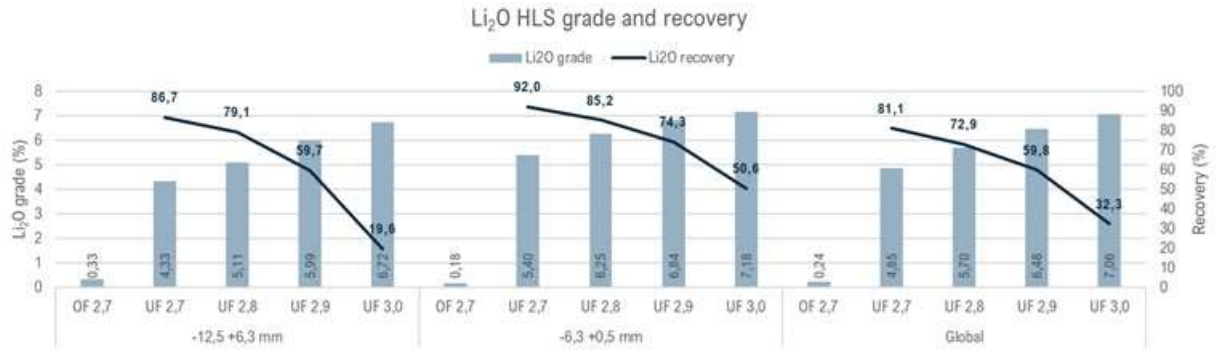

Figure 13-6 – Li2O Recovery and Grade per HLS Step

Source: Lithium Ionic 2024

13.3.2 Vendors Tests

Some test work has been conducted by vendors like:

- Ore Sorter
- Crushing Work Index (CWI)
- Crushing equipment to determine BWI (Bond Work Index), ore abrasiveness, equipment working capacity.

13.3.2.1 Ore Sorter at TOMRA

A composite sample from 6 drill holes (ITDD-22-013, 015, 029, 032, 035, and 036) with lithium oxide (Li2O) content ranging from 1.31 to 1.52% was sent to TOMRA in Germany to evaluate the applicability of the Ore Sorter in the pre-concentration stage. The material was crushed to achieve 100% passing at 31.5 mm and separated into 3 particle size ranges (-31.5 +19.1 mm; -19.1 +9.5 mm; and -9.5 mm). Tests were conducted on two particle size ranges, -31.5 +19.1mm and -19.1 +9.5 mm, while the -9.5 mm material was weighed, and its content determined to complete the metallurgical balance of the test. A preliminary analysis on the sample indicated the use of X-ray Transmission (XRT) sensor for conducting the test.

The X-ray Transmission sensor is related to the atomic density of the material, where higher transmitted X-ray intensity corresponds to lower absorption and lower atomic density. Electromagnetic radiation, between 90 and 200 keV, is directed onto the sample, and the transmitted radiation is detected pixel by pixel, converted into an electrical signal to generate a grayscale image. Hence, a lighter shade indicates lower absorption, thus lower atomic density. To distinguish thickness and atomic density, two sensors are utilized, acquiring different energy bands (VERAS, 2018; WOTRUBA & HARBECK, 2012).

The tests were conducted using the principle of cascade classification, as depicted in Figure 13-7. The sample was fed via a vibratory feeder onto a conveyor belt and analyzed by the Duoline X-ray sensor. The initial configuration of the equipment was programmed to eliminate all particles with at least 30% of high atomic density pixels. Subsequently, the previously classified low-density material was reclassified, eliminating all particles with at least 80% of high and medium atomic

density pixels. Lastly, the particles not ejected in the intermediate stage underwent further classification, where particles with at least 50% of high and medium density pixels were eliminated, while those with low atomic density pixels were retained, constituting the ore sorter concentrate.

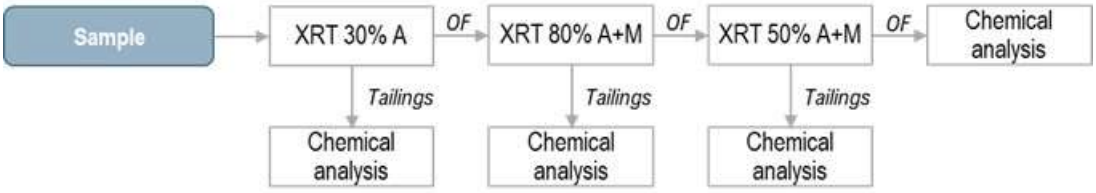

Figure 13-7 – Ore Sorter Test Procedure Using XRT Sensor

Source: Lithium Ionic 2024

The results obtained are presented in Table 13-4 and Table 13-5 for the particle size ranges of -31.5 +19.1 mm and -19.1 +9.5 mm, respectively. The fine fraction (-9.5 mm) accounted for 16.9% of the mass, which will be sent to the dense medium concentration stage. From the results, it is possible to observe that with the decrease in the ore sorter's average atomic density cut-off, the concentrate grade increases, and the metallurgical recovery decreases for both particle size ranges. Therefore, configuration 2 was selected as the most promising, as it was possible to enrich the dense medium feed grade by 25 to 26%, recovering 91 to 94% of the lithium.

Table 13-4 – Ore Sorter Results for the Size Fraction of -31,5 +19.1 mm

Source: Lithium Ionic 2024

Configuration	Mass reduction (%)	Conc. Li_2O grade (%)	Reject Li_2O grade (%)	Li_2O Recovery (%)	Enrichment (%)
1	17.15	1.46	0.23	96.85	17
2	24.81	1.56	0.30	93.97	25
3	48.43	1.74	0.73	71.69	39

Table 13-5 – Ore Sorter Results for the Size Fraction of -19.1 + 9,5 mm

Source: Lithium Ionic 2024

Configuration	Mass reduction (%)	Conc. Li_2O grade (%)	Reject Li_2O grade (%)	Li_2O Recovery (%)	Enrichment (%)
1	16.49	1.52	0.29	96.37	16
2	26.86	1.65	0.43	91.26	26
3	55.01	1.95	0.80	66.51	50

Subsequently, tests were conducted at TOMRA to evaluate the effect of dilution with shale on the equipment's performance. For this purpose, two drill holes, ITDD-22-054 and ITDD-22-098, with 10% dilution at the intersection with the pegmatite, were selected. The samples were crushed to achieve 100% passing at 31.5 mm and separated into 4 particle size ranges (-31.5 +19.1 mm; -19.1 +9.5 mm; -9.5 mm +0.85 mm; and -0.85 mm). Tests were conducted for two particle size ranges, -31.5 +19.1 mm and -19.1 +9.5 mm, while the material from the other size ranges was weighed, and its content determined to complete the metallurgical balance.

The tests were conducted using the same cascade classification principle applied previously, as shown in Figure 13-7. Table 13-6 and Table 13-7 present the results of the ore sorter test for the particle size range -19.1 +9.5 mm for the two drill holes. It is possible to observe that the results obtained for both samples were similar and indicate that configuration 1 is the most suitable. This is because, in this setup, enrichment between 19 and 20% was achieved with 94-96% recovery.

Table 13-6 – Ore Sorter Results for the Size Fraction of -19.1 + 9.5 mm (ITDD-22-054)

Source: Lithium Ionic 2024

Configuration	Mass reduction (%)	Conc. Li_2O grade (%)	Reject Li_2O grade (%)	Li_2O Recovery (%)	Enrichment (%)
1	20.81	1.77	0.43	94.00	19
2	27.15	1.83	0.56	89.83	23
3	50.68	2.29	0.70	76.09	54

Table 13-7 – Ore Sorter Results for the Size Fraction of -19.1 +9.5 mm (ITDD-22-098)

Source: Lithium Ionic 2024

Configuration	Mass reduction (%)	Conc. Li_2O grade (%)	Reject Li_2O grade (%)	Li_2O Recovery (%)	Enrichment (%)
1	19.90	1.61	0.26	96.19	20
2	30.89	1.72	0.48	88.94	29
3	54.45	1.98	0.80	67.28	48

The results for the particle size range -31.5 +19.1 mm are presented in Table 13-8 and

Table 13-9 for drill holes ITDD-22-054 and ITDD-22-098, respectively. There were discrepancies in the results between the two samples for the coarse particle size range, despite the difference in Li2O content in the test feed being less than 5% (1.31% for ITDD-22-054 and 1.26% for ITDD-22-098). Since no significant variation was observed in the results of the tests with and without dilution for the particle size range of -19.1 +9.5 mm, and no relevant effect of particle size on the undiluted test was observed, the result of drill hole ITDD-22-054 for coarse particle size was not considered in the ore sorter application analysis, as it differs from the other results obtained. Therefore, the second configuration is indicated as the most interesting, as it achieved a recovery of almost 93% of lithium, with an enrichment of 17%.

Table 13-8 – Ore Sorter Results for the Size Fraction of -31.5 +19.1 mm (ITDD-22-054)

Source: Lithium Ionic 2024

Configuration	Mass reduction (%)	Conc. Li_2O grade (%)	Reject Li_2O grade (%)	Li_2O Recovery (%)	Enrichment (%)
1	21.35	1.47	0.74	87.97	12
2	30.63	1.62	0.62	85.54	23
3	48.03	1.93	0.65	76.32	47

Table 13-9 – Ore Sorter Results for the Size Fraction of -31.5 +19.1 mm (ITDD-22-098)

Source: Lithium Ionic 2024

Configuration	Mass reduction (%)	Conc. Li_2O grade (%)	Reject Li_2O grade (%)	Li_2O Recovery (%)	Enrichment (%)
1	14.90	1.39	0.49	94.17	11
2	20.71	1.47	0.43	92.84	17
3	42.17	1.70	0.65	78.24	35

13.3.2.2 SGS Chile – CWI (Crushability Work Index)

The Bond Low Energy Impact test was conducted at SGS Chile to determine the Crushing Work Index (CWi), a factor indicating the power required for crushing. For the assay, 20 pieces cut to a thickness of 51 mm were sent. Each specimen was subjected to the impact of two hammers mounted on a pendulum. The test was repeated with an increase in the pendulum angle, thus increasing the impact, until the sample fractured. Cwi results varies from 4.1kWh/t to 10.2 kWh/t. The average result was 7.0 kWh/t, characterizing medium crushability work index. Table 13-10 and Table 13-11 shows the results obtained for this test.

Table 13-10 – Average CWi Results for the Bond Low-Energy Impact Tests

Source: Lithium Ionic 2024

Specimen No	Impact Energy, Joules	Work Index, kWh/t
1	14.9	5.9
2	10.4	4.1
3	14.9	5.9
4	10.4	4.1
5	14.9	5.9
6	26	10.2
7	26	10.2
8	20.1	7.9
9	10.4	4.1
10	26	10.2
11	10.4	4.1
12	14.9	5.9
13	26	10.2
14	26	10.2
15	20.1	7.9
16	14.9	5.9
17	14.9	5.9
18	20.1	7.9
19	20.1	7.9
20	14.9	5.9

Table 13-11 – Test Work Statistics

Source: Lithium Ionic 2024

Parameter	kWh/t
Maximum Impact Work Index	10.2
Minumum Impact Work Index	4.1
Average Impact Work Index	**7**
Standard Deviation	2.3

The specific gravity for the specimens were determined and found the result de 2.68 g/cm3.

13.3.2.3 Metso Outotec Tests

Crushability tests were performed to define crushing size with three composite samples of minimum 50 kg. According to tests the following parameters were determined, as shown in Table 13-12. The material was classified as abrasive and very easy to crush. In general, the results did not vary between the composites samples.

Table 13-12 – Crushability Tests Results

Source: Lithium Ionic 2024

	COMPOSITE 1	COMPOSITE 2	COMPOSITE 3
Samples	ITDD-22-023T/030T and ITDD-23-083T	ITDD-22-048T	ITDD-23-093T/087T
Abrasion index (Bond)	Average (0,295 g)	Average (0,300 g)	Average (0,212 g)
Abrasion index (Macon)	Abrasive (1698 g/t)	Abrasive (1602 g/t)	Abrasive (1600 g/t)
Crushability (Macon)	69,0 % (very easy)	68,8 % (very easy)	79,0 % (very easy)
Work index (Bond)	Average (12,25 kWh/st)	Average (11,35 kWh/st)	Average (10,50 kWh/st)
Bulk density	1,56 t/m³	1,61 t/m³	1,60 t/m³
Specific gravity	2,66 t/m³	2,71 t/m³	2,70 t/m³
Jaw crusher crushability	Crusher 75x50mm - Smooth Jaw Plates. CSS=4,5mm - Load Cell on Toggle	Crusher 75x50mm - Smooth Jaw Plates. CSS=4,5mm - Load Cell on Toggle	Crusher 75x50mm - Smooth Jaw Plates. CSS=4,5mm - Load Cell on Toggle
Volumetric capacity index	Standard methods (107,84 %)	Standard methods (107,40 %)	Maximum value (116,47 %)
Strength index	Smallest leaflet setting (96,21 %)	Smallest leaflet setting (106,96 %)	Minimum setting reduced 20% (88,57 %)
Product flakiness index	Cubical material (13,29 %)	Cubical material (5,45 %)	Cubical material (4,91 %)

13.3.3 Ore Variability

A variability study was conducted to understand the geological and metallurgical ore variability. First, eight drill holes without schist was selected to evaluate the HLS performance for different samples. Then, fifteen new samples from eleven drill holes were selected to evaluate the ore sorter and HLS performance in different area and depth with schist dilution.

13.3.3.1 Undiluted Samples – HLS tests

Figure 13-8 indicates the location of the eight drill holes selected, those has maximum 100m depth and minimum 5m interception, except ITDD-23-134T only used to Bond Low Energy Impact Test. A total of 906 kg was sent to SGS Geosol to be prepared, which includes crushing, screening, and sampling. The HLS was performed in duplicate at two particle size ranges -12.7 +6.3mm and -6.3 +0.85mm for three densities 2.8 g/cm³, 2.7 g/cm³ and 2.4 g/cm³, simulating a rougher-scavenger circuit and a polishing step for petalite recovery.

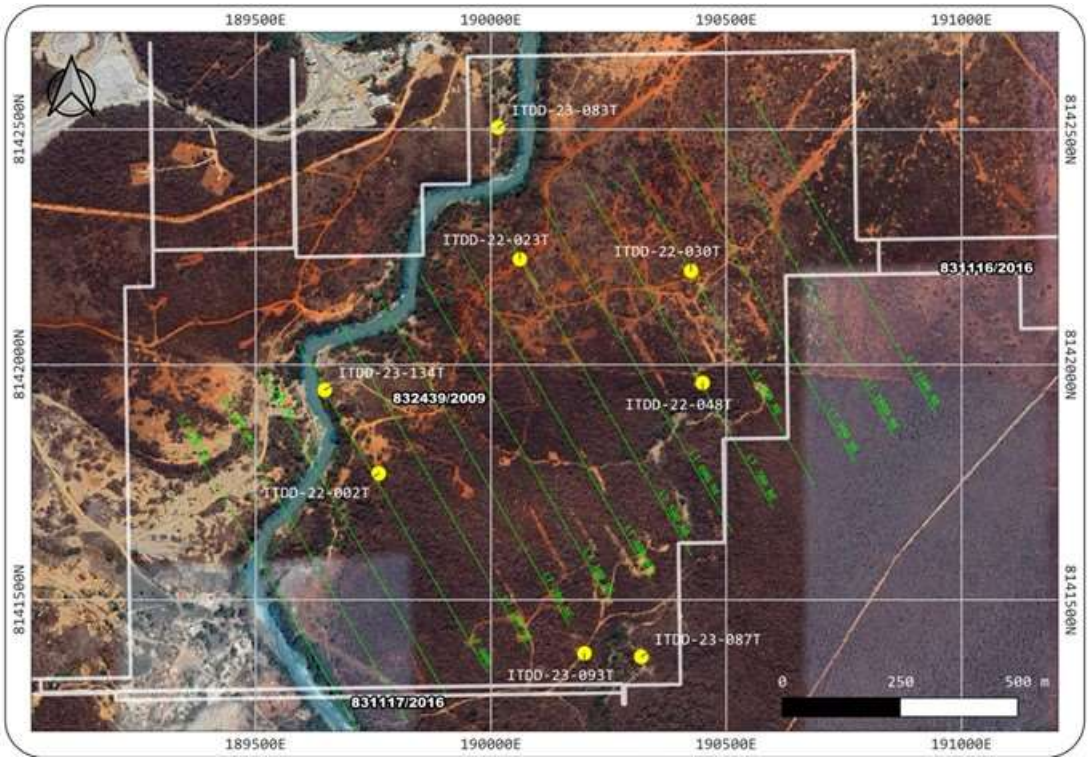

Figure 13-8 – Variability Study Drill Holes Map

Source: Lithium Ionic 2024

HLS rougher-scavenger results are presented in Table 13-13 and Table 13-14 for each particle size range. The 2.4 g/cm³ step did not presented significative mass for all samples, which indicates minor presence of petalite. In general, rougher concentrate presented Li2O grade above 5.5% with average global recovery of 84% for the coarse and 89% for the fine fraction.

Composite samples were tested to evaluate the combined behavior of the cluster. The composite results fit to the polynomial adjustment as shown in Figure 13-9 and Figure 13-10. The metallurgical recovery polynomial adjustment adherence with the composite results is shown in

Figure 13-11 with a R^2=0.89.

Table 13-13 – HLS Results for Coarse Fraction (-12.7+6.35 mm)

Source: Lithium Ionic 2024

Drill Hole	Li_2O Feed Grade (%)			Li_2O Float Grade (%)			Li_2O Sink Grade (%)			Li_2O Global Recovery (%)		
	T1	T2	$\bar{x}$	T1	T2	$\bar{x}$	T1	T2	$\bar{x}$	T1	T2	$\bar{x}$
ITDD-22-002T	1.10	1.40	1.25	0.33	0.26	0.29	4.18	3.95	4.06	76.80	88.18	82.50
ITDD-22-023T	1.60	1.48	1.54	0.22	0.23	0.23	5.82	5.55	5.68	89.90	89.30	89.61
ITDD-22-030T	0.83	1.63	1.23	0.38	0.35	0.36	7.13	7.65	7.39	60.40	84.49	72.42
ITDD-22-048T	1.26	0.95	1.10	0.26	0.28	0.27	5.40	5.43	5.41	86.20	78.00	82.08
ITDD-23-083T	1.61	2.14	1.88	0.10	0.14	0.12	6.76	6.33	6.55	95.30	95.93	95.61
ITDD-23-087T	1.53	2.12	1.83	0.38	0.21	0.30	4.96	5.57	5.27	83.20	94.43	88.81
ITDD-23-093T	0.60	0.59	0.60	0.19	0.13	0.16	6.75	6.15	6.45	72.30	81.80	77.06
Composite 1	1.40	-	-	0.27	-	-	4.52	-	-	87.20	-	-
Composite 2	1.33	-	-	0.29	-	-	5.50	-	-	84.40	-	-

Table 13-14 – HLS Results for Fine Fraction (-6.35+0.85 mm)

Source: Lithium Ionic 2024

Drill Hole	Li_2O Feed Grade (%)			Li_2O Float Grade (%)			Li_2O Sink Grade (%)			Li_2O Global Recovery (%)		
	T1	T2	$\bar{x}$	T1	T2	$\bar{x}$	T1	T2	$\bar{x}$	T1	T2	$\bar{x}$
ITDD-22-002T	1.14	1.07	1.10	0.17	0.17	0.17	5.59	4.98	5.29	88.32	87.71	88.01
ITDD-22-023T	1.59	1.33	1.46	0.22	0.17	0.19	6.75	6.01	6.38	89.57	90.25	89.91
ITDD-22-030T	1.44	1.36	1.40	0.31	0.27	0.29	7.37	6.56	6.96	82.64	84.37	83.51
ITDD-22-048T	0.96	1.00	0.98	0.18	0.13	0.16	6.25	6.83	6.54	85.33	89.91	87.62
ITDD-23-083T	1.45	1.48	1.46	0.12	0.12	0.12	7.15	7.25	7.20	93.48	93.89	93.69
ITDD-23-087T	1.51	1.58	1.54	0.19	0.21	0.20	6.55	6.37	6.46	91.25	90.26	90.76
ITDD-23-093T	1.04	1.19	1.12	0.16	0.15	0.15	6.99	6.74	6.87	87.67	90.48	89.08
Composite 1	1.34	-	-	0.19	-	-	6.74	-	-	89.1	-	-
Composite 2	1.42	-	-	0.18	-	-	6.54	-	-	90.8	-	-

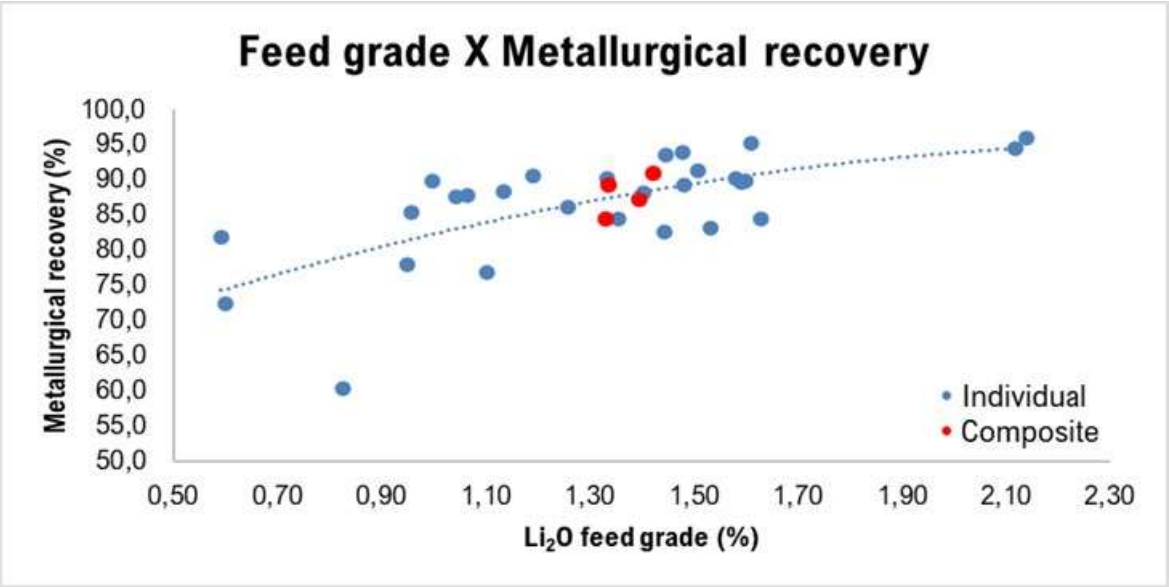

Figure 13-9 – HLS Metallurgical Recovery in Function of Feed Grade

Source: Lithium Ionic 2024

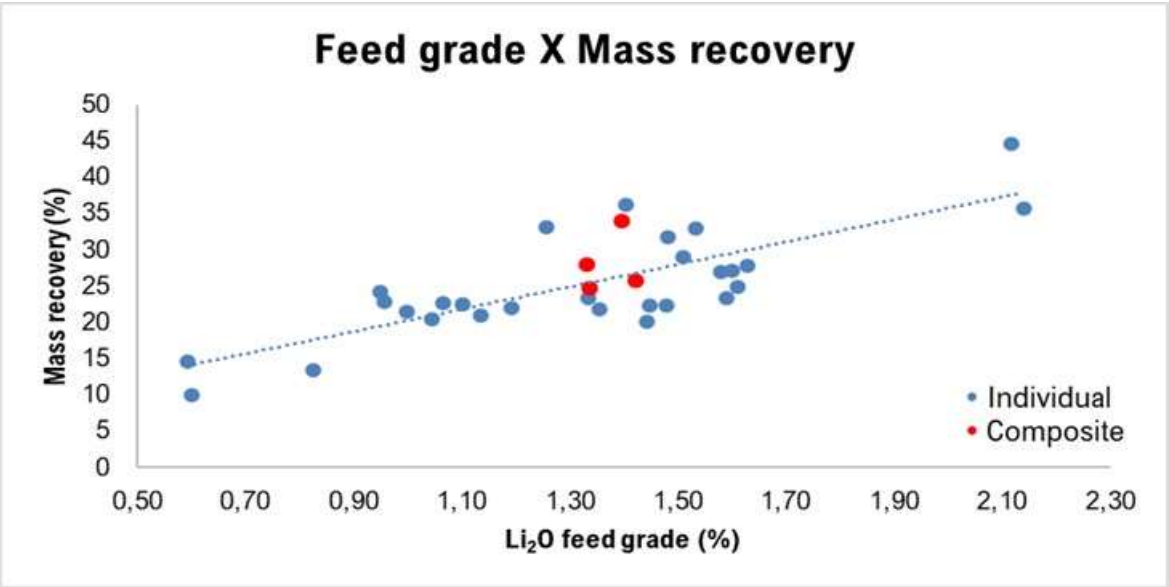

Figure 13-10 – HLS Mass Recovery in Function of Feed Grade

Source: Lithium Ionic 2024

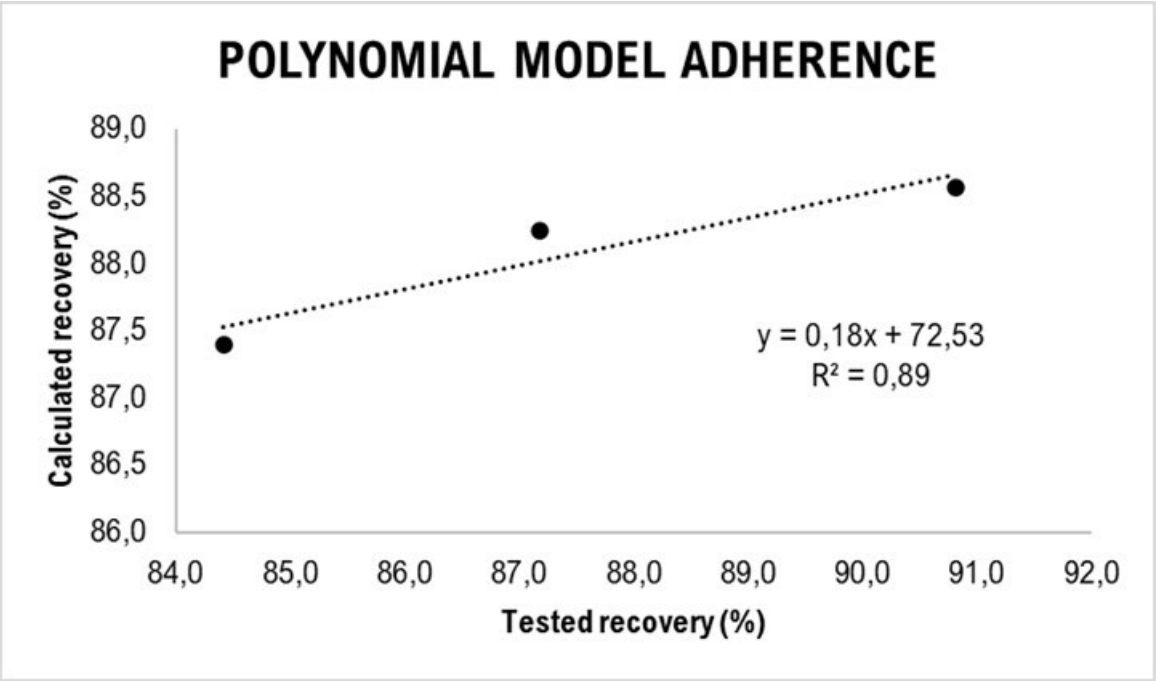

Figure 13-11 – Metallurgical Polynomial Model Adherence

Source: Lithium Ionic 2024

All HLS samples was analyzed by X-ray diffraction to understand the mineralogical behavior at HLS. The main lithium bearing minerals founded was spodumene, montebrasite, petalite and elbaite. According to Figure 13-12 and Figure 13-13 spodumene is mainly in the concentrate for both particle size distribution. Montebrasite distribution is presented in Figure 13-14 and Figure 13-15 and it is reported mainly in the tailing fraction. The same behavior happens to petalite distribution as shown in Figure 13-16 and Figure 13-17. Elbaite distribution has no concentration preference, as shown in Figure 13-18 and Figure 13-19 following the mass distribution.

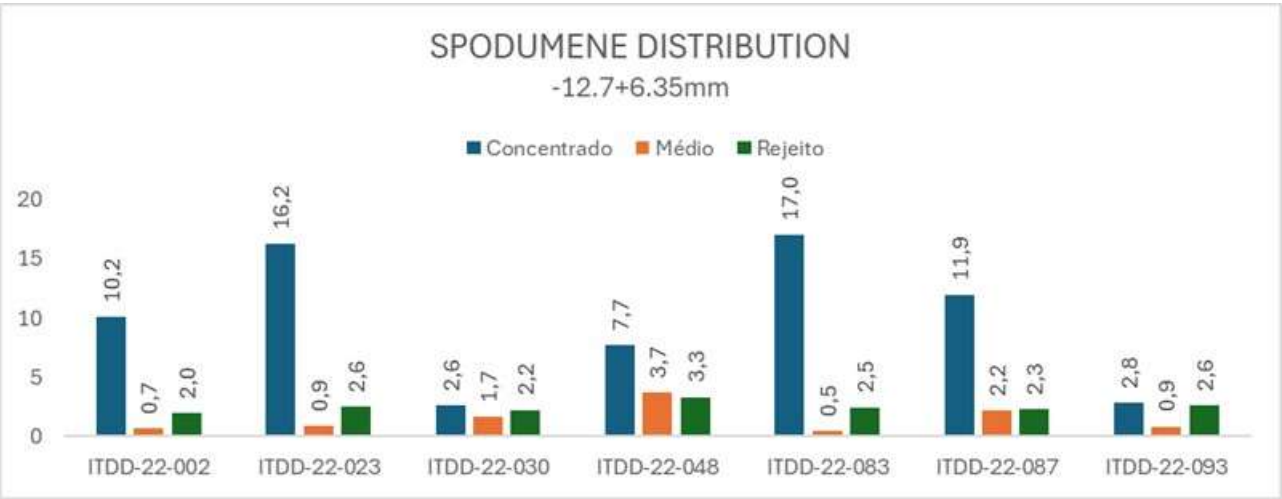

Figure 13-12 – Spodumene Mass Distribution in HLS tEst for Coarse Material (-12.7+6.35 mm)

Source: Lithium Ionic 2024

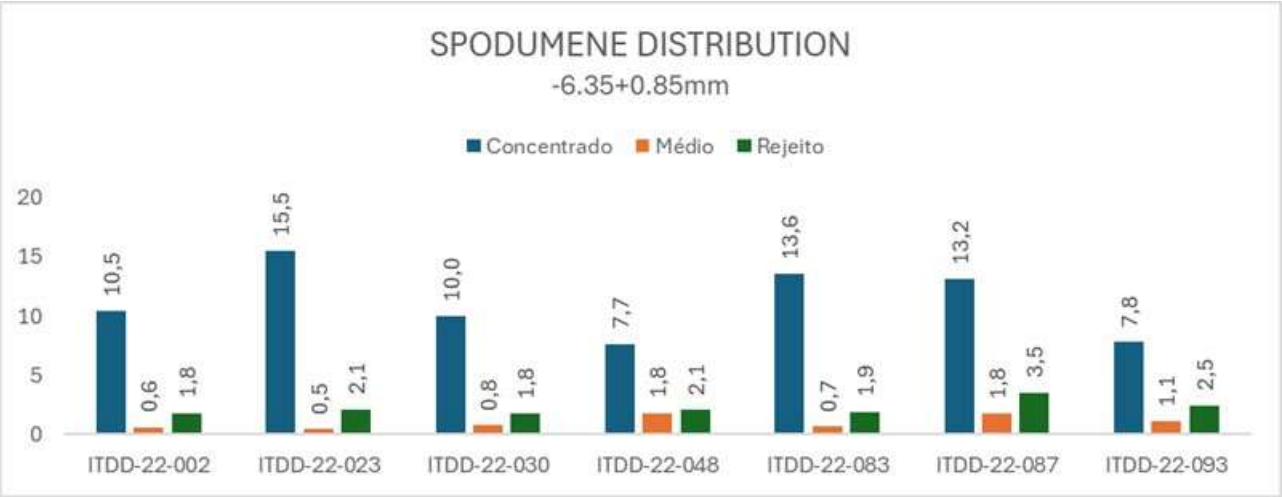

Figure 13-13 – Spodumene Mass Distribution in HLS Test for Fine Material (-6.35+0.85 mm)

Source: Lithium Ionic 2024

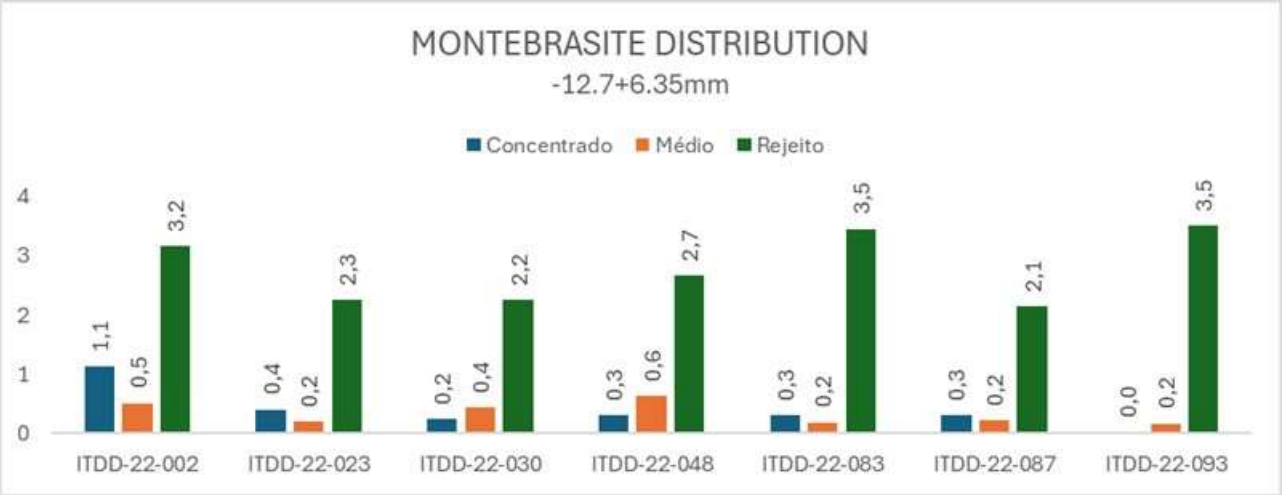

Figure 13-14 – Montebrasite Mass Distribution in HLS Test for Coarse Material (-12.7+6.35 mm)

Source: Lithium Ionic 2024

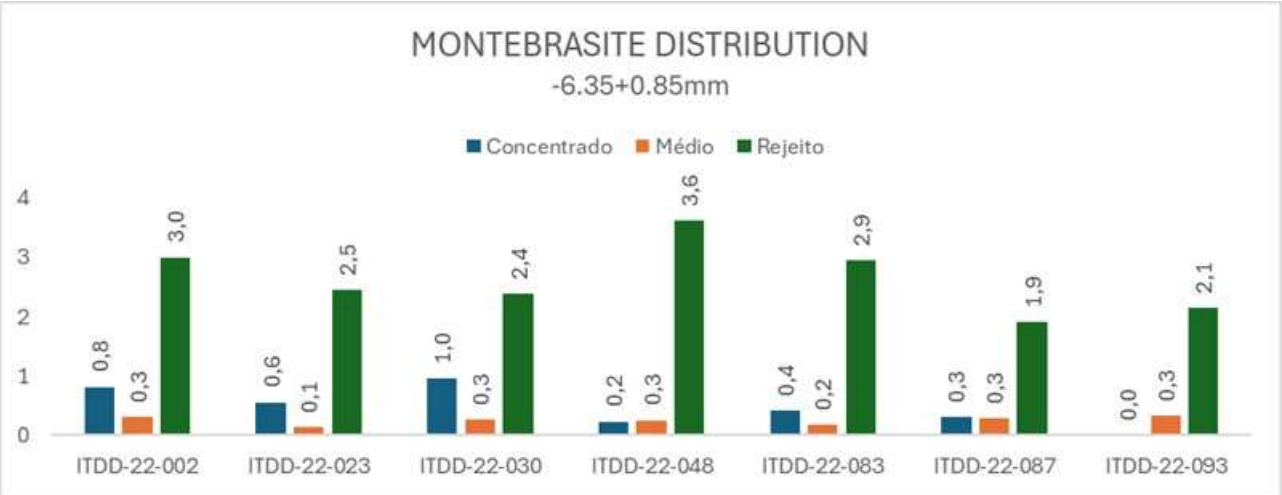

Figure 13-15 – Montebrasite Mass Distribution in HLS Test for Fine Material (-6.35+0.85 mm)

Source: Lithium Ionic 2024

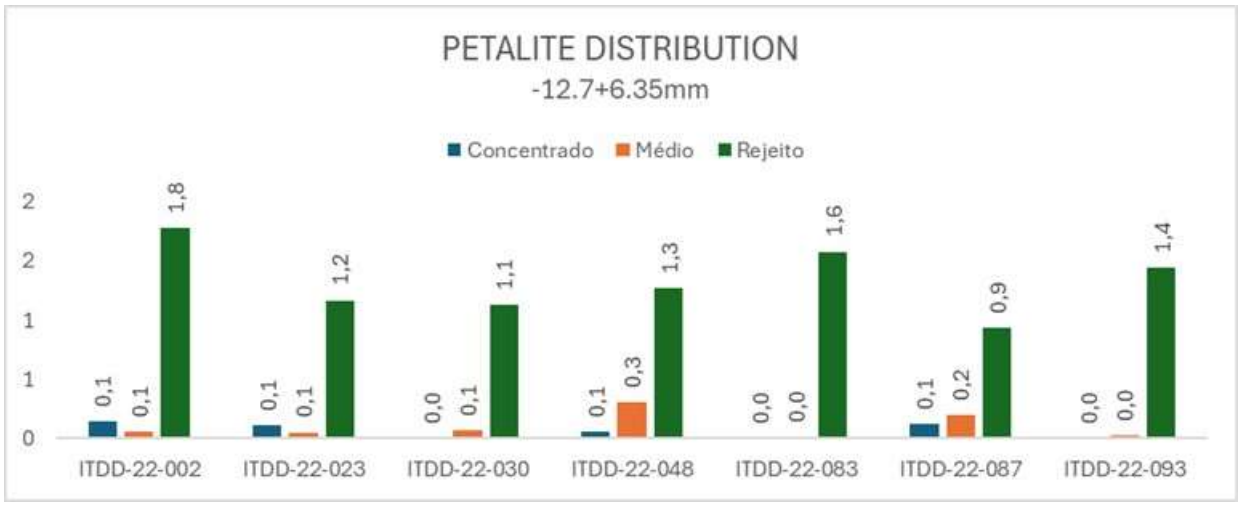

Figure 13-16 – Petalite Mass Distribution in HLS Test for Coarse Material (-12.7+6.35 mm)

Source: Lithium Ionic 2024

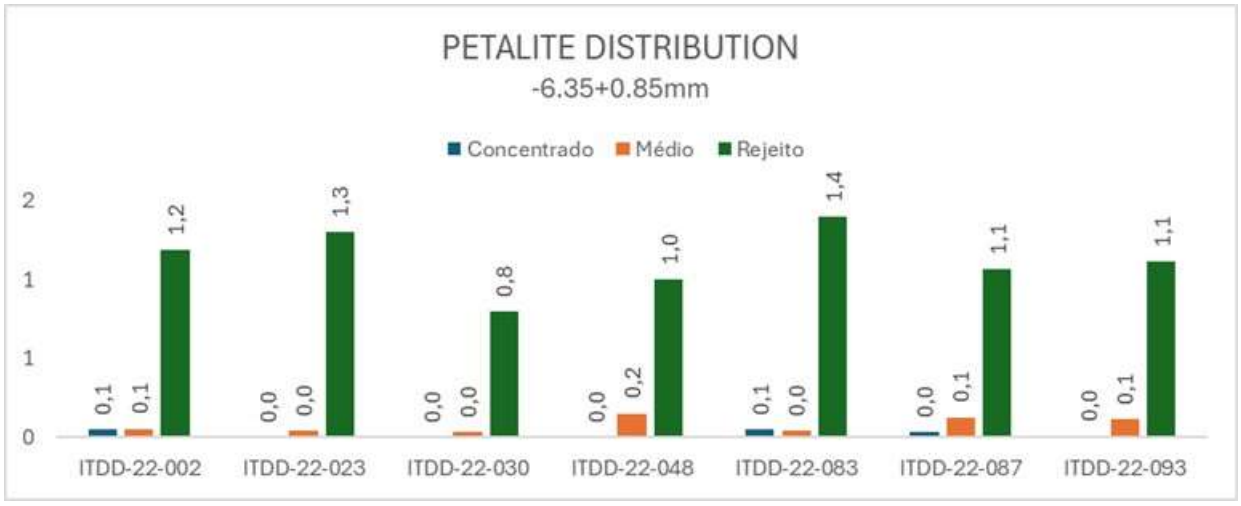

Figure 13-17 – Petalite Mass Distribution in HLS Test for Fine Material (-6.35+0.85 mm)

Source: Lithium Ionic 2024

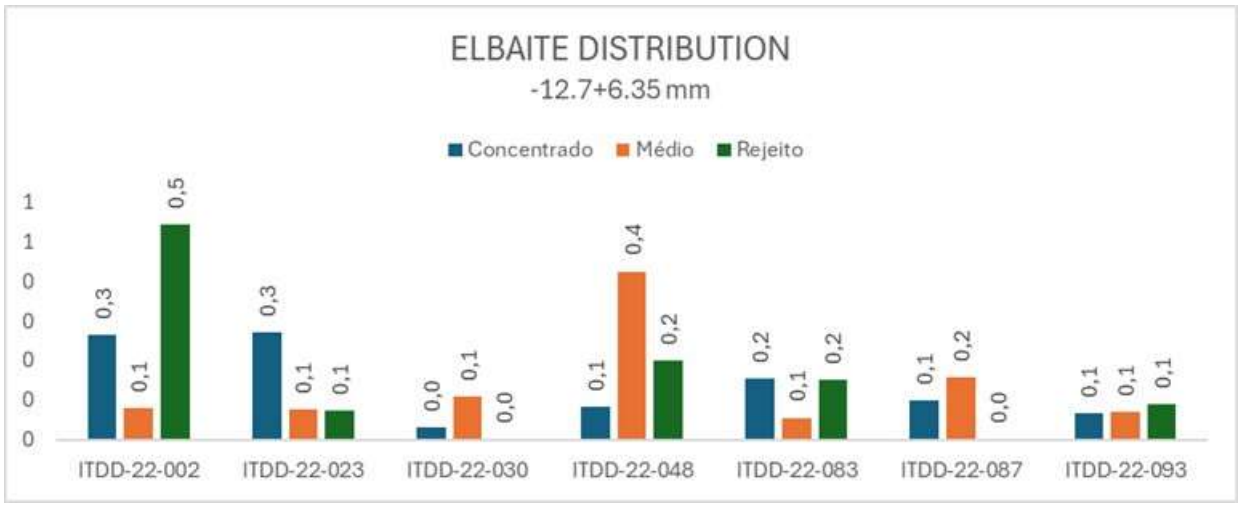

Figure 13-18 – Elbaite Mass Distribution in HLS Test for Coarse Material (-12.7+6.35 mm)

Source: Lithium Ionic 2024

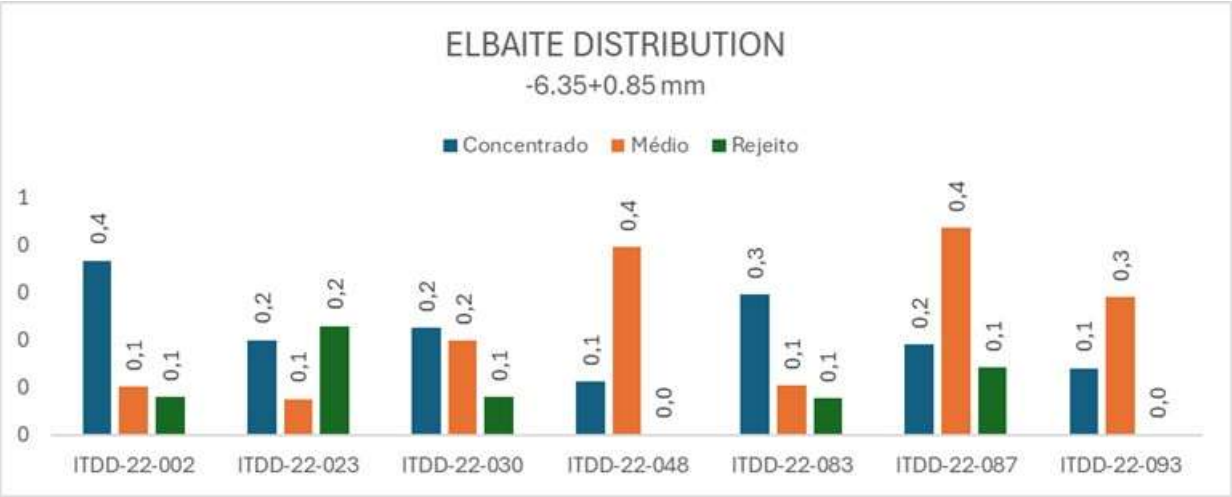

Figure 13-19 – Elbaite Mass Distribution IN Hls Test FOR Fine Material (-6.35+0.85 mm)

Source: Lithium Ionic 2024

13.3.3.2 Diluted Samples – Ore Sorter & HLS Tests

Figure 13-20 indicates the location of the 11 new drill holes (phase 2 in blue) among those two drill holes (ITDD-23-065 and ITDD-23-073) were selected three in different depths, to evaluate the metallurgical response over the LOM. For these samples, were performed ore sorter tests and HLS.

Ore sorter tests were done in two particle size range -31.5+19.1 mm and -19.1+7.5 mm. Then both concentrates were combined jointly together with the fraction size below 7.5 mm, that did not pass through ore sorter concentration. These composite samples were used to perform HLS tests in two particle size range -12.7+6.35 mm and -6.35+0.5 mm in three densities (2.8 g/cm³, 2.7 g/cm³ and 2.45 g/cm³).

Ore sorter results are presented in Figure 13-21 below for lithium and iron. In general, average lithium recovery was 93.6% and 92.6% respectively.

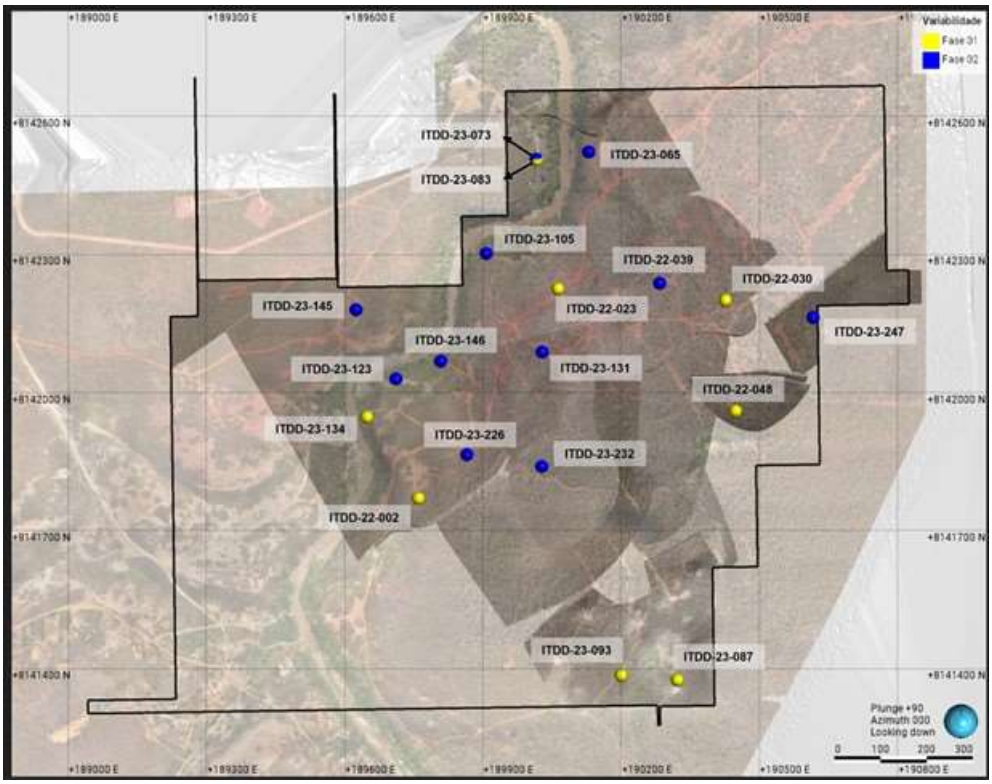

Figure 13-20 – Variability Additional Drill Hole Location Map

Legend: phase 2 in blue. Source: Lithium Ionic 2024

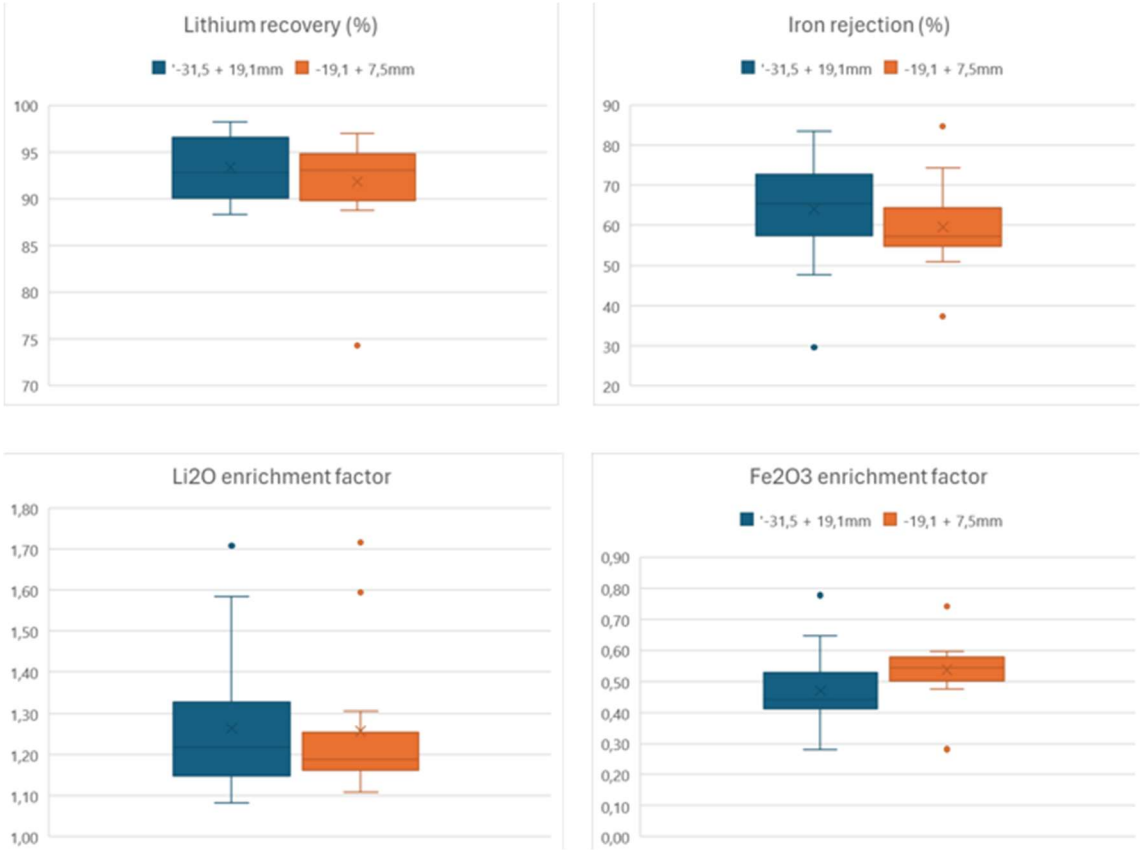

Figure 13-21 – Ore Sorter Results for Lithium and Iron

Source: Lithium Ionic 2024

Coarse and fine ore sorter concentrate were combined with fine fraction -7.5+0.5 mm to perform HLS tests. The particle size in HLS was -12.7+6.35 mm and -6.35+0.5 mm. A 3-stage circuit was simulated by HLS test in 2.80 g/cm³, 2.70 g/cm³ and 2.45 g/cm³. Table 13-15,

Table 13-16 and

Table 13-17 present HLS results. Rougher average metallurgical recovery was 77.8% with 22.1% of mass recovery. Scavenger step may increase the metallurgical recovery up to 86.1% with 34.0%. The step in 2.45 g/cm³ to may increase average metallurgical recovery up to 88.2% and mass recovery up to 2.1%. Figure 13-22 indicates the polishing effect.

Table 13-15 – HLS Rougher Step Results

Source: Lithium Ionic 2024

Sample	Size	Rec. Mas (%)	Rec. Met (%)	Li_2O feed (%)	Li_2O conc (%)	Li_2O tail (%)
ITDD-23-065 270.2 a 277.97	Fine	28.7	85.1	2.22	6.57	0.46
ITDD-23-065 351.23 a 380.7	Fine	8.7	47.4	0.97	5.27	0.56
ITDD-23-065 455.28 a 462.88	Fine	12.4	81.0	0.70	4.59	0.15
ITDD-23-073 76.82 a 84.66	Fine	25.1	90.0	1.83	6.55	0.24
ITDD-23-073 205.62 a 214.3	Fine	24.4	88.2	2.01	7.25	0.31
ITDD-23-073 406.21 a 428.35	Fine	15.0	71.9	1.17	5.60	0.39
ITDD-23-146 266.31 a 277.18	Fine	19.1	81.7	1.53	6.56	0.35
ITDD-23-145 289.82 a 303.05	Fine	19.1	82.0	1.59	6.84	0.35
ITDD-23-226 170.61 a 180.57	Fine	16.4	73.1	1.53	6.83	0.49
ITDD-22-039 85.24 a 96.86	Fine	25.7	85.4	1.59	5.29	0.31
ITDD-23-247 84.62 a 99.58	Fine	12.0	79.1	0.81	5.36	0.19
ITDD-23-232 137.7 a 146.95	Fine	20.6	80.6	1.53	6.00	0.38
ITDD-23-105 219.44 a 230.59	Fine	14.3	80.4	1.16	6.54	0.27
ITDD-23-123 148.16 a 160.4	Fine	14.2	81.2	1.08	6.19	0.24
ITDD-23-131 97.48 a 103.88	Fine	25.4	88.9	1.36	4.76	0.20
ITDD-23-065 270.2 a 277.97	Coarse	44.6	89.7	3.30	6.63	0.61
ITDD-23-065 351.23 a 380.7	Coarse	7.8	37.0	1.07	5.04	0.73
ITDD-23-065 455.28 a 462.88	Coarse	23.5	74.7	0.90	2.85	0.30
ITDD-23-073 76.82 a 84.66	Coarse	30.3	82.9	2.10	5.75	0.51
ITDD-23-073 205.62 a 214.3	Coarse	31.0	85.7	2.25	6.23	0.47
ITDD-23-073 406.21 a 428.35	Coarse	25.2	68.6	1.99	5.41	0.84
ITDD-23-146 266.31 a 277.18	Coarse	29.4	83.9	2.19	6.27	0.50
ITDD-23-145 289.82 a 303.05	Coarse	34.2	83.7	2.03	4.95	0.50
ITDD-23-226 170.61 a 180.57	Coarse	25.1	69.3	2.08	5.73	0.85
ITDD-22-039 85.24 a 96.86	Coarse	31.5	84.7	2.14	5.74	0.48

Sample	Size	Rec. Mas (%)	Rec. Met (%)	Li_2O feed (%)	Li_2O conc (%)	Li_2O tail (%)
ITDD-23-247 84.62 a 99.58	Coarse	13.0	64.9	0.87	4.32	0.35
ITDD-23-232 137.7 a 146.95	Coarse	25.8	71.6	1.59	4.42	0.61
ITDD-23-105 219.44 a 230.59	Coarse	14.0	71.0	1.25	6.33	0.42
ITDD-23-123 148.16 a 160.4	Coarse	20.3	84.8	1.65	6.90	0.32
ITDD-23-131 97.48 a 103.88	Coarse	27.2	86.4	1.60	5.07	0.30

Table 13-16 – HLS Scavenger Step Results

Source: Lithium Ionic 2024

Sample	Size	Rec. Mas (%)	Rec. Met (%)	Li_2O feed (%)	Li_2O conc (%)	Li_2O tail (%)
ITDD-23-065 270.2 a 277.97	Fine	13.4	32.7	0.46	1.13	0.36
ITDD-23-065 351.23 a 380.7	Fine	5.6	6.2	0.56	0.62	0.55
ITDD-23-065 455.28 a 462.88	Fine	10.9	38.4	0.15	0.53	0.11
ITDD-23-073 76.82 a 84.66	Fine	13.8	44.9	0.24	0.79	0.16
ITDD-23-073 205.62 a 214.3	Fine	8.2	23.5	0.31	0.89	0.26
ITDD-23-073 406.21 a 428.35	Fine	15.5	25.8	0.39	0.64	0.34
ITDD-23-146 266.31 a 277.18	Fine	9.2	25.9	0.35	0.98	0.28
ITDD-23-145 289.82 a 303.05	Fine	15.1	46.5	0.35	1.09	0.22
ITDD-23-226 170.61 a 180.57	Fine	6.5	24.9	0.49	1.89	0.40
ITDD-22-039 85.24 a 96.86	Fine	12.2	48.4	0.31	1.24	0.18
ITDD-23-247 84.62 a 99.58	Fine	9.5	47.7	0.19	0.97	0.11
ITDD-23-232 137.7 a 146.95	Fine	14.7	62.8	0.38	1.60	0.16
ITDD-23-105 219.44 a 230.59	Fine	14.6	47.7	0.27	0.87	0.16
ITDD-23-123 148.16 a 160.4	Fine	13.5	43.9	0.24	0.77	0.15
ITDD-23-131 97.48 a 103.88	Fine	38.7	75.3	0.20	0.39	0.08
ITDD-23-065 270.2 a 277.97	Coarse	18.1	50.7	0.61	1.72	0.37
ITDD-23-065 351.23 a 380.7	Coarse	6.4	12.4	0.73	1.41	0.68
ITDD-23-065 455.28 a 462.88	Coarse	20.9	71.9	0.30	1.02	0.11
ITDD-23-073 76.82 a 84.66	Coarse	11.4	18.4	0.51	0.83	0.47
ITDD-23-073 205.62 a 214.3	Coarse	8.7	27.9	0.47	1.49	0.37
ITDD-23-073 406.21 a 428.35	Coarse	28.9	45.2	0.84	1.31	0.65
ITDD-23-146 266.31 a 277.18	Coarse	13.7	45.2	0.50	1.64	0.32
ITDD-23-145 289.82 a 303.05	Coarse	17.4	36.8	0.50	1.06	0.38
ITDD-23-226 170.61 a 180.57	Coarse	13.5	49.5	0.85	3.12	0.50
ITDD-22-039 85.24 a 96.86	Coarse	10.4	46.9	0.48	2.17	0.28
ITDD-23-247 84.62 a 99.58	Coarse	11.3	52.8	0.35	1.64	0.19
ITDD-23-232 137.7 a 146.95	Coarse	19.7	57.8	0.61	1.79	0.32
ITDD-23-105 219.44 a 230.59	Coarse	19.1	46.9	0.42	1.04	0.28
ITDD-23-123 148.16 a 160.4	Coarse	19.8	29.5	0.32	0.47	0.28
ITDD-23-131 97.48 a 103.88	Coarse	45.9	12.7	0.30	0.08	0.48

Table 13-17 – Polishing HLS Results

Source: Lithium Ionic 2024

Sample	Size	Mas Rec (%)	Met Rec (%)	Li_2O feed (%)	Li_2O conc (%)	Li_2O tail (%)
ITDD-23-065 270,2 a 277,97	Fine	2.3	27.4	0.36	0.27	4.22
ITDD-23-065 351,23 a 380,7	Fine	5.7	48.8	0.55	0.30	4.72
ITDD-23-073 205,62 a 214,3	Fine	0.8	6.6	0.26	0.24	2.05
ITDD-23-073 406,21 a 428,35	Fine	1.0	13.5	0.34	0.30	4.84
ITDD-23-065 351,23 a 380,7	Coarse	8.9	49.4	0.68	0.38	3.79
ITDD-23-073 205,62 a 214,3	Coarse	2.2	6.2	0.37	0.36	1.06
ITDD-23-073 406,21 a 428,35	Coarse	4.5	30.7	0.65	0.47	4.45

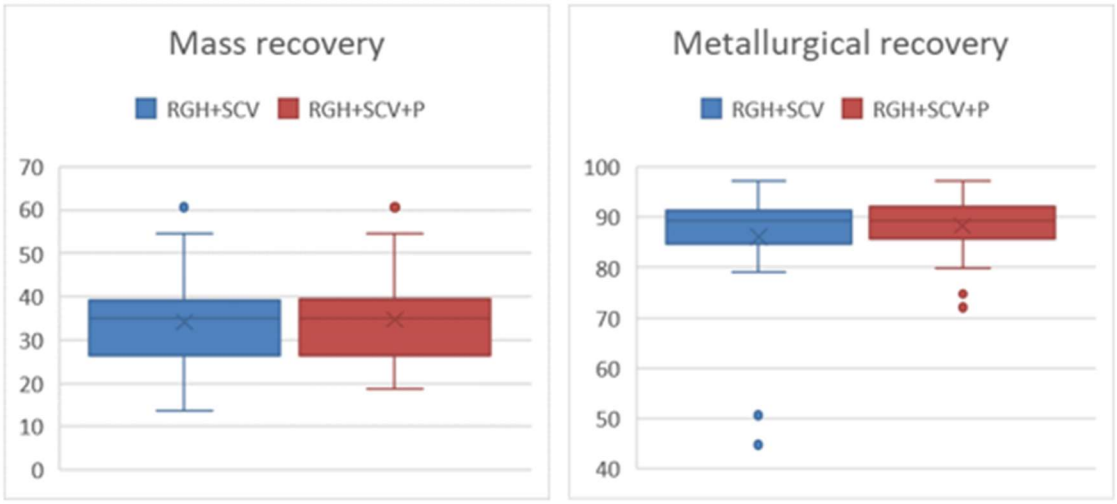

Figure 13-22 – Comparative Recovery for 2-Stage and 3-Stage Circuit

Source: Lithium Ionic 2024

13.3.4 Pilot Plant – Ore Sorter (Steinert) & DMS (SGS Geosol)

After completing the variability study from 7(seven) drill holes, the reserved samples were tested by ore sorter equipment and DMS pilot plant, as shown in Figure 13-23. Besides it, a composite sample was selected to perform HLS test by size to evaluate liberation.

Ore sorter tests were performed as describe in Figure 13-23. For the coarse material (-25.4+6.35 mm) each sample had mass around 7 kg. Two samples were tested individually, and the others five samples were composed in one to improve test representative. The fine material (-12.7+6.35 mm) was tested individually.

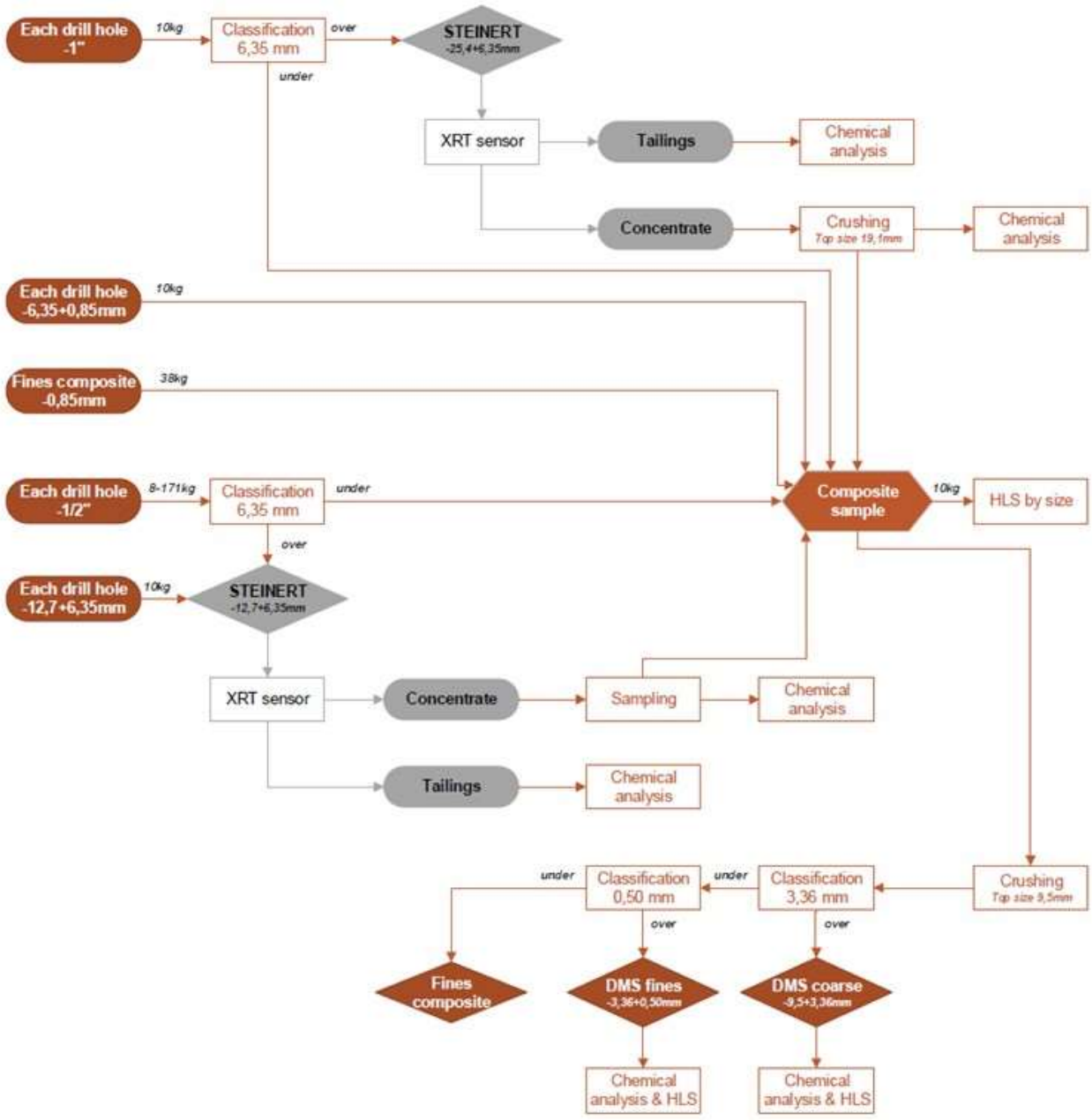

Figure 13-23 – Pilot Plant Flowsheet

Source: Lithium Ionic 2024

Ore sorter results are shown in Table 13-18. Lithium recovery ranged from 88.1 to 96.1% with average mass loss of 18.1% and enrichment factor of 1.12. Mass recovery to the concentrate should be lower to increase lithium recovery, once were used undiluted samples. New tests using diluted samples were completed to validate the ore sorter results. Regarding iron and potassium, tailings enrichment factor was 1.37 and 2.34, respectively, with good results of discharging schist and feldspar to tailings.

The liberation particle size was evaluated by performing HLS test in 7 particle size range, from top size of 19.1 mm to 0.5 mm. To avoid sampling error all the mass retained in 15.9 mm sieve was used in the coarser HLS test. For HLS test with particle size below 15.9 mm up to 1.7 mm, 500 g were sampled from the total mass retained in each sieve and for the finer samples 150 g

were used. This procedure was recommended by SGS Geosol as their best practice.

The tests used two densities, 2.8 g/cm³ and 2.7 g/cm³, simulating rougher and scavenger stages. The results for each particle size range are shown in Table 13-19. In general, the results indicate that the recovery tends to decrease as the particle size increases. On the other hand, the Li2O grade decreases as the particle size increases.

Table 13-20 presented the grade and recovery results accumulated by mass distribution. Figure 13-24 shows the results of each HLS size particle range.

Table 13-18 – Ore Sorter Pilot Plant Results

Source: Lithium Ionic 2024

SAMPLE	PARTICLE SIZE	FEED			CONCENTRATE			TAILING			RECOVERY			
		Li2O (%)	Fe (%)	K (%)	Li2O (%)	Fe (%)	K (%)	Li2O (%)	Fe (%)	K (%)	Mass	Li2O	Fe	K
ITDD-23-087T	-25.4 +6.35mm	1.36	0.51	1.62	1.43	0.45	1.37	0.61	1.08	4.19	91.3	96.1	81.3	77.4
ITTD-22-002T	-25.4 +6.35mm	0.96	0.68	1.90	1.07	0.48	1.47	0.53	1.51	3.74	80.9	89.5	57.4	62.4
Composite	-25.4 +6.35mm	1.21	0.54	1.74	1.29	0.51	1.27	0.46	0.75	5.77	89.5	96.0	85.3	65.3
ITTD-22-048T	-12.7 +6.35mm	1.03	0.73	1.83	1.11	0.67	1.34	0.67	1.01	4.00	81.6	88.1	74.6	59.8
ITDD-23-087T	-12.7 +6.35mm	1.59	0.65	1.79	1.76	0.63	1.29	0.82	0.72	4.03	81.6	90.5	79.6	58.7
ITTD-23-083T	-12.7 +6.35mm	1.80	0.48	1.84	2.02	0.48	1.15	0.90	0.47	4.60	79.9	89.9	80.3	49.9
ITTD-22-002T	-12.7 +6.35mm	1.23	0.88	2.16	1.59	0.53	1.56	0.31	1.79	3.71	72.1	93.0	43.3	52.1
ITTD-23-093T	-12.7 +6.35mm	0.66	0.51	1.82	0.72	0.54	1.37	0.35	0.36	3.82	81.7	90.2	87.0	61.5
ITTD-22-030T	-12.7 +6.35mm	1.19	0.46	1.83	1.33	0.50	1.14	0.63	0.32	4.56	79.8	89.3	86.0	49.6
ITTD-22-023T	-12.7 +6.35mm	1.53	0.40	2.07	1.72	0.39	1.42	0.73	0.42	4.79	80.8	90.8	79.6	55.5

Table 13-19 – HLS Results for Each Particle Size Range for Spodumene Liberation

Source: Lithium Ionic 2024

	-19.1+15.9mm		-15.9+12.7mm		-12.7+9.5mm		-9.5+6.3mm		-6.3+3.4mm		-3.4+1.7mm		-1.7+0.5mm	
	Li_2O Assay, %	Li_2O Dist, %	Li_2O Assay, %	Li_2O Dist, %	Li_2O Assay, %	Li_2O Dist, %	Li_2O Assay, %	Li_2O Dist, %	Li_2O Assay, %	Li_2O Dist, %	Li_2O Assay, %	Li_2O Dist, %	Li_2O Assay, %	Li_2O Dist, %
Feed	1.25	100.0	1.36	100.0	1.54	100.0	1.51	100.0	1.40	100.0	1.34	100.0	1.30	100.0
Sink 2.8 g/cm³	4.13	59.0	4.97	77.9	5.32	74.1	5.87	75.4	6.02	82.3	6.75	84.2	6.48	89.4
Sink 2.7 g/cm³	1.76	25.1	2.48	10.9	2.09	11.7	1.83	16.2	1.43	8.5	1.22	7.3	0.80	3.2
Float 2.7 g/cm³	0.31	15.9	0.21	11.1	0.31	14.1	0.19	8.4	0.18	9.2	0.15	8.6	0.13	7.4

Table 13-20 – Accumulated HLS Results by Particle Size

Source: Lithium Ionic 2024

	-19.1+15.9mm	**-15.9+12.7mm**	**-12.7+9.5mm**	**-9.5+6.3mm**	**-6.3+3.4mm**	**-3.4+1.7mm**	**-1.7+0.5mm**
Mass retained, %	1.53	7.96	12.03	12.72	15.58	12.05	13.28
Li_2O grade by size, %	4.13	4.97	5.32	5.87	6.02	6.75	6.48
Li_2O recovery by size, %	84.1	88.9	85.9	91.6	90.8	91.4	92.6
	-19.1+0,5mm	**-15,9+0,5mm**	**-12,7+0,5mm**	**-9,5+0,5mm**	**-6,3+0,5mm**	**-3,4+0,5mm**	**-1,7+0,5mm**
Li_2O grade accumulated, %	5.93	5.97	6.09	6.26	6.39	6.61	6.48
Li_2O recovery accumulated, %	90.2	90.3	90.5	91.6	91.6	92.0	92.6

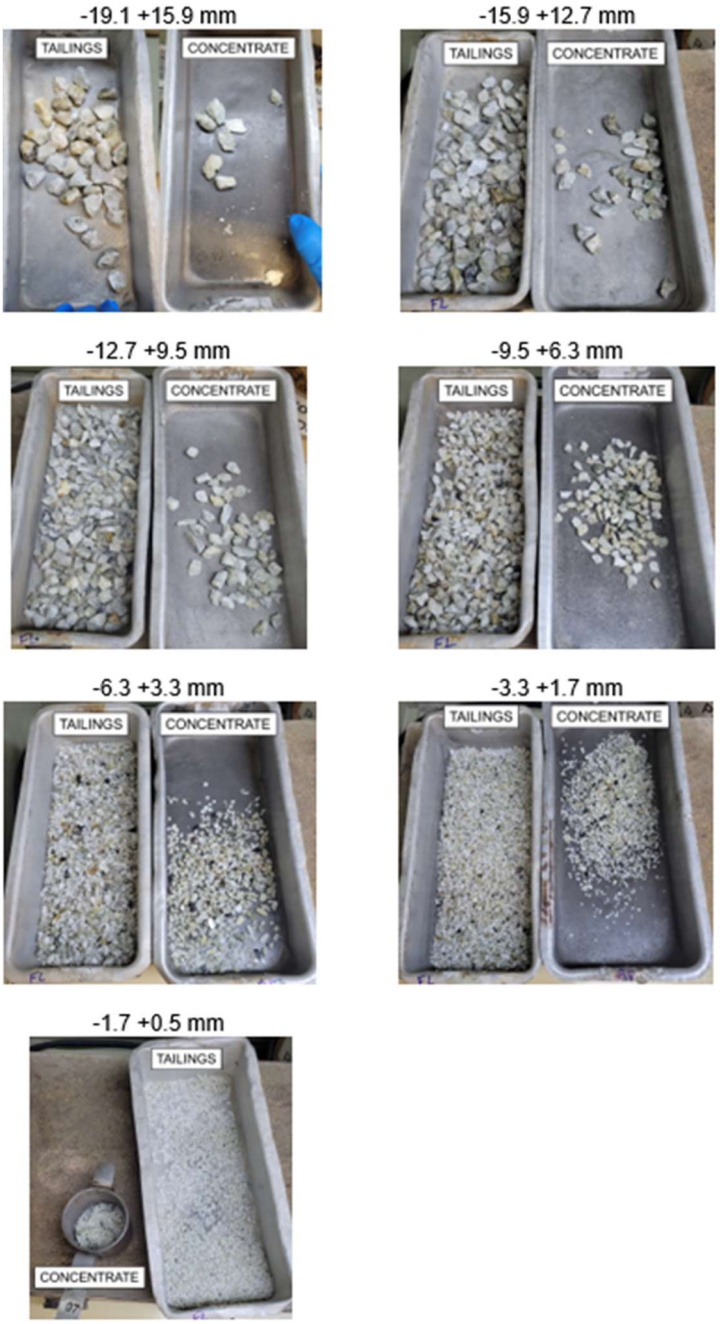

Figure 13-24 – HLS Separation for Rougher Stage

Source: Lithium Ionic 2024

The tests at the DMS pilot plant were conducted using composite samples from the seven drill holes of the variability tests. These samples underwent testing in an Ore Sorter at Steinert for the removal of schist and feldspar, followed by particle size adjustment to meet the specification of the DMS pilot plant. The DMS tests were conducted in two size fractions. The coarser fraction was prepared at -9.5 mm +3.55 mm, and the finer fraction was prepared at -3.55 mm +0.5 mm. Below is the list of drill holes from which the samples were composed:

- ITDD-22-048T
- ITDD-23-093T

- ITDD-23-087T
- ITDD-22-023T
- ITDD-22-002T
- ITDD-23-083T
- ITDD-23-030T

Figure 13-25 presents a flowchart reproducing the unit operations in the SGS Geosol DMS pilot plant. 25 DMS pilot plant tests were performed (21 Rougher and 4 Scavenger) to obtain supporting information for the Bandeira process development.

The circuit includes a hopper, manually fed with ore, connected to a vibrating feeder responsible for feeding this ore into the static mixer. The solid dense media (Iron Silicon) is fed directly into the agitated tank. This dense media undergoes a dilution process and subsequent pulp density adjustment by injecting water into the tank or the first section of the screen's chute.

The prepared dense media with the appropriate density feeds by gravity into the chute of the first section of the screen. From this point, the dense media is pumped through a demagnetizing coil and a flow divider with manual valves. The flow divider directs part of the dense media to the screen, and the rest recirculates to the agitated tank. The screen's function is to protect the system and retain undesirable or inadequately sized materials. The screen underflow feeds the static mixer, positioned just above the DMS cyclone. This static mixer promotes the mixing of the ore from the vibrating feeder and the dense media from the screen underflow. The gravity feed of the DMS cyclone establishes a cyclone feed pressure based on the height of the liquid column relative to the vertical distance between the DMS cyclone feed flange and the pulp level in the static mixer.

The DMS cyclone, positioned at a 20-degree incline relative to its centerline, separates the mixture by density, partitioning it into sink (underflow) and float (overflow). In this process, the concentrate is directed to the sink flow, and the reject is directed to the float flow. The dewatering screen has a partition into two parallel sections and two underflow chutes. Each chute receives drainage from half of the parallel sections' area. The cyclone sink is directed to the first section of the screen, and the float is directed to the second section. In the first screen chute, the dense media concentrate is drained. From the second chute, wash water is injected to remove residual dense media and drain this diluted flow. The diluted dense media is then pumped to the magnetic separator, which retains Iron Silicon particles and removes excess water, concentrating the dense media mixture. The concentrated dense media is then recirculated to the agitated tank, while the water is discarded. The DMS concentrate is equivalent to the oversize from the first section of the dewatering screen, and the DMS reject is equivalent to the oversize from the second section of the screen.

To conduct the scavenger stage test, this process is repeated by refeeding the reject obtained in the rougher stage.

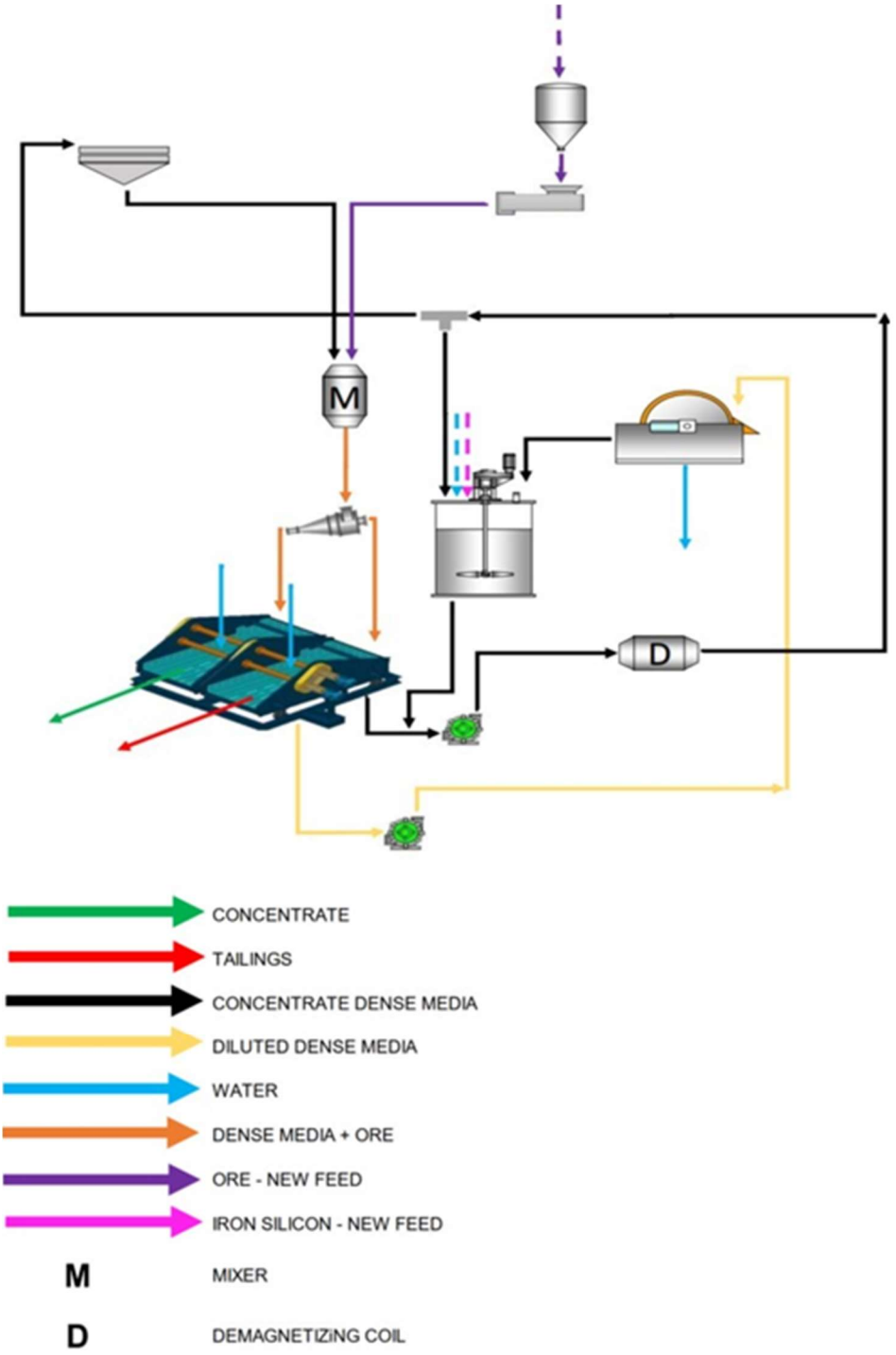

Figure 13-25 – DMS Pilot Plant Flowchart

Source: Lithium Ionic 2024

The results of the pilot tests were presented in graphical representations to define trend lines and points of coherence for a comprehensive analysis of the results.

The initial rougher tests for the coarse fraction were discarded as they were part of the pilot plant's calibration period. The results of the tests considered for the rougher stage indicated the following trend curve (Metallurgical Recovery x Li2O Grade in Concentrate) for the -9.5 mm +3.35 mm fraction is presented in Figure 13-26.

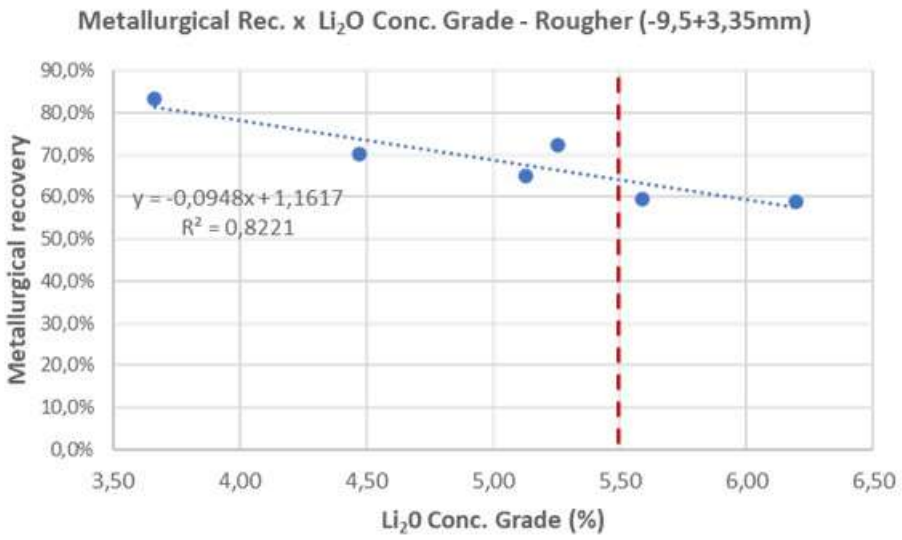

Figure 13-26 – Rougher Coarse Metallurgical Recovery x Li2O Grade in Concentrate

Source: Lithium Ionic 2024

The analysis of these data converges to achieve a metallurgical recovery of about 64,0% to obtain a concentrate with a Li2O grade of 5.50% in the -9.5 mm +3.35 mm fraction.

The initial rougher tests for the fine fraction were discarded as they were part of the pilot plant's calibration period. The results of the tests considered for the rougher stage indicated the following trend curve (Metallurgical Recovery x Li2O Grade in Concentrate) for the -3.35 mm +0.5 mm fraction is presented in the Figure 13-27.

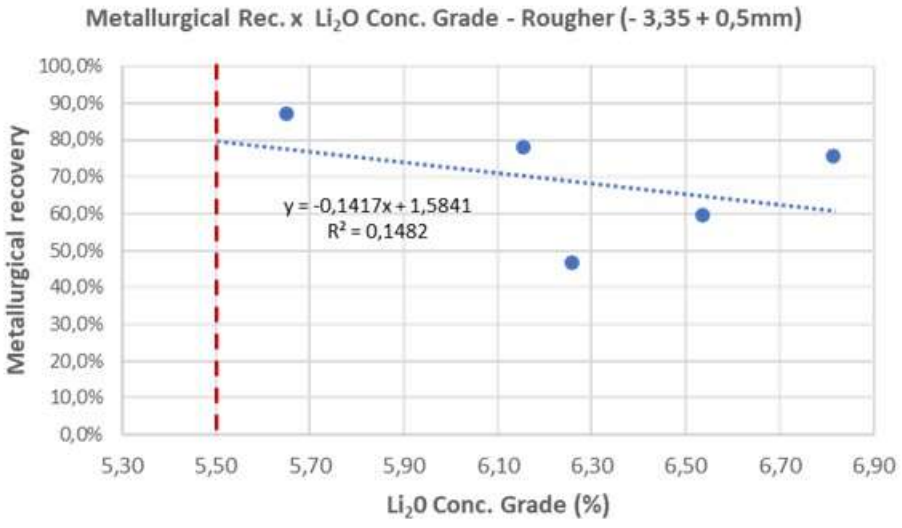

Figure 13-27 – Rougher Fine Metallurgical Recovery x Li2O Grade in Concentrate

Source: Lithium Ionic 2024

Although this trend line does not fit the points as well as in the coarse fraction, the analysis of these data converges to achieve a metallurgical recovery of about 80,5% to obtain a concentrate with a Li2O grade of 5.50% in the -3.35 mm +0.5 mm fraction. The combination of the most

coherent result points obtained in the two fractions, -9.5 mm +3.35 mm and -3.35 mm +0.5 mm, presented the following trend curve, showed below in Figure 13-28.

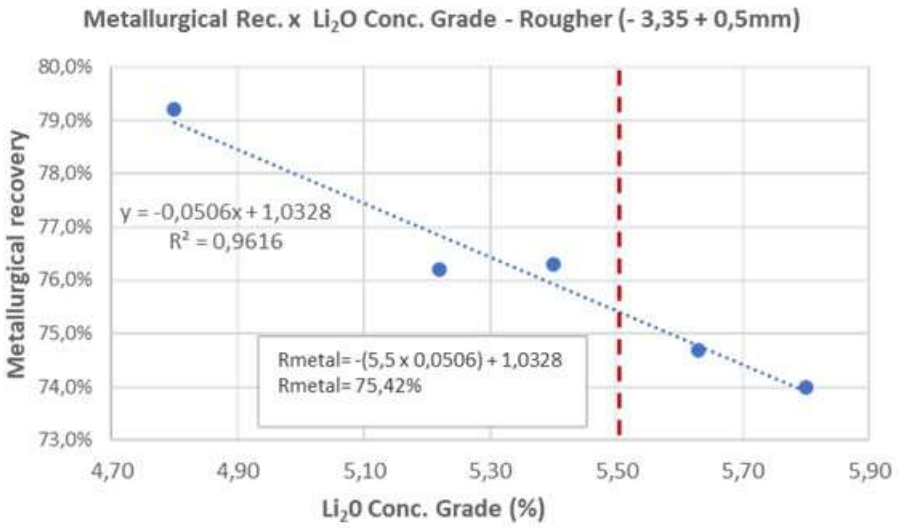

Figure 13-28 – Rougher Composite Metallurgical Recovery x Li2O Grade in Concentrate

Source: Lithium Ionic 2024

The analysis of these data converges to achieve a metallurgical recovery of about 75.42% to obtain a concentrate with a Li2O grade of 5.50% in the rougher stage, considering the combination of the two tested size fractions. To achieve this metallurgical recovery, the results of tests 16 and 17 were adopted as references. Since both produced concentrates with Li2O grades higher than 5.50%, it was necessary to recalculate the metallurgical recoveries. The Figure 13-29 presents the results of tests 16 and 17, as well as the adjusted metallurgical recoveries to obtain a 5.50% concentrate and an overall rougher stage metallurgical recovery of 75.42%.

Testwork n°	Li_2O Grade Conc.	Metall. Rec.
test 16	5,65	87,06%
test 17	5,59	59,48%
Rougher Mass Balance		
-9,5 + 3,35 mm	5,50	60,41%
-3,35 + 0,5mm	5,50	88,42%
-9,5+ 0,5 mm	5,50	75,42%

Figure 13-29 – Rougher Test Work Results and Metallurgical Recovery

Source: Lithium Ionic 2024

Therefore, the rougher stage of the DMS plant considered the following recoveries:

- Coarse Fraction DMS Rougher Metallurgical Recovery: 60.41%
- Fine Fraction DMS Rougher Metallurgical Recovery: 88.42%
- Composite DMS Rougher Metallurgical Recovery: 75.42%

13.3.4.1 Bandeira Project Simplified Mass Balance – Global Recovery on Rougher Stage

The metallurgical recoveries mentioned in the previous item and applied to a macro mass balance of the project indicate the mass distribution as shown in the Figure 13-30:

Material	Mass Production (tons/year)	Mass Distribuition (%)	Li_2O Grade (%)	Li_2O Production (tons/year)	Li_2O Distribution (%)
Run of Mine	1,300,000	100.0%	1.16%	15,080	100.0%
Coarse DMS Feed	407,655	31.4%	1.44%	5,862	38.9%
Fines DMS Feed	436,476	33.6%	1.55%	6,765	44.9%
DMS Total Feed	844,131	64.9%	1.50%	12,627	83.7%
Coarse DMS Concentrate	64,383	5.0%	5.50%	3,541	23.5%
Fines DMS Concentrate	108,767	8.4%	5.50%	5,982	39.7%
DMS Total Rougher Concentrate	173,149	13.3%	5.50%	9,523	63.2%
Schist	193,508	14.9%	0.35%	683	4.5%
Coarse DMS Tailings	238,966	18.4%	0.36%	850	5.6%
Fines DMS Tailings	256,916	19.8%	0.14%	366	2.4%
DMS Medium (Coarse)	104,307	8.0%	1.41%	1,471	9.8%
DMS Medium (Fines)	70,793	5.4%	0.59%	418	2.8%
Fine Material -0,5 mm	262,361	20.2%	0.67%	1,770	11.7%

Figure 13-30 – Rougher Stage Mass Balance

Source: Lithium Ionic 2024

Thus, the analysis of the test results suggests that the rougher stage of the DMS circuit can establish an overall metallurgical recovery of 63.15%.

13.3.4.2 DMS Scavenger Stage Potential Gains – Global Recovery

For the Scavenger stage, the results of the same tests adopted as references in the rougher stage (16 and 17) were considered. The Figure 13-31 presents the metallurgical recoveries and grades of the Scavenger concentrates.

Scavenger		
Testwork n°	Li_2O Grade Conc.	Metall. Rec.
test 16	0,59	53,33%
test 17	1,41	63,38%

Figure 13-31 – Scavenger Test Work Results and Metallurgical Recovery

Source: Lithium Ionic 2024

From the Scavenger concentrate, there is a possibility of increasing the overall metallurgical recovery. To achieve this, this material needs to undergo a new crushing stage to increase ore liberation, and then be re-fed into the DMS circuit. This reprocessing was not tested in the pilot plant. However, considering similar operations and the Rougher/Scavenger test work results, it is estimated that a potential gain of up to 5.71% in the overall plant metallurgical recovery could be achieved through this reprocessing. Thus, it would be possible to obtain an overall metallurgical recovery of 68.86%.

14 MINERAL RESOURCE ESTIMATES

GE21 conducted comprehensive 3D geological modelling, statistical and geostatistical studies, and grade estimation for the Lithium Ionic Bandeira Property. This estimation considered various factors, such as the quantity and distribution of available data, interpreted controls on mineralization, mineralization style, and the quality of the sampling data.

The geological modelling and estimation processes were executed utilizing Leapfrog 2023.2.1 software. The UTM Projection – Zone 23 South in SIRGAS 2000 Datum was adopted as the reference coordinate system for the database in this project.

14.1 Drilling Database

The database underwent a comprehensive visual validation, considering the interrelation of tables, identifying gaps and overlaps, and ensuring the inclusion of crucial information. Using Leapfrog Geo software, GE21 also conducted validation checks on the Collar, Survey, Assay, and Lithology tables. This stage of the work did not reveal any significant inconsistencies, as these had already been verified during the Data Verification stage.

Mineral Resource estimates were based on data derived from drill hole and trench databases, incorporating lithology logs and assay results from HQ drill core samples. The topographic surface bounds the extent of these estimates. Figure 14-1 illustrates the spatial distribution of the utilized drill holes.

The original dataset provided by Lithium Ionic encompassed data from 267 surface diamond drill holes (totalling 54,116 meters) and 31 trench channels (2,245 meters) executed by Lithium Ionic data available from 2022 until March 5th, 2024.

Until March 5th, 2024, the Bandeira database contains 8,693 assay intervals covering 8,168 meters, comprising 105 assays from trenches totalling 100 meters and 8,588 assay intervals from drill holes totalling 8,068 meters.

The assay table includes data for various elements, including Li (ppm), Li2O (%), Al (%), As (ppm), B (%), Ba (ppm), Be (ppm), Ca (%), Cd (ppm), Co (ppm), Cr (ppm), Cu (ppm), Fe (%), K (%), La (ppm), Mg (%), Mn (ppm), Mo (ppm), Nb (ppm), Ni (ppm), P (%), Pb (ppm), Sb (ppm), Sc (ppm), Sn (ppm), Sr (ppm), Ta (ppm), Ti (%), V (ppm), W (ppm), Y (ppm), and Zn (ppm). Following a thorough review of the database, the Li2O (%) data was extracted explicitly for subsequent statistical analysis, block modelling, and resource estimation.

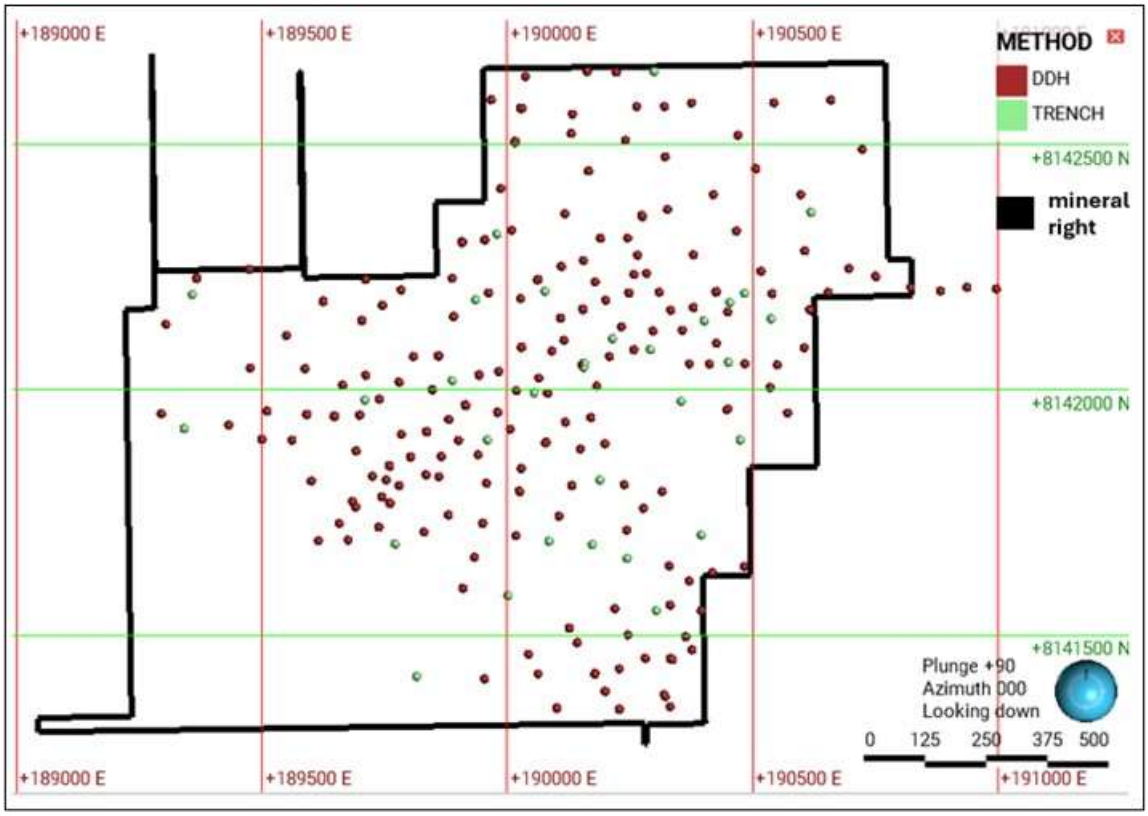

Figure 14-1 – Drillhole Location Map

Source: GE21 2024

14.2 Geological Modeling

Lithium Ionic undertook a geological interpretation encompassing all documented pegmatite intervals within the Bandeira deposits. Initially, cross-sectional interpretations were crafted utilizing traditional manual techniques and advanced cartographic software platforms such as QGIS, ArcGIS, and Leapfrog. These initial steps laid the groundwork for a robust modelling process.

The Lithium Ionic team interpreted a set of grade shell sections, with an envelope delimiting a zone with a cut-off grade of 0.3% Li2O (%) (Figure 14-2 and Figure 14-3). The resulting interpretations were developed into a series of implicit 3D models aligned with two prevailing strike directions: 235° and 140° (Figure 14-4 and Figure 14-5).

Lithium Ionic also conducted weathering modelling, basing the analysis on the descriptions provided in the logs (Figure 14-6).

The Qualified Person thinks the geological interpretations and modelling suit a Mineral Resource Estimation study. Quality assurance procedures follow the industry's best practices, and the model honours the mineralized pegmatite intervals and has adequate continuity of the modelled bodies.

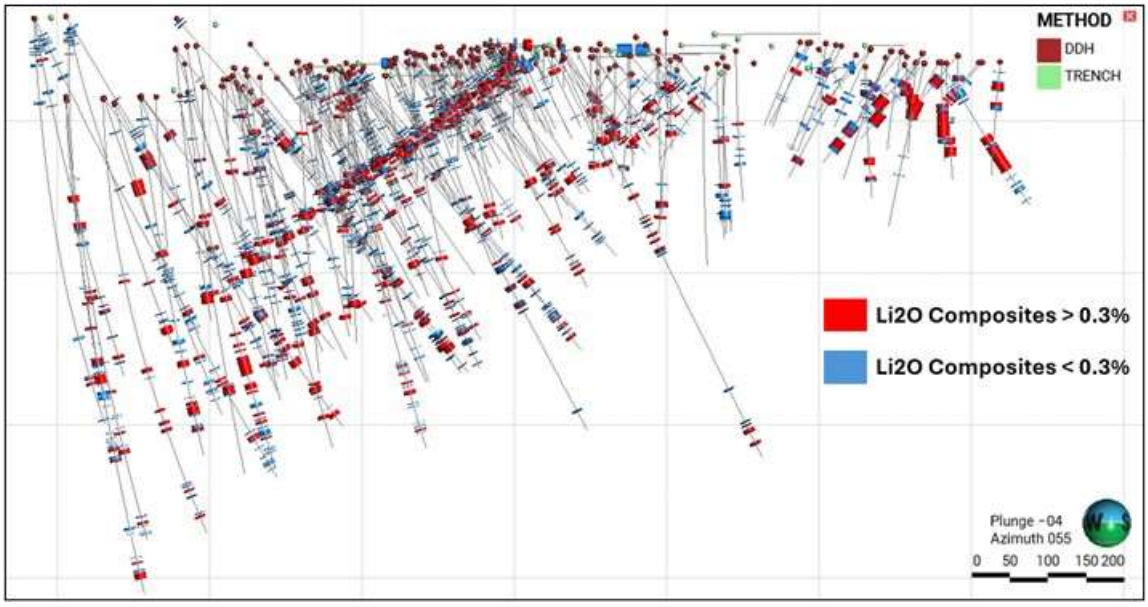

Figure 14-2 – Assay Composites Classified by Li2O > 0.3% Grade Limit in Pegmatites Veins, Oblique view NW-SE

Source: GE21 2024

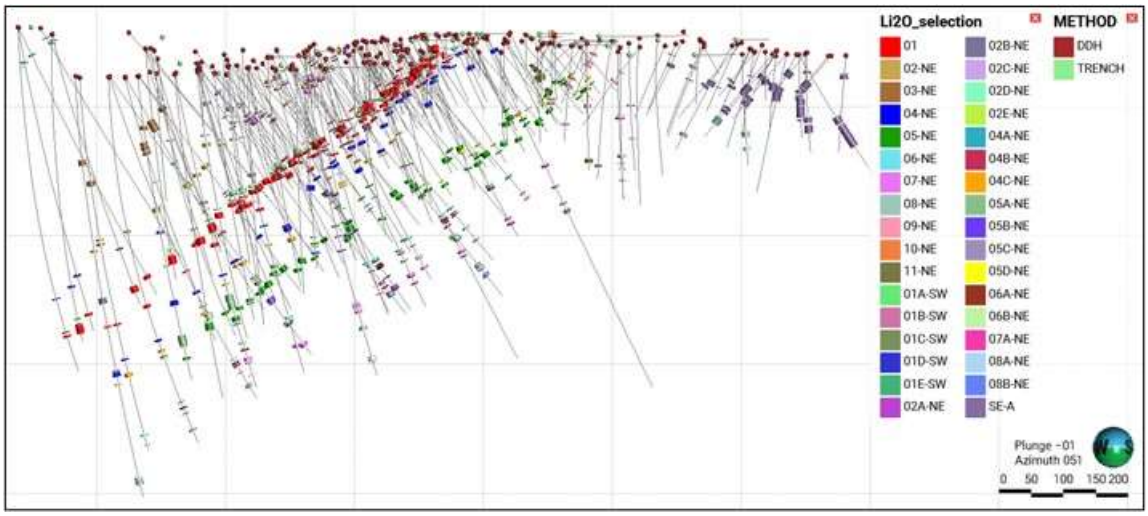

Figure 14-3 – Assays Composites within the Li2O > 0.3% Limit in Pegmatite Veins Grouped by Separated Lenses and Dykes

Source: GE21 2024

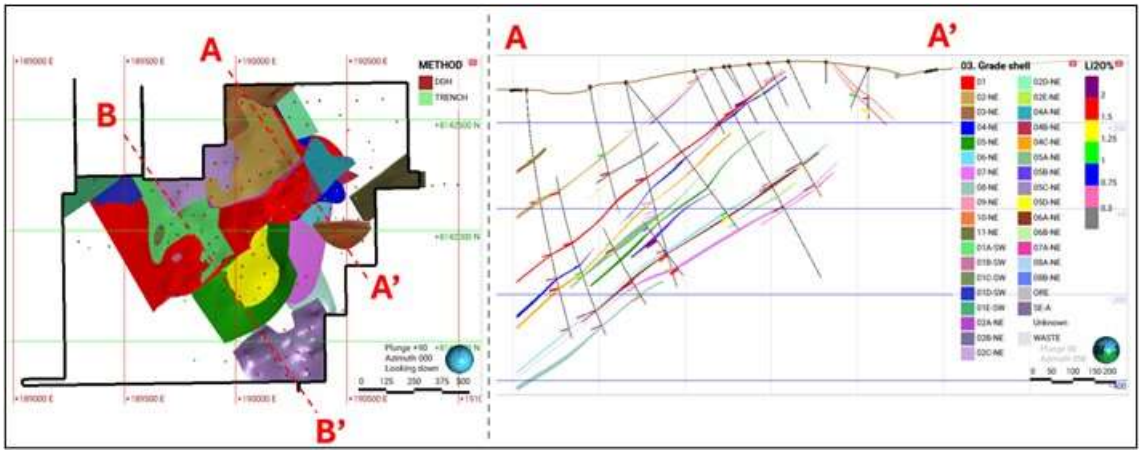

Figure 14-4 – Spodumene Grade Shells Modelled with Assays Composites Li2O > 0.3 %

Legend: horizontal view plan (left side) and section view (right view plan).
Source: GE21 2024

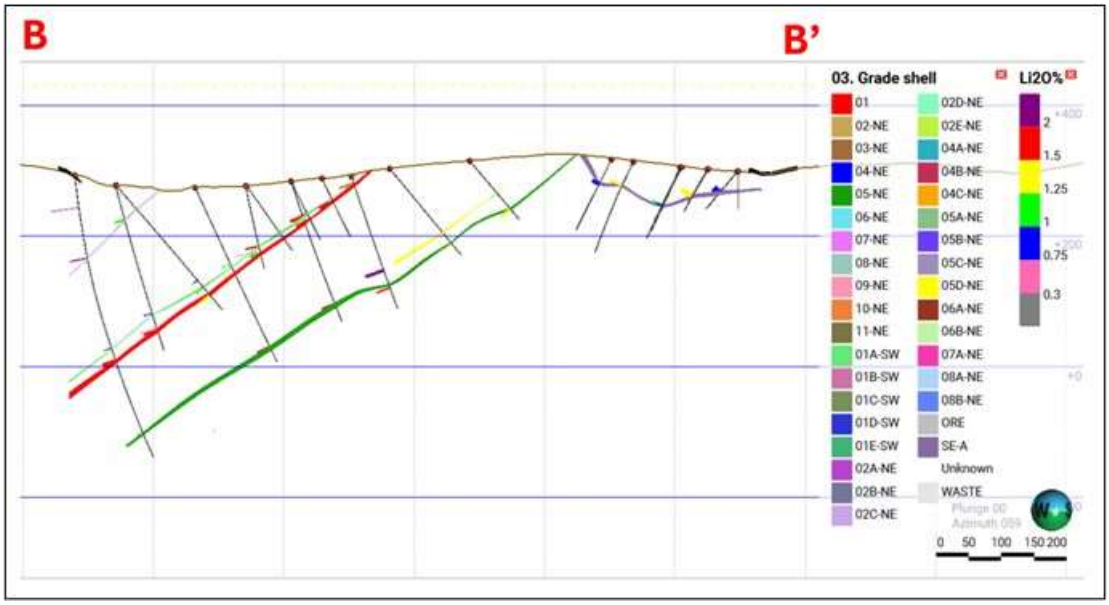

Figure 14-5 – Spodumene Grades Shells Model – Assays Composites Li2O > 0.3 % – Section View

Source: GE21 2024

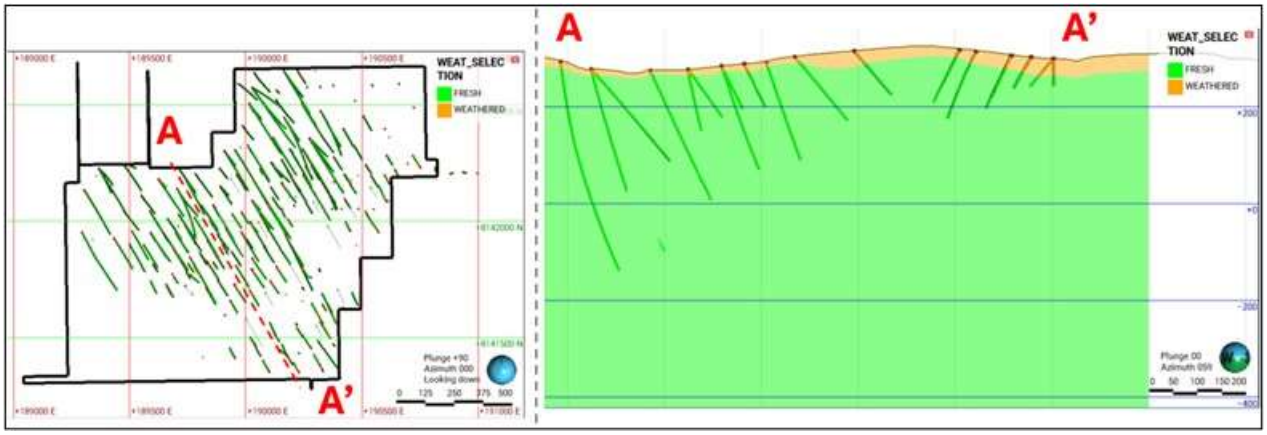

Figure 14-6 – Weathering Zone Model

Legend: horizontal view plan (left side) and section view (right view plan).
Source: GE21 2024

14.3 Geostatistical Structural Analysis

14.3.1 Regularization of Samples

The analysis of the sample support showed that more than 95% of the drilling samples have a length equal to 1 meter. GE21 regularly analyzed samples in 1 meter for complementary studies of statistics and geostatistics (Figure 14-7).

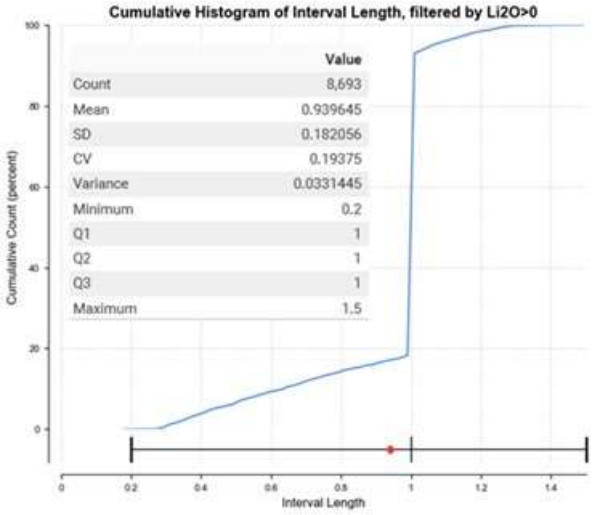

Figure 14-7 – Bandeira Assays Interval Length Statistics

Source: GE21 2024

14.3.2 Exploratory Data Analysis (EDA)

Statistical analysis on composited drilling samples was performed for the Li2O% variable inside each modelled typology. Figure 14-8 and Table 14-1 shows the statistics for pegmatite veins.

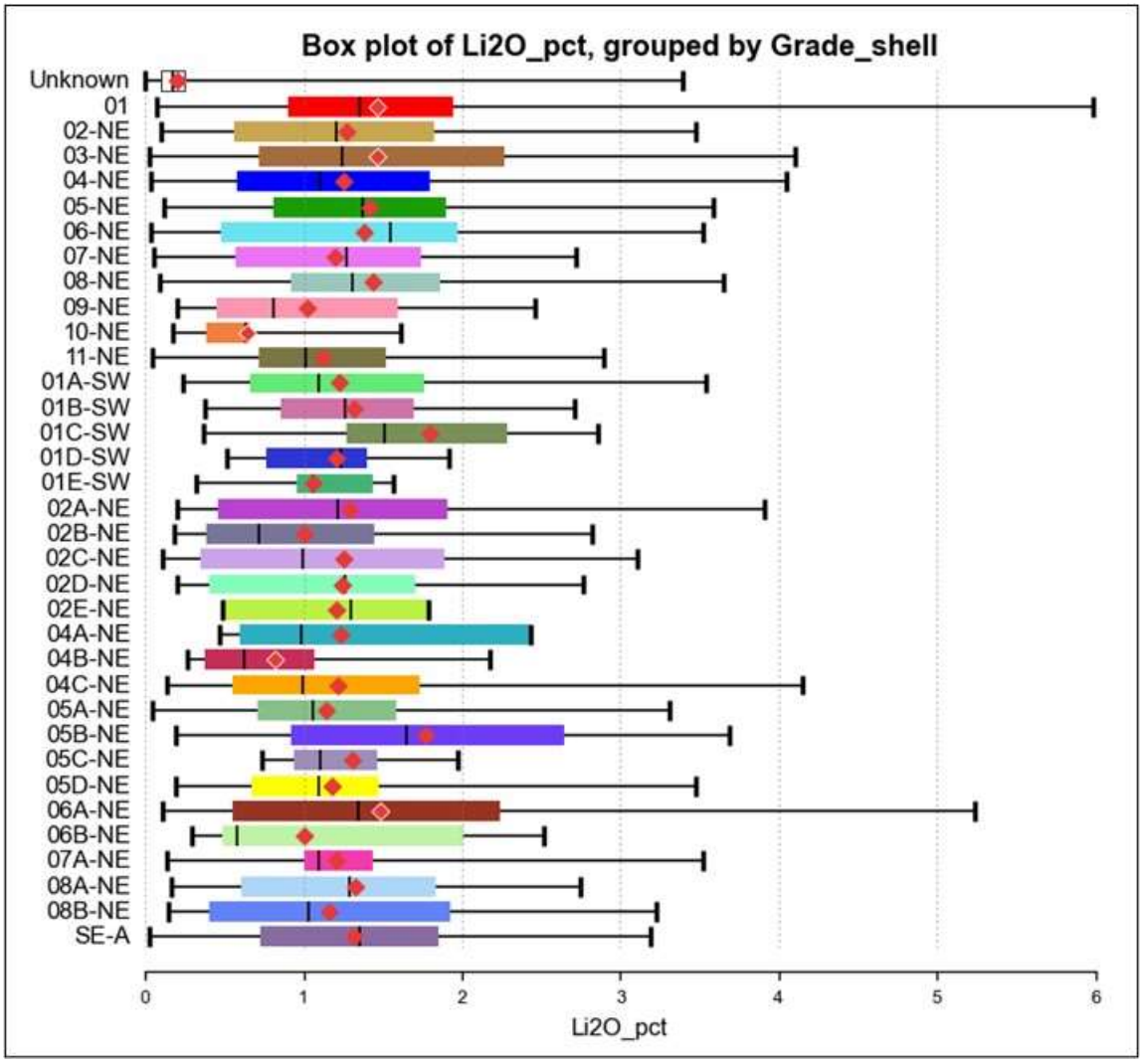

Figure 14-8 – Li2O (%) Spodumene Pegmatites Veins Model Statistics

Legend: boxplots (left side). Source: GE21 2024

Table 14-1 – Li2O (%) Spodumene Pegmatites Veins Model Statistics – Statistics Table

Source: GE21 2024

Li2O%											
Domain	**Count**	**Length**	**Mean**	**Standard deviation**	**Coefficient of variation**	**Variance**	**Minimum**	**Lower quartile**	**Median**	**Upper quartile**	**Maximum**
Total	8901	8870.23	0.52	0.68	1.30	0.46	0.00	0.12	0.22	0.57	5.99
1	625	611.79	1.46	0.77	0.53	0.60	0.07	0.90	1.36	1.94	5.99
02-NE	110	109.40	1.27	0.80	0.63	0.64	0.10	0.56	1.20	1.82	3.48
03-NE	69	69.19	1.47	1.03	0.70	1.05	0.02	0.71	1.25	2.27	4.10
04-NE	176	175.02	1.25	0.80	0.64	0.63	0.04	0.58	1.10	1.80	4.05
05-NE	309	304.55	1.42	0.75	0.53	0.57	0.12	0.81	1.38	1.89	3.58
06-NE	45	43.78	1.38	0.94	0.68	0.89	0.04	0.48	1.55	1.98	3.52
07-NE	85	84.74	1.20	0.70	0.58	0.48	0.06	0.57	1.27	1.74	2.71
08-NE	78	77.67	1.43	0.74	0.51	0.54	0.09	0.92	1.31	1.86	3.65
09-NE	25	24.55	1.02	0.67	0.66	0.45	0.20	0.45	0.81	1.60	2.46
10-NE	11	10.57	0.64	0.40	0.62	0.16	0.17	0.38	0.63	0.66	1.61
11-NE	55	54.54	1.13	0.59	0.52	0.34	0.04	0.72	1.01	1.52	2.90
01A-SW	110	105.74	1.22	0.71	0.58	0.50	0.24	0.66	1.10	1.76	3.54
01B-SW	24	22.90	1.32	0.63	0.48	0.40	0.38	0.86	1.26	1.70	2.71
01C-SW	10	9.17	1.80	0.73	0.40	0.53	0.37	1.27	1.51	2.29	2.86
01D-SW	10	10.00	1.21	0.46	0.38	0.21	0.52	0.76	1.23	1.40	1.91
01E-SW	10	9.54	1.06	0.45	0.42	0.20	0.32	0.95	1.06	1.44	1.56
02A-NE	58	55.57	1.29	0.84	0.65	0.70	0.21	0.46	1.22	1.91	3.91
02B-NE	26	26.42	1.00	0.75	0.75	0.56	0.18	0.39	0.71	1.45	2.82
02C-NE	26	25.39	1.26	0.93	0.74	0.87	0.11	0.35	0.99	1.89	3.10
02D-NE	11	10.61	1.24	0.82	0.66	0.67	0.20	0.40	1.26	1.71	2.76
02E-NE	4	4.02	1.21	0.57	0.47	0.33	0.48	0.48	1.30	1.78	1.78
04A-NE	5	5.13	1.24	0.86	0.69	0.74	0.47	0.60	0.98	2.43	2.43
04B-NE	10	9.97	0.82	0.62	0.76	0.39	0.27	0.38	0.62	1.07	2.17
04C-NE	60	61.02	1.21	0.80	0.66	0.64	0.14	0.56	1.00	1.73	4.15
05A-NE	79	79.38	1.14	0.65	0.57	0.42	0.05	0.71	1.06	1.58	3.31
05B-NE	28	27.42	1.77	1.00	0.56	0.99	0.19	0.92	1.65	2.65	3.69

Li2O%											
Domain	**Count**	**Length**	**Mean**	**Standard deviation**	**Coefficient of variation**	**Variance**	**Minimum**	**Lower quartile**	**Median**	**Upper quartile**	**Maximum**
05C-NE	5	4.05	1.31	0.51	0.39	0.26	0.74	0.94	1.10	1.47	1.97
05D-NE	30	28.52	1.18	0.76	0.64	0.58	0.19	0.68	1.10	1.47	3.47
06A-NE	45	46.24	1.48	1.07	0.72	1.14	0.10	0.55	1.34	2.24	5.23
06B-NE	17	17.18	1.01	0.80	0.80	0.64	0.29	0.49	0.58	2.01	2.51
07A-NE	14	13.46	1.20	0.81	0.67	0.66	0.14	1.00	1.10	1.44	3.52
08A-NE	28	27.19	1.32	0.74	0.56	0.55	0.17	0.60	1.29	1.83	2.75
08B-NE	13	12.03	1.16	0.95	0.82	0.91	0.15	0.40	1.03	1.92	3.23
SE-A	317	316.28	1.32	0.70	0.53	0.50	0.03	0.73	1.35	1.85	3.19
Waste	6373	6377.22	0.20	0.20	0.99	0.04	0.00	0.10	0.17	0.25	3.39

14.3.3 Variographic Analysis

The structural analysis of the domains was conducted to determine the variographic parameters, which are essential for determining the spatial continuity model of the grade variables and for the grade estimate.

Variograms were generated explicitly for Li2O% within the spodumene veins suite. This approach considered the geological similarity among them, enhancing the robustness of the variograms. Two distinct sets of veins were considered:

- NW Veins Suite.
- SE Veins Suite.

The variographic analysis was executed using Leapfrog Edge software. Figure 14-9 to Figure 14-12 show the variograms for the Li2O% variable for each set of vein domains. Additionally, Table 14-2 presents the variographic parameters obtained from all conducted analyses. These parameters were applied in the process of grade estimation.

Table 14-2 – Variographic Parameters

Variogram Name	Variance	Nugget	Normalized Nugget	Structures	Sill	Normalized sill	Structure	Major	Semi-major	Minor	Dip	Dip Azi.	Pitch
NW	0.60	0.13	0.22	Structure 1	0.21	0.35	Spherical	82	17	1.6	37	323	0
				Structure 2	0.26	0.43	Spherical	95	68	2.7	37	323	0
SE	0.50	0.06	0.13	Structure 1	0.62	0.19	Spherical	35	14	1.8	20	128	28
				Structure 2	0.25	0.48	Spherical	56	50	3.8	20	128	28

Source: GE21 2024

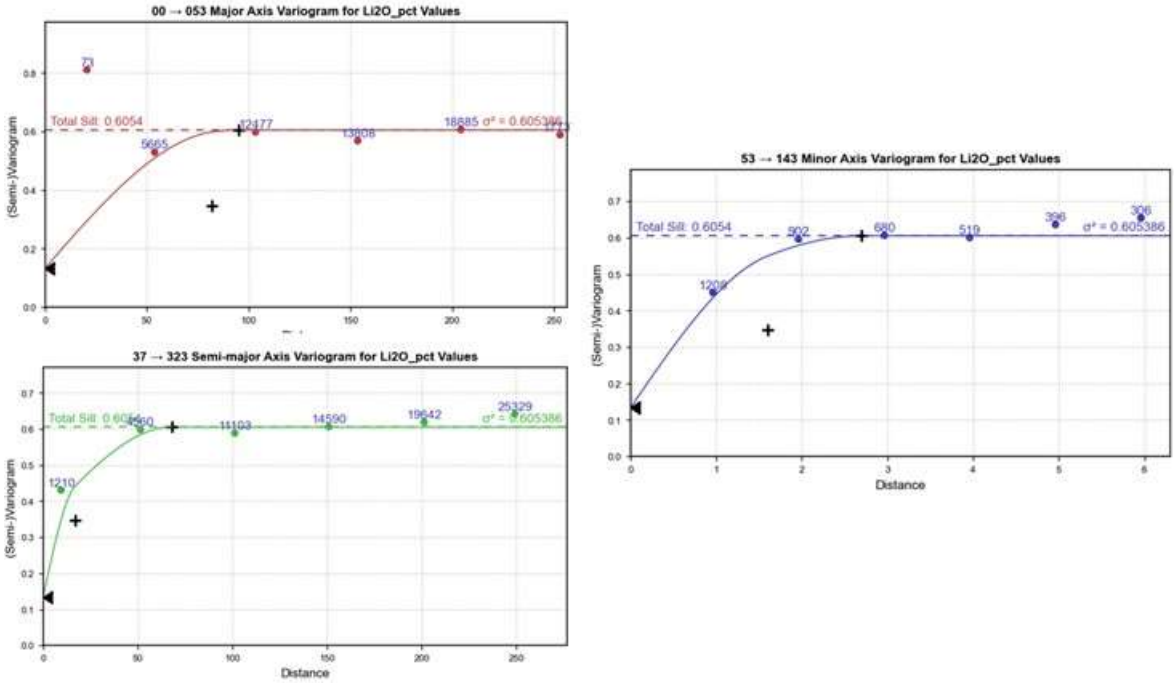

Figure 14-9 – Variographic Model – Domains Set NW

Source: GE21 2024

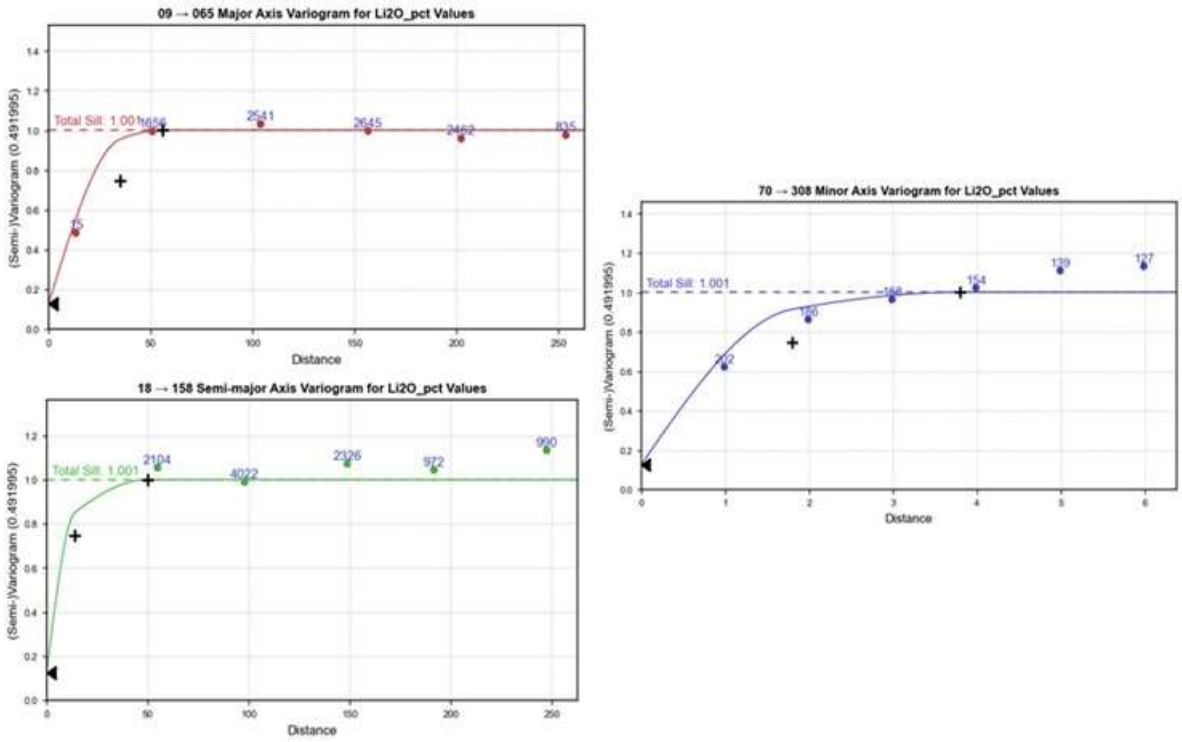

Figure 14-10 – Variographic Model – Domains Set SE

Source: GE21 2024

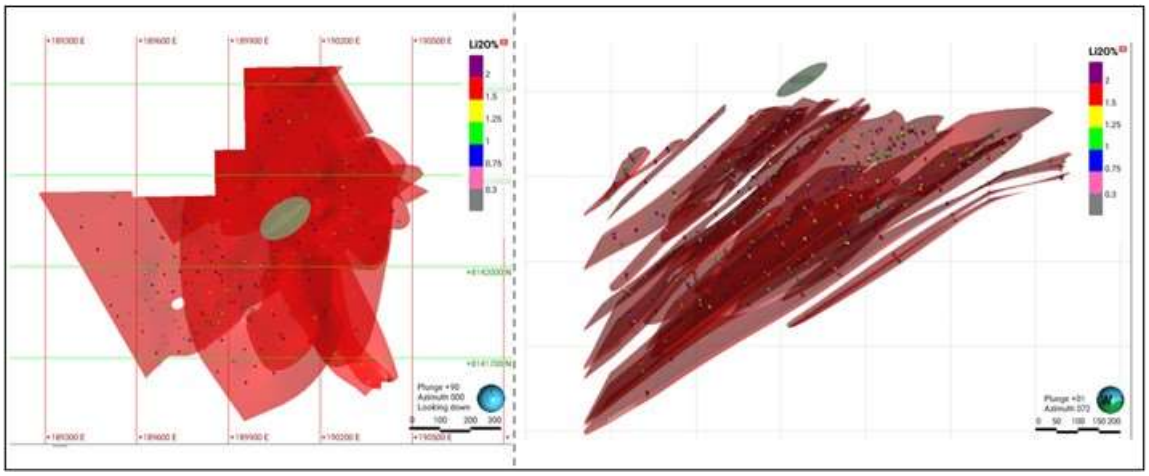

Figure 14-11 – Variographic Ellipsoid – Domains Set NW

Source: GE21 2024

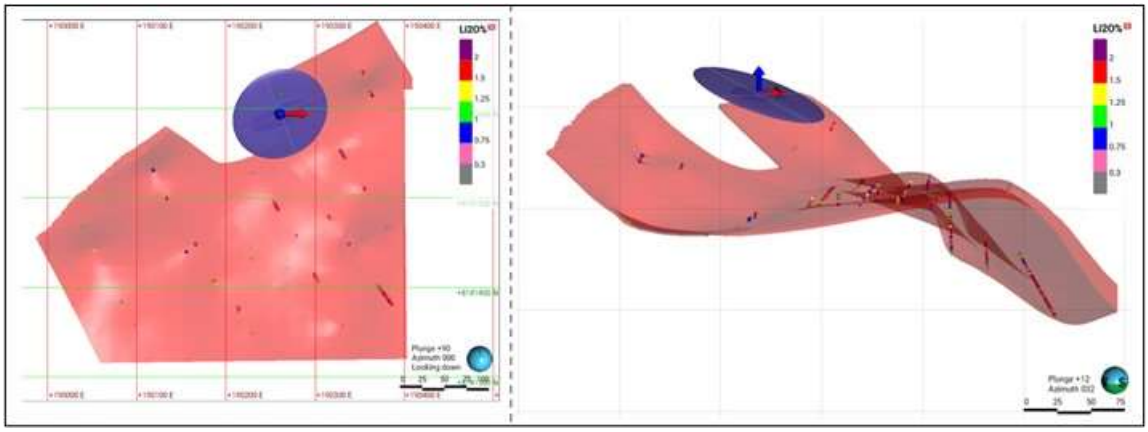

Figure 14-12 – Variographic Ellipsoid – Domains Set SE

Source: GE21 2024

14.4 Block Model

A block model was built to carry out the grade estimation. The model's dimensions (12m x 12m x 4m) were defined based on the minimum spacing of the drilling grid. The sub-blocks model was set in a 1,5m x 1,5m x 2m size to ensure the geometric adherence of the modelled bodies.

The dimensions of the block models and the attributes are shown in Table 14-3 and Table 14-4.

Table 14-3 – Block Model Dimensions

Source: GE21 2024

	X	Y	Z
Minimum Coordinates (Center) (m)	**189,206**	**8,141,277**	**-467**
Maximum Coordinates (Center) (m)	190,934	8,142,705	409
Minimum Coordinates (Corner) (m)	189,200	8,141,271	-469
Maximum Coordinates (Corner) (m)	190,940	8,142,711	411
Number of nodes	145	120	220
Block size (m)	12	12	4
Sub-Block	1,5	1,5	2
azimuth: 0 degrees (rotate clockwise around the Z axis when looking down) dip: 0 degrees (then turn around the X' axis down from the horizontal plane) pitch: 0 degrees (then rotate clockwise around the Z'' axis when looking down)			

Table 14-4 – Block Model Variables Summary

Source: GE21 2024

Attribute Name	Type	Deals	Background	Description
GM_weat	Character	-		Weathering Model
GM_ grad	Character	-		Spodumene Veins Model
Class	Character	-		Mineral Classification
Density	Real	4	-99	Density Values
GM_miner	Character	-		Bandeira Mineral Right
Li2O_ok	Real	4	-99	Li2O OK estimation

14.5 Grade Estimation

The Ordinary Kriging (OK) was carried out in the Leapfrog Edge software and was used on the Li2O (%) variable estimation based on the structural analysis results described in this work.

Each mineralized vein was estimated independently, using a hard boundary strategy to ensure that samples from one domain did not influence neighbouring domains. The variograms were initially modelled considering the structural continuity across the entire set of domains, followed by an adjustment for honouring the specific behaviour for each domain. Table 14-5 shows the main parameters of the Kriging strategy applied in the grade estimation.

Table 14-5 – Kriging Parameters

Source: GE21 2024

Type	Steps	Ellipsoid Ranges			Number of Samples	
		Maximum	Intermediate	Minimum	Minimum	Maximum
Li2O	Step 1	50	50	4	6	16
	Step 2	100	100	8	6	16
	Step 3	150	150	16	4	16
	Step 4	1500	1500	1600	4	16

Notes:
1. Dynamic Variable Orientation for Estimation was applied to each domain in Leapfrog software.
2. Moving neighbourhood from ellipsoid, Dip = 37° Dip Azimuth = 323° Pitch = 00° (NW Veins).
3. Moving neighbourhood from ellipsoid, Dip = 20° Dip Azimuth = 128° Pitch = 28° (SE Veins).
4. Maximum number of samples per Drill = 2.

14.6 Estimation Validation

The QP carried out the validation of the estimate through visual verification and by the Global and Local bias verification. Global and Local bias checks used The Nearest Neighbour as the comparison estimate. NN-Checks plots, Figure 14-13 and Figure 14-14 show the results for global bias analysis of the estimated Li2O% and density variables. It allowed verification of the expected estimation smoothing by Ordinary Kriging within the acceptance limits. The comparison showed that Ordinary Kriging globally respected the average grades, and the global bias in the estimated grades is within the limits of acceptance.

The local bias assessment by the Swath-Plot method aims to analyze the occurrence of local bias by comparing the average grades for the model through Ordinary Kriging and the Nearest Neighbour method in swath coordinates intervals graphs along the X, Y, and Z axes. Figure 14-15 and Figure 14-16 show the validation results of the Li2O% and Density swath plots.

The results from the grade estimate validation by Ordinary Kriging show that the smoothing effect or local and global bias are inside acceptance limits for mineral resource estimation.

14.7 Density

The density (g/cm³) in the spodumene pegmatites was estimated using Inverse Distance Weighting (IDW). How parameters were utilized for exponent 2, with minimum samples one and maximum samples 28.

The schists density was defined as the mean of the 4,830 samples from the Lithium Ionic database. The weathered zone doesn't have measurements, and GE21 has adopted the value 1.8 g/cm³ for this domain, a common value used by other companies in the Jequitinhonha Valley region. GE21 recommends that additional density tests be carried out in weathered zones.

Table 14-6 shows the average IDW densities of each estimated pegmatite domain and the adopted densities of the host rocks.

Table 14-6 – Density Values

Source: GE21 2024

Spodumene Domains	Density
	g/cm³
01	2.68
02-NE	2.66
03-NE	2.68
04-NE	2.66
05-NE	2.69
06-NE	2.69
07-NE	2.71
08-NE	2.71
09-NE	2.48
10-NE	2.44
11-NE	2.46
01A-SW	2.69
01B-SW	2.68
01C-SW	2.67
01D-SW	2.71
01E-SW	2.34
02A-NE	2.56
02B-NE	2.70
02C-NE	2.65
02D-NE	2.64
02E-NE	2.71
04A-NE	2.53
04B-NE	2.49
04C-NE	2.68
05A-NE	2.66
05B-NE	2.69
05C-NE	2.69
05D-NE	2.72
06A-NE	2.70
06B-NE	2.69
07A-NE	2.72
08A-NE	2.74
08B-NE	2.74
SE-A	2.63
Mean	**2.68**

Domains	Density
	g/cm³
Shists Rocks	2.8
Weathered Zone	1.8

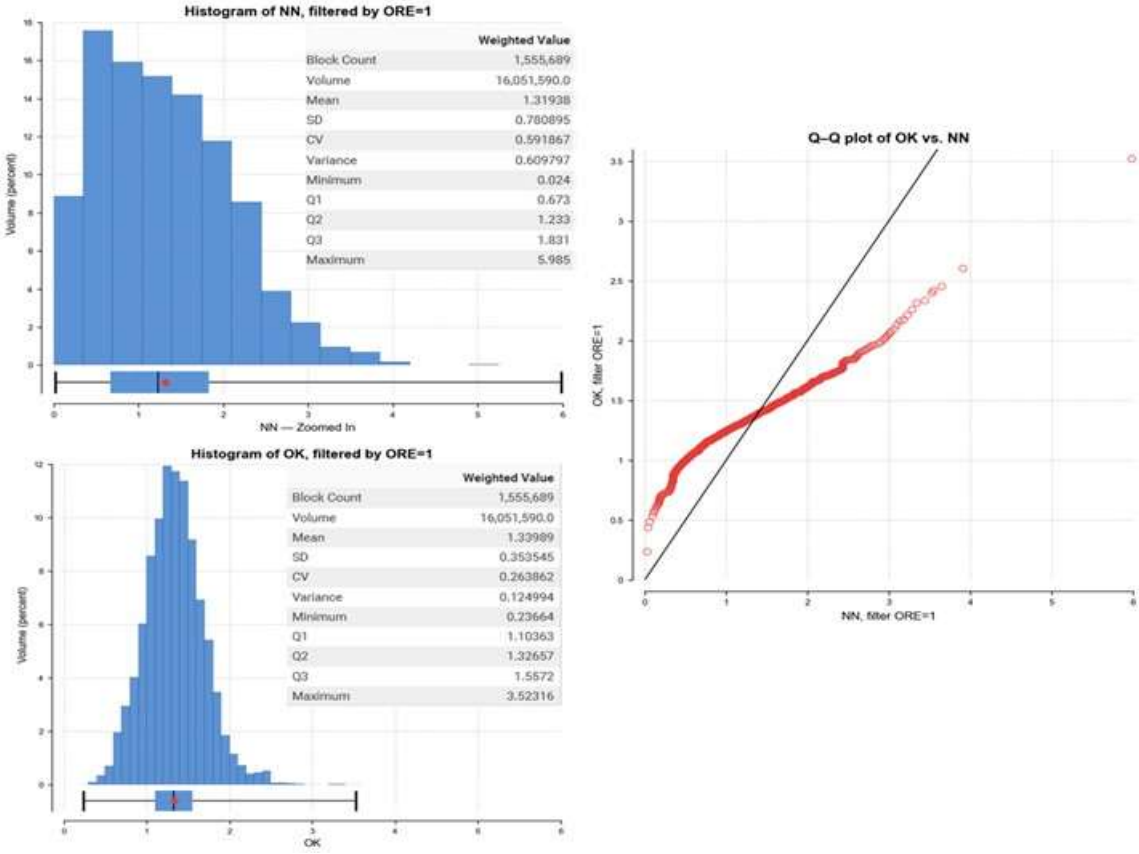

Figure 14-13 – Estimation Validation – NN Check to Li2O

Source: GE21 2024

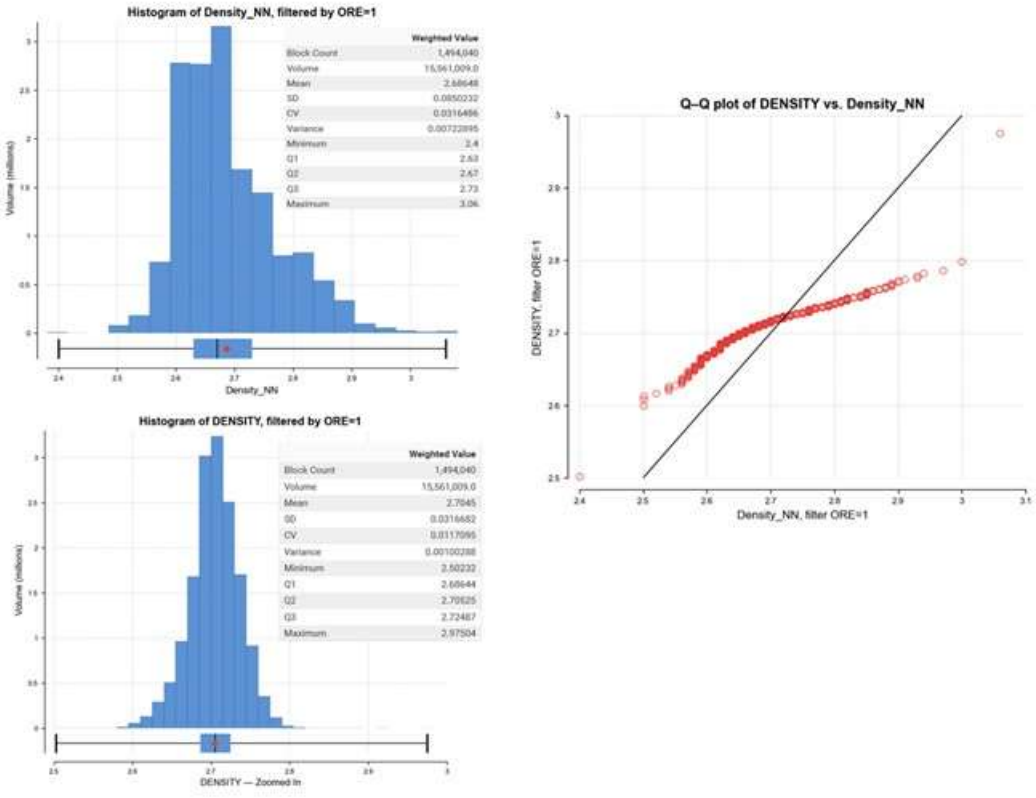

Figure 14-14 – Estimation Validation – NN Check to Density

Source: GE21 2024

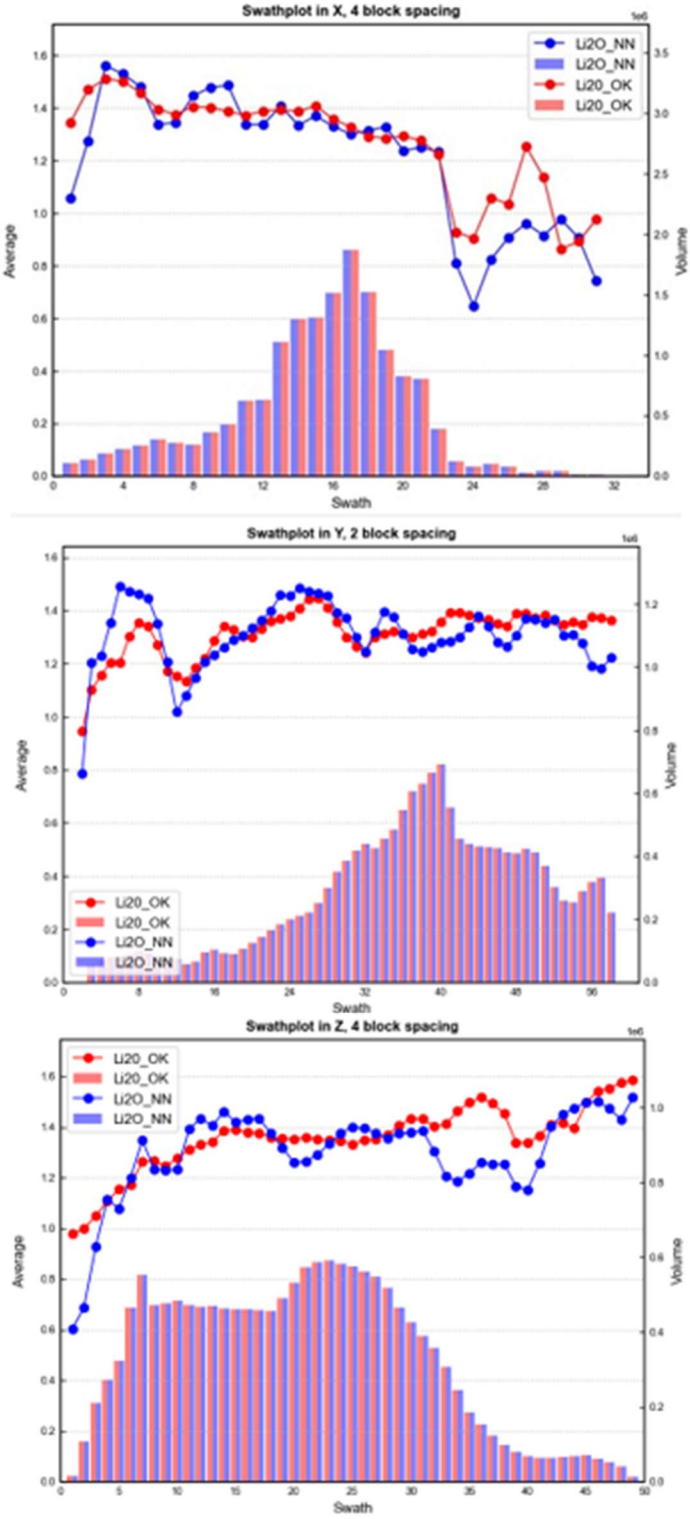

Figure 14-15 – Estimation Validation – Swath Plot Li2O

Source: GE21 2024

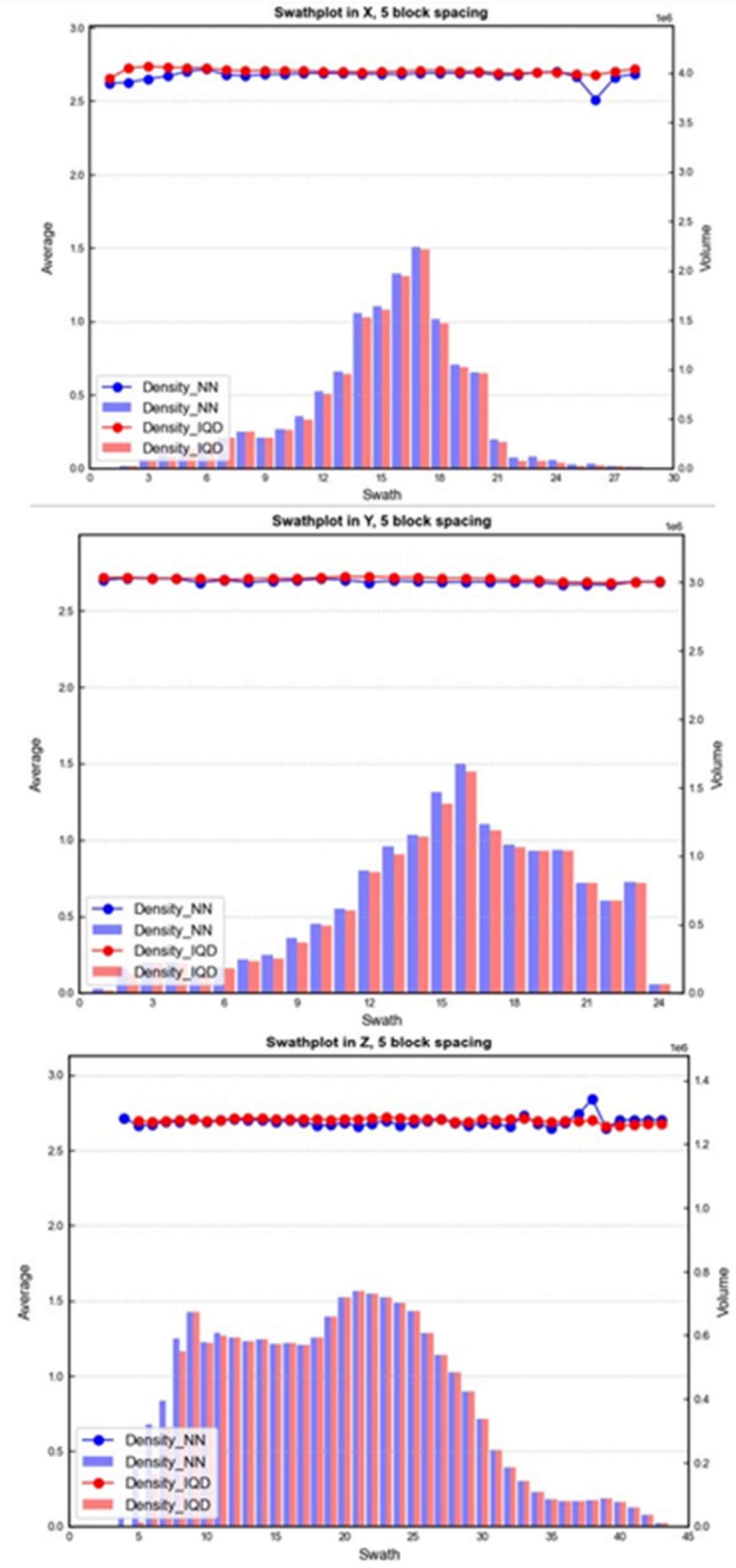

Figure 14-16 – Estimation Validation – Swath Plot Density

Source: GE21 2024

14.8 Classification of Mineral Resources

The Mineral Resource was classified per CIM Standards and CIM Guidelines, utilizing geostatistical and classical methods and economically and mining-appropriate parameters relevant to the deposit type.

The Resource definitions by CIM are transcribed below:

- A Mineral Resource is a concentration or occurrence of diamonds, a natural solid inorganic material or natural fossilized solid organic material, including base and precious metals, coal and industrial minerals in the earth's crust or the earth's crust in such form and quantity and of such grade or quality that allows reasonable prospects of economic extraction. The location, quantity, level, geological characteristics, and continuity of a Mineral Resource are known, estimated, or interpreted from specific geological evidence and knowledge.
- An "Inferred Mineral Resource" is that part of a Mineral Resource for which the quantity and level or quality can be estimated based on geological evidence and limited sampling and reasonably presumed but not verified geological and grade continuity. The estimation is based on limited information and sampling collected using appropriate techniques from locations such as outcrops, trenches, wells, and drill holes.
- An "Indicated Mineral Resource" is that part of a Mineral Resource for which quantity, grade or quality, densities, shape and physical characteristics can be estimated with a level of confidence sufficient to allow the appropriate application of technical and economic parameters to support mine planning and assessment of the deposit's economic viability. The estimation is based on thorough and reliable exploration and testing information gathered using appropriate techniques from locations such as outcrops, trenches, wells, works, and drill holes spaced far enough apart for geological and level continuity to be reasonably assumed.
- A "Measured Mineral Resource" is that part of a Mineral Resource for which quantity, level or quality, densities, shape, and physical characteristics are so well established that they can be estimated with sufficient confidence to allow the appropriate application of technical and economic parameters, to support production planning and assessment of the deposit's economic viability. The estimation is based on thorough and reliable exploration, sampling, and analysis of information gathered using appropriate techniques from locations such as outcrops, trenches, wells, works, and drill holes spaced far enough apart to confirm geological and level continuity.

The classification boundaries made by GE21 for the Measured, Indicated, and Inferred categories were established through an approach that considered a comprehensive set of factors.

These factors included the sampling procedure analysis, the sample grid spacing, the survey methodology, and the quality of assay data.

Additionally, drilling spacing and the progressive expansion of the search radius during grade estimation stages were also considered, as well as the average anisotropic distance of the samples and the continuity of pegmatite mineralization.

This multi-faceted approach ensured the robustness and accuracy of the classification process.

- The Measured Mineral Resource classification referenced the 50 meters of the Average Euclidean distance to sample (AvgD) used in ordinary kriging estimation with a minimum of seven composites in at least three different drill holes.
- The Indicated Mineral Resource classification referenced the 100 meters of the Average Euclidean distance to sample (AvgD) used in ordinary kriging with a minimum of seven composites in at least three different drill holes.
- The Inferred Mineral Resource classification is all remaining estimated blocks.
- The total mineral resources were limited to the boundaries of the mining rights.

The resource classification was supported by a grade shell representing the underground mining appliance (Reasonable Prospect for Eventual Economic Extraction – RPEEE), performed through a restricted wireframe based on a grade shell elaborated considering a cut-off of 0.5% Li2O. this value is commonly adopted for SRP-type pegmatites in the Lithium Valley province.

The Bandeira Mineral Resources Estimates results are shown in Table 14-7, Figure 14-17 and Figure 14-18.

Table 14-7 – Bandeira Mineral Resource Estimates (base case cut-off grade of 0.5 % Li2O)

Source: GE21 2024

Deposit / Cut-Off Grade	Category	Resource (Mt)	Grade (% Li2O)	Contained LCE (kt)
Bandeira *(0.5% cut-off)*	Measured	3.32	1.38	113.1
	Indicated	20.36	1.33	669.6
	Measured + Indicated	23.68	1.34	783.0
	Inferred	18.25	1.37	618.4

Notes:
1. The spodumene pegmatite domains were modelled using composites with Li2O grades greater than 0.3%.
2. The mineral resource estimates were prepared following the CIM Standards and the CIM Guidelines, using geostatistical and/or classical methods, plus economic and mining parameters appropriate to the deposit.
3. Mineral Resources are not ore reserves or demonstrably economically recoverable.
4. Grades reported using dry density.
5. The effective date of the MRE is March 05, 2024.
6. The QP responsible for the MRE is the geologist Carlos Silva (MAIG #7868).
7. The MRE numbers provided have been rounded to the estimated relative precision. Values cannot be added due to rounding.
8. The MRE is delimited by Lithium Ionic Bandeira Target Claims (ANM).
9. The MRE was estimated using ordinary kriging in 12m x 12m x 4m blocks.
10. The MRE report table was produced in Leapfrog Geo software.
11. The reported MRE only contains fresh rock domains.
12. The MRE was restricted by RPEEE with grade shell using 0.5% Li2O cut-off.

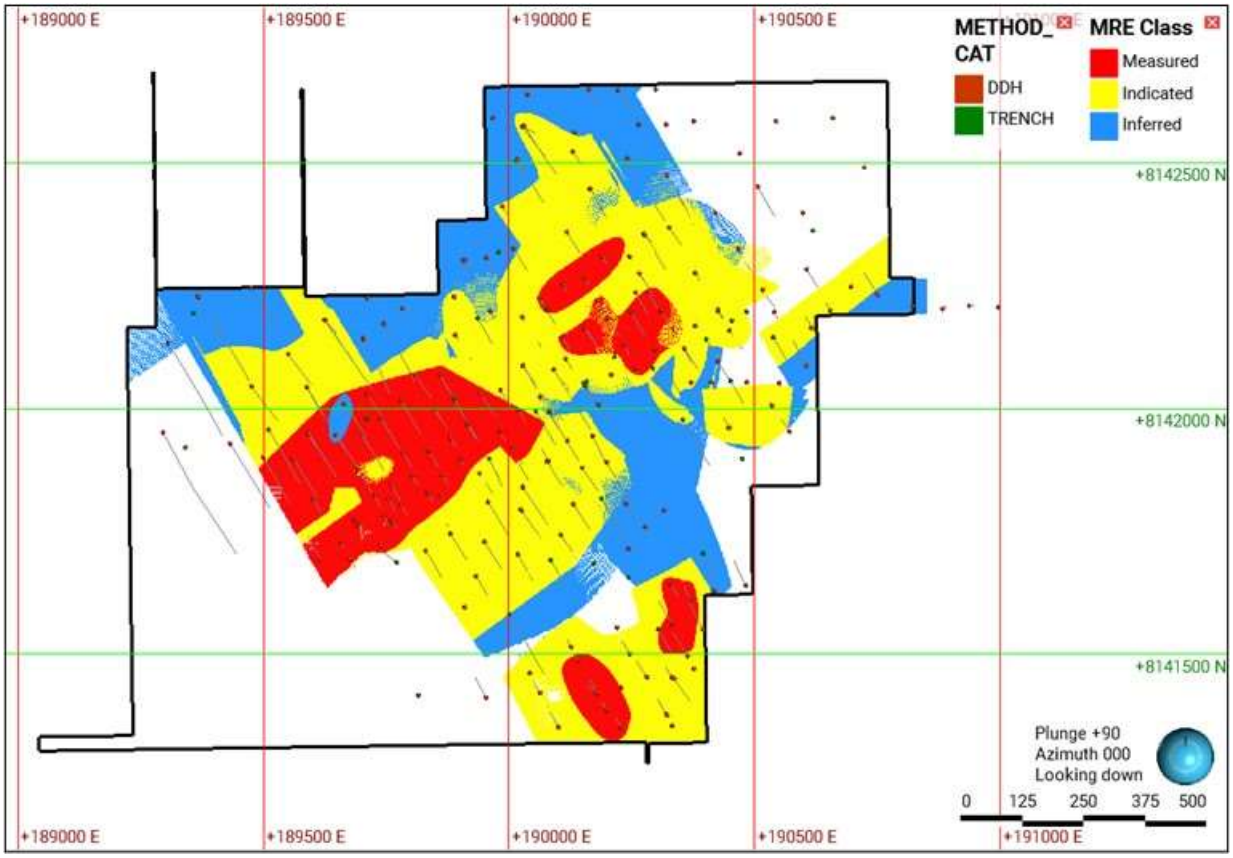

Figure 14-17 – Resource Classification with RPE3 – Horizontal View

Source: GE21 2024

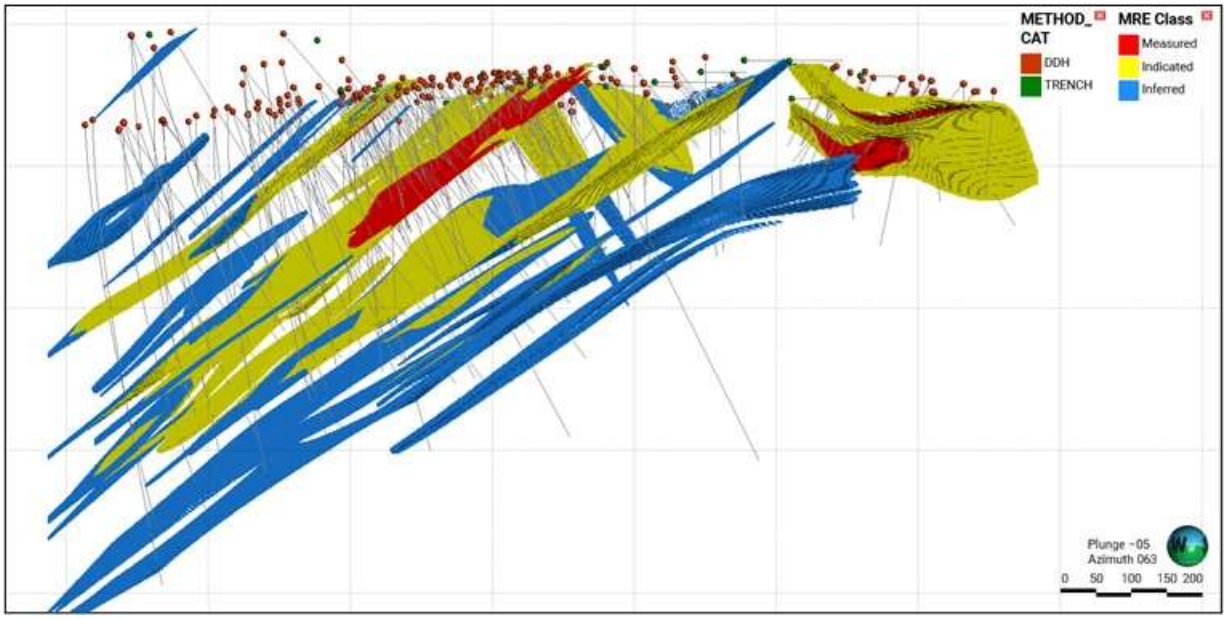

Figure 14-18 – Resource Classification with RPEE – Oblique view.

Source: GE21 2024

15 MINERAL RESERVES ESTIMATES

Not applicable.

16 MINING METHODS

Not applicable.

17 RECORVERY METHODS

Not applicable.

18 PROJECT INFRAESTRUCTURE

Not applicable.

19 MARKET STUDIES AND CONTRACTS

Not applicable.

20 ENVIRONMENTAL STUDIES, PERMITTING, AND SOCIAL OR COMMUNITY IMPACTS

Not applicable.

21 CAPITAL AND OPERATING COSTS

Not applicable.

22 ECONOMIC ANALYSIS

Not applicable.

23 ADJACENT PROPERTIES

The Araçuaí Pegmatitic District, situated in the northeastern sector of Brazil's Eastern Pegmatitic Province, encompasses the region bounded by Salinas, Araçuaí, and Capelinha to the west, and Itinga and Caraí to the east. In this district, Brazil's is a lithium producer, including lithium-bearing pegmatites, gemological pegmatites, and pegmatites that produce ceramic minerals and ornamental rocks. Many of these have been exploited by mineral exploration and mining companies, as well as by artisanal miners, for over a century.

The lithium-bearing pegmatites in the Araçuaí Pegmatitic District include complex zoned bodies with highly diverse mineralogy type, as well as simply to complexly zoned pegmatites rich in disseminated spodumene within a quartz-feldspar matrix that is rich in albite and relatively poor in accessory minerals. Current lithium exploration focuses on spodumene, which typically makes up deposits that can exhibit ore mass volumes of 5 to 30 million tons, with economic grades of lithium oxide.

The Araçuaí Pegmatitic District, particularly the Itinga Pegmatitic Field, is of extreme importance for prospecting projects, considering its production history and its geological and metallogenetic characteristics in this district, in terms of history and prospects for spodumene production, are the Brazilian Lithium Company (CBL) and the Sigma Lithium Corporation (successor to Arqueana de Minérios e Metais Ltda.).

The Bandeira lithium ore deposit, registered under ANM 832439/2009, is located adjacent to the mineralized areas of spodumene-bearing pegmatites, which include the Cachoeira deposits of the Companhia Brasileira de Lítio (CBL) and the Barreiro, Murial, and Lavra do Meio deposits of Sigma Lithium Corporation.

Figure 23-1 shows the locations of the mineral rights of CBL and Sigma Lithium surrounding the mining right 832.439/2009.

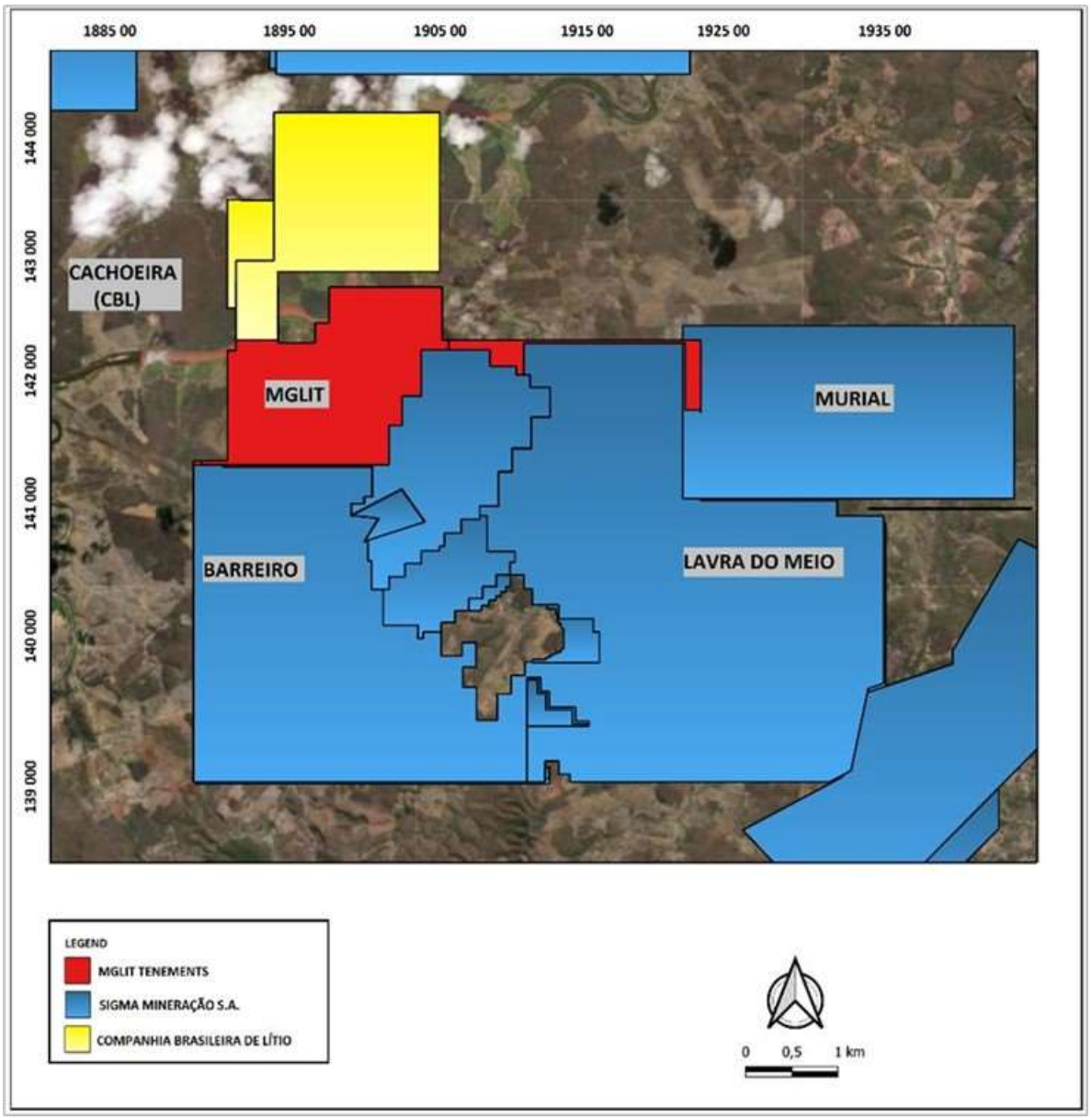

Figure 23-1 – Mining Right

Legend: MGLIT 832.439/2009 (red), surrounding areas CBL (yellow), and Sigma (blue).
Source: GE21 2024

24 OTHER RELEVANT DATA AND INFORMATION

There is no relevant information which affect the opinions offered in this Report.

25 INTERPRETATION AND CONCLUSIONS

Mineral Resources were estimated and limited to the areas outlined using the Mining Rights polygonal that comprise the Bandeira Property and the Reasonable Prospect for Eventual Economic Extraction - RPEEE.

The original dataset provided by Lithium Ionic encompassed data from 267 surface diamond drill holes (totalling 54,116 meters) executed by Lithium Ionic data available from 2022 until March 5th, 2024. This Bandeira database contains 8,693 assay intervals covering 8,168 meters.

A set of solid-grade shells for estimation domains was created using a 0.3% Li2O (%) threshold. These interpretations were then transformed into a series of implicit 3D models, aligned with the dominant strike directions of 235° and 140°. Additionally, weathering modelling was performed, considering the information provided in the logs. The model was built from implicit modelling using the Leapfrog 2023.2 software.

The Ordinary Kriging (OK) estimation method was used on the Li2O% and Density variables based on the structural analysis results.

The mathematical/geostatistical criterion for classifying the resource was based on:

- The Measured Mineral Resource classification had as a reference the 50 meters of the Average Euclidean distance to sample (AvgD) used in ordinary kriging estimation with a minimum of five composites in at least three different drill holes.
- The Indicated Mineral Resource classification had as a reference the 100 meters of the Average Euclidean distance to sample (AvgD) used in ordinary kriging with a minimum of five composites in at least three different drill holes.
- The Inferred Mineral Resource classification is all remaining estimated blocks.

The Bandeira Mineral Resources are summarized in Table 25-1.

Table 25-1 – Bandeira Mineral Resources

Source: GE21 2024

Deposit / Cut-Off Grade	Category	Resource (Mt)	Grade (% Li2O)	Contained LCE (kt)
Bandeira *(0.5% cut-off)*	Measured	3.32	1.38	113.1
	Indicated	20.36	1.33	669.6
	Measured + Indicated	23.68	1.34	783.0
	Inferred	18.25	1.37	618.4

Notes:

The spodumene pegmatite domains were modelled using composites with Li2O grades greater than 0.3%.

1. The mineral resource estimates were prepared following the CIM Standards and the CIM Guidelines, using geostatistical and/or classical methods, plus economic and mining parameters appropriate to the deposit.
2. Mineral Resources are not ore reserves or demonstrably economically recoverable.
3. Grades reported using dry density.
4. The effective date of the MRE is March 05, 2024.

5. The QP responsible for the MRE is the geologist Carlos Silva (MAIG #7868).
6. The MRE numbers provided have been rounded to the estimated relative precision. Values cannot be added due to rounding.
7. The MRE is delimited by Lithium Ionic Bandeira Target Claims (ANM).
8. The MRE was estimated using ordinary kriging in 12m x 12m x 4m blocks.
9. The MRE report table was produced in Leapfrog Geo software.
10. The reported MRE only contains fresh rock domains.
11. The MRE was restricted by RPEEE with grade shell using 0.5% Li2O cut-off.

26 RECOMMENDATIONS

GE21 proposes the following recommendations for the continuous improvement of the Mineral Resource estimate:

- A 50x50m infill drilling program in the domain of the indicated resource classification that will focus on resource delineation improvement.
- A 100x100m infill drilling program in the domain of the inferred resource classification that will focus on resource delineation improvement.
- A density campaign to measure the density of drill hole cores by drying the samples in an oven, as well as waterproofing them. Compare the results with the methodology used in the current project procedure to check whether there is a bias in the results.
- Conduct an on-site density survey in the weathered zone.
- An updated mineral resource assessment is currently underway through the ongoing infill drilling program.
- Detail Geotechnical analysis, including a geotechnical-oriented diamond drilling campaign and logging, including sampling collecting for tensile, compressive and shear strength tests.
- Perform supplementary geotechnical investigations of planned infrastructure sites including at waste pile areas; supplementary geochemical tests (ARD); large-scale waste rock and tailings co-disposal stockpile field test.
- To implement the hydrological and hydrogeological studies for the project's next phases.

27 REFERENCES

Afgouni K., Sá, J., Haroldo, S. Lithium Ore in Brazil, Energy Vol 3, páginas 247 – 253, Pergamon Press Ltd, Printed in Great Britain,1978.

Afgouni, K., and Marques, F. F., 1997. Depósitos de lítio, berílio e césio de Araçuaí/Itinga, Minas Gerais. In: Schobbenhaus, C., Queiroz, E. T., & Coelho, C. E. S. (Coords.). 1997. Principais Depósitos Minerais do Brasil. Brasília: DNPM/CPRM. v. 4B. p. 373-388.

Alkmim, F. F., Marshak, S., Pedrosa-Soares, A. C., Peres, G. G., Cruz, S. C. P., Whittington, A., 2006. Kinematic evolution of the Araçuaí-West Congo orogen in Brazil and Africa: Nutcracker tectonics during the Neoproterozoic assembly of Gondwana. Precambrian Research, 149, 43–64.

Aquino, J. A.; Oliveira, M. L. M.; Braga, P. F. A. Ensaios em meio denso. IN: Tratamento de Minérios: práticas laboratoriais. Rio de Janeiro: CETEM/MCTI, 2007. p. 297-318.

Arenare, D. S., Rodrigues, O. M. S., Araujo, A. C., Viana, P. R. M., 2009. Espirais concentradoras no tratamento de minérios de ferro: uma breve revisão. Tecnol. Metal. Mater, volume 5, p. 224-228.

Bamber AS (2008) Integrated mining, pre-concentration and waste disposal systems for the increased sustainability of hard rock metal mining. Ph.D. thesis, University of British Columbia, Vancouver, Canadá.

Bradley D., and McCauley A., (2013): A Preliminary Deposit Model for Lithium-Cesium-Tantalum (LCT) Pegmatites: U.S. Geological Survey, Open-File Report 2013–1008 Version 1.1, December 2016.

Burt, R. O. Gravity concentration technology. Amsterdam: Elsevier, 1984, p.139-183.

Campos, A. R.; Luz, A. B.; Braga, P. F. A. Separação em meio denso. In: Tratamento de minérios. 6. ed. Rio de Janeiro: CETEM/MCTIC, 2018. Cap.7, p.303-338.

Cerný, P. and Ercit, T., 2005. The classification of granitic pegmatites revisited. The Canadian Mineralogist, 43, 2005-2026.

Cerný, P., 1991. Rare-element granite pegmatites. Part I: anatomy and internal evolution of pegmatite deposits. Part II: regional to global relationships and petrogenesis. Geoscience Canada 18: 49-81

Cerný, P., London, D., Novak, M., 2012. Granitic pegmatites as reflections of their sources.

Elements, 8, 289-294.

Chaves, M. L. S. C., Dias, C. H., Cardoso, D. K., 2018. Lítio. In: Pedrosa-Soares, A. C, Voll, E., & Cunha, E. C. (orgs.). Recursos Minerais de Minas Gerais. Belo Horizonte: Companhia de Desenvolvimento de Minas Gerais (Codemge). p. 1-21. http://recursomineralmg.codemge.com.br

Correia-Neves, J.M., Pedrosa-Soares, A.C. & Marciano, V.R. (1986). A Província Pegmatítica Oriental do Brasil à luz dos conhecimentos atuais. Revista Brasileira de Geociências, vol. 16(1): 106-118.

Costa Sena, J.C. de (1982). Notícia sobre a mineralogia e geologia de uma parte do norte e nordeste da Província de Minas Gerais. Annaes da Escola de Minas de Ouro Preto, n. 2, pp. 113-136.

Costa, A. G., 1989. Evolução petrológica para uma sequência de rochas metamórficas regionais do tipo baixa pressão, Itinga, NE de MG. Revista Brasileira de Geociências, 19, 440–448.

Costa, A. G., Neves, J. M. C., & Mueller, G. (1984). Feições polimetamórficas de metapelitos da região de Itinga (Minas Gerais, Médio Jequitinhonha). In: Congresso Brasileiro de Geologia, 33, Rio de Janeiro, Anais, 6. Sociedade Brasileira de Geologia, 3166–3180.

Castañeda, C.; Addad J. E.; Liccardo, A. (org.). Gemas de Minas Gerais. 1.ed. Belo Horizonte: Sociedade Brasileira de Geologia-Núcleo Minas Gerais, v. único, p. 16-33.

Delboni Jr., H., Laporte, M-A, Quinn, J., Rodriguez, P.C., O'Brien, N., 2023. Grota do Cirilo Lithium Project, Araçuaí and Itinga regions, Minas Gerais, Brazil, Updated Technical Report (https://www.sigmalithiumresources.com)

Deluca, C., Pedrosa-Soares, A., Lima, S., Cordani, U., Sato, K., 2019. Provenance of the Ediacaran Salinas Formation (Araçuaí Orogen, Brazil): Clues from lithochemical data and zircon U-Pb (SHRIMP) ages of volcanic clasts. Brazilian J. Geol. 49, 1–19. https://doi.org/10.1590/2317-4889201920190017

Dias, C. H., 2015. Mineralogia, tipologia e causas de cor de espodumênios da Província Pegmatítica Oriental do Bra¬sil e química mineral de Nb-tantalatos da mina da Ca¬choeira (Minas Gerais). Belo Horizonte, IGC- UFMG. (Dissert. Mestrado). URL: https://repositorio.ufmg.br/han¬dle/1843/BUBD-9ZWPNA.

Ferraz, L.C. (1928). Compêndio dos minerais do Brasil. Imprensa Nacional, Rio de Janeiro.

Ferraz, L.C. Compêndio dos minerais do Brasil. Imprensa Nacional, Rio de Janeiro, 1928.

GE21 Consultoria Mineral Ltda. Leonardo Silva Santos Rocha. (2023). QA/QC Assessment: Lithium Ionic Corp 2022 Diamond Drilling Campaign Results – Draft Technical Memo, Project 220210, January 25, 2023.

IDE SISEMA (2022) / IBGE (2022). https://idesisema.meioambiente.mg.gov.br/webgis

London, D., (1984): Experimental Phase Equilibria in the System LiAlSiO4- SiO2-H2O; a Petrogenetic Grid for Lithium-rich Pegmatites, American Mineralogist, 69(11-12), pp. 995-1004

London, D., 2008. Pegmatites. Canadian Mineralogist Special Publication, 10, 347 pp.

Luiz, C.R., 2023. Como garantir segurança geotécnica em minas subterrâneas: O exemplo da Mina da Cachoeira da Companhia Brasileira de Lítio. Invited lecture in Lithium Business 2023, Vale do Rio Jequitinhonha, Araçuaí, Brazil. Video available in YouTube (https://www.youtube.com/watch?v=5QKjPYJtV8k).

MGLIT Empreendimentos Ltda, 2022. QA/QC Protocol for Diamond Drilling, Itinga Project, April 2022.

MGLIT Empreendimentos Ltda, 2023. Relatorio dos testes com Ore Sorter TOMRA Solutions – Alemanha, July 10, 2023.

Mining legislation classes notes of UNI-BH Geology bachelor's degree, 2015.

Paes, V. J. C., Heineck, C. A., and Drumond, J. B. V. (2010). Folha SE.24-V-A-IV Itaobim. Belo Hori¬zonte: CPRM, Programa Geologia do Brasil, 1:100000.

Paes, V.J.C., Santos, L.D., Tedeschi, M; F., 2016. Avaliação do Potencial do Lítio no Brasil: Área do Médio Rio Jequitinhonha, Nordeste de Minas Gerais. Programa Geologia do Brasil. CPRM, Belo Horizonte, 276p.

Paiva, G. (1946). Províncias Pegmatíticas do Brasil. Bo¬letim DNPM/DFPM, 78, 13-21.

Paulo F. A. Braga A., Sílvia C. A. França A., Ronaldo L. C. dos Santos – Panorama da indústria do lítio no Brasil, II simpósio de minerais industriais do Nordeste, páginas 237 – 247 – CETEM Centro de Tecnologia Mineral, Ministério de Ciência e Tecnologia.

Paulo F. A. Braga A., Sílvia C. A. França A., Ronaldo L. C. dos Santos – Panorama da indústria do lítio no Brasil, II simpósio de minerais industriais do Nordeste, páginas 237 – 247 – CETEM Centro de Tecnologia Mineral, Ministério de Ciência e Tecnologia.

Pedrosa-Soares A.C., Correia-Neves J.M., Leonardos O.H., 1990. Tipologia dos pegmatitos de

Coronel Murta – Virgem da Lapa, Médio Jequitinhonha, MG. Revista Escola de Minas: 44-54.

Pedrosa-Soares, A. C. (1997). Mapa Geológico da Folha Araçuaí, Minas Gerais, Brasil. Belo Horizonte, Pro¬jeto Espinhaço, 1:100.000. Mapa e relatório, CODEMIG, http://www.portalgeologia.com.br/index.php/mapa

Pedrosa-Soares, A. C., De Campos, C. P., Noce, C., Silva, L. C., Novo, T., Roncato, J., Alkmim, F. (2011): Late Neoproterozoic-Cambrian granitic magmatism in the Araçuaí orogen (Brazil), the Eastern Brazilian Pegmatite Province and related mineral resources. Geological Society, London, Special Publications, 350(1), 25–51. doi:10.1144/sp350.3

Pedrosa-Soares, A. C., Leonardos, O. H., Correia-Neves, J. M., 1984. Aspectos metamórficos de sequências supracrustais da Faixa Araçuaí em Minas Gerais. In: Congresso Brasileiro de Geologia, 33, Rio de Janeiro, Anais, 6. Sociedade Brasileira de Geologia, 3056–3065.

Pedrosa-Soares, A., Chavez, M., Scholz, R (2009): Field Trip Guide Eastern Brazilian Pegmatite Provinces, 4th International Symposium on Granitic Pegmatite, 28 p.

Pedrosa-Soares, A.C., Alkmim, F.F., Tack, L., Noce, C.M., Babinski, M., Silva, L.C., Martins-Neto, M.A., 2008. Similarities and differences between the Brazilian and African counterparts of the Neoproterozoic Araçuaí-West Congo orogen. Geol. Soc. Spec. Publ. 294, 153–172. https://doi.org/10.1144/SP294.9

Pedrosa-Soares, A.C., de Campos, C.P., Noce, C., Silva, L.C., Novo, T., Roncato, J., Medeiros, S., Castañeda, C., Queiroga, G., Dantas, E., Dussin, I., Alkmim, F., 2011. Late Neoproterozoic-Cambrian granitic magmatism in the Araçuaí orogen (Brazil), the Eastern Brazilian Pegmatite Province and related mineral resources. Geol. Soc. Spec. Publ. 350, 25–51. https://doi.org/10.1144/SP350.3

Pedrosa-Soares, A.C., De Campos, C.P., Noce, C.M., Silva, L.C., Novo, T., Roncato, J., Medeiros, S., Castañeda, C., Queiroga, G., Dantas, E., Dussin, I., Alkmim, F., 2011. Late Neoproterozoic-Cambrian Granitic Magmatism in the Araçuaí Orogen (Brazil), the Eastern Brazilian Pegmatite Province and Related Mineral Resources. In: Sial, A.N., Bettencourt, J.S., De Campos, C.P., Ferreira, V.P. (Eds.), Granite-Related Ore Deposits. London, Geological Society of London, Special Publication 350, 25–51.

Pedrosa-Soares, A.C., Deluca, C., Araujo, C.S., Gradim, C.S., Lana, C.C., Dussin, I., Silva, L.C., Babinski, M. 2020. Capítulo 11: O Orógeno Araçuaí à luz da Geocronologia: um tributo a Umberto Cordani. In: Bartorelli, A., Teixeira, W., Brito Neves B.B. Geocronologia e evolução tectônica do Continente Sul-Americano: a contribuição de Umberto Giuseppe Cordani. – 1. ed. – São Paulo: Solaris Edições Culturais, p. 250-272.

Pedrosa-Soares, A.C., Diniz, H.B., Costa, C.H.C., Guimarães, A., Costa, R., 2023. Lithium ore in the Eastern Brazilian Pegmatite Province: a review and new discoveries of spodumene-rich pegmatites. (Article to be submitted).

Pedrosa-Soares, A.C., Monteiro, R., Correia-Neves, J.M., Leonardos, O.H., Fuzikawa, K. 1987. Metasomatic evolution of granites, Northeast Minas Gerais, Brazil. Revista Brasileira de Geociências, 17, 512-518.

Pedrosa-soares, A.C., Noce, C.M., Wiedemann, C.M., Pinto, C.P., 2001. The Araçuaí-West-Congo Orogen in Brazil: an overview of a confined orogen formed during Gondwanaland assembly. Precambrian Res. 110, 307–323. https://doi.org/10.1016/S0301-9268(01)00174-7

Pedrosa-Soares, A.C.; Baars, F.J.; Lobato, L.M.; Magni, M.C.V.; Faria, L.F. 1993. Arquitetura tectono-metamórfica do setor central da Faixa Araçuaí e suas relações com o Complexo Guanhães. In: 4 Simpósio Nacional de Estudos Tectônicos, Belo Horizonte. Anais: SBG Núcleo MG, p. 176-182.

Pedrosa-Soares, A.C.; Chaves, M.; Scholz, R. 2009. Eastern Brazilian Pegmatite Province. PEG 2009, Fieldtrip Guide: https://www.researchgate.net/publication/234037120_Eastern_Brazilian_Pegmatite_Province

Pedrosa-Soares, A.C.; Leonardos, O.H.; Ferreira, J.C.H.; Reis, L.B. 1996. Duplo Regime Metamórfico na Faixa Araçuaí: Uma reinterpretação à luz de novos dados. In: 39 CONGRESSO BRASILEIRO DE GEOLOGIA, 1996, Salvador. Anais. Salvador: SBG Núcleo Bahia-Sergipe, v. 6. p. 5-8.

Pedrosa-Soares, A.C.; Pinto, C. P.; Custódio Netto; Araújo, M. C.; Castañeda, C.; Achtschin, A.B.; Basilio, M. S. 2001. A Província Gemológica Oriental do Brasil. In:

Pedrosa-Soares, A.C.; Romeiro, J.C.P.; Castañeda, C. 1997. Papel do Controle Estrutural de Pegmatitos Graníticos em suas Mineralizações. In: VI Simpósio Nacional de Estudos Tectônicos, 1997, Pirenópolis. Anais. SBG-Núcleo Brasília, 1997. p. 357-359.

Peixoto, A., Ferreira, D., Mattos, I. Catálogo de minerais do laboratório de mineralogia. Fortaleza: UFCE, 2016.

Peixoto, A., Ferreira, D., Mattos, I. Catálogo de minerais do laboratório de mineralogia. Fortaleza: UFCE, 2016.

Peixoto, E., Alkmim, F.F., Pedrosa-Soares, A.C., 2018. The Rio Pardo salient, northern Araçuaí orogen: an example of a complex basin- controlled fold-thrust belt curve. Brazilian J. Geol.

48(1), 25–49. https://doi.org/10.1590/2317-4889201820170134

Peixoto, E.; Alkmim, F.F.; Pedrosa-Soares, A.; Lana, C.; Chaves, A.O. 2017. Metamorphic record of collision and collapse in the Ediacaran-Cambrian Araçuaí orogen, SE-Brazil: Insights from P-T pseudosections and monazite dating. Journal of Metamorphic Geology, p. 1-26.

Quéméneur, J. and Lagache, L. (1999). Comparative study of two pegmatitic fields from Minas Gerais, Brazil, using the Rb and Cs contents of micas and feldspars. Revista Brasileira de Geociências, 29(l): 27-32.

Revuelta, M. B. (2018). Mineral resources: from exploration to sustentability assessment. Madrid: Springer

Romeiro, J. C. P. (1998). Controle da mineralização de lítio em pegmatitos da Mina da Cachoeira, Companhia Bra¬sileira de Lítio, Araçuaí, MG. Belo Horizonte: Instituto de Geociências, UFMG. (Dissertação de Mestrado).

Romeiro, J. C., Pedrosa-Soares, A.C. (2005). Controle do minério de espodumênio em pegmatitos da Mina da Cachoeira, Araçuaí, MG. Geonomos, 13, 75-85.

Sá, J.H.S. (1977). Pegmatitos litiníferos da região de Itinga-Araçuaí, Minas Gerais. Tese de Doutorado, Universidade de São Paulo.

Saadi., A., Pedrosa-Soares, A.C., 1990. Um graben cenozóico no Médio Jequitinhonha, Minas Gerais. In: Workshop sobre Neotectônica e Sedimentação Cenozoica Continental no Sudeste Brasileiro. Belo Horizonte: SBG-MG. Bol. 11, p. 101-124.

Sahoo, S. K; Tripathy, S. K; Nayak, A.; Hembrom, A. C; Dey, S. Rath, R. K; Mohanta, M. K. Beneficiation of lithium bearing pegmatite rock: a review. Mineral Processing and Extractive Metallurgy Review, 2022.

Sampaio, J. A.; BRAGA, P. F. A. Ensaios em espirais concentradoras. In: Tratamento de Minérios: práticas laboratoriais. Rio de Janeiro: CETEM/MCTI, 2007. p. 281-293.

Santos, R. F., Alkmim, F. F., Pedrosa-Soares, A. C., 2009. A Formação Salinas, Orógeno Araçuaí, MG: História deformacional e significado tectônico. Revista Brasileira de Geociências, 39, 81–100.

Santos, R.F. dos Alkmim, F.F., Pedrosa-Soares, A.C., 2009. A Formação Salinas, Orógeno Araçuaí (MG): história deformacional e significado tectônico. Rev. Bras. Geociências 39, 81–100. https://doi.org/10.25249/0375-7536.200939181100

Sepro Laboratories Inc.: Aaron Bazzana and Tanner Parkes, 2023. Lithium Ionic Dense Media

Separation Teswork Report, July 7, 2023.

SGS Geosol: Alberto Antonio de Faria, 2022. Preliminary test work, Final Report Rev 01, Lithium Ionic/MGLIT, Lithium Project, December 22, 2022.

Simmons, W.B., Webber, K.L., Falster, A.U., and Nizamoff, J.W. (2003): Pegmatology: Pegmatite Mineralogy, Petrology and Petrogenesis.: By Published by Rubellite Press, New Orleans, Louisiana 70122, 176 pages. (ISBN 0–9740613–0–1).

Spix, J.B. von & Martius, C.F.P. von. (1823). Viagem pelo Brasil, volume 2. Imprensa Nacional, Rio de Janeiro.

Stevanato, R., Intergeo Comércio E Serviços Em Geofísica Aplicada Ltda – Me, 2022: Projeto Lítio – Araçuaí-MG (Polarização Induzida e Resistividade na Exploração Mineral), prepared for MGLIT Empreendimentos Ltda & Grupo GE21.

VERAS, M. M. Detecção de minério ortador de elementos de terras raras do depósito de Pitinga/AM, Brasil assistido por tecnologia de sensor-based sorting. Universidade Federal do Rio Grande do Sul, Porto Alegre. 2018

VERAS, M. M., YOUNG, A. S., SAMPAIO, C. H. e PETTER, C. O., 2016. A mining breakthrough, preconcetration by sensor-based sorter. mining engineering magazine, Volume 01, pp. 38-42.

VERAS, M. M; YOUNG, A. S; SAMPAIO, C. H; PETTER, C. O. A mining breakthrough; Pre concentration by sensor-based sorting. Mining Engineering, 68, p. 38-42. 2016

Viana, R.R., Manttari, I., Kunst, H., and Jordt-Evangelista, H., (2003): Age of Pegmatites from Eastern Brazil and Implication of Mica Intergrowths on Cooling Rates and Age Calculation, Journal of South American Earth Sciences, Vol. 16, pp.493-501.

wills, B. A., Napier-Munn, T. J., 2006. Wills' mineral processing technology: an introduction to the practical aspects of ore treatment and mineral recovery. 7 ed. s.l.:Elsevier.

wills, B.A. Heavy medium separation. In: Mineral Processing Technology. New York: Pergamon Press, 4 ed., cap. 11, p. 420-456, 1988.

Wotruba, H., Harbeck, H., Sensor-Based Sorting. Ullmann’s encyclopedia of industrial chemistry, vol. 32, p. 395-404

Young, A. S. Uso da separação automática por sensor de raio X na pré-concentração de minérios: ferro e zinco. Universidade Federal do Rio Grande do Sul, Porto Alegre. 2017.

28 CERTIFICATE OF QUALIFIED PERSON

28.1 Carlos José Evangelista da Silva

I, Carlos José Evangelista da Silva, am a GE21 Consultoria Mineral Geologist at Avenida Afonso Pena, 3130 – 12th and 13th floor, Belo Horizonte, MG, Brazil, CEP 30.130-910. This certificate applies to the Technical Report entitled "NI 43-101 Technical Report – Mineral Resource Update on Bandeira Project, Araçuaí and Itinga, Minas Gerais State, Brazil", with an effective date of March 5th, 2024.

1. I hold the following academic qualifications:
    - a B.A.Sc. in Geology from the Federal University of Minas Gerais, in Belo Horizonte, Brazil,
    - a master's degree in engineering in Mineral Technology from the Postgraduate Program in Mining, Metallurgical and Materials Engineering (PPGE3M) at the Federal University of Rio Grande do Sul, Brazil,
2. I am a professional Geologist with more than 17 years of experience in the mining industry. My relevant experience for this Technical Report includes:
    - I have 12 years of experience as a specialist geologist in Mineral exploration:
        - 2006 to 2011 – Geologist in Coffey Mining Brazil, which provides advice, assistance, and audits for the mineral exploration, project development, and geological assessments for JORC and NI 43-101.
        - 2011 to 2014 – Geologist in Colossus Minerals, Serra Pelada - Gold Project in Curionópolis – Pará – Brasil. Which assists in brownfield exploration projects.
        - 2014 to 2016 - Geologist in SMCA - Sociedade Mineira de Cobre de Angola, Mavio Copper Project – Maquela do Zombo – Uige - Angola, which provides mineral resource management.
    - I have six years of experience in consultancy companies as a specialist in resource estimate and geostatistics:
        - 2018 to present – Resource Geologist of GE21 Consultoria Mineral, which provides advice, assistance, and audits for the Mineral Resource Estimation and mineral exploration for JORC and NI 43-101 reports.
3. I am a member of the Australian Institute of Geoscientists (#7868).
4. I meet all the education, work experience, and professional registration requirements of a "Qualified Person" as defined in Section 1.1 of National Instrument 43-101.
5. I inspected the property subject to this Technical Report between the 13th and 14th of September 2023 and the 13th of December 2023.
6. I am responsible for Sections 2 to 12, 14, 23 and jointly for Sections 1, 11, 12, 25 and 26 of this Technical Report.
7. I previously signed as QP the MRE of the Bandeira Project PEA dated November 30, 2023, named "Bandeira Project, Araçuaí and Itinga, Minas Gerais State, Brazil "
8. Independent Technical Report – Preliminary Economic Assessment "
9. I am independent of the Issuer, Lithium Ionic Holdings Corp, and its subsidiaries.
10. I have read National Instrument 43-101, and the parts of the Technical Report I am responsible for have been prepared in compliance with this Instrument, including the CIM Definition Standards on Mineral Resources and Mineral Reserves.

At the effective date of the Technical Report, and at the date it was filed, to the best of my knowledge, information, and belief, the parts of the Technical Report for which I am responsible contain all scientific and technical information that is required to be disclosed to make the Technical Report not misleading.

Belo Horizonte, Brazil, May 27th, 2024.

<signed & sealed in the original>

_____

Carlos José Evangelista da Silva

28.2 Certificate of Leonardo Silva Santos Rocha

I, Leonardo Silva Santos Rocha, MAIG, (#7623), as an author of the technical report titled "NI 43-101 Technical Report – Mineral Resource Update on Bandeira Project, Araçuaí and Itinga, Minas Gerais State, Brazil", dated May 27th, 2024, with an effective date of March 5th, 2024 (the "Technical Report"), prepared for "Lithium Ionic Corp." (the "Issuer"), do hereby certify that:

1. I am a geologist for GE21 Consultoria Mineral Ltda., which is located on Avenida Afonso Pena, 3130, 12th and 13th floor, Savassi, Belo Horizonte, MG, Brazil - CEP 30130-910.
2. I am a graduate of the Federal University of Minas Gerais, located in Belo Horizonte, Brazil, and hold a Bachelor of Science Degree in Geology (2013). I have practiced my profession continuously since 2013.
3. I am a Professional enrolled with the Australian Institute of Geoscientists ("AIG") Member - ("MAIG") #7623.
4. I am a professional geologist with over twenty (11) years of experience in economic geology, mineral exploration, and Mineral Resource Estimation.
5. I have read the definition of "qualified person" set out in National Instrument 43-101 – Standards of Disclosure for Mineral Projects ("NI 43-101") and certify that, by reason of my education, affiliation with a professional association as defined in NI 43-101, and past relevant work experience, I fulfill the requirements to be a "qualified person" for the purposes of NI 43-101.
6. I have supervised the preparation of the Technical Report for Chapters 11, 12 with co-responsibility for the corresponding sections within Chapters 1, 25 and 26 that are related to the foregoing Chapters of this Technical Report.
7. I personally inspected the property that is the subject of this Technical Report on April 11th, 2024.
8. As of the effective date of the Technical Report, to the best of my knowledge, information, and belief, the sections of the Technical Report that I have authored and am responsible for contain all scientific and technical information that is required to be disclosed to make the Technical Report not misleading.
9. I have had no prior involvement with the property that is the subject of this Technical Report.
10. I have no personal knowledge, as of the date of this certificate, of any material fact or material change which is not reflected in this Technical Report.
11. I am independent of the Issuer, Lithium Ionic Holdings Corp, and its subsidiaries, applying all the tests in section 1.5 of NI 43-101.
12. I have read NI 43-101 and Form 43-101F1 – Technical Report and, in my opinion, the Technical Report has been prepared in compliance with such instrument and form.

Belo Horizonte, Brazil, May 27th, 2024.

<signed & sealed in the original>

_____

Leonardo Silva Santos Rocha, MAIG

28.3 Certificate of Paulo Bergman

I, Paulo Bergman, am a Mining Engineer associated to GE21 Consultoria Mineral, located at Avenida Afonso Pena, 3130 – 12th and 13th floor, Belo Horizonte, MG, Brazil, CEP 30.130-910. This certificate applies to the Technical Report entitled "NI 43-101 Technical Report – Mineral Resource Update on Bandeira Project, Araçuaí and Itinga, Minas Gerais State, Brazil", with an effective date of March 5th, 2024.

1. I hold the following academic qualifications: a B.A.Sc. in Mining Engineering from the Federal University of Minas Gerais, in Belo Horizonte, Minas Gerais, Brazil.
2. I am a professional Mining Engineer, with more than 40 years of experience in the mining industry. My relevant experience for the purpose of this Technical Report includes:
    - 30 years in mining and plant operation management, including AngloGold, Yamana, Jaguar Mining and Buritirama Mineração.
    - 10 years as engineering development and consultancy in the mining industry, including gold, iron, manganese, rare earth elements and others.
3. I am a Member of the Australasian Institute of Mining and Metallurgy (#333121).
4. I meet all the education, work experience, and professional registration requirements of a "Qualified Person" as defined in Section 1.1 of National Instrument 43-101.
5. I am responsible for Technical Report sections 13 and jointly responsible for Sections 1, 25 and 26 of this Technical Report.
6. I previously signed as QP Chapter 13 of the Bandeira Project PEA dated November 30, 2023, named "Bandeira Project, Araçuaí and Itinga, Minas Gerais State, Brazil "
7. I am independent of the Issuer, Lithium Ionic Corp, and its subsidiaries.
8. I have read National Instrument 43-101 and the parts of the Technical Report for which I am responsible have been prepared in compliance with this Instrument, including the CIM Definition Standards on Mineral Resources and Mineral Reserves.
9. At the effective date of the Technical Report, and at the date it was filed, to the best of my knowledge, information, and belief, the parts of the Technical Report for which I am responsible contain all scientific and technical information that is required to be disclosed to make the Technical Report not misleading.

Belo Horizonte, Brazil, May 27th, 2024.

<signed & sealed in the original>

_____

Paulo Bergman